HYDROGEOCHEMICAL MODELING OF THE SPECIATION AND LEACHING OF FLY ASH CO-DISPOSED WITH WATER, BRINES AND ORGANICS: A CASE STUDY OF SASOL-ESKOM COAL ASH DISPOSAL, SOUTH AFRICA

JOHN MWAI MBUGUA

Submitted in fulfilment of the academic requirements for the degree of

Doctor of Philosophy

School of Chemistry and Physics

University of KwaZulu-Natal, Westville Durban, South Africa

Supervisor: Prof J. Catherine Ngila

Co-Supervisors: Prof Andrew Kindness

Prof Chris Buckley

Dr Molla Demlie

October 2012

HYDROGEOCHEMICAL MODELING OF THE SPECIATION AND LEACHING OF FLY ASH CO-DISPOSED WITH WATER, BRINES AND ORGANICS: A CASE STUDY OF SASOL-ESKOM COAL ASH DISPOSAL, SOUTH AFRICA

JOHN MWAI MBUGUA (B. Ed (Sci), Hons, KU; MSc, JKUAT)

2012

A thesis submitted to the School of Chemistry, Faculty of Science and Agriculture, University of KwaZulu Natal, Westville, Durban for the degree of Doctor of Philosophy.

This thesis has been prepared according to Format 2 as outlined in the guidelines from the Faculty of Science and Agriculture which states:

"Format 2: This is a thesis in which the chapters are written as a set of discrete research papers, with an overall introduction and a final discussion. These research papers are not published yet, but would be in the format for publication."

As the candidate's supervisor, I have approved this thesis for final printing.

Supervisor

Name: Prof J. Catherine Ngila

Signed.....

Date...23 October 2012.

PREFACE

The modeling work described in this thesis was carried out in the School of Chemistry & Physics and the School of Chemical Engineering, both in the University of KwaZulu-Natal, from February 2009 to May 2012, under the supervision of Prof Chris Buckley of the Pollution Research Group, (in the School of Chemical Engineering), Prof Catherine Ngila, Prof Andrew Kindness both of the School of Chemistry & Physics, and Dr Molla Demlie of the School of Geological Sciences.

This thesis has been prepared according to Format 2 as outlined in the guidelines from the Faculty of Science and Agriculture of UKZN, (FHDR Approved 13 March 2007) which states that:

"Format 2: This is a thesis in which the chapters are written as a set of discrete research papers, with an overall introduction and a final discussion. These research papers are not published yet, but would be in the format for publication."

The studies represent original work by the author and have not been submitted in any form for any degree or diploma to any tertiary institution. Where use has been made of the work of others, particularly the calibration data of the acid neutralization capacity (ANC) from collaborating institutions involved in the ash-brine project and the original ash recipe by Mr. S. Hareeparsad (of Sasol), the author wishes to state that such work has been duly acknowledged in this thesis.

DECLARATION 1- PLAGIARISM

I, ……..……., declare that:

1. The modeling research reported in this thesis, except where otherwise indicated, is my original research.
2. This thesis has not been submitted for any degree or examination at any other university.
3. This thesis does not contain other person's data, pictures, graphs or other information unless specifically acknowledged as being sourced from other persons. In this respect I do declare that the data used for calibration of the model related to ANC of ash was obtained from Dr Gitari of Chemistry Department at UWC through personal communication. This data has been used in **chapters 3** and **4**, and hereby duly acknowledged. The data is already available in the public domain in form of publications and is cited accordingly.
4. This thesis does not contain other persons' writing, unless specifically acknowledged as being sourced from other researchers. Where other written sources have been quoted, then:
    a) Their words have been re-written but the general information attributed to them has been referenced
    b) Where their exact words have been used, then their writing has been placed in italics and inside quotation marks, and referenced.
5. This thesis does not contain text, graphics or tables copied and pasted from the Internet, unless specifically acknowledged, and the source being detailed in the thesis and in the References sections.

Signed……

DECLARATION 2 – PUBLICATIONS AND CONFERENCES

DETAILS OF CONTRIBUTION TO THE PUBLICATION (current or future) that form part and /or include research presented in this thesis (include publications in preparations or manuscript submitted or to be submitted for review and publication; and give details of the contributions of each author). The manuscripts will have to be reformatted to conform to selected journals format. The specific journals have been identified for each manuscript and listed.

Manuscript 1 (Chapter 3): To be submitted to the Journal of Environmental and Earth Science

Mbugua, J.M., Ngila, J. C., Kindness, A., Buckley, C., Demlie, M., Hareeparsad, S.,
Hydrogeochemical Modeling of the Effect of Brines and Organics on Metal Leaching, Acid Neutralization Capacity and Mineralogy of South African Fly Ash. **2012, School of Chemistry & Physics, University of KwaZulu-Natal, Durban, South Africa: Durban. p. 40.**

Contribution: I performed the PHREEQC modeling research work, data analysis and write up; Shameer Hareeparsad assisted me in ash-recipe modeling for the PHREEQC work. All the other co-authors are my supervisors who provided guidance and insightful ideas as well as editing the manuscript.

Manuscript 2 (Chapter 4): To be submitted to the Journal of Chemistry and Physics of the Earth

Mbugua, J.M., Ngila, J. C., Kindness, A., Buckley, C., Demlie, M., Hareeparsad, S.,
Reactive-Transport Modeling of Fly Ash-water-Brines Interactions from Laboratory-Scale Column Studies. **2012, School of Chemistry & Physics, University of KwaZulu-Natal, Durban, South Africa: Durban. p. 47.**

Contribution: I performed the PHREEQC modeling research work, data analysis and write up; Shameer Hareeparsad assisted me in ash-recipe modeling for the PHREEQC work. All the other co-authors are my supervisors who provided guidance and insightful ideas as well as editing the manuscript.

Manuscript 3 (Chapter 5): To be submitted to the Journal of Contaminant Hydrology

Mbugua, J.M., Ngila, J. C., Kindness, A., Buckley, C., Demlie, M., Hareeparsad, S.,
Application of Hydrogeochemical Modeling in Simulating the Transportation of Elements in Fly Ash Heap under Different Disposal Systems in South Africa. **2012, School of Chemistry & Physics, University of KwaZulu-Natal, Durban, South Africa: Durban. p. 20.**

Contribution: I performed the PHREEQC modeling research work, data analysis and write up; Shameer Hareeparsad assisted me in ash-recipe modeling for the PHREEQC work. All the other co-

authors are my supervisors who provided guidance and insightful ideas as well as editing the manuscript.

Conferences Attended

1. John M. Mbugua, J. Catherine Ngila, Chris Buckley, Andrew Kindness, Demlie Molla. *Hydrogeochemical modeling of multi-species release and transport in fly ash-brine co-disposal systems, using PHREEQC*. **Poster presentation during Faculty of Science and Agriculture Research day, Pietermaritzburg, September 23rd 2010.**

2. John M. Mbugua, J. Catherine Ngila, Chris Buckley, Andrew Kindness, Demlie Molla, Shameer Hareeparsad. *Hydrogeochemical modeling of fly ash co-disposed with brines: Effect of brines on acid neutralization capacity of a South African fly ash.* **Poster presentation in 2nd Tanzania Chemical Society International Conference proceedings, Dar es Salaam, Tanzania, October 5-7, 2011.**

3. John M. Mbugua, J. Catherine Ngila, Chris Buckley, Andrew Kindness, Demlie Molla. *Reactive-Transport Modeling of Fly Ash-Water-Brines Interactions from Laboratory-Scale Column Studies.* **Poster presentation in 13th WaterNet /WARFSA/GWP-SA International Symposium on Integrated Water Resource Management, Johannesburg, South Africa, October 31-November 2, 2012.**

Signed:…….

ABSTRACT

Two coal utility plants in South Africa selected (one from Sasol and another from Eskom) for this study produce large volumes of fly ash (over 40 Mt from Eskom at Tutuka, and 3 Mt from Sasol Synfuels at Secunda annually), and brines as by-products during coal processing. Co-disposal of the brines and fly ashes has been a normal practice in these coal-utility plants for decades. Long-term management of fly ash is necessary and requires an understanding and knowledge of how the different waste materials interact with water and brines in different chemical situations. However the geochemistry of their interactions, the leaching and mobility of elements in these disposal systems has not been fully understood. This work gives insights into the chemical processes taking place in the brine-water/brines systems that govern the concentrations of major and minor elements in ash leachates under different environmental conditions. The possible presence of organic compounds (subsequently referred to as 'organics') in brines and their effects on the leaching chemistry of fly ash was also studied. Sustainability and long term impact of the co-disposal of fly ash and brines on the environment was studied through static (batch tests) modeling of the pH-dependent acid neutralization capacity (ANC) tests and columns modeling for dynamic leach tests. The modeling was based on experimental results from other Sasol-Eskom ashbrine project collaborators. Modeling results of the ANC tests were in good agreement with the reported experimental results, which revealed that the release trends of various elements (including trace, heavy elements and contaminants) contained in fly ash into solution is highly pH dependent. However Na, K, Mo and Li exhibited constant solubilisation which was independent of pH changes from all the scenarios. The presence of different constituents of brines subjected to ANC resulted to different ANC capacities ranging from 0.98 moles H^+/Kg dry ash (of ash-organics mixed with Mg-brines) to 3.87 H^+/Kg dry ash for those with the C(4) brines. As expected, those constituents from the cationic brines were found on the lower region of acid addition (in the order Mg-brines < Ca-brines < Na-brines) while the anionic brines were found at the upper region of acid addition (in the order S(6)-brines < Cl-brines < C(4)-brines). In the middle region of acid addition were three important scenarios: that of ash with brine, ash without brines (i.e. ash with DMW) and ash with both ASW organics and combined brines. It was from these three scenarios that a generalization of the effect of brines and organics on the ANC was inferred. The ANC of ash with demineralised water (DMW) was 2.33 mol H^+/Kg dry ash and that of ash with ASW organics lower at 2.12 mol H^+/Kg dry

ash which was the same value as that of ash with combined brines. This indicated that brines decreased the ANC of ash by about 9.01 % and which could be attributed to the acid-base neutralization process and the dynamics of solid phase dissolutions in response to the acid addition. Both fly ashes exhibited a typical pH > 12 (suspension in demineralised water) and the predominant cation even at this high pH is Ca^{2+} (at concentration > 0.002 mmol/L). This indicates that dissolution of CaO and formation of OH^- species at pH > 10 contributes to acid neutralisation capacity of both fly ashes and is the greatest contributor to the acid neutralizing capacity of both fly ashes. Two broad leaching behaviours as a function of pH were observed from the three fly ash-ASW organics-brines scenarios (i) leaching of Ca, Mg, Ni and Sr follows a cationic pattern where the concentration decreases monotonically as pH increases; (ii) leaching of Al, Fe, Ti and Zn follow an amphoteric pattern where the concentration increases at acidic and alkaline pH, although Al showed some anomaly from pH 11 where the concentration decreased with the increase in pH. Al showed an amphoteric pattern in which its release increased between pH 12.8 and 11 for all the scenarios and then decreased with decrease in pH down to neutral pH of 7.

The batch leaching simulation results from hydrogeochemical modeling also showed that mineral dissolution, precipitation and new phase formation during ash-organics-brines interactions was controlled by pH. The newly formed phases however remain in equilibrium with the ash-brines-organics mixture. Each individual mineral phase dissolution/precipitation/formation system controls the concentration and speciation of the respective constituent elements as evidenced by the log C-pH diagrams obtained from the modeled scenarios. The ash-brines-organics interactions do exhibit and affect the mineralogical chemistry of fly ash. However the extent to which these interactions occur and their effect, varies from one scenario to another, and are dependent on the amounts and type of the constituent brine components. Organics do have a significant effect on dissolution characteristics of few minerals such as calcite, mullite, kaolinite, Ni_2SiO_4, and $SrSiO_3$ due to complexation effect. The effect is quantitatively conspicuous for calcite mineral phase and for the formation of some new phases such as $Fe(OH)_3$(am)-CF and portlandite.

The composition of the liquid phase from acid neutralisation capacity experiments was successful.

Hydrogeochemical modeling was used as a means to provide insights and understanding of the complex reactions taking place, speciation and mineralogical changes occurring. These changes would serve to predict future environmental scenarios when pH conditions change. In this study, an extension of the application field of PHREEQC hydrogeochemical code for modeling and simulation of equilibrium; kinetic and transport mechanisms associated with the interaction of water; and organics and brines with fly ash during their co-disposal is successfully demonstrated.

The parameters associated with these mechanisms were used as inputs into the PHREEQC program using modified Lawrence Livermore National Laboratory (LLNL) database for inorganic brines and MINTEQ.V4 database for organics, and used to model the results of ANC test data for the fly ashes. A special reference is made to two separate modeled mineralogical ash recipes from two of the South African power utility plants' fly ash systems, namely, Tutuka and Secunda. The effects of brines in the leaching of major, minor and trace elements at various pH values and the mineralogical changes associated with the intermediate and final products from the interactions of ash-brines systems under different scenarios are qualitatively and quantatively discussed. Multiphase saturation characteristics have been determined for mineral species in contact with water and brines.

The modeling results indicated that several mineral phases could be controlling the species concentration in the leachates, and the ANC and column modeling results corroborated well in many aspects with the experimental results obtained from collaborating institutions (South Africa Universities and Research institutions). In addition, application of the PHREEQC model to the ash heap under different disposal systems was carried out to predict the heap leachate composition and geochemical transformations taking place in a period of time. Pore water chemical analysis, and moisture content analysis revealed that contact of the ash with water is a crucial factor in the mobilization of the contaminants with time. Maximum weathering/dissolution of the ash is observed in the top layer (1-3) m and at the point of contact with the subsurface water level which was in good agreement with the model results. The surface layer and the very lowest layers of the dump in contact with lateral flows experience the highest degree of weathering leading to depletion of species. The geophysical transformation of fly ash was also captured through the porosity change calculations and the results revealed that geochemical reactions do affect the porosity of fly ash during the weathering processes. These modelling results were in agreement with the hydraulic tests and

salt leaching tests conducted during Sasol-Eskom ashbrine project in Phase I which suggested that salts captured in the ash will become mobile and leach from the fly ash over time. The data therefore indicates that ash dumps may not act as sustainable salt sinks. These findings may have some bearing on engineering decisions on fly ash reuse. From the above observations, it is apparent that release of large quantities of the salts in the ash depends on the extent of its interaction with brines being used for irrigation or with water, either through plug-in flow after a rainfall event or contact with groundwater. The results revealed effects of brine-water contact time with fly ash, the flow volume and velocity, the pH, the degree of saturation, hydrogeology and ash heap geometry as important factors that affect fly ash transformation and weathering.

Overall, the ash heap modeling enhanced the understanding of the ash-brines interactions and demonstrated that leachate composition is determined by the following factors; (i) the mass flows from the pores of fly ash, (ii) the surface dissolution of the mineral phases, (iii) the various chemical reactions involved during the ash-brine and ash-water interactions, (iv) the interactions with a gas phase (atmospheric CO_2), (v) the composition of the initial fly ash, and (vi) by the leachate flow and hydrodynamics as captured in the conceptual model. Any ash handling system should therefore be designed to take these criteria into consideration to prevent environmental contamination. The modeling results also gave indications that the ash-brine co-disposal in dry ash systems would be an unsustainable way of locking up brine salts in the long run.

In this Thesis, modeling results were used to support experimental data which further reaffirmed the important role hydrogeochemical modeling plays in liquid and solid waste management. Furthermore, hydrogeochemical modeling complements the work of analytical/environmental scientists as well as guiding the future solid waste management and engineering decisions.

ACKNOWLEDGMENT

I wish to thank my supervisor Prof Catherine Ngila and co-supervisor Prof Chris Buckley who first introduced me into the field of hydrogeochemical modeling and have patiently guided me through the academic ladder, every step of the way. My special thanks also to my other co-supervisors Professor Andrew Kindness and Dr Demlie Molla for their invaluable discussions, suggestions, direction and continued encouragement. To you all, you will remain very special people, mentors in my life.

Shameer Hareeparsad of Sasol, with whom I worked very closely during the first phase of the project supervised by Prof Chris Buckley, is hereby acknowledged for his initial guidance and whose work became the basis of my modeling study in the second phase of the Sasol-Eskom ash-brine project. I wish to thank Prof. David Parkhurst (the architect of PHREEQC code in USGS) whose online help and ready answers to my questions enriched me greatly in my modeling activities.

I would also like to thank Prof Leslie Petrik, Dr Wilson Gitari and Mr Ojo Fatoba of the University of Western Cape who did all the laboratory experimental work and whose data on ash-water interactions was used for the initial calibration and validation of my models.

The entire Sasol-Eskom ashbrine project team, who provided a forum for knowledge sharing in various workshops in the Eskom premises in Johannesburg, is greatly appreciated.

The project could not have been possible were it not for the financial support of the University of KwaZulu-Natal's fees remission and the bursary from the Pollution Research Group through Prof Chris Buckley, and not forgetting Prof Catherine Ngila for her financial support. I am very grateful to them all.

I also wish to acknowledge the Faculty of Science and Agriculture, UKZN for awarding me conference funding to present some of the research results of this Thesis during the 2nd Tanzania Chemical Society International Conference in Dar es Salaam.

Equally so is my acknowledgement of the Kenya Polytechnic University College for granting me study leave and supplementary funding during my entire studies.

My fellow postgraduate students in the Analytical Research Group and the entire Staff in the School of Chemistry & Physics, and friends, who supported me and made me feel at home, are gratefully acknowledged.

Last but not least, my family, for the patience, support, encouragement and love.

School of Chemistry and Physics, UKZN, Durban South Africa, June 2012

DEDICATION

This work is dedicated to my beloved wife Reginah Wanja, my two sons Joseph Mbugua Mwai and Raymond Mwangi Mwai, and my lovely daughter Salome Njeri Mwai.

TABLE OF CONTENTS

LIST OF FIGURES

LIST OF TABLES

LIST OF ABBREVIATIONS

ADR	Advective-Dispersive Reactive
ANC	Acid neutralization capacity
ASW	Artificial sewage waste
BDL	Below detection limit
CAE	Clear ash effluent
CCRs	Coal combustion residues
Csh_gel	Calcium silicate hydrate gel (also C-S-H gel)
CUB	Coal utilization by-products
D	Dimensional
DMW	Demineralised water
EC	Electrical conductivity
EDR	Electro-dialysis reversal
FTIR	Fourier Transform Infra red
IC	Ion chromatography
ICP-MS	Inductively coupled plasma-mass spectrometer
L/S	Liquid-Solid ratio
LLNL	Lawrence and Livermore National Laboratory
mM	milli molarity
mmol	milli molality
pe	Potential of electrons
PHREEQC	pH, redox, Equilibrium Calculations
PRG	Pollution Research Group
Redox	Reduction-oxidation
RO	Reverse Osmosis
RTM	Reactive Transport Models
S/L	Solid-liquid ratio
SC	Secunda column
TC	Tutuka column
TDS	Total Dissolved Solids

Temp	Temperature
TOT	Total
TRO	Tubular Reverse Osmosis
UFS	University of the Free State
UKZN	University of KwaZulu-Natal
USGS	United States Geochemical Survey
UWC	University of Western Cape
XRF	X-ray Diffraction
Log	Logarithm

NOMENCLATURE

(NB. The units used are given in the respective sections where the parameters are used in the Thesis.)

Parameter	Description
d_phase	delta
d^1	absolute change in delta, (delta_delta)
Rc_d^1	relative change of delta_delta,
TOT	Total elemental concentration
S(6)	PHREEQC convention for S(VI) species
C(4)	PHREEQC convention for C(IV) species
K	Equilibrium constant
ΔH	Enthalpy change
ΔG	Gibb's free energy change
ΔS	Entropy change
a	activity
γ	activity coefficient
m	molality
ρ_w	density of water
% H_2O	Moisture content (of fly ash due to wet packing)
m_c	Weight of empty Column
$m_c + m_{w\text{-}ash}$	Weight of Colum + wet fly ash
$m_{w\text{-}ash}$	Weight of wet fly ash only
m_{H2O}	mass of water

$m_{d\text{-}ash}$	dry weight of fly ash before leaching
$m_{w\text{-}ash\text{-}l}$	Dry weight of fly ash after leaching
$m_{leached}$	leached amounts
$\%m_{leached}$	% leached
d	diameter of column
H	Column height
h	height of compacted ash in column
r	column radius
V	column total volume (includes voidage)
Vo	pore water volume of column($A*h*\varepsilon$)
PV	pore volumes = V/Vo
Q	flow rate
ε	porosity
A	cross-sectional area
i	hydraulic gradient=Q/KA
v	pole water flow velocity($Q/\varepsilon A$)
D	Darcy flow velocity
K	Hydraulic conductivity
t	total time (duration of simulated experiment)
ρ_b	bulk density of wet ash=$m_{w\text{-}ash}/V_{w\text{-}ash}$
ρ	dry ash density
Kd	distribution coefficient
R	Retardation, R = (1 + dq/dc)=1+Kd
q	concentration in the solid (mol/L of pore water)

c	solute concentration (mol/L)
D_L	Hydrodynamic dispersion coefficient
α_L	longitudinal dispersitivity
L/S	L/S=leachate volume/mass of dry ash=(ε/ρ).V/Vo)
1d, 2d, 3d	1 day, 2 days, 3 days etc
1 y	1 year
Kd	normalized distribution coefficient = q/c = ρb/ε
R	Retardation = 1+q/c = 1+ Kd
mixf	mixing factor between two consecutive cells
v	pole water flow velocity (Q/εA)
Δx	cell length
α_L	dispersitivity
Tot x	total column length or flowline
N_{cell} (or n)	number of cells = Tot x/Δx
Tot t (or t)	total time of injection or simulation
Δtv	for maximal value of Δt: = Δx , hence Δt < Δx/v (integer value)
N_{shifts}	timesteps
Δt	Time for each shift (Tot t/Nshifts)
ppt	parts per trillion (ng/Kg = ng/L = pg/g)

PHREEQC nomenclature on charge on species and valence states:

Charge on a chemical species--The charge on a species may be defined by the proper number of pluses or minuses following the chemical formula or by a single plus or minus followed by a integer number designating the charge. Either of the following is acceptable, Al^{+3} or Al^{+++}. However, Al^{3+} would be interpreted as a molecule with three aluminium atoms and a charge of plus one.

Valence states--Redox elements that exist in more than one valence state in solution are identified for definition of solution composition by the element name followed by the formal valence in parentheses. Thus, sulphur that exists as sulphate is defined as S(6) and total sulphide (H_2S, HS^-, and others) is identified by S(-2).

GLOSSARY

Within the context of this study and in this Thesis, the following terms will assume the specified meaning.

Aqueous speciation – the distribution of individual ions and ion pairs in water

Breakthrough volume - leachate volume at which a particular solute pumped continuously through a column begins to be eluted. It is dependent on the column volume and the retention factor of the solute and is useful in the determination of the total sample capacity of the column for a particular solute.

Brine – effluent saline solutions of the species Na, K, Ca, Mg carbonates (and hydrogen carbonates), sulphates and chlorides and of varying concentrations emitted from the Sasol & Eskom coal utility plants. After brines are applied on fly ash, they generate leachates.

Cementitious - Any of various building materials which may be mixed with a liquid, such as water, to form a plastic paste, and to which an aggregate may be added; includes cements, limes, and mortar [1].

Chemical speciation - describes the amounts and types of the different species and phases present in a system, or the process of identifying and quantifying these species or phases.

Closed system – a system in which exchange of material does not occur between the system and the environment, but energy exchange may occur and change of phase within the system is possible

Groundwater - Refers to water filling the pores and voids in geological formations below the water table

Hydraulic conductivity - The hydraulic conductivity is the constant of proportionality in Darcy's law. It is defined as the volume of water that will move through a porous medium in a unit time under a unit hydraulic gradient through a unit area measured at right angles to the direction of flow [2].

Kinetics – the rates of geochemical reactions

Leachate – liquid material that results from the fly ash-brines interaction which contains dissolved salts of varying quantities.

Mass transfer – moving mass between phases: solid, liquid or gases

Open system – a system in which exchange of matter and energy occurs between the system and the environment

Organics - organic compounds commonly found in sewage waste such as the

Permeability - The ease with which a fluid can pass through a porous medium,(unit: darcy or cm^2). It is defined as the volume of fluid discharged from a unit area of an aquifer under unit hydraulic gradient in unit time. It is an intrinsic property of the porous medium and is independent of the properties of the saturated fluid; (NB. Should not be confused with hydraulic conductivity (unit: m/d), which relates specifically to the movement of water [2].

Pollution - The introduction into the environment of any substance by the action of man that is, or results in, significant harmful effects to man or the environment.

Porosity - The porosity of the fly ash is its property of containing pores or voids.

Pozzolan - a siliceous or siliceous and aluminous material, which in itself possesses little or no cementing property, but will in a finely divided form - and in the presence of moisture - chemically react with calcium hydroxide at ordinary temperatures to form compounds possessing cementitious properties [1].

Reactive transport – coupling of flow and chemical reactions

Recharge - Groundwater recharge or deep drainage or deep percolation is a hydraulic process where water moves downward from surface water to groundwater [3]. This process usually occurs in the vadose zone below plant roots and is often expressed as a flux to the water table surface. Recharge occurs both naturally (through the water cycle) and anthropogenically (i.e. "artificial groundwater recharge "), where rainwater and or reclaimed is touted to the subsurface.

Saturated zone - The subsurface zone below the water table where interstices are filled with water under pressure greater than that of the atmosphere [4].

Saturation – the state of an aqueous solution in chemical equilibrium with a particular solid phase

Supersaturation – the phase is considered thermodynamically favoured to be formed

Undersaturation – the phase is considered thermodynamically favoured to dissolve

Unsaturated zone - The part of the geological stratum above the water table where interstices and voids contain a combination of air and water, synonymous with zone of aeration or vadose zone [4].

Water table - The upper surface of the saturated zone of an unconfined aquifer at which pore pressure is at the atmospheric pressure, the depth to which many fluctuate seasonally [4].

CHAPTER 1: INTRODUCTION

1.1 Background of the study

Sasol Synfuels at Secunda and the Eskom power station at Tutuka are two of the largest consumers of coal in South Africa, generating over 40 million tons of ash annually from their coal processing facilities [5, 6]. They heavily depend on coal and coal based technologies with each having large coal processing facilities situated inland in water scarce areas. The combustion of coal results in coal ash being produced as a by-product, which is disposed of in either terrestrial or aquatic environments (ash disposal basins). Environmental concerns and questions arise regarding the feasibility of ash disposal and the impact that it has on the environment, especially since coal ash is seen as a possible source of pollution due to its chemical makeup. Several published reviews have tried to answer some of these questions by examining the environmental impact of coal combustion residue disposal; however these reviews have focused on a few aspects of the disposal of coal waste [7-9]. Therefore some important knowledge gaps exist with regards to understanding the geochemistry and the leaching chemistry arising from the fly ash-brines interactions. This prompted Sasol and Eskom to undertake research which will help them understand the chemical and physical behaviour of ash produced from their facilities and the interactions occurring during their respective disposal situations. The Sasol-Eskom ash-brine project was undertaken in collaboration with various academic institutions in South Africa which included University of KwaZulu-Natal (UKZN), University of the Western Cape (UWC) and the Institute of Groundwater Studies (IGS) at the University of the Free State (UFS). Each of these institutions had specific mandate. All the experimental work dealing with fly ash characterization of fresh and weathered ash, (mineralogy, surface properties, particle size, surface area, CEC and influence on alkaline chemistry), brine chemistry, leaching tests, ash-water-brine chemistry interaction and hydrogeology were done was contracted to the Environmental and Nano Sciences group of UWC. The Pollution Research group of the UKZN under which my research work is based was contracted to carry out all the hydrogeochemical modeling work for fly ash-water-brine interaction chemistry: (chemical speciation modelling of brines, modelling of the ash recipe, computer modelling of equilibrium, kinetic and transport mechanisms associated with the interaction of solutions (water and brines) with ash during their disposal, mineralogical changes associated with the intermediate and final products, effects of adsorption and exchange, multi phase saturation characteristics, role of organics for different water brine qualities, knowledge development and transfer). The Institute for Groundwater Studies group at UFS was contracted to provide data on hydrogeology of ash dumps and numerical model of brine hydraulics.

The project was spread into two phases of which phase I was completed in December 2008 and whose findings became the basis for the current study carried out in phase II of the so called Sasol-Eskom

ashbrine project. The overall objectives in phase I and II were to understand the chemistry, microbiology and hydrogeology of ash-water- brine interactions [6]. Establishment of the environmental and physical variables that would have an influence on the capacity of various ash sources to act as salt sink for a variety of brine streams was to be carried out. Boundary conditions between saturated and unsaturated zones of ash were to be defined as part of hydrogeology and subsequently a predictive model was to be developed. Phase I studies concentrated on the fly ash-water interaction studies and characterization of the ash and brines, and geohydrological studies.

The following **section 1.1.1** gives some excerpts from the phase I results' summary by Roux and co-workers [6] and [10, 11]) as important highlights of the results in phase I of the Sasol-Eskom ashbrine project. This is meant to give a better understanding of the background of my work as some of the phase I results were subsequently used in my modeling studies in phase II of the project. The (ANC) batch experimental results were used for coming up with the model ash recipes from Secunda and Tutuka coal utility plants. The column experiment data with demineralised water was used for model calibration while cores data from drilled weathered samples between 15 and 20 years was used for ash heap model validation.

All the modelling work in phase I dealt with fly ash-water interactions only and carried out by Hareeparsad and co-workers. My modeling studies carried out in phase II was to address the fly ash–water and fly ash-brines chemistry interactions as well as the effect of organics in the brines.

1.1.1 Results highlights of Phase I (Excerpts from Sasol-Eskom ashbrine reports [6] and [10, 11])

Within the general scope of the Sasol-Eskom ashbrine project, understanding the development and extent of mineral phases that might lock-up the salts over time in the ash dumps required that the following crucial questions be considered [6]: (a) is the process of mineral formation sustainable to any extent? (b) does demineralization, for example due to rain water, lead to release of the salts to groundwater? (c) what are the chemical processes leading to the mineral formation and what factors control these processes? (d) can the reactions be modelled for predictive purposes?

To address these questions, several experiments were designed which included; chemical characterisation of Secunda and Tutuka fly ash and the hyper saline effluents, leaching tests with demineralised water and buffered solutions (acid neutralisation capacity tests) and long-term equilibrium dissolution of the fly ash (up-flow percolation and batch equilibration at a liquid to solid (L/S) ratio of 10 and 20). These experiments were carried out at various S/L ratios in an attempt to identify the chemical reactions and kinetics of dissolution in the fly ash-water system. The ANC

results data (**Appendix 6**) for the composition of solution was further utilized to identify the role of certain mineral phases by calculating saturation indices (SI) [6].

In order to better understand the mineralogy under the real disposal conditions, cores were drilled at Tutuka ash dump as a function of age. Their mineralogical analysis by depth coupled to extracted interstitial or pore water studies and fractionation by sequential extraction was applied to increase our understanding of mobility of contaminants under disposal conditions. The following are the highlights of the experimental results of phase I.

- **Chemical characterization of fresh ash samples and equilibrium tests**

  Chemical analysis of fresh, fine fly ash samples from Tutuka and Secunda revealed the major elements are Al_2O_3, SiO_2, Fe_2O_3, CaO and MgO and trace elements Cr, Sr, Ba Ce and Zr for both sources of fly ash. Results from DIN-S4 tests reveals that species highly leached include Ca (15-24.23 %), K (0.23-0.45 %), Na (0.58-0.82 %), Mg (0.0047-0.007 %), Ba (0.96-3.33 %), SO_4^{2-} (0.012-1.51 %), Se (2.17-8.75 %), Mo (2.96-13.92 %) and Cr (0.22-2.18 %) per dry weight of fly ash for both Secunda and Tutuka [6].

  XRD revealed the presence of major phases of mullite, quartz and lime. Leaching tests revealed that the major soluble components in solution at equilibrium for both fly ashes were Ca, Na, SO_4^{2-} and K. [6].

  Results of the acid neutralization capacity (ANC) tests results (**Table 1.1** and **Appendix 6)** revealed that the release trends of various toxic elements and contaminants contained in fly ash into solution is highly pH dependent. Both fly ashes exhibited a natural pH > 12 (suspension in ultra-pure water) and the predominant cation even at this high pH is Ca^{2+} (at concentration > 0.002 mmol/L). This indicates that dissolution of CaO and formation of OH- species at pH > 10 contributes to acid neutralisation capacity of both fly ashes and is the greatest contributor to the acid neutralizing capacity of both fly ashes [6].

- **Dissolution kinetic and upflow column tests**

A difference has been observed in release patterns of the species analysed in the leachates for dissolution kinetics over 60 days (closed system) and upflow column tests over 90 days (open system). The pH for both systems remained above 12 for both fly ashes over the period of the study. By measuring the difference in the weight of Secunda and Tutuka fly ashes before and after exposure to leaching tests (up-flow percolation test) it was shown that during the 90 day period of leaching 3.42% of the ash constituents were leached from Secunda fly ash and 4.40% from Tutuka ash.

The results of the upflow column leaching test showed that the initial leachates from the fly ashes contained high concentrations of species such as Ca, Mg, Na, K, S, Sr, Ba, which decreased as the

leaching continued until steady states were reached. Fe, Mn, Se, As, Cu, Pb, Mo and Cr concentrations were also high at the beginning of the leaching test before decreasing over time [6].

In addition the results show that more precipitation/adsorption takes place in a closed system (dissolution kinetics experiments where the L/S ratio was fixed) with sufficient equilibration time and no recharge than in an open system (upflow column tests with changing L/S ratios) where recharge is continuous, flow is progressive and contact time is low, and this is bound to cause a difference in the leachate concentration. This explains the linear relationship of the concentration of some species such as K, Na, Cl, Li with upflow column experiments [6].

- **Mineral phases saturation states**

This study showed the possibility of the formation of small amounts of secondary phases in the ash at the ash dump which could reduce the release of some minor and trace toxic species into the environment. Major ash components such as Ca and SO_4^{2-} were predicted to be controlled by portlandite ($Ca(OH)_2$), anhydrite and gypsum precipitation; Barite ($BaSO_4$) and celestite ($SrSO_4$) were predicted by PHREEQC as the mineral phases controlling release of Ba and Sr in the leachates; Mg was controlled by sepiolite [$Mg_4Si_6O_{15}(OH)_2.6H_2O$]. Preliminary calculations of saturation indices (SI) showed that the leachates were slightly supersaturated with respect to brucite ($Mg(OH)_2$), which could control the release of Mg. Pyrochroite [$Mn(OH)_2$], ferrihydrite ($Fe(OH)_3$), $Ba_3(AsO_4)_2$, $SrSeO_4$, $Cu(OH)_2$, $Pb(OH)_2$, $CaMoO_4$ and $BaCrO_4$ were predicted as the secondary mineral phases controlling the release of Mn, Fe, As, Se, Cu, Pb, Mo and Cr respectively. Saturation indices (SI) also predicted the formation of mineral phases such as cupricferrite ($CuFe_2O_4$), cuprousferrite ($CuFeO_2$), diaspore(AlOOH), goethite (FeOOH), magnetite (Fe_3O_4), manganite (MnOOH), and nsutite (MnO_2) [6].

- **Physical, chemical and mineralogical analysis of weathered ash samples/drilled core samples**

Samples were obtained from the five drilled boreholes on the ash dump irrigated with fresh and brine water at Tutuka power station. Drilled cores were taken across the Tutuka ash dump to sample either freshly placed ash (1 y) or older weathered ash (up to 30 y old cores sample site labelled AMB 79).

The pH profile of the extracted interstitial water as a function of the age of the dumped ash for the Tutuka ash dump revealed that pH of the top ash layers of various cores stabilises at about 8-9 as the fly ash ages. This indicates the chemical weathering of the ash had reached the region where dissolution of aluminosilicates controls the pH of the pore water [12]. Weathering of the cores was observed to follow a similar trend. The pH profile of the various cores indicated that contact with atmosphere and consequent ingress of carbon dioxide and leaching by percolation of rainwater through the dump had a great effect on the weathering of the disposed fly ash. The greatest

weathering was observed to take place at the top layer (0.55-3 m depth) in the older cores (15 years and older), showing that infiltration of rain water has a profound effect on the decrease of the pore water pH. This would probably be due to rapid dissolution and initial rapid flushing out of the fly ash of the soluble species that also act as pH buffering constituents. The implications of these results are that soluble fly ash components are highly mobile. Thus run off or permeates from the dump will be immediately enriched in these soluble contaminants [6].

XRD analysis of surface samples taken from the surface ash dump layers exposed to the atmosphere at Tutuka dump revealed the formation of either gypsum or calcium sulphate hydrate ($CaSO_4$. $0.6H_2O$).

- **Analysis of the extracted pore water**

Table 1.1 gives an extracted version of the data from drilled cores of the AMB 79 site at Tutuka. Analysis of the extracted pore water in each of the different Tutuka cores at a specific depth profile reveals that many elements were mobile and are moving through the ash in a progressive leaching pathway. The elements can be roughly grouped into two classes. Species such as Al, Cr, Si, B, Sr, Mg, Na, K, Ca, Cl^-, SO_4^{2-} and NO_3^- were observed in the pore water of all cores. Species B, Sr, Mg, Al, Na, K, Ca, Ti, Ba, Pb, Cr, Cl^- and SO_4^{2-} show a similar general trend in each of the different Tutuka cores at a specific depth profile, being highly weathered in the top layers of the cores and accumulating at about 6-10 m down the core profile. Concentrations in pore waters at a core depth of about 6-8 m ranged from 200 mg/L for Na; 80 mg/L for Ca down to 30 mg/L for K. The Na, Mg, K, Ca and SO_4^{2-} trends closely resemble each other indicating that these species could be present as soluble sulphate salts. These elements are highly mobile [6]. The elements Ba, Pb, Se, Fe, V, As, Zn, Cu, Ni and Ti were generally present in low concentrations in pore waters and Pb species present in the cores did not weather to any significant extent. Peaks in concentrations observed for Fe, Al, Si, V, Se, Zn, Mg, Pb in the water soluble fraction suggest mineralization at 4-5 m depth. Pore waters from this depth were generally higher in electrical conductivity, and cation exchange capacity data suggests some enhancement of sorption capacity of ash in this region. This suggests that some species solubilised at the top layer through weathering are trapped temporarily in this deeper region of the dump as result of transient mineral phase formation. Very low levels of Mo, Cr, Al, Fe, Na, K were observed in pore waters of the top section namely the weathered layers of the core, whereas these elements were present at higher concentrations between a core depth of 6-10 m. Cr and Mo were present at concentrations above 8000 μ g/L and 1000 μ g/L respectively in pore waters extracted at a core depth of 9 m in the core of ash dumped 20 years ago. A significant decrease in levels of almost all mobile contaminant species was observed in pore waters of the cores sampled at the deepest levels of the ash dump which is in direct contact with lateral flows occurring at the contact point with the

water table level present under the ash dump, indicating the very likely continuous elution of contaminants into ground water after permeation through the ash dump [6].

Table 1.1: Acid consumption of Secunda and Tutuka fresh fly ashes (UWC ANC data) [13]

Acid consumption capacity of Secunda fly ash

Vol. (ml) of 2M HNO_3	Final pH	EC (mS/cm)	TDS (ppt)
-	12.48	9.16	4.80
7.4	11.29	10.33	5.37
9.1	10.68	11.78	6.11
12.7	9.58	15.41	7.99
14.0	8.78	16.69	8.66
15.5	7.25	18.14	9.43
16.80	5.83	19.46	>10.00
17.50	4.77	>20.00	>10.00

Acid consumption capacity of Tutuka fly ash

Vol. (ml) of 2M HNO_3	Final pH	EC (mS/cm)	TDS (ppt)
-	12.34	6.39	3.32
3.2	11.83	6.51	3.39
5.4	10.73	7.87	4.09
6.8	9.59	9.37	4.86
9.2	8.12	12.21	6.34
9.8	7.30	12.94	6.72
10.0	6.31	13.11	6.81
10.5	5.46	13.16	7.63
11.5	4.36	14.74	7.65

Table 1.2: Extracts of UWC-analytical data of drilled cores samples from sample site AMB 79 [13]

Depth	(m)	1	3	5	7	9	10	12	14	15	
pH	pH	8.6	10.75	10.8	11.1	10.9	11.1	9.5	8.5	8.3	
EC	mS/cm	0.3	0.5	1.15	1.15	1.5	1.3	1.2	0.9	0.9	RAM
Sr	mg/L	2.2	3	1.9	1.2	3.2	5	0.9	0.5	0.5	87.6
Na	mg/L	20	22	198	201	240	205	190	140	142	23
Mg	mg/L	16	25	1.5	0.5	0.5	4.2	6	4.2	6.2	24.3
Ca	mg/L	30	45	30	25	55	85	40	35	45	40.1
K	mg/L	4	3.5	26	25.8	32	20	7.6	5	5.3	39.1
S(6)	mg/L	170	288	360	420	828	840	490	360	270	32.1
Cl	mg/L	0	0	10	10	65	180	285	300	330	35.5
Mo	µg/L	50	58	200	250	1200	925	600	468	480	95.9
Fe	µg/L	20	20	30	90	10	10	20	60	280	55.8
Cr	µg/L	0.5	0.55	0.5	2.5	8.5	3.5	2	1.5	2	52
Ti	µg/L	75	112.5	75	65	115	197.5	92	70	100	47.9
Al	mg/L	0.2	0.22	4.8	3.6	3.6	1.8	0.1	0.15	0.2	27
Si	mg/L	6.5	6	6.2	9.6	5.7	7.2	6	5.5	5.3	28.1
CEC	meq/100g	160	160	350	155	185	210	x	x	x	
	fresh ash, CEC = 100 meq/100g							x = no results available			
	water level at 10 m and EC=3.35 mS/cm										
	pH of fresh ash = 12.7										
	ash/soil interface at 11.9 m										

- **Moisture content determination**

There was generally a gradual increase in the moisture content of the ash dumps as a function of sample depth, particularly in older areas of the ash dump. However, the very variable moisture content observed for some of the cores could be attributed to uneven or haphazard placement methods resulting in greater or less packing density and void volume differences of the dump or could be due to ambient weather conditions during placement. A significant increase in moisture content was observed for the core samples in direct contact with the water table present under the ash dump. Another observation was that the older ash cores had a lower moisture content at the top than at the bottom which is consistent with the hydraulics of the ash dump [6].

- **X-ray fluorescence (XRF) Analysis of drilled cores**

The weathering and mobility patterns of species in the solid fraction sampled from different Tutuka cores seem to follow a similar pattern to the trends shown in the pore waters. Trace elements Pb, V, Zn, Cr, Ni and Co are enriched in solids for the entire depth of the core compared to fresh ash. This could be due to flushing of the soluble salts leading to positive enrichment of relatively insoluble components in the weathered ash. These trace toxic elements are normally associated with the sparingly soluble aluminosilicate (such as mullite ($Al_6Si_2O_{13}$) and kaolinite $Al_2Si_2O_5(OH)_4$) matrix of fly ash. The leaching studies have shown that their relatively insoluble nature is pH dependant. These elements also constitute the group that are enriched in fly ash, especially from bituminous coal. Ca, K, Mg, Ba, Sr, P, Zr are depleted especially at the top layer (1-7 m). Depletion of Fe is observed which could be an indication of the existence of some Fe as a soluble phase [6].

- **X-ray Diffraction (XRD) analysis of drilled Cores**

XRD mineralogical compositions of the solid ash samples extracted at different depths of these cores are generally similar. The major mineral components in all cases are quartz, calcite and mullite regardless of sampling depth. The quartz peaks of the core samples (fly ashes) are quite prominent and have a tendency to obscure other less crystalline mineral phases and this would be the major limitation of XRD analysis [6].

- **Hydrogeological perspective**
  - **Geophysics**

Groundwater, through the various dissolved salts it contains, is electrically conductive and enables electric currents to flow into the ground. To identify the presence of groundwater from resistivity measurements, one can look to the absolute value of the ground resistivity, but most of the time it is the relative value of the ground resistivity which is considered for detecting groundwater. Measurement of the resistivity of the ash dumps was carried out by transmitting a controlled current (I) between two electrodes pushed into the ground, while measuring the potential (V) between two other electrodes. Direct current (DC) or a very low frequency alternating current was used, and the method is often called DC-resistivity. The resistance (R) is calculated using Ohm's law. The resistivity mapping was used to site the core drilling in old highly weathered areas as well as recently placed areas and revealed the relative degree of saturation between wet and dry ash handling systems [6].

The distribution and the potential pathways of the salts could be mapped according to the geophysics lines over the ash dump. The geophysics on both wet and dry ashing systems showed large quantities of salts that are captured in some areas of the ash dams/dumps. The geophysics also showed the areas where these salts leach into the subsurface. The laboratory salt leach tests on sections of cores confirmed that a large volume of the salts in the cores are still mobile [6].

- **Drilling**

A combination of Air Flush Coring and direct circulation air percussion drilling were used to drill the boreholes at Tutuka. Air Flush Coring uses a conventional drilling rig and compressor with a specialized drill bit that cores the ash without the need for water or lubrication for cooling of the drill bit. The advantage of this air drilling technique is that the coring method does not use water to cool down the drill bits as in normal rock coring. The samples therefore remained chemically unchanged and physically intact. The borehole depths varied from 10 to 30 m, depending on the depth of the ash. No drilling took place at Secunda. The geophysical data and ash core drilling provided the basis for a detailed descriptive assessment of the ash dumps [6].

- **Hydraulic Tests**

The Darcy equation relates the hydraulic gradient (i) and flow area (A) to the discharge (Q) through the use of the hydraulic conductivity (K). The Darcy tests on the Tutuka cores suggested that water flow through the ash has high initial hydraulic conductivity with a reduction in hydraulic conductivity over time hinting to clay like swelling and reduction in flow. High concentrations of salt were also mobilised from the initial flush of water through the cores. Both the hydraulic conductivity and salt concentration decreased over time to reach a steady state. The hydraulic conductivity values obtained on the ash dump using tension infiltrometers and double-ring infiltrometers suggests that the texture of the ash plays a role in the hydraulic properties. The field scale work was completed for both sites using different hydraulic infiltration methods and both sites showed similar hydraulic conductivities. Fine textured ash and hard pan ash had K-values in the order of 10^{-2} m/day. Undisturbed ash had a K-value of about 10^{-1} m/day. Very coarse consolidated ash, reworked ash and fresh ash have the highest K-values at a magnitude higher (between 1 and 10 m/day) compared to finer texture ash cores.

Measurement of electrical conductivity (Total Dissolved Solids) leaching from the cores during the Darcy tests shows that between 1 and 3 kg of salt could leach from 0.007 m^3 of ash in a 24 h period. The hydraulic and salt leach tests show initial high rates of flow through and salt leaching from the ash cores and a reduction to a steady state thereafter. The leaching of the salts did not approach zero during the test periods [6].

Salt capturing under steady state conditions of older leached ash might be more efficient. Some of the sections from ash cores had no transmissivity under constant head lab conditions and could not be tested. The salt leaching from these cores was limited. The processes under which the salts were captured resulting in the low transmissivity unleachable conditions are unclear at this stage. Some data therefore indicate that the total salt content of an ash dump may not leach, but it cannot yet be confirmed how to achieve these conditions over larger areas of the dump to ensure a sustainable salt sink. More work is required to identify the mechanisms under which these unleachable core sections were formed. Studies of mini ash dumps under controlled conditions could shed some light on this aspect [6].

The presence of cementitious reactions were not well resolved by the characterization performed but based on observation, cementation based on pozzolanic activity of the ash was present in some areas of most of the cores, highlighting the relative inhomogeneity resulting from the dry ashing system at Tutuka [6].

- **Porosity**

Effective Porosity is defined as the portion of the soil through which chemicals move, or the portion of the media, which contribute to flow. Effective porosity (n_e) can be expressed as the specific discharge (q) or Darcy velocity divided by the average velocity of a tracer (v). The effective porosity is less than the total porosity since not all of the water-filled pores are interconnected and therefore not all pores contribute to flow. Three methods were used to estimate porosity values for the ash. A tracer test was conducted on the ash cores, yielding a value of 0.35. Total porosity values were calculated from dry and wet moisture content, yielding values between 0.4 and 0.6. Porosity values calculated from the geophysical data compare well with laboratory and tracer test estimates, yielding values between 0.13 and 0.5. When ash dries out it may crack and could result in preferred pathways through the dump. Coring revealed crack formation in some zones of the ash dumps. The fractures may create a preferential pathway and transmit flows of rain water past the salts captured in the matrix of the ash, instead of allowing it to percolate through. Comparison with ash dam studies where saturated conditions are constantly experienced might shed more light on this aspect [6].

- **Water Level Behaviour**

Borehole monitoring for the ash dump was implemented to establish the water levels on a daily basis. The motive for measuring the water levels was to establish rainfall impact on the water level in the ash dump in the short term. Water level monitoring data showed that no drastic water level changes are taking place in the Tutuka rehabilitated areas. The water level is about 2 m above the original land surface resulting in the bottom 2 m of ash being permanently saturated with groundwater/ brine mixture. This has implications in terms of the continuous leaching of ash constituents into ground water as was highlighted by the pore water and resistivity mapping studies [6].

The procedures developed during Phase I of the project were further developed and extended during Phase II. All the above results of phase I were put into consideration in coming up with the conceptual models used in phase II. The aim of the project was to model and predict the release (leaching) of the chemical elements which may directly impact on the environment created by co-disposal of ash and brines. Leach column tests needed to be undertaken in order to provide the linkage between changes in the ash chemistry and the transport properties of the ash.

Long term leaching studies from fly ash –water and brines systems was to be achieved by modeling the effect of a flux of waters and contaminants (brines) into the aquifer from an assumed ash heap in order to determine a no-effect condition for any abstraction or outflow from the aquifer. The study also covered the effect of the organic components in the brines on the solubilisation of ash and the speciation of the elements of concern. Depending on the outcome, these results were then to be fed into the ash heap modeling exercises. The chemical models of ash brine transformations and transport needed to be refined and improved so that predictions can be made. The results of the modeling are to be grounded in data from cores from existing ash heaps. These predictions should then be used to develop scenarios for the management of ash heaps.

At the end of phase II, it was expected that the collaboration in the research among the concerned institutions (Sasol/ Eskom/ Universities) would be able to provide predictive modeling of long term ash disposal systems and explain the geochemical transformations under different disposal scenarios. The knowledge gained from this study would be used to assess the potential risks associated with ash disposal and its effect on ground and surface water, and also assess the effect of brines on the possible enhancement of the ash utilization. These results will further be used to guide future sustainable management practices and enhancement of more reuse of the fly ashes.

1.2 Scope of the study and research questions

The Pollution Research Group at the University of KwaZulu-Natal (UKZN) was contracted through the Eskom-Sasol joint research initiative to address the modeling aspect of the fly ash-brines interactions and the chemistry associated therein. This formed part of this PhD work, thereby demonstrating the power of collaboration between research institutions, universities and industries towards addressing environmental challenges. Apart from the need to meeting the waste regulatory requirements, the industries have refocused their attention to the development of more economically sustainable waste management methods with the possibility of enhanced reuse of the fly ash solid wastes. The focus areas of our study were (i) hydrogeochemical modeling of the chemical speciation of brines, (ii) the leaching chemistry of the fly ash under different disposal conditions with brines, (iii) modeling of equilibrium aqueous chemistry of ash-brines-organics interactions, (iv) modeling of kinetic and transport mechanisms associated with interactions of water and brines with fly ash during their disposal, and (v) mineralogical transformations associated with intermediate and final products. In so doing, a hydrogeochemical model which would be capable of predicting the speciation and release of multielement species from brines-fly ash disposal systems, would be developed and used to model an ash heap. In this study the use of hydrogeochemical modeling software (PHREEQC) [14] was demonstrated. During the study, knowledge development and transfer amongst the collaborating parties was to be enhanced through the medium of confidential reports, seminars and one-on-one training sessions.

The following research questions were used as a guide towards addressing the scope of the work.

1. How do the interactions of South African fly ash and brine affect the leachability of major and trace elements from the fly ash-brine systems?

2. What are the geochemical factors that may influence the release of major and minor species from the fly ash-brine systems?

3. What are the mineral phases likely to form as a result of fly ash-brine interactions?

4. Do the secondary mineral phases formed disintegrate over time to release contaminants on continuous interactions with aqueous solutions?

5. Can modeling aid in providing substantial solutions towards best practices of operational management of existing and new ash disposal facilities to safeguard the environment?

6. Can modeling support experimental leaching studies in a column of ash?

7. Can the long term effluent (leachate) quality from ash heap /ash column be predicted?

In this study, the application of PHREEQC hydrogeochemical code for modeling and simulation of equilibrium, kinetic and transport mechanisms associated with the interaction of water, organics and brines with fly ash during their co-disposal is demonstrated. It specifically addresses the speciation and leaching chemistry, quantification and characterization of the products formed when ash is in contact with brines. Special reference is made to two separate modeled mineralogical ash recipes from two of the South African power utility (Sasol and Eskom) plants' fly ash systems. This study is the first of its kind to be carried out jointly by the two leading coal utility plants in South Africa in which hydrogeochemical modeling code PHREEQC was employed as an important tool in enhancing better understanding of ash-brines interactions. From the work so far accomplished, modeling results were used to support experimental data and further reaffirmed the important role hydrogeochemical modeling play in solid waste management as it augments or complements the work of analytical/environmental scientists as well as guiding the future solid waste management and engineering decisions.

Evidence of chemical reactions occurring between fly ash and the salt species in the brines as well as that organics do participate in products/compounds formation, has been reported [10, 15-17]. However, the chemical and physical interaction of highly saline effluents and atmospheric O_2 and CO_2 with fly ash is not fully understood. Understanding the chemical processes responsible for development of stable mineral phases that would lock-up the salts over time in the ash dumps will be crucial in assessing the benefit, and predicting the impact of this practice on the environment.

Fly ash is known to undergo dissolution on contact with aqueous solutions [18-22], and which increases the pH of brine. Moreover, species released react with the brine components leading to cleaner effluents [23].

It is expected that the possibility of the formation of small amounts of secondary phases in the ash at the ash dump could reduce the release of some minor and trace toxic species into the environment. The modeling of the above scenarios will be used to build-up knowledge towards the prediction of leaching of chemical elements which may directly impact on the environment, particularly with regard to impacts on groundwater. These predictions may then be used to develop scenarios and offer potential guidance for future sustainable waste management practices as a way of addressing the co-disposal of brines within inland ash dams and heaps.

1.3 Hypothesis

Hydrogeochemical modeling of fly ash-brines interactions will provide better understanding of the speciation, release and transport of multi elements, and it is sufficient enough to support experimental data and engineering decisions towards sustainable fly ash-brines waste management.

1.4 Aim and objectives

1.4.1 Aim

The aim of the study was to adapt a suitable modeling software to model and understand the science associated with the chemical and hydraulic interaction of brine solutions and organics with ash dams and heaps during their co-disposal.

1.4.2 Specific objectives

The specific objectives were:

i. To learn and gain competency in PHREEQC modeling

ii. Acid Neutralization Capacity (ANC) modeling

To model the effect of the brines and organics on Acid Neutralization Capacity (ANC) of fly ash under the following batch-based scenarios in order to understand:

- PHREEQC modeling of ANC tests + Demineralised water (DMW) on ash recipes,
- PHREEQC model ANC + brine on ash recipes
- PHREEQC model ANC + organics on ash recipes
- PHREEQC model ANC + brine + organics on ash recipes

iii. Column modeling

- To study PHREEQC code on reactive-transport modeling in columns
- To model Secunda and Tutuka ash column with DMW using PHREEQC
- To model Secunda and Tutuka ash column with brines using PHREEQC
- To investigate the influence of brines on column simulations

- To study the dynamic leaching effects of ash-brine interaction on mineralogy of ash
- To study PHREEQC column model effect of chemical reactions and porosity
- To validate the model simulations by extrapolating with experimental column data

iv. To model Tutuka ash heap irrigated with rain water (atmospheric CO_2 included) and with brines in order to predict the long term quality of the leachate released from ash heap under different disposal scenarios:

1.5 Modeling approach / methodology

As a strategy towards achieving the above objectives the modeling scheme Figure 1.1 was adopted in the study.

Chemical and transport models were based on laboratory-scale experiments conducted by UWC, one of the Sasol-Eskom ash-brine project collaborating institutions. Equilibrium ANC tests based on the Pr EN 14429 European standard (Influence of pH on leaching with initial acid/base addition) [24] were employed for the batch tests of fly ash with water and brines. This provided the chemical model with the relevant mineralogical phases and reactions in fly ash- water and fly ash-brines interactions. Up-flow column tests were done as part of the dynamic leach tests. The dynamic tests provided information on transport mechanisms of the elements in the leachate from the coal ash water and brines long term interactions. The fitting of the model and experimental results was used for validating the laboratory-scale chemical and transport models. If proper fitting was not achieved, then some of the respective model parameter inputs were re-adjusted until good agreement between the model and experimental data was obtained. The calibration input parameters were further used in the modelling of the ANC of fly ash with brines.

The initial scope of this study was to cover both the laboratory and field-scale chemical and transport modeling as indicated in Figure 1.1. Further validation of the model was to be carried out using lysimeters and core-samples data drilled from selected ash dump sites in the respective Secunda and Tutuka fly ashes, at a field-scale level. Validation of the ash heap- brine model and quality of the leachate after 20 years was based on the cores analytical data supplied by UWC. The scope of chemical and transport modeling was reviewed and restricted to laboratory-scale only as the commissioning of lysimeters by Sasol was delayed and could not be done within the time frame of the study. Lysimeter data could form part of future work that may be carried out to validate the model further.

PHREEQC code, (version 2.15.0) [14] was used as the hydrogeochemical modeling tool with its modified LLNL database for inorganics and MINTEQ.V4.DAT for the organics.

In the PHREEQC simulation, the fly ash was modelled as a collection of pure mineral phases which come to equilibrium with the liquid phase.

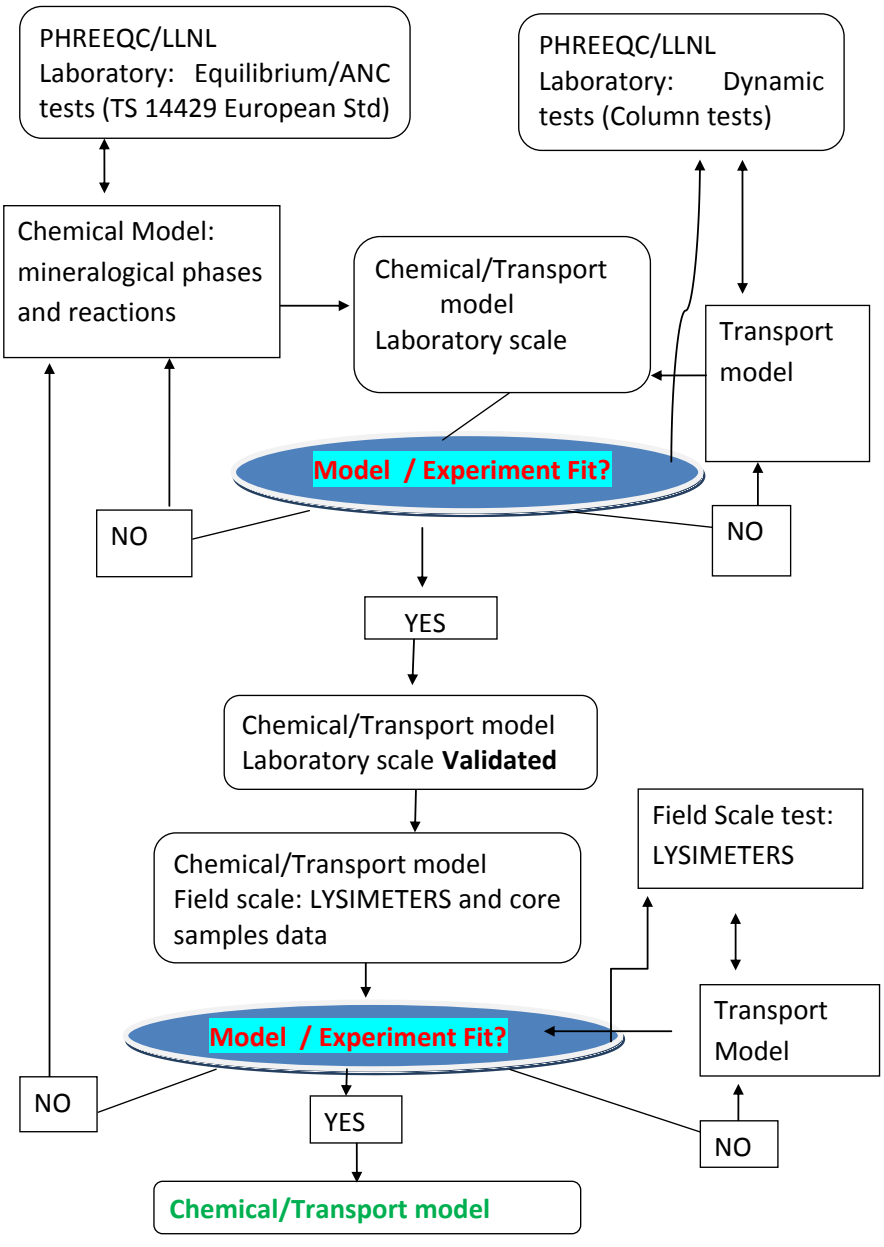

Figure 1.1: Scheme of the approach adopted for previous studies [25] and modified for current PHREEQC model development

1.5.1 Modeled fly ash recipes, brines and organics

Modeling of the fly ash recipes was based on the characterization studies and modeling carried out in phase I (2007) of the collaborative Sasol-Eskom research initiative with UWC and UKZN. Two modeling ash recipes of Secunda and Tutuka were derived from experimental work carried out by Ojo [15] and modeling work of Hareeparsad and co-workers [26], during phase I of the project. This involved elemental analysis of the leachates from the ANC tests, (using inductively coupled plasma-mass spectrometry (ICP-MS) at pH of 2 (by acidification with 65% HNO_3) for cations and by ion-chromatography (IC) for anions. For XRD analysis, fly ash samples were analysed before and after leaching in order to determine the major mineralogical composition and transformations [13]. They exhibited similar mineral phases composition but only differed quantatively. Hareeparsad and co-workers [26] improved further the mineralogical characterization in the previous study by Ojo [15] using computer controlled scanning electron microscopy (CCSEM) technique which characterized further mineral phases that would otherwise not be observed with other techniques. Tiruta-Barna and co-workers [27] have described the steps involved in obtaining the hypothetical modeling ash recipe, which were used for the development of our mineralogical ash recipe in this study. These steps take into account the rapid dissolution of some solid phases, test results and mechanisms for ash-demineralised water column tests; as well as susceptibility to precipitation as hydroxides in the experimental conditions (the most soluble hydroxide being chosen from the database following the Ostwald priority rule) [28].

In the case of modeling involving brines, the levels of the major elements in brines generated from Secunda and Tutuka power plants were characterised by Gitari and co-workers, and Ojo and others [11, 13, 15, 29] and which were used in the geochemical model calibration. Artificial sewage waste was used as the modeling recipe for the organics in brines. This is because any sewage waste recipe contains important organic ligands that are commonly found in the environmental waste, such as acetate, glycinate, tartrate, glutamate, salicylate and phthalate, as prescribed by Wadley and Buckley [30].

1.5.2 Conceptual model development

Conceptualization of a geochemical model is the first critical step in developing a model; it includes defining the approach to the geochemical problem at hand, initial solution, mass transfer, and nature of equilibrium that occurs over the course of the reaction processes [31]. Specific conceptual models were developed for each of the modeled scenarios to reflect the specific conditions and are detailed in the respective subsequent chapters.

1.5.3 Modeling PHREEQC input data: the initial conditions

The simulations are executed by using an input file in which the problem is specified via KEYWORDS and associated data-blocks [14]. These KEYWORDS are described in the subsequent **Chapter 2**. The input file specifies the initial conditions in terms of solution composition, temperature, pH, pe, density of solution, reactants and their quantities (in moles), equilibrium phases present, transport parameters and the selected output required. These input file parameters are described in details for each of the modeled scenarios in the respective subsequent chapters.

For dynamic leach test, modeling reactive transport involved describing mass balances of species and reactions among species. The column experimental parameters were adopted from the work of Ojo [19] and Hareeparsad and co-workers [26]. Other column parameters and hydraulic property calculations were performed in programmed spreadsheets by MS EXCEL and formed part of the input column and hydraulic parameters in PHREEQC code. Flux-type boundary conditions (also known as third type or Cauchy boundary condition) were employed. Closed-system conditions were applied which prevented, or at least minimised, CO_2 and other atmospheric gases uptake. The dynamic leaching test was made at constant temperature (20°C).

For ash heap modeling, Tutuka ash heap was considered under different disposal conditions. The model definitions included geometry and boundary conditions, initial conditions, and selection of chemical reactions. These conditions are explained in **Chapter 5** of this thesis. The flow rates, the volumes of the leachates and the specific solid/liquid (S/L ratio) were imposed at the laboratory scale. Conceptual models were developed and mechanisms involved were used as the input parameters for the PHREEQC program using a modified LLNL database.

1.5.4 Data output and interpretation

The simulation data output formed the modeling results discussed in each subsequent chapters. The data were presented in the form of MS EXCEL spreadsheets generated from the unique feature of PHREEQC capability and linkage data sourcing tool with MS EXCEL. The total elemental concentration (TOT), species concentration (m_species), change in phase assemblage data (delta d_phase) and saturation indices (SI) for the formed phases at each pH were some of the parameters generated by PHREEQC simulation. From the spreadsheet data output, Log C-pH diagrams of elemental concentration (TOT) and that of various species with concentration greater than or equal to 10^{-6} M were drawn as well as graphs relating to ANC and mineralogical phases transformation and quantification. In the case of mineral phase quantification, phase assemblage data was expressed in either of the following parameters against pH; delta (d_phase), absolute change of delta (d^1), and relative change of delta (Rc_d^1). These parameters are explained in **Chapter 3** in order to understand their significance in the study.

The main achievement of the study project is that the developed model was validated by comparison with experimental batch and column data. It was therefore expected that the model should predict the leaching of chemical elements which may directly impact on the environment, particularly with regard to impacts on ground water. These predictions may then be used to develop scenarios and offer potential guide for future sustainable waste management practices as a way of addressing the co-disposal of brines within inland ash dams and heaps.

1.6 Thesis presentation review

Chapter 1

This chapter highlights the introduction which gives an insight on the background of the study as well as the scope, study hypothesis and objectives. It also presents an outline of the entire thesis organization.

Chapter 2

Chapter 2 captures some important literature review on the areas of our study, mainly the fly ash chemistry and mineralogy, the brines, and the challenges for the coal utility plants in their co-disposal. It also highlights hydrogeochemical modeling and its role as an important tool for environmental scientists and industry. The literature review also identifies the knowledge gaps in the understanding of the leaching, speciation and transport of elements from the fly ash–brines interactions and for which the application of hydrogeochemical modeling code PHREEQC will be demonstrated in this study.

Chapter 3

This chapter is a discreet manuscript that gives the results for the static/batch leaching modeling of the effects of organics and brines on the metal leaching and acid neutralization capacity (ANC) as well as the mineralogical transformations of the Secunda fly ash only. The manuscript discusses the modeling results of the Secunda fly ash as the ash recipe was similar to that of Tutuka and therefore would give similar results. However, it should be noted that the Tutuka fly ash is studied in the subsequent chapters. The simulation results obtained are presented, discussed and conclusions drawn. Part of this work was presented in the conference proceedings of the 2nd Tanzania Chemical Society International Conference held in Dar es Salaam, Tanzania, from 5th - 7th October 2011.

Chapter 4

This chapter is also presented as a discreet manuscript on the modeling results for the dynamic column modeling of Secunda and Tutuka fly ashes with brines over a period of time (90 days). It captures the leaching and mobility of the elements in an upflow column generated from reactive-transport modeling using the PHREEQC code. The results of the simulations are discussed and conclusions drawn.

Chapter 5

This chapter presents the application of PHREEQC reaction-transport modeling in an ash heap of Tutuka fly ashes under different disposal scenarios (water and brines). The study was limited to Tutuka ash only because the method of ash heap disposal applies to Tutuka while Secunda disposes its fly ash in ash dams. The chapter gives an insight to the long term time-dependent leaching and mobility of the multispecies elements during co-disposal of fly ash and brines. The ability of the model to predict long term leaching and mobility of elements and ultimately the quality of leachate is illustrated.

Chapter 6

This chapter gives the conclusions drawn on from the study based on the research findings and data obtained. It gives a recapitulation of what the project entails and summarizes the results of the project. It highlights the outcomes, challenges encountered and also outlines future scientific work desired or being sought.

Appendices

Hydrogeochemical modeling simulations with PHREEQC generate enormous amount of data, all of which may not be presented in the manuscripts because of its bulkiness and details. This section therefore presents supplementary data and information relevant to the study and specific to each of the chapters discussed, which may not have been captured in the main thesis.

CHAPTER 2: LITERATURE REVIEW

2.0 Fly ash, Co-disposal with Brines and Modeling Techniques

This section gives insights on fly ash generation from coal utility plants, its morphology and mineralogy, chemical composition, classification, disposal and utilization. The fly ash co-disposal with brines, leaching chemistry and modelling techniques of fly ash-brines systems are highlighted.

2.1 Fly ash

Recent years have seen an increase in the demand for coal-based electricity production as a result of growing population and economic development [32] as well as rapid industrialization. Coal, by far, is the world's most abundant recoverable hydrocarbon resource. The world's proven coal reserves are estimated to be 985-billion tons, with the largest known reserves being in the United States, Russia, China, India, Australia, Germany and South Africa [33]. Coal processing facilities worldwide have been known to produce large quantities of coal combustion residues (CCRs) such as fly ash and some brine effluents [34, 35] which pose a big environmental and economic challenge to industries. Other CCRs include boiler slag, and bottom ash from different types of boilers as well as desulphurisation products like spray dry absorption product and flue gas desulfurization (FGD) gypsum. In South Africa, Sasol and Eskom use coal feed for their respective processes. Eskom uses coal for generation of electricity while Sasol uses coal for the production of synthesis gas (using Fischer-Tropsch process - a chemical process used to convert synthetic gas (syngas) from coal, natural gas, biomass into valuable, high quality liquid fuels) [33]. Fly ash is one of the coal combustion by-products (besides CO_2 and brines) which is generated from South African coal processing facilities of Eskom and Sasol. Coal firing power thermal stations are still the main source of power generation in South Africa and these stations are situated in close vicinity of the coalfields, all in the North of the Country (Gauteng, Mpumalanga, Limpopo and Free State). Sasol, which is one of the Africa's major producers of chemicals and liquid fuels, while Eskom, a major power producer in South Africa are some of the biggest consumers of coal in South Africa with Sasol utilizing about 28 million tons of coal for its gasification process at Sasol synfuels in Secunda and 6 million tons at Sasol Infrachem in Sasolburg annually. These facilities are all located in the interior countryside in water sensitive catchment areas, where the re-use and recycling of water are mandatory. One of the facilities is situated on the site of Eskom's Tutuka Power Station located 25 km, north-east of the town of Standerton, and the second, at Sasol, the synthetic fuel production plant at Secunda. Both towns are situated in the Mpumalanga Province of the Republic of South Africa.

Eskom is a state-owned enterprise that generates approximately 95 percent of the electricity used in South Africa and approximately 47 percent of the electricity generated in Africa [5, 36]. The Eskom's core business is to generate, transmit and distribute electricity to industrial, mining, commercial, agricultural and residential customers and redistributors. The rising demand of electricity in South Africa and Africa in general has necessitated the building of additional power stations which will result in increased fly ash generation.

Sasol on the other hand, in its Secunda facilities, utilises a low rank bituminous coal for gasification and combustion to produce synthesis gas and steam respectively. The amount of coal used during the gasification process amounts to approximately 28 million tons/y, (70 % of the coarse coal feedstock) which produces 7 million tons of gasification ash [37]. A finer coal fraction, which accounts for the remaining 30 %, is combusted to produce steam for electric power generation, with fly ash produced as a by-product. South Africa currently produces more than 25 million tons of ash per annum [38].

2.1.1 Fly ash generation

Combustion of coal produces large volumes of coal combustion residues (CCRs) like fly ash and bottom ash [39]. As the coal is burnt at temperature zones of about 1400 $^{\circ}$C – 1600 $^{\circ}$C, complex chemical transformations takes place. Flow diagram of coal combustion and related processes leading to the formation of the various coal combustion products is given by Figure 2.1. All the mineral matter is condensed, charred and transformed to ash. The minerals associated with it become molten and form a spherical shape. They experience rapid cooling as they pass out of furnace and solidify as amorphous, glassy materials of spherical shape [40, 41]. About 20 % of this material falls down due to gravity and is removed as bottom ash and the remaining part is fly ash. The fly ash is then collected by mechanical or electrostatic precipitators. The varied quality of coal makes the task of proper analysis or utilization of these coal combustion residues more difficult. Approximately 80 % of the solid residue released from the combustion of coal is released as fly ash, while the rest consist of larger particles that are retained within the furnace as bottom ash [35]. Fly ash is the dust-like material that results from the combustion of either hard (bituminous) coal or brown coal (lignite) in a wide variety of combustion processes, e.g. dry bottom power plant furnaces and fluidized bed boilers, and which is recovered from the flue gas by electrostatic or mechanical precipitation [42]. Since the particles solidify while suspended in the exhaust gases, fly ash particles are generally very fine (silt size, 0.074 - 0.005 mm) and spherical in shape [43-45]. Sasol and Eskom plants were reported to have generated 7 million tons of gasification ash and 1.5 million tons of ash respectively in 2005 [37]. This

production has since increased so that by 2010, Eskom produced over 36.1 million tons/y of coal combustion fly ash [46].

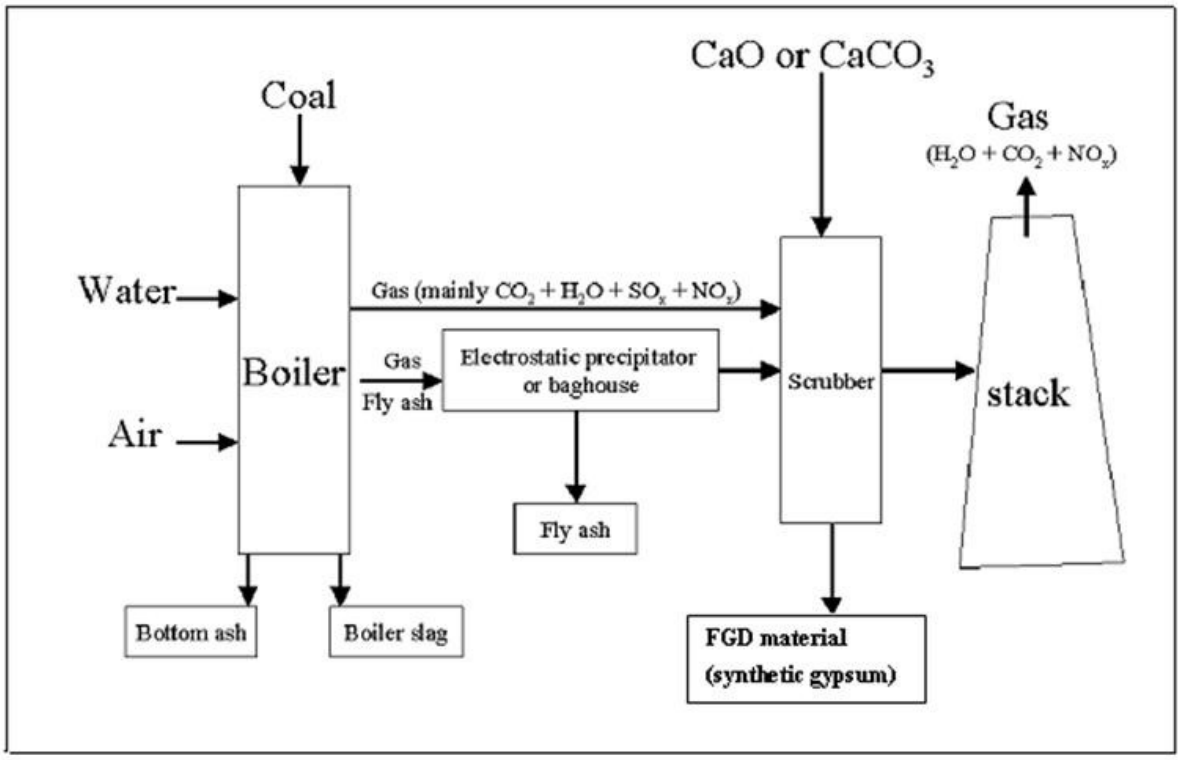

Figure 2.1: Flow diagram of typical coal combustion and related processes leading to the formation of the various coal combustion products [12].

2.1.2 Morphology and mineralogy

A number of authors have reported various but similar morphologies of fresh fly ash [40, 47]. They made conclusions to the effect that the spherical shape is an indication that the particles were formed under un-crowded freefall conditions and a relatively sudden cooling, which helps to maintain the spherical shape while the agglomerated nature of some particles is an indication that the particles were produced due to high temperature sintering reactions. Morphological study of fly ashes is of importance as morphology has a bearing on the leachability of heavy metals as reported by Ramesh and Kozinski [48], in which the presence of the non-porous continuous outer surface and a dense particle interior may prevent heavy metal leachability from the fly ash. Most fly ashes are rich in SiO_2, Al_2O_3, and Fe_2O_3, and contain also significant amounts of CaO, MgO, MnO, TiO_2, Na_2O, K_2O, SO_3, etc [41, 49].

Mineralogical characterization of two South African fresh fly ashes (Secunda and Tutuka ashes) indicated the presence of mullite, quartz, hematite, magnetite as well as lime as the major phases [26, 50]. Both fly ashes showed some similarities, with quartz, glass and mullite being the most commonly identified mineral phases. Previous studies of fly ashes from South African Power stations have shown mineral phases most commonly to be detected were quartz, mullite, hematite, magnetite, maghemite, anhydrite, portlandite, lime, periclase and titanium oxides [29, 37].

2.1.3 Chemical and elemental composition

Coal ash chemistry is usually determined by the type of coal from where it is generated [7, 15, 42, 51-54]. Coal fly ash is a fine-grained material which is mostly made up of spherical, glassy particles. Elemental analysis shows that the main components are silicon, aluminium and calcium. Coal fly ash is very poorly soluble in water. Heavy metals, tightly bonded to ash particles, typically make up less than 1 % of the total mass. Due to its composition and genesis, coal fly ash exhibits pozzolanic properties; it reacts with dissolved calcium hydroxide and water at normal temperature to form strength-developing minerals in a similar manner to cement [55].

From elemental analysis, fly ash is observed to be enriched in silica, alumina and ferric oxides. The fly ash is also enriched in traces of Zn, Pb, Rb, Zr, Sr, Sc, S, Th, Cu, Ni, Mn, Cr, V, Rb, U, Y and Ba [47]. Presence of these trace elements in fly ash makes it an environmental hazard as the traces can leach into the ground water.

2.1.4 Fly ash classification

The American Society for Testing and Materials (ASTM) categorizes coal combustion fly ash into class C and F [49], based on the sum oxides content of Si, Al and Fe(III), i.e $SiO_2 + Al_2O_3 + Fe_2O_3$ in the ash. When the sum is between 50 % and 70 % the ash is classified as class C while when over 70 % it is classified as class F. The Class F fly ashes are normally generated due to combustion of anthracite or bituminous coal which gives a sum oxide content greater than 70 % in the ash. The class C fly ashes are produced due to burning of lignite or sub-bituminous coal [49]. Most fly ashes are rich in SiO_2, Al_2O_3, and Fe_2O_3, and contain also significant amounts of CaO, MgO, MnO, TiO_2, Na_2O, K_2O, SO_3, etc. ASTM class C fly ashes (high-lime fly ashes) typically contain CaO in excess of 10 % up to 40 %, and class F fly ashes (low-lime fly ashes) generally contain less than 10 % CaO. Due to high CaO content, class C fly ashes participate in both cementitious and pozzolanic reactions whereas class F fly ashes predominately participate in pozzolanic reaction during the hydration process. Therefore, class C fly ashes are classified as cementitious and pozzolanic admixtures/additives and class F fly ashes as normal pozzolans for use in concrete [22, 41, 42, 49, 56].

2.1.5 Fly ash utilization

The varied quality of coal makes the task of proper analysis or utilization of these coal combustion residues more difficult. Depending on the type of coal and the type of boiler siliceous, silico-calcareous or calcareous fly ashes with pozzolanic and/or latent hydraulic properties are produced throughout Europe. The utilisation of fly ash across European countries is different and is mainly based on national experience and tradition [32]. The utilisation of coal combustion products (CCPs) is well established in some countries of the world, based on long term experience and technical as well as environmental benefits [57]**.** The CCPs are mainly utilised in the building material industry, in civil engineering, in road construction, for construction work in underground coal mining as well as for re-cultivation and restoration purposes in open cast mines. The majority of the CCPs are produced to meet certain requirements of standards or other specifications with respect to utilisation in certain areas. Due to different boundary conditions regarding climate, taxes and legislation the utilisation rate of CCPs is different across European countries and worldwide [57].

Within the South Africa context, it currently produces more than 30 million tons of ash per annum, of which nearly 1.2 million tons are utilized for different purposes [38]. Some of these include use as back mine fill, as soil stabilizer in geotechnical application. Other fly ash uses include land fill as well as an extender and pozzolan for cement and concrete applications, and as adsorbent for inorganic wastes. Coal ash can be mixed with cement and other pozzolanic materials to form a stabilized construction material [41, 45, 49, 58], and their interaction with seawater is an intensively researched subject as reviewed by [20, 45] with a view of seeking alternative fly ash disposal methods into the oceans and potential environmental impacts. As stated in the previous section, the cementitious and pozzolanic properties of class C fly ashes and class F fly ashes (predominantly pozzolanic) find use in concrete making [41, 49]. Coal ash may reach and affect the marine environment as a dumped waste, or as a construction material for different marine applications such as artificial islands, artificial reefs and land reclamation of coastal areas. Coal ash can serve as filling material, with no contact with seawater or can be in direct contact with it during dumping operations [20].

The potential and opportunities that coal ash offers our society with environmental and economic benefits without harm to public health and safety when properly managed has attracted research [58, 59]. The coal based industry refers to these materials as coal combustion products (CCPs) to emphasize the fact that they have significant commercial value. A multibillion-dollar industry has arisen over the past 50-plus years around the use of these materials, which include fly ash, bottom ash, boiler slag, and various forms of flue gas emission control/ desulfurization materials [60]. Each of these varies by coal source and composition, combustion technologies, emissions controls technologies, amongst other factors.

2.2 Brines

Coal processing facilities in South Africa (Sasol and Eskom) are located in water-scarce areas and as such the decreasing water availability and quality has been cited as one of the emerging risks and challenges for these industries [60, 61]. Various processes currently being employed by Sasol and Eskom for maximum utilization, upgrading, and reuse of various industrial effluents include, desalination, evaporation, softening and ion exchange [62]. The desalination technology commonly employed by these facilities inevitably produces a highly saline effluent solution referred to as brine. Evaporation in the pipes surrounding the boilers that produce steam in order to rotate the turbines responsible for electricity generation also leads to preconcentration of dissolved salts in water which lead to formation of some brine. These industries have therefore developed strategies for water recovery from the effluent, resulting in reuse and recycling, and have embraced the modern technology for advanced water and wastewater treatment at the power plants. These efforts are geared towards significant reduction of operating costs and increased efficiency [63].

The continuous re-use and recycling of the effluent streams have resulted in the accumulation of salts in the fly ash water system. In Sasol Synfuels facilities, the total salts accumulating in the complex are a combination of chemicals used, raw water, mine water and salts originating from coal and ash. These salts enter the Synfuels complex at a rate of approximately 250 tons/day, and end-up in water that circulates the complex [64, 65]. Typical saline brines that occur at Sasol Synfuels contain the following components based on the fraction of the total salts present: Na^+ (2 % - 4 %), Cl^- (5 %), SO_4^{2-} (5 %), Ca^{2+} (0.12 %), K^+ (0.38 %), Mg^{2+} (0.06 %) ions and trace elements such as Fe, Mn, Cr, V, Ti, P, Si, and Al [62]. These salts, in the form of waste brine effluents, are continuously introduced into the Clear Ash Effluent (CAE). The CAE is sent to the Tubular Reverse Osmosis (TRO) unit where the stream is concentrated by desalination, resulting in TRO brine. The TRO brine is recycled and returned to the Secunda ash water system, and as a result lead to the accumulation of salts. This accumulation exceeds the salt encapsulation limits of the fine ash, on which the system has relied on for many years. A situation has been reached in which some salts components (especially gypsum) have exceeded their saturation limits in the ash effluent streams[11, 66]. Brines are heavily loaded with salts that can seep to the ground water and even may make the soil saline.

The burden of wastes namely brines and fly ash from the coal fired power plants is a threat to sustainable energy production. Thus the power generation industry has been at the forefront in looking for alternatives to the usual disposal methods so as to make coal based power generation not only more environmentally friendly but also more sustainable [47].

2.3 Fly ash - brine disposal systems and environmental impact

The production of large amounts of coal combustion by-products such as fly ash and brines presents a global disposal challenge to coal-utility industries [67, 68]. This has been of great concern to the power generating industry due to high cost implications involved and also their potential to harm the environment particularly to ground water pollution [7, 8]. The handling and disposal of saline effluents (brines) and fly ashes is a difficult and complex problem to Sasol and Eskom coal processing facilities. Most of the fly ash generated from Sasol and Eskom is dumped in landfills covering several hectares of valuable land near the plants. For the unutilized fly ash and the brine, common disposal practices involve holding ponds, lagoons, landfills and slag heaps. These are usually regarded as unsightly, environmentally undesirable and a non-productive use of land resources. They also present an on-going financial burden through their long-term maintenance [69].

Two main fly ash disposal systems are employed by Sasol and Eskom, namely the dry and wet ash disposal mechanisms.

For dry ash placement, the fly ash does not drain water except during rainfall and irrigation. The ash is transported by truck or conveyor belt at the site and disposed of by constructing a dry embankment (dyke) which with time builds into an ash heap (also known as ash dump). Eskom in its Tutuka power station employs this type of disposal in which the fly ash from the precipitators is moistened with low amounts (about 16 %) of brine [5] and is taken to the ash dumps via conveyor belt for disposal. At the ash dump, the ash is irrigated with brine (generated from water treatment plants) to keep the ash moist as a way of suppressing the dust. Although both dry and wet ash disposal methods have an impact on both surface and groundwater, dry ash disposal dumpsites (heaps), when properly constructed, are unlikely to produce leachate for many years. Factors that possibly play a role in reducing the leachate impact from dry ash are the pozzolanic property of dry ash [44, 55, 70, 71] and its inherent dry nature, and the saline (brine) content of water used to irrigate the heaps. The pozzolanic action of a dry ash system has been reported to be very different from that of a wet ash system.

Wet placement (dense slurry disposal) is any method that results in an excess of water that must be handled after the ash has been placed, that is, the fly ash is transported as slurry through pipes and disposed off in an impoundment called an ash pond [19, 69]. Sasol in its Secunda plant employs this type of disposal in which the ash is added from the hoppers to a stirring tank with continuous addition of brine to make slurry with controlled density (ash-to-water ratios of 1:10 to 1:5 by volume) [72]. This is then pumped continuously via pipes to the ash dam where the ash particles immediately settle out and the ash-water is either drained away via a penstock to the clear ash effluent dam, or percolates

through the ash dam and is collected in a toe drain. The ash water goes to the clear ash effluent dam, where it mixes with other wastewaters. After settling, the mixture is pumped back for treatment using reverse osmosis (RO) and electro-dialysis reversal (EDR). The waste product, brine (highly concentrated salt laden), from these treatment processes is again used for hydraulic transport of more ash from the hoppers thereby being co-disposed with the fly ash. With the growing environmental awareness that hydraulic ash removal systems are costly with regard to water and land usage, emphasis has been placed on finding a better system [69]. The wet ash disposal systems have been the preferred methodology in South African power stations. However, its management is being re-evaluated because of the cost of disposal and the potential for contamination of surface and ground waters by trace elements leached from the ash dams. The question always arise as to how can they (Eskom and Sasol) better manage their ash dams to not only satisfy all legal requirements and possible pressure from social awareness groups but also, more importantly, prevent, or at least limit, pollution of the natural environment.

The major potential impacts of ash disposal on terrestrial ecosystems have been reported [9]. These include:

- leaching of potentially toxic substances into soils and groundwater
- reductions in plant establishment and growth due primarily to adverse chemical characteristics of the ash
- changes in the elemental composition of vegetation growing on the ash
- increased mobility and accumulation of potentially toxic elements throughout the food chain
- visual intrusion

Despite the co-disposal of fly ash with brine, the interaction chemistry of the species in the system is yet to be well understood. The interactions of some species in the fly ash and brine could result in precipitation of salts due to super-saturation or adsorption. It is necessary to study the chemical interactions in fly ash-brine systems. This will give an insight into the effect of the interaction on the brine quality as well as the sustainability of the co-disposal scenario over time when fly ash and brine are co-disposed. Research into quantification and dynamic leaching studies for both Secunda and Tutuka ash disposal systems through modeling by use of PHREEQC has not been addressed. Results from column modeling studies are useful in enhancing further understanding of long term time-dependent leaching mechanisms.

2.4 Leaching studies of fly ash

Fly ash as a by-product of coal combustion has been previously handled as a waste and as such has attracted a lot of interests to researchers with regards to guidelines on the assessment of the waste with respect to improved levels of re-use and safe disposal. Accordingly, several leaching studies of coal ash have been conducted with acids, distilled or freshwater, and with seawater [20, 73-81]. Literature survey conducted by Hesbach and co-workers [82, 83] revealed over 100 leaching methods therefore raising the question as to the "best method" for ash leaching for a given type of ash.

2.4.1 Leaching methods and release mechanisms

Confronted by the question as to which of the many leaching methods could be the best, some standard leaching tests (also known as methodologies or protocols) have been developed and are currently in use [84]. Some of these methods are regulatory methods, mandated to characterize materials. Others are approved by professional and government organizations for establishing compliance to particular specifications [85]. Some methods are also intended to mimic natural (field or on-site) conditions or to obtain information about the nature of the extractable material within a particular solid. The methods vary in the mass and particle size of the sample, the type and volume of leachant solution(s), the leachant delivery method, and time. Most procedures are performed at ambient temperature, although a few decrease the time required to solubilise components by increasing the temperature. Although many were developed for application to municipal solid waste or industrial wastes, most leaching methods have been applied to a variety of materials, including coal utilization by-products (CUB) such as fly ash [32, 57].

In choosing a method, the scientist ought to be guided by the ability and effectiveness of results from the method used to answer the following pertinent questions as highlighted by Fallman and Aurell [78]:

i. How much of the total content of a pollutant can be released in leaching processes?

ii. What is the time-dependent release from the material by equilibrium or diffusion controlled leaching?

iii. What changes will the material undergo with time by atmospheric impact (CO_2, O2, rain, etc), chemical changes, or by leaching?

iv. What influence do pH and redox potential have on the leaching process and what changes in these parameters are likely to occur in the leachate from the wastes?

v. What is the time-dependent release from the waste with the proposed technique for utilisation/disposal?

Leaching tests have been classified broadly into two aspects: those that aim at equilibrium conditions during leaching (usually performed as batch-type or with controlled pH), or at the dynamic (time-dependent) aspects of leaching [86]. Diffusion tests for monolithic materials [87] and column leaching tests for granular materials [88] fall under dynamic leaching tests. Further classification of the leaching methods is reported by van der Sloot [86] and based on distinction in relation to practice. These include: (i) characterization tests aimed at understanding the leaching behaviour of materials under a variety of exposure conditions (typical testing times run from a few days to weeks or even a month), (ii) compliance tests, which are generally of much shorter duration, that are often aimed at a direct comparison with thresholds values (test duration up to one or two days), and (iii) on-site verification tests, which are aimed at verifying a previous evaluation of a charge or batch arriving at a processing plant (test duration typically within an hour). The latter distinction has been adopted in CEN, the European Standardization Organisation, as the basis for leach test development [86].

For coal ash residues, there exist some laboratory leaching tests which have been used in several leaching studies of coal ash by [11, 26, 77, 78, 80, 89-91]. These include (i) Dissolution Kinetics, (ii) Acid Neutralization Capacity based on European and Dutch standards: PrEN 14429, which deals with influence of pH on leaching with initial acid/base addition, (iii) Compact Granular Leaching Test (NVN 7347), (iv) Column Percolation Test: (PrEN 14405 also known as up-flow percolation test), and (vi) ENV 12920-European pre-standard for characterisation of waste [27]. These tests are used as characterization tests in order to identify the chemical reactions and the reaction kinetics in the ash-water system. The leaching information is then used to develop a mineralogical model and to identify the main transport mechanisms [35, 75].

From the static and dynamic leach tests conducted in recent years, a number of factors have been cited to affect the leaching mechanisms from different studies. Common among them are solubility, adsorption, pore water chemistry and solid phase chemistry [35, 62, 92, 93]. The release mechanisms from fly ash have been reported to be either one or a combination of the following release types [94]:

(i) Rate-limited release - this occurs in non-equilibrium situations and the concentration of the leachate depends on the rate of dissolution. The leachate concentrations remain unchanged over time unless the precipitated compounds are fully dissolved or the rate of release changes.

(ii) Solubility-controlled release - controlled release also occurs in non-equilibrium situations when the dissolution rate is infinite, and dissolution is controlled by solubility. The concentration of the leachate depends on the solubility of a compound in pore water and remains at the solubility limit of the compound.

(iii) Adsorption-controlled release – in this type of release, the concentration of metals in pore fluid continually changes, because the metal concentrations in the solid and liquid phase are controlled by the partition coefficients. Adsorption-controlled release corresponds to an equilibrium condition where adsorption and desorption occurs instantaneously.

On-site verification tests and validation usually follow the characterization and compliance testing. All of this information serves as the basis for the development of a geochemical model and which will provide the necessary background to make such long term evaluations of environmental impact. It also provides information which influences decisions on potential utilization, treatment, recycling and disposal of such materials [86]. The focus in this project is the coal ash residues.

Prior to the Sasol-Eskom collaborative research initiative [19], not much literature was available documenting the understanding and release mechanisms of the fly ash-water and fly ash-brine interaction in South African disposal systems. It is envisaged that the fundamental studies on the co-disposal of brines in inland ash dams and geochemical modeling studies would provide the necessary and better understanding of the geochemical processes involved and the potential environmental implications of the ash-brines co-disposal.

2.5 Hydrogeochemical modeling

Hydrogeological and geochemical models have become important numerical modeling tools used in the environmental, scientific and technical community worldwide. The term hydrogeochemical modeling constitutes this body of science which combines both hydrogeological and geochemical models. Both of these models comprise three major components [95], namely:

- Specific information describing the system of interest
- The equations that are solved in the model
- The model output

Geochemical models incorporates an additional component, the equilibrium and kinetic prescriptions for chemical reactions among the chemical components of concern [96]. Modeling and computer simulation is a valuable tool that can be used to gain a greater understanding of geochemical processes both to interpret laboratory experiments and field data as well as to make predictions of long term behaviour. In spite of its increasing application, geochemical modeling still remains the preserve of a limited group of specialists.

A general modeling scheme of inorganics is presented in Figure 2.2 which gives the basic components of the inputs, processing and outputs in any numerical model.

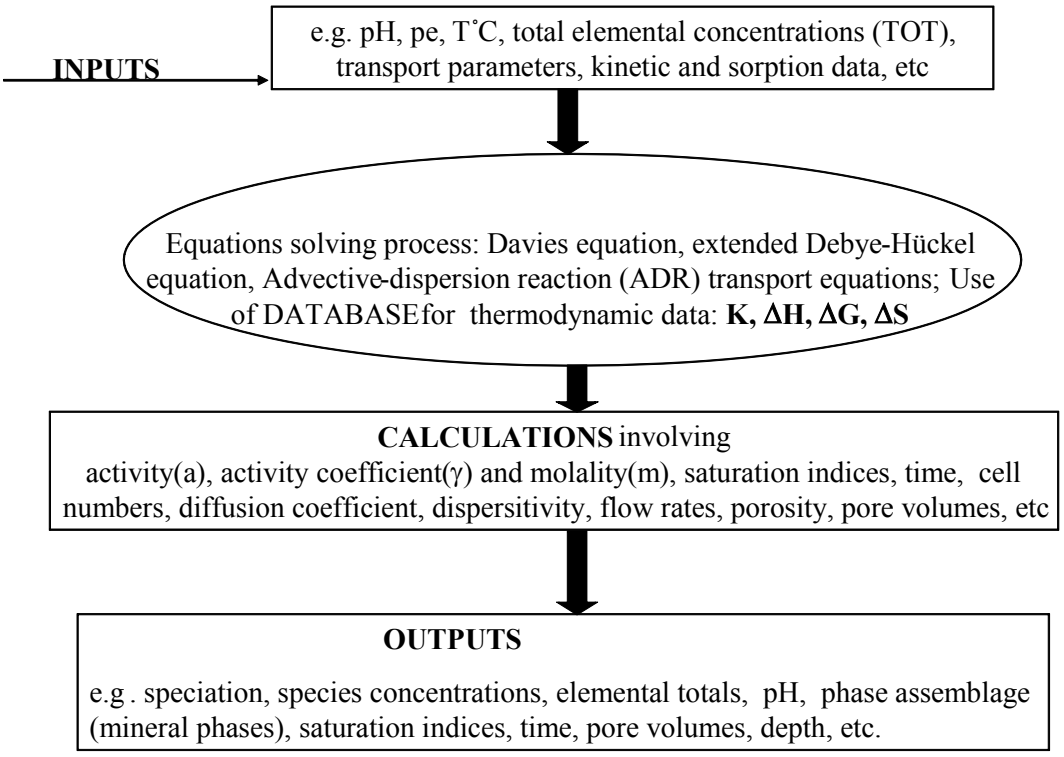

Figure 2.2: General hydrogeochemical modeling scheme of inorganics and organics using computers (Adapted but modified from [97])

The equations solving processes involves providing useful solutions to some partial differential or algebraic equations representing laws governing speciation, advective-dispersion transport phenomena, geochemical processes using prescribed principal numerical methods [98]. Activities of aqueous species are usually calculated using the Davies equation, the Debye-Hückel equation, or the extended Debye-Hückel equation [14, 99]. This approach limits the field of applicability for these models to solution ionic strengths less than or equal to that roughly corresponding to seawater [14].

Some programs can be used to simulate high ionic strength aqueous solutions such as brines, using the specific interaction approach proposed by Pitzer [100]. The Pitzer method for activity calculation, however, is weakened at the present time by a lack of reliable literature data, particularly for redox sensitive species [101].

The term hydrogeochemical modeling has therefore been used to refer to the numerical modeling which combines both hydrogeological and geochemical models. It simulates the chemical and physical processes affecting the distribution of chemical species in liquid, gas, and solid phases. In this context, hydrogeochemical modeling addresses most environmental hydrogeochemical problems, which are: hydrochemistry, geochemistry, hydrogeology and reactive solute transport.

Hydrogeochemical models as applied in solid waste have been extensively reviewed in the literature [99, 101-104], with respect to speciation and solubility [49, 105], reaction paths (e.g. titration, buffering, flushing) [106], kinetic reaction paths [21, 104, 107, 108], inverse mass balance [109, 110] and coupled mass transport [96, 107, 111]. However, literature is scarce on hydrogeochemical modeling application towards helping better understand the chemistry of fly ash-water and brines interactions, in particular within the South African coal utility facilities. The Sasol-Eskom ash-brine project initiative was geared towards filling some of these gaps in fly ash-solution interactions.

Development of a conceptual model is the most important part of the modeling process. The conceptual model is the foundation of the quantitative, mathematical representation of the field site (i.e., the mathematical model), which in turn is the basis for the computer code used for simulation [69]. In the present study, application of PHREEQC computer code with modified LLNL database has been undertaken to study the Sasol-Eskom fly ash interactions.

2.5.1. Geochemical modeling tools/software

There are over 100 computer programs associated with geochemical modeling that have been reviewed [101] and which are available both commercially and in the public domain, for the simulation of geochemical reaction systems. Some of these programs are specifically designed for batch-type simulations, whilst others incorporate transport capabilities. Some of these programs have become enormously sophisticated and allow the simulation of very complex aquifer systems.

The continuous development of these programs has been necessitated by the complexity of the ever changing chemical environment and the nature of the studied materials. There has therefore been the need for high-performance numerical tools coupled with huge thermodynamic databases. Some of these geochemical softwares have been in existence for decades and include: AquaChem, MINTEQA2, EQ3/6, UNSATCHEM-2D, WATEQ4F, and PHREEQC, some of which work on a Windows platform while others work on other platforms such as DOS and UNIX. The above mentioned are available as public-domain coupled transport and geochemical reaction programs. PHREEQC and MINTEQA2 have a wide range of capabilities that are similar and the choice between the two is more of preference than capability differences. MINTEQA2 has additional sorption models relative to PHREEQC, triple layer, constant capacitance, Langmuir, and Freundlich isotherms. PHREEQC has capabilities for speciation, kinetics, solid-solution, cation exchange, and gas-phase calculations, which are also present in MINTEQA2. PHREEQC has only one sorption model, the diffuse double layer model of Dzombak and Morel, but Freundlich and Langmuir isotherms can be modeled by using some careful (obscure) definitions [112]. PHREEQC has also the 1D-transport and coupled reactive transport modeling capabilities which are not in MINTEQA2. Further limitations of MINTEQ2A are with respect to the assumption that water exist at a constant thermodynamic activity in the model, errors arising from changes in temperatures (high temperatures), not able to evaluate systems with significant kinetic constraints, and wrong databases for some components [113]. On the overall, PHREEQC has more capabilities and a better interface than MINTEQA2.

Among the commercial softwares include: Geochemist's workbench (GWB), CHESS, HYDRUS, MODFLOW-SURFACT, SWIFT-98, WinTran, AQUA3D, and AQUACHEM. In his review of geochemical modeling tools, Crawford [101, 114] noted that it was possible to determine the technical capabilities of most public-domain programs by examining the software, user manuals, and test examples that could be downloaded from internet. This was not always possible for commercial programs and product descriptions available from software vendors were heavily relied upon. In some cases it was not possible to ascertain exactly if a program was capable of a certain technical feature owing to an incomplete product description, poor documentation, or exaggerated claims made by the vendor. Most of the commercially available programs are tailor-made to address specific tasks and for

those that have multiple capabilities, theirs are relatively fewer than those of the public-domain programs. Most of them are not user friendly due to being in DOS and some in uncompiled Fortran code platform. Other limitations include the high cost, inavailability in the internet and the lack of multitasking and interfacing capabilities. Geochemist's workbench however stands the most highly rated and robust among the aforementioned commercially available programs. With its crisp user interface, fully integrated graphics, highly optimized algorithms, and advanced software architecture, the GWB makes quick work of geochemistry tasks small and large. With a few clicks, you can balance reactions, figure equilibrium constants, and make Eh-pH diagrams. It also integrates kinetic rate laws for mineral dissolution and precipitation, complex association and dissociation, sorption and desorption, redox transformation, and gas transfer. Geochemist's workbench also models microbial metabolism and growth apart from simulating equilibrium and kinetic reactions in heterogeneous, and dual-porosity media [115].

Softwares coupling geochemistry and transport are more fewer and they are more specific for hydrogeology problems (like HYTEC, PHAST, FEFLOW) [91, 101, 112, 116] and whose use requires specialised (high level) competence on numerical modeling, thus limiting their day-to-day application by the average person.

2.5.2. PHREEQC: hydrogeochemical modeling code

PHREEQC is one of the advanced geochemical models that performs simulations based on the principles of thermodynamic equilibrium [14]. The acronym PHREEQC stands for the most important parameters of the model; namely PH (pH), RE (redox), EQ (equilibrium), C (programming language C). Since its inception, it has undergone numerous transformations each time a new version developed with additional capabilities. The original version (PHREEQE) was used to address the two major types of geochemical problems: forward and inverse [14], then followed by the PHREEQC-1. The latest version (PHREEQC-2, V2.18.5314) was released in August 2011 by Parkhurst, who developed and usually maintains the running of the PHREEQC in the public domain.

PHREEQC is used for simulating a variety of geochemical reactions and processes in natural waters or laboratory experiments [14]. The simulations are executed by using an input file in which the problem is specified via KEYWORDS and associated data-blocks. Table 2.1 gives a summary and description of the keywords used in PHREEQC.

Table 2.1: Keywords used in PHREEQC input file

KEYWORD	DESCRIPTION
SOLUTION (*m-n)*	For composition and quantity of solutions in flasks *m* to *n (m, n are integers:1,2,3,4,5etc)*
USE	For specific solution
MIX	fractions of solutions in one flask
EQUILIBRIUM_PHASES	Various reactants can be added to the flask: for a combination of minerals and/or gases which react reversibly to a prescribed equilibrium
EXCHANGE	for the capacity and composition of an exchanger
SURFACE	For the capacity and composition of surface complexers
REACTION	For stepwise adding or removing chemicals, minerals or water
KINETICS	For chemicals which react depending on time and composition of the solution
GAS_PHASE	For a combination of gases in a specified volume or at a given pressure
SOLID_SOLUTIONS	For adding solid solutions of minerals or liquid solutions of organic chemicals
REACTION_TEMPERATURE	For changing the temperature of the flask
END	To signal for PHREEQC to calculate the composition of the solution and the reactants in what is termed a *simulation*
SAVE	The compositions can be stored in computer memory with **SAVE** solution no., **SAVE** exchange no. etc
PRINT	To limit printout to specific items and to suspend/resume print options
SELECTED_OUTPUT	To obtain results in spreadsheet type format
USER_PRINT, **USER_PUNCH** and **USER_GRAPH**	For defining tailor-made, specific output
TRANSPORT	For 1D dispersive/diffusive transport including mobile/immobile zones: For 3-D transport, the code PHAST can be used from United States Geochemical Survey (USGS).
INVERSE_MODELING	Chemical reactions which led to a given water quality can be recovered using this keyword

PHREEQC has four databases that are distributed with the code, namely: PHREEQC.DAT, WATEQ4F.DAT MINTEQ.DAT, and LLNL.DAT. The PHREEQC.DAT database is extended with many heavy metals and is a subset of WATEQ4F.DAT, which is essentially equivalent to the database in WATEQ4F.DAT and it includes some organic compounds. The database LLNL.DAT is derived from the EQ3/6 and is nearly identical to the database for EQ3/6 and Geochemist's Workbench. It is currently the largest database containing many elements with a large temperature range [14, 112].

A full description of many alternatives for input and the mathematical backgrounds can be found in the manual of the program by Parkhurst and Appelo [14] and further updated in the file 'release.txt' distributed with the program from the USGS website.

Generally, the PHREEQC-2 model used for the study's simulations is capable of speciation, batch-reaction, one-dimensional transport and inverse geochemical calculations, both in natural or polluted water. It is based on equilibrium chemistry of aqueous solutions interacting with minerals, gases, solid solution, exchange phase and sorption surfaces in which minerals and soluble species are equilibrated simultaneously. The one dimensional transport module is comprised of dispersion, diffusion and various options for dual porosity media. The inverse modeling capability enables identification of reactions that account for observed water compositions along a flow line or in the time course of an experiment. It also has an extensive chemical database which allows application of the reaction, transport and inverse modeling to almost any chemical reaction that is recognized to influence soil, surface water and groundwater quality [14].

PHREEQC offers a number of advantages for most users as an all-purpose geochemical model, with some of the programs advantages listed below:

- It is a well established model with a long history. A large number of papers have been published in the literature over the years that have used PHREEQC models to solve geochemical problems. However its application in fly ash chemistry within the South African context has not been done except by Hareeparsad and co-workers [26].

- The current manifestation, PHREEQC, is versatile in that it can solve a wide range of problems, including those entailing surface chemistry phenomena and reaction kinetics.

- It is based upon a robust numerical engine that rarely crashes

- It can access thermodynamic data from large, well-established databases or rely on user-provided data, depending on user specifications

- PHREEQC is public domain software that can be easily and freely downloaded from the internet.

Despite the many capabilities presented above, PHREEQC has some limitations that relate to the following aspects as detailed in the PHREEQC manual [14]:

- Aqueous model: whereas PHREEQC uses ion-association and Debye Hückel expressions to account for the non-ideality of aqueous solutions aqueous model is adequate at low ionic strength but may break down at higher ionic strengths (in the range of seawater and above). This limitation has since been addressed by incorporating the Pitzer equation in the new versions of PHREEQC. The other limitation of the aqueous model is lack of internal consistency in the data in the databases. Careful selection of aqueous species and thermodynamic data is left to the users of the program.

- Ion Exchange: The ion-exchange model assumes that the thermodynamic activity of an exchange species is equal to its equivalent fraction. Optionally, the equivalent fraction can be multiplied by a Debye-Hückel activity coefficient to define the activity of an exchange species. Other formulations use other definitions of activity (mole fraction instead of equivalent fraction, for example) and may be included in the database with appropriate rewriting of species or solid solutions. No attempt has been made to include other or more complicated exchange models. In many field studies, ion-exchange modeling requires experimental data on material from the study site for appropriate model application.
- Surface Complexation: PHREEQC incorporates the Dzombak and Morel [117] generalized two-layer model, a two-layer model that explicitly calculates the diffuse-layer composition, and a non-electrostatic surface-complexation model. Other models, including triple- and quadruple-layer models have not been implemented in PHREEQC. Sorption according to Langmuir or Freundlich isotherms can be modeled as special cases of the non-electrostatic model.
- Solid Solutions: only non-ideal, binary solid solutions are considered in the current PHREEQC versions. Ternary non-ideal solid solutions are not implemented. It is possible to model two or more component solid solutions by assuming ideality. However, the assumption of ideality is usually an oversimplification except possibly for isotopes of the same element.
- Transport Modelling: An explicit finite difference algorithm is included for calculations of 1D advective-dispersive transport and optionally diffusion in stagnant zones. The algorithm may show numerical dispersion when the grid is coarse. The magnitude of numerical dispersion also depends on the nature of the modeled reactions; numerical dispersion may be large in the

many cases--linear exchange, surface complexation, diffusion into stagnant zones, among others--but may be small when chemical reactions counteract the effects of dispersion. It is recommended that modeling be performed stepwise, starting with a coarse grid to obtain results rapidly and to investigate the hydrogeochemical reactions, and finishing with a finer grid to assess the effects of numerical dispersion on both reactive and conservative species.

- Convergence Problems: PHREEQC tries to identify input errors, but it is not capable of detecting some physical impossibilities in the chemical system that is modeled, arising for example from charge imbalances. At present, the numerical method has proved to be relatively robust. All known convergence problems (cases when the numerical method fails to find a solution to the non-linear algebraic equations) have been resolved. Occasionally it has been necessary to use the scaling features of the KNOBS keyword.
- Inverse Modelling: the numerical method has shown some inconsistencies in results due to the way the solver handles small numbers.

PHREEQC version 2 is a modification of PHREEQC version 1 but which keep on being updated into other new sub-versions (e.g. 2.15.0, 2.18.5314 etc). Some of the limitations cited above have been addressed in subsequent revised versions of the program. All of the capabilities and most of the code for version 1 are retained in version 2 and several new capabilities have been added such as isotopes balancing, kinetics, simple adsorption, surface complexation, (humic/fulvic), Pitzer activity model, diffusion/dispersion, solid solutions, etc, as outlined and clearly demonstrated in the PHREEQC manual [14]. Bug fixing, new BASIC functions (e.g. ceil and floor) and improving on convergence tolerance are some of the features continuously being reviewed and posted in PHREEQC newer versions [118].

This study employed PHREEQC version 2.15.0 for hydrogeochemical modeling of fly ash co-disposed with brines and organics for Sasol-Eskom coal ash.

CHAPTER 3

HYDROGEOCHEMICAL MODELING OF THE EFFECT OF BRINES AND ORGANICS ON METAL LEACHING, ACID NEUTRALIZATION CAPACITY AND MINERALOGY OF FLY ASH (SOUTH AFRICA)

John M. Mbugua[1]*, J. Catherine Ngila[1,2], Andrew Kindness[1], Chris Buckley[3], Molla Demlie[4] and Shameer Hareeparsad[5]

[1] University of KwaZulu-Natal, School of Chemistry and Physics, Westville Campus, Private Bag X54001, Durban 4000, South Africa

[2] University of Johannesburg, Department of Chemical Technology, P.O Box 17011, Doornfontein, Johannesburg 2028, South Africa

[3] University of KwaZulu-Natal, Pollution Research Group, Howard College Campus, Durban 4041, South Africa

[4] University of KwaZulu-Natal, Department of Geological Sciences, Westville Campus, Durban 4000, South Africa

[5] Sasol Synfuels (Pty) Ltd, Environmental Sciences and Engineering Research and Development, Secunda, Mpumalanga 2302, South Africa

*Corresponding author: jmmwai@gmail.com, Tel: +27312601498; +27799228187

Abstract

Two major coal utility plants (Sasol and Eskom) in South Africa produce vast volumes of fly ash and brines as by-products during coal processing. Co-disposal of the brines and fly ashes has been a normal practice in these coal-utility plants for decades. However, the geochemistry of brine-fly ash interactions, the leaching and mobility of elements in these disposal systems has not been fully understood. Sustainability and long term impact of their co-disposal on the environment was studied through modelling of pH-dependent acid neutralization capacity (ANC) tests. Modeling results of the ANC tests were in good agreement with the reported experimental results, which revealed that the release trends of various toxic elements and contaminants contained in fly ash into solution is highly pH dependent. Both fly ashes exhibited a natural pH > 12 (suspension in demineralised water) and the predominant cation even at this high pH is Ca^{2+} (at concentration > 0.002 mmol/L). This indicates that

dissolution of CaO and formation of OH^- species at pH > 10 contributes to acid neutralisation capacity of both fly ashes and is the greatest contributor to the acid neutralizing capacity of both fly ashes.

The batch leaching simulation results from hydrogeochemical modeling also showed that mineral dissolution, precipitation and new phase formation during ash-organics-brines interactions was controlled by pH. The newly formed phases however remain in equilibrium with the ash-brines-organics mixture. Each individual mineral phase dissolution/precipitation/formation system controls the concentration and speciation of the respective constituent elements as evidenced by the log C-pH diagrams obtained from the modeled scenarios. The ash-brines-organics interactions do exhibit and affect the mineralogical chemistry of fly ash. However, the extent to which these interactions occur and their effect, varies from one scenario to another, and are dependent on the amounts and type of the constituent brine components. Organics do have a significant effect on dissolution characteristics of few minerals such as calcite, mullite, kaolinite, Ni_2SiO_4, and $SrSiO_3$. The effect is quantitatively conspicuous for calcite mineral phase and for the formation of some new phases such as $Fe(OH)_3$(am)-CF and portlandite.

Hydrogeochemical modeling was used as a means to provide insights and understanding of the complex reactions taking place; speciation and mineralogical changes occurring; and to predict future environmental scenarios when pH conditions change. In this study, PHREEQC hydrogeochemical code was applied for modeling and simulation of equilibrium, kinetic and transport mechanisms associated with the interaction of water and brines with fly ash. In this study, a special reference is given to modelled mineralogical ash recipe from one of the South African power utility plant's fly ash system. The PHREEQC program using modified Lawrence Livermore National Laboratory (LLNL) database for inorganic brines and MINTEQ database for organics, were used to model the results of ANC test data for the fly ashes. The effects of brines and organics in the leaching of major, minor and trace elements at various pH values and the mineralogical changes associated with the intermediate and final products from the interactions of ash-brines systems under different scenarios, are qualitatively and quantitatively reported. Modeling results were used to support experimental data which could be used to guide future waste management decisions. Furthermore the hydrogeochemical modeling results of the current study can play a role in solid waste management as they may augment or complement the practical activities of environmental scientists.

Keywords: Acid neutralization capacity (ANC), Brines, Fly ash, Hydrogeochemical modeling, Mineral phases, PHREEQC

3.1 Introduction

Coal processing facilities worldwide have been known to produce large quantities of coal combustion residues such as fly ash and some brine effluents [34, 35] which pose a huge environmental challenge. Other than the environmental concerns associated with fly ash, these coal utility plants are exploring on increased commercial utilization of fly ash. The fly ash has been used as by-product in numerous environmental and commercial applications due to its pozzolanic, cementitious and alkaline properties [18]. Some of the applications of fly ash include; cement production where it is used as admixture to blend cements; in agriculture to improve soil structure and water holding capacity; as a liming agent to neutralize acidic soils; and as an essential source of micronutrients for agricultural crops [93, 119, 120]. However fly ash heaps and dams are potential long-term sources of contamination to surface-water and groundwater systems due to their possible enrichment in major and trace elements relative to normal geological materials.

The release of different kinds of ions, including heavy metals, may have the potential to pollute the environment and thus affects the extent of further utilization of fly ash. The pollution may occur if the ions are released into the environment in sufficient amounts. There is need therefore to assess the release and mobilization of elements that result from weathering of fly ash. Understanding the factors controlling the leaching behaviour of major and minor elements is therefore critical in predicting potential impacts of fly ash on the environment. The two types of coal fly ash reported in this study were from two of the South African coal processing plants, Sasol and Eskom. These facilities are both located in the interior of South Africa in water stressed areas, where the re-use and recycling of water are mandatory. Despite the reuse of the water in the industrial plants, the brine effluents still remain which require to be disposed off.

This study focuses hydrogeochemical modeling of chemical, mineralogical and geochemical properties of coal fly ash co-disposed with brines possibly containing some organics, by use of PHREEQC. Geochemical reactions that occur between fly ash components and the chemical species in the brine solutions have been reported in related studies of the larger Sasol-Eskom ash-brine project [11, 13, 26, 62]. The interactions between the various species in the fly ash and the brine may result either in neoformed phases (as secondary phases) or in dissolution of the primary phases. This mutual interaction of individual wastes determines the long-term quality of the leachate [121]. Using the PHREEQC modeling code, the effect of the brines-fly ash interactions together with the possible organics in the brines was investigated. The modeling was carried out with a view to quantify and characterize the products formed.

It was based on the ANC of fly ash and the leaching capacity of the major and minor elements from brine-organics-fly ash interactions, with reference to the batch leaching tests (or static leaching tests).

It is envisioned that the modeling of the batch leach tests will form the basis for understanding and predicting further the leaching chemistry associated with fly ash-brines interactions. These predictions may then be used to develop scenarios and offer potential guide for future sustainable waste management practices as a way of addressing the co-disposal of brines within inland ash dams and heaps. The modeling results would be used to support experimental data and hence may be used to guide future waste management decisions.

3.2 Methodology and hydrogeochemical modeling tools

3.2.1 Background on Phase I studies

The modeling work was based on experimental work carried out by Ojo [15] during phase I of the Sasol-Eskom ash-brine project. The total content of the elements present in the fly ash samples was determined by total acid digestion (HF + aqua regia + H_3BO_3) of the samples followed by analysis of the resulting solution. The elemental analysis of the leachates from the ANC tests was done using inductively coupled plasma-mass spectrometry (ICP-MS) at pH of 2 (by acidification with 65% HNO_3) for cations and by ion-chromatography (IC) for anions. For XRD analysis, fly ash samples were analysed before and after leaching in order to determine the major mineralogical composition and transformations [13]. From the experimental work of Ojo [11, 15, 19] and modeling work of Hareeparsad and co-workers [26], two modeling ash recipes of Secunda and Tutuka were derived. They exhibited similar mineral phases composition but only differed quantatively. Hareeparsad and co-workers [26] improved further the mineralogical characterization in the previous study by Ojo [15] using computer controlled scanning electron microscopy (CCSEM) technique which identified further mineral phases that would otherwise not be observed with other techniques. These modeling ash recipes and their amounts are given by Table 3.1.

3.2.2 Experimental work in Phase II

The input parameters for phase II project (this study) were based on the phase I studies conducted by others [6, 10, 11, 13, 19, 26, 29, 93, 122].

Hydrogeochemical modeling of the leaching behaviour of elements in fly ash was studied using PHREEQC [14], developed on the basis of laboratory-scale experimental results based on the prescribed protocol Pr EN 14429 (Influence of pH on leaching with initial acid/base addition) [24]. In the PHREEQC simulation, the fly ash is modelled as a collection of pure mineral phases which come to equilibrium with the liquid phase. Two fly ash recipes from Secunda (Sasol) and Tutuka (Eskom) given in Table 3.1 were previously developed in phase 1 of the project by Hareeparsad and co-workers [26] and were used for the ANC modeling. The elements Na, K and Li were also considered to be existing as free ions in the ash recipe and whose values were:

- Tutuka fly ash (mM): Na (0.5), K (0.1) and Li (0.2)
- Secunda fly ash (mM): Na (10), K (2) and Li (4)

Table 3.1: Modeled fly ash recipe composition for Secunda and Tutuka [26]

Name	Formula	Secunda ash recipe (moles/L)	Tutuka ash recipe (moles/L)	Dissolves only
Anhydrite	$CaSO_4$	7.66E-03	6.90E-03	
Chromatite	$CaCrO_4$	1.96E-05	3.00E-05	
Calcite	$CaCO_3$	1.36E-02	6.90E-03	
Powellite	$CaMoO_4$	1.32E-06	1.80E-07	
Hematite	Fe_2O_3	1.41E-03	3.00E-02	TRUE
Kaolinite	$Al_2Si_2O_5(OH)_4$	2.35E-03	5.32E-04	TRUE
Lime	CaO	6.15E-02	4.41E-02	
Millerite	NiS	1.16E-07	0.00E+00	TRUE
Mullite	$Al_6Si_2O_{13}$	1.26E-05	5.00E-03	TRUE
Liebenbergite	Ni_2SiO_4	2.14E-06	3.00E-06	TRUE
Periclase	MgO	4.16E-02	2.10E-02	
Pyrite	FeS	5.50E-04	3.00E-04	
$SrSiO_3$	$SrSiO_3$	6.09E-04	4.59E-04	TRUE
Zn_2TiO_4	Zn_2TiO_4	2.67E-07	2.00E-06	TRUE

In this part of the study, fly ash from Secunda (Sasol) was chosen for the modeling purposes.

The modeling results of the ANC test carried out in phase 1 of the project by Hareeparsad and co-workers [26] were used for the development of the modeling ash recipe. The ANC test results were also developed by utilizing the saturation indices (SI) calculations from experimental results of the composition of the solution. These SI results when supplemented by literature information would give the proposed solid model simulated in the fly ash-demineralised water system of the ANC. The

simulation of other test samples in which acid or base was added permitted to fit the proposed mineralogical model and semi-quantification of the pure mineral phases constituting the modeling ash recipe. Tiruta-Barna and co-workers [27] have described the steps involved in obtaining the hypothetical modeling ash recipe, which were used for the development of our mineralogical ash recipe in this study. These steps take into account the rapid dissolution of some solid phases, test results and mechanisms for ash-demineralised water column tests; as well as susceptibility to precipitation as hydroxides in the experimental conditions (the most soluble hydroxide being chosen from the database following the Ostwald priority rule) [28]. The possibility of some solid phases going in to solution and not able to precipitate, was also taken into consideration similar to the case of silicates and oxides when formed at high temperatures. From the work of Hareeparsad and co-workers [26], there were also some phases that were considered likely to be formed during the leaching transformation paths. These phases were also incorporated in the present modeled ash recipe and are given in Table 3.2

Table 3.2: Phases absent in fresh ash but likely to be formed and thus incorporated in the ash recipe [26]: (am or A = amorphous, mC = microcrystalline, Csh = C-S-H)

Mineral Name	Alternative Formula
$Al(OH)_3$(mC)	$Al(OH)_3$
Brucite	$Mg(OH)_2$
Bunsenite	NiO
Celestite	$SrSO_4$
$Cr(OH)_3$(A)	$Cr(OH)_3$
Csh_gel_0.8	$Ca_{0.8}SiO_{2.8}$:H_2O
Ettringite	$Ca_6Al_2(SO_4)_3(OH)_{12}$:$26H_2O$
$Fe(OH)_3$(am)-CF	$Fe(OH)_3$
Gypsum	$CaSO_4$:$2H_2O$
Magnesite	$MgCO_3$
$Ni(OH)_2$	$Ni(OH)_2$
$NiCO_3$	$NiCO_3$
Portlandite	$Ca(OH)_2$
SiO_2(am)	SiO_2
$Sr(OH)_2$	$Sr(OH)_2$
$Zn(OH)_2$(gamma)	$Zn(OH)_2$
Csh_gel_1.1	$(CaO)_{1.1}SiO_2$:nH_2O
Csh_gel_1.8	$(CaO)_{1.8}SiO_2$:nH_2O

The levels of the major elements in brines generated from Secunda and Tutuka power plants were characterised by Gitari and co-workers, and Ojo and others [11, 13, 15, 29], as shown in Table 3.3 and which was used in the geochemical model. Artificial sewage waste was used as the modeling recipe for the organics in brines. This is because any sewage waste recipe contains important organic ligands that are commonly found in the environmental waste, such as acetate, glycinate, tartrate, glutamate, salicylate and phthalate, given in Table 3.4 as prescribed by Wadley and Buckley [30].

Table 3.3: Elemental levels in brines from Secunda and Tutuka coal utility plants [19]

Elements	Secunda TRO brine (moles/L)	Tutuka RO brine (moles/L)
Ca	2.05E-02	4.30E-03
Mg	3.39E-04	8.38E-03
K	6.61E-03	4.30E-03
Na	1.09E-01	2.87E-01
CO_3^{-2}	4.00E-03	6.00E-03
SO_4^{-2}	4.54E-02	1.11E-01
Cl^-	4.64E-02	8.83E-02

Table 3.4: Artificial sewage waste (ASW) recipe used for modeling of organics [30]

Name of Ligand	Concentration (mmol/L)
Acetate	5.00E-01
Glycinate	5.00E-01
Tartrate	2.50E-01
Glutamate	2.00E-01
Salicylate	1.55E-01
Phthalate	1.25E-01

The major cations present in brines were Na^+, K^+, Ca^{2+} and Mg^{2+} whereas major anions were SO_4^{2-}, CO_3^{2-} and Cl^-. Each of the cations was input together with all the three anions for every PHREEQC simulation, and each anion was also alternately input together with all the cations (Appendix B). Within the scope of this paper, four modeling scenarios were simulated using the PHREEQC software and which included:

i. Ash interaction with demineralised water (DMW): This was used to calibrate the subsequent models
ii. Ash interaction with artificial sewage waste (ASW) organics and individual brines
iii. Ash interaction with artificial sewage waste (ASW) organics and combined brines
iv. Ash interaction with combined brines

PHREEQC simulations were done using a modified Lawrence Livermore National Laboratories (LLNL) database to obtain pH range between the natural fly ash pH of 13 and pH 4. A modified MINTEQ.V4 database was used to simulate ash interactions with model ASW organics in brines. In all simulations, HNO_3 acid was used as the neutralizing reagent to lower pH values whereas NaOH was used to raise the pH values in those cases where the natural pH of the mineral recipe was initially lower than the natural fly ash pH of 13. The liquid-solid (L/S) ratio was maintained at 10:1 as per the experimental work of Petrik and others [29].

3.2.3 PHREEQC data input

The brines components (cations and anions) given in Section 3.2.2 (Table 3.3) were the inorganics input parameters for the SOLUTION data block while the organic ligands found in the artificial sewage waste (ASW) and given by Table 3.4 were used as input parameters for the SOLUTION data block in PHREEQC according to the specific modeling scenario being simulated. An input file for the ANC of fly ash with ASW organics and combined brines is presented in **Appendix 1**. Temperature input in the SOLUTION data block was maintained at 20 $^{\circ}$C and the electron activity (pe) set at the default value of 4. The Secunda 'Sept2009 fly ash' recipe comprising the mineral phases in Table 3.2 and Table 3.3 (**section 3.2.2**) were input in the EQUILBRIUM_PHASES data block for all the simulations in each modeling scenario. Some phases were imposed to undergo dissolution only as they cannot precipitate in the experimental conditions used, hence the column with the term 'dissolves only' in Table 3.2 and entered as 'true' for such mineral phases.

3.2.4 PHREEQC data output and presentation

The simulation data output obtained from the PHREEQC runs, was presented in the form of MS EXCEL spreadsheet generated from the unique feature of PHREEQC capability and linkage data sourcing tool using MS Excel. The total elemental concentration (TOT), species concentration (m_species), change in phase assemblage data (delta d_phase) and saturation indices (SI) for the formed phases at each pH were some of the parameters generated by PHREEQC simulation. From the spreadsheet data output, Log C-pH diagrams of elemental concentration (TOT) and that of various species with concentration greater than or equal to 10^{-6} M were drawn as well as graphs relating to ANC and mineralogical phases transformation and quantification. In the case of mineral phase quantification, phase assemblage data was expressed in either of the following parameters against pH; delta (d_phase), absolute change of delta (d^1), and relative change of delta (Rc_d^1). These parameters are explained in the following **section 3.2.5** in order to understand their significance in the study.

3.2.5 Phase assemblage parameters: interpretation and significance.

Three important phase assemblage parameters will be discussed under this section, namely; delta (d_phase), absolute change in delta, delta_delta (d^1) and relative change of delta_delta, (Rc_d^1). These parameters relate to the amount of mineral phase dissolved, precipitated or newly formed when given phase(s) interact with aqueous media.

(i) delta (d_phase)

The dissolution/precipitation chemistry of the ash mineral phases and formation of new (secondary) mineral phases when ash is in contact with water, brines and/or organics under the aforementioned modeling scenarios, is captured in the phase assemblage output data of the PHREEQC. To give an insight on the important information that phase assemblage yields, a section of a PHREEQC output file showing the phase assemblage of ANC of ash + organics + combined brines at pH 12, is shown in Table 3.5.

Table 3.5: Phase assemblage data from PHREEQC simulation

```
-------------------------------Phase assemblage-------------------------------

                                                    Moles in assemblage
Phase                  SI log IAP  log KT      Initial       Final       Delta

Al(OH)3(mC)         -4.59    4.76    9.35   0.000e+000           0  0.000e+000
Anhydrite           -0.27   -4.61   -4.34   7.656e-003           0 -7.656e-003
Brucite              0.00   17.18   17.18   0.000e+000  4.197e-002  4.197e-002
Bunsenite           -2.20   10.55   12.74   0.000e+000           0  0.000e+000
CaCrO4              -5.33   -7.59   -2.27   1.960e-005           0 -1.960e-005
Calcite              0.00   -8.46   -8.46   1.365e-002  1.768e-002  4.028e-003
------------------------------------------------------------------------------
```

The delta parameter (d_phase) is calculated by the program as the difference between the initial moles and the final moles of the mineral phase after reactions/interactions at that particular pH.

Thus, the change in the amount of mineral phase, given as delta (d_phase), was calculated using the following expression in Equation 1:

d_phase = initial moles of phase – final moles of phase……..Equation 1

When the calculated d_phase from the output file is negative, it indicates that the mineral phase has dissolved by that amount and when d_phase is positive, the number of moles of that mineral phase will have increased from the initial amount, indicating precipitation; or a new mineral phase is formed if initial amount was zero.

From Table 3.5, all anhydrite and $CaCrO_4$ mineral phases dissolved (7.656e-003 and 1.960e-005 moles, respectively) at pH 12, but both remain in solution as the solution is still undersaturated with them since the saturation index is negative.

For calcite, 4.028e-003 moles precipitated from the solution while 4.197e-002 moles of brucite were formed as a new (secondary) phase since the mineral phase was absent in the starting mineralogical recipe. This is similar to the case of $Al(OH)_3$(mC) and Bunsenite phases whose respective initial moles were zero. Both calcite and brucite were in equilibrium with the solution as the saturation indices recorded for both was zero.

When the saturation index is positive it is an indicator that the solution is supersaturated with the mineral phase and hence the phase is likely to precipitate. Often when there is no equilibrium, then the saturation state merely indicates the direction the processes may go. In the case of sub-saturation, dissolution is expected, whereas supersaturation suggests possible precipitation [123, 124].

Delta, d_phase is therefore a very significant parameter in hydrogeochemical modeling as it gives both qualitative and quantitative information about a mineral phase as to whether or not, it dissolves, precipitates or whether a new (secondary) phase has been formed, from different ash-water-brines-

organics systems/modeling scenarios. Secondly, it shows how much of the mineral phase gets dissolved, precipitated or formed at particular pH values. In this study delta values are given in moles of phase/Kg dry ash modelled.

Phase dissolution graphs showing the amount of phase dissolved and/or remaining during the ANC leaching simulation were also drawn. It is from such simulation data that the leaching chemistry of the interaction of fly ash in different ash-water-brines-organics systems/modeling scenarios was inferred.

(ii) Absolute change in phase assemblage, delta_delta; (d^1)

This parameter gives the difference in delta d_phase values of each mineral phase as generated from two distinct modeling scenarios of the same pH, one of which is kept as the reference.

In this study, the simulation of the ash recipe with demineralised water (DMW) was maintained as the reference, i.e. $d\_phase_{(ash+DMW)}$. All other modeling scenarios were carried out with a view to compare the effect of the interactions of ash, and how much of that effect, in different ash-water-brines-organics systems. The absolute change is given in Equation 2

$$\text{Absolute change in delta, delta\_delta } (d^1) = d\_phase_{(scenario)} - d\_phase_{(\text{reference scenario})} \quad \text{Equation 2}$$

In this study, reference scenario is that of ash and DMW; where DMW denotes demineralised water.

When $d^1 > 0$, two cases are likely: either $d\_phase_{(reference\ scenario)} > d\_phase_{(scenario)}$ in which case the mineral dissolves more in demineralised water (reference scenario) than in the other scenario, or $d\_phase_{(scenario)} > 0$, meaning that there is precipitation of the mineral phase taking place at the respective pH values.

For instance, in order to capture the effects of combined brines on the ANC of ash, d^1_anhydrite was calculated as shown in Equation 3.

$$d^1\_anhydrite = d\_anhydrite_{(ash+combined\ brines)} - d\_anhydrite_{(ash + DMW)} \quad \text{Equation 3}$$

(iii) Relative change of delta_delta, (Rc_d^1)

This parameter is considered as the one that gives comparative influence of a given component in any of the modeling scenarios with respect to the reference scenario. It is a ratio of the absolute change of delta d^1 to that of the reference modeling scenario, (i.e., $d^1\_phase/d^1\_phase_{(ash+DMW)}$) as given by the following general expression, Equation 4:

$$Rc\_d^1 = (d\_phase_{(scenario)} - d\_phase_{(reference\ scenario)}) / d\_phase_{(reference\ scenario)} \quad \text{Equation 4}$$

and in our study as indicated in Equation 5:

$$Rc\_d^1 = (d\_phase_{(scenario)} - d\_phase_{(ash+DMW)}) / d\_phase_{(ash+DMW)} \quad \text{Equation 5}$$

In this study, the relative change in delta_delta (Rc_d^1) is taken as a very important parameter which compares the absolute change to the reference scenario value. It gives information as to how many times a phase is more soluble (or less soluble) in a given scenario, compared to that of ash-water system (reference scenario). This is significant for prediction purposes, in terms of determining how much a given phase is likely to dissolve or precipitate when subjected to environmental scenarios. This would be possible if the quantitative dissolution chemistry of that phase is known in the DMW reference scenario at a given pH.

3.3 Results and Discussion

The modeling results of leaching behaviour of fly ash when in contact with brines and organics contained in brines are presented. The main highlights are; (i) the mineralogical changes that ash undergoes; (ii) the effects on the ANC of ash and; (iii) insights of the metal leaching capacity of fly ash under different leaching scenarios. PHREEQC modeling output data was graphically presented and analyzed to determine the potential significance of the impact of organic ligands (in sewage waste) on the ANC of ash with brines in different scenarios. For neo-formed phases, the quantification and characterisation of the products formed and the species they control quantatively in solution was also reported, which gives insights as to the relation of leachate chemistry to the mineral phases of the fly ash modelled. Graphs for Log C-pH diagrams of elemental totals giving the total dissolved elements species for each pH were drawn. An increase in elemental totals (TOT, in molality) indicated that mineral dissolution was occurring, whereas a decrease indicates that the elements in solution are precipitate out or new mineral formation is taking place. When TOT does not change with pH yet some species show an increase and others a decrease, this could be a pointer of ion exchange or possible simultaneous processes of mineral dissolution and precipitation.

3.3.1 Model calibration of the ANC of fly ash with demineralised water (DMW)

The value of any model's predictions is only as good as the model's ability to be effectively calibrated. There should always be an attempt to calibrate a model, whether it's a numerical or analytical model. Without model calibration it would not be possible to assess whether predictions made with the model are reasonable. Our model calibration was carried out with an attempt to demonstrate that the model and its parameter values were reasonably representative of the experimental conditions carried out by Petrik and co-workers [11] for the ANC of fresh fly ash from Secunda with demineralised water.

The simulation (model) and experimental results for elemental leaching of major and minor elements against pH were given in Figures 3.1a and 3.1b as released from the originally modeled Secunda ash recipe during the ANC with demineralised water. The experimental and simulation results are in the same order of magnitude for most of the elements (Ca, Mg, Na, Li, Al, Sr, Ni, S(6), Cr and Mo) and showed very good fitting between the experimental and modeled data under the modeled conditions. The Ca and Sr plots showed similar trend in the model and experimental, which shouldn’t be surprising due to similar calibration. The discrepancy between the modeled and experimental results for Si, and Cr at lower pH value less than 6 could possibly be attributed to some experimental errors in the analysis. A general agreement between the simulations (model) and experimental (Expt) results in the distribution of the main cations and anions in the aqueous solution (Figures 3.1a and 3.1b) would indicate that the assumption of local equilibria among the aqueous species and the secondary mineral phases was reasonable for static neutralizing processes of the fly ash. This agreement therefore lends support to our equilibrium model for the major neutralization reactions in an ash-water closed system. The modeling parameters used for the calibration were therefore used for modeling the subsequent ANC scenarios of Secunda fly ash with artificial sewage waste organics and brines.

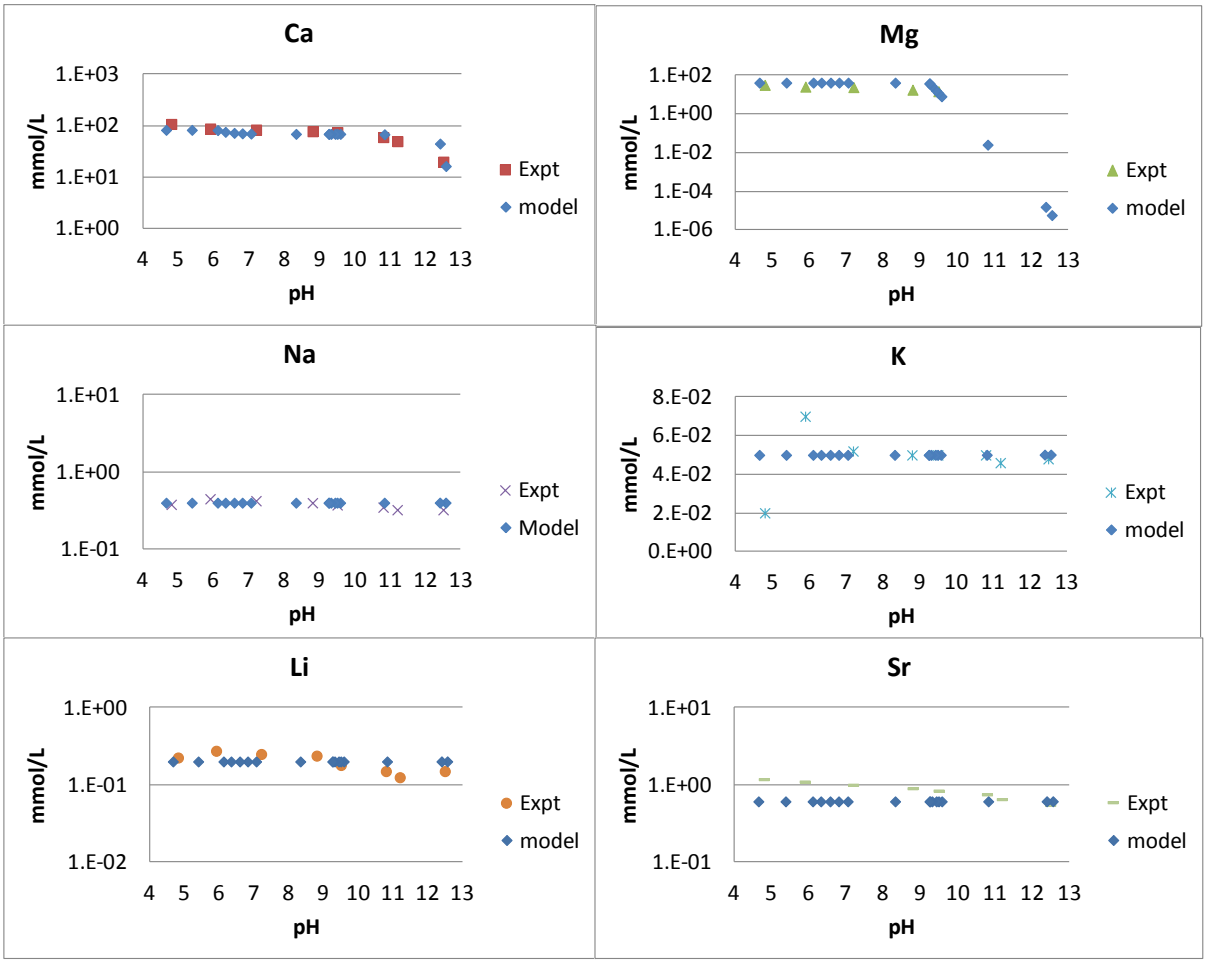

Figure 3.1a: Model calibration graphs comprising of major and minor elemental concentrations in leachate (Ca, Mg, Na, K, Li and Sr) against pH during ANC of fly ash with dimineralised water (DMW): (Expt = Experimental, and model = simulated data).

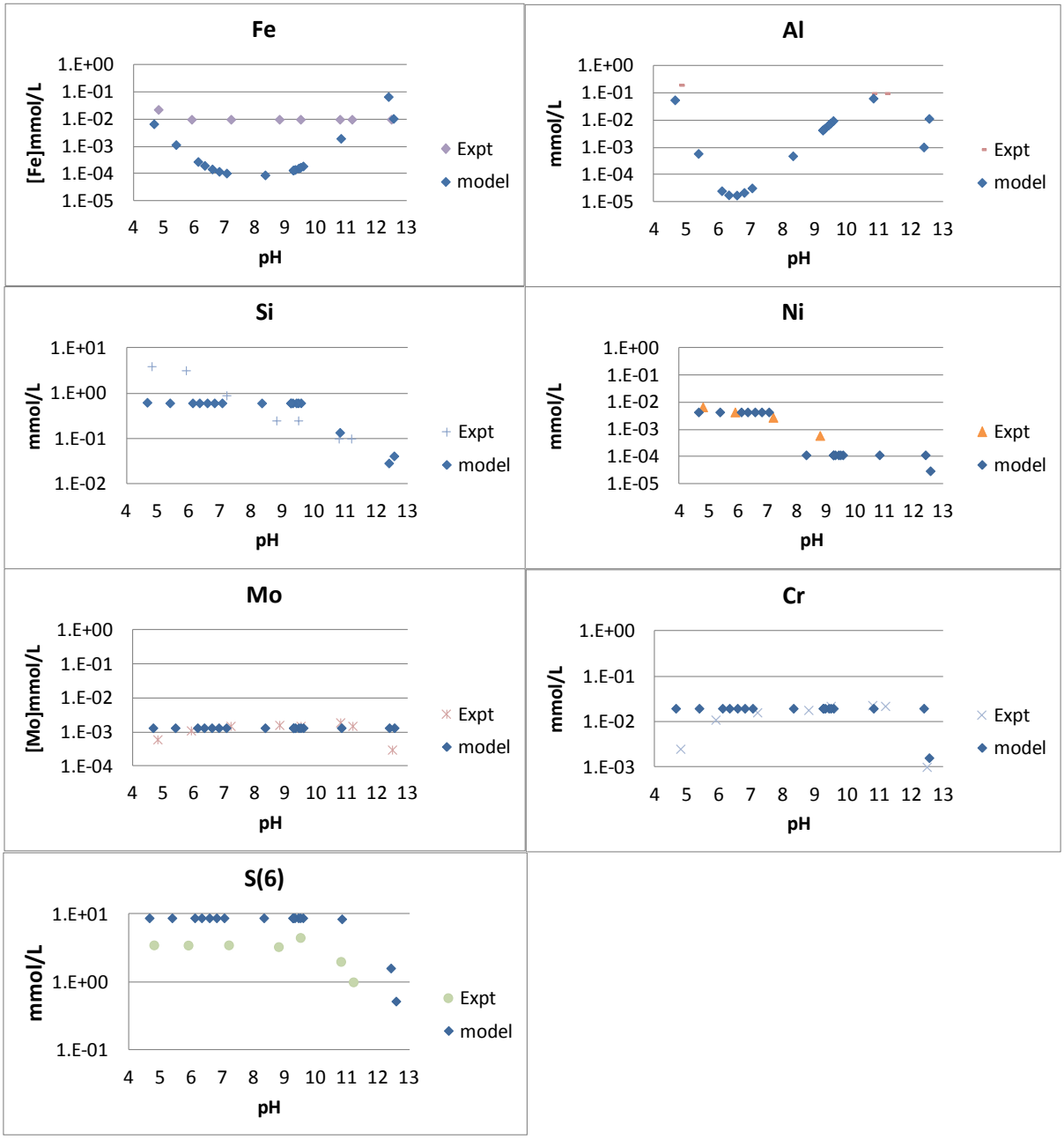

Figure 3.1b: Model calibration graphs comprising of major and minor elemental concentrations in leachate (Fe, Al, Si, Ni, Mo, Cr, and S) against pH during ANC of fly ash with demineralised water (DMW): (Expt = Experimental, and model = simulated data).

3.3.2 Effect of artificial sewage waste (ASW) organics and combined brines on acid neutralization capacity (ANC) and mineralogy of fly ash

Nine modeling scenarios were considered in order to capture the effect of the ANC of fly ash with organics and with brines. These scenarios were;

i. ANC of ash with combined brines

ii. ANC of ash with no brines (with DMW)

iii. ANC of ash with ASW organics and combined brines

iv. ANC of ash with ASW organics and individual brines (Ca^{2+}, Mg^{2+}, Na^{+}, SO_4^{2-}, CO_3^{2-} and Cl^{-} brines); this constituted six scenarios (**Appendix 1: Table A2**).

The ANC simulation results of the modelled scenarios were presented as titration curves given in Figure 3.2.

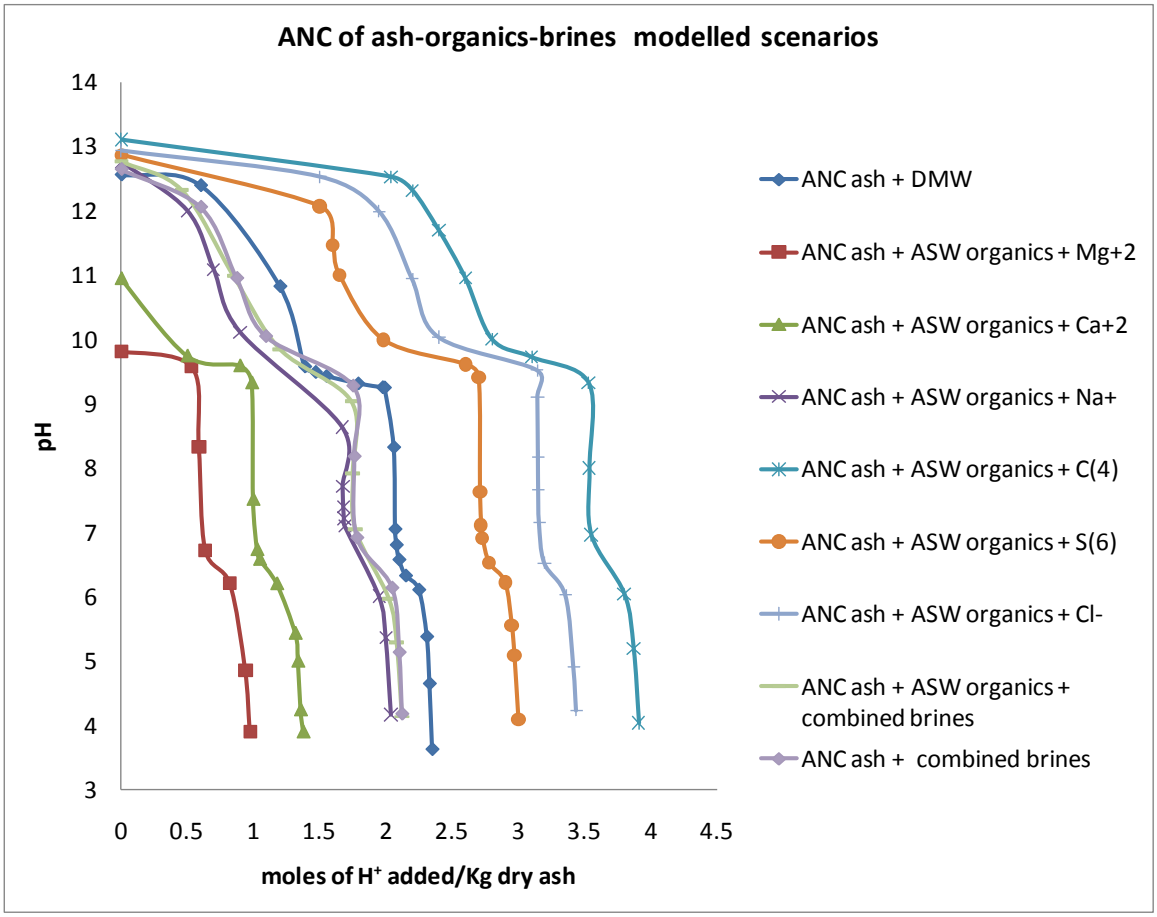

Figure 3.2: ANC simulation results of various scenarios for Secunda fresh fly ash with demineralised water (DMW), brines and artificial sewage waste (ASW) organics

The acid neutralization behaviour of the fresh Secunda ash under different modeling scenarios was evaluated by plotting the pH attained as a function of equivalent moles of acid added per kilogram of dry ash as given by Figure 3.2. Acid neutralization capacity was calculated as the amount of moles equivalent of HNO_3 acid required to lower the fly ash pH to 4.5. Normally, target pH values between 4.5 and 4.7 are common analytical tools used as a measure of the capacity of solutions to absorb acid (ANC) without major ecological consequences [125]. From Figure 3.2, the fly ash showed high alkalinity during the early stages of batch leaching (at lower acid addition), having a pH range between 9.8 (for ASW organics in Mg-brines) and 13.1 (for ASW organics in carbonate brines) before any acid addition. The curves from Figure 3.2 indicate a pH region of high buffer capacity occurring between pH 9 and 10.2 and also at initial higher pH between pH 12.5 and 13.1 which may be possibly due to some newly formed minerals during the ANC modeling. The presence of different constituents of brines subjected to ANC resulted to different ANC capacities ranging from 0.98 moles H^+/Kg dry ash (of ash-organics mixed with Mg-brines) to 3.87 H^+/Kg dry ash for those with the C(4) brines. As expected, the ones of the cationic brines were found on the lower region of acid addition (in the order

Mg-brines < Ca-brines < Na-brines) while the anionic brines were found at the upper region of acid addition (in the order S(6)-brines < Cl-brines < C(4)-brines). In the middle region of acid addition were three important scenarios: that of ash with brine, ash without brines (i.e. ash with DMW) and ash with both ASW organics and combined brines. It was from these three scenarios that a generalization of the effect of brines and organics on the ANC was inferred. The ANC of ash with demineralised water (DMW) was 2.33 mol H^+/Kg dry ash and that of ash with ASW organics lower at 2.12 mol H^+/Kg dry ash which was the same value as that of ash with combined brines. This indicated that brines decreased the ANC of ash by about 9.01 % decrease and which could be attributed to the dynamics of solid phase dissolutions in response to the acid addition. The presence of ASW organics did not show significant contribution to the change in the ANC of ash as evidenced from Figure 3.2 in which the major cations and anions of the individual brines could have been the major contributor on ANC changes. It was also observed that in the pH regions of low buffer capacity such as the initial pH range of 10 to 12 and generally between the range of 7 to 9, the slopes of the curves generated for all scenarios are essentially the same or similar.

3.3.3 Comparison of three modeled scenarios and chemistry of elements: Ash with demineralised water (Ash-DMW), ash with demineralised water with artificial sewage organics (Ash-ASW Organics) and ash with combined brines

The leaching of the elements was studied from the simulation results of the ANC of fly ash in three main scenarios; ash with brines, ash without brines (i.e. ash with DMW) and ash with both ASW organics and combined brines. The simulation results were presented by drawing log C-pH diagrams given by Figure 3.3, which shows mainly the major and minor elements found in the fresh Secunda fly ash recipe for the three modeled scenarios. The log concentration was based on the molal (moles/Kg of water) concentration of the elements.

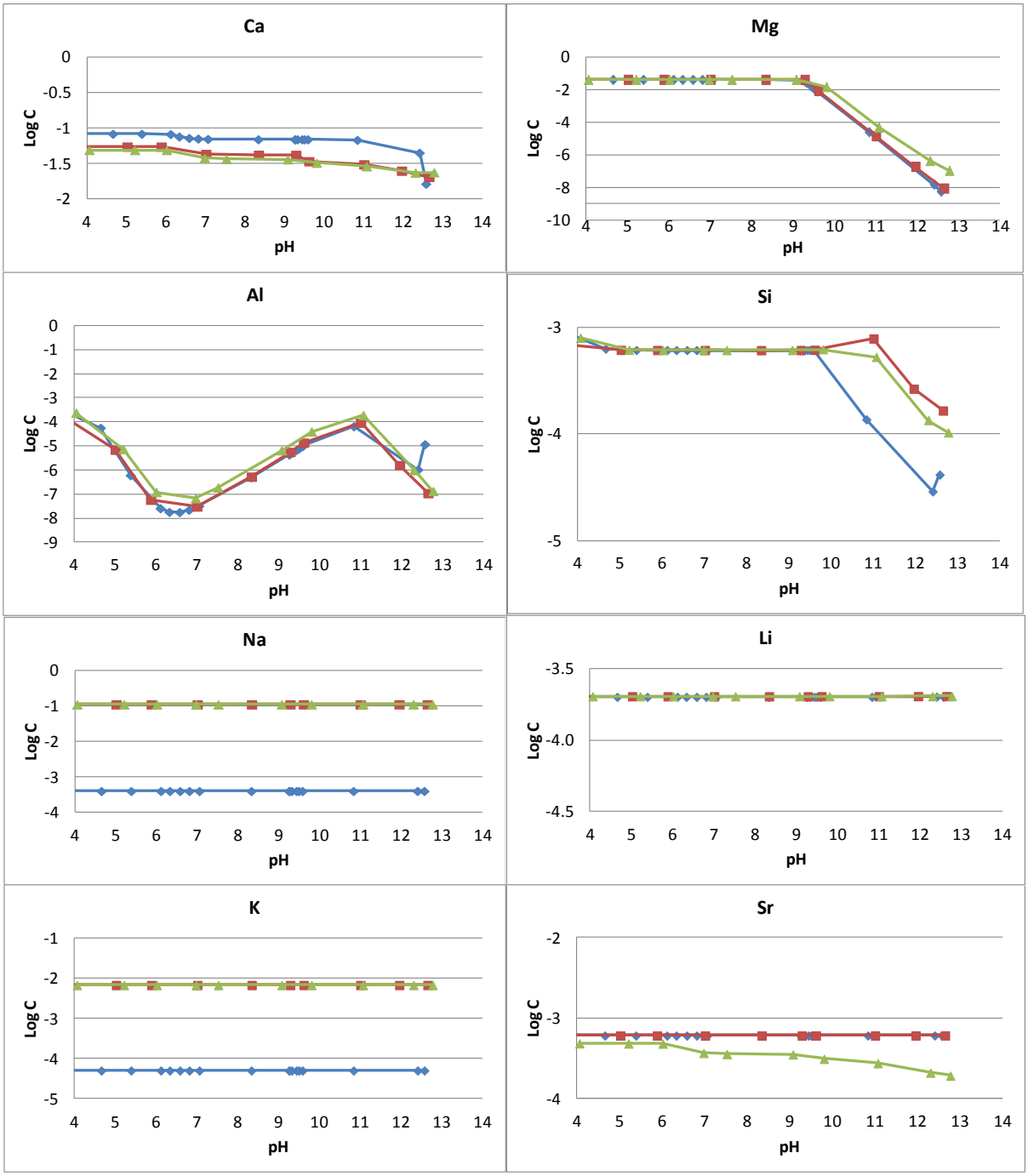

Figure 3.3a: Simulated Log C-pH diagrams for the release of major and minor elements from ANC of Secunda fly ash modeled with (i) demineralised water (DMW), (♦), (ii) combined brines, (■) and (iii) artificial sewage waste (ASW) organics in brines, (▲).

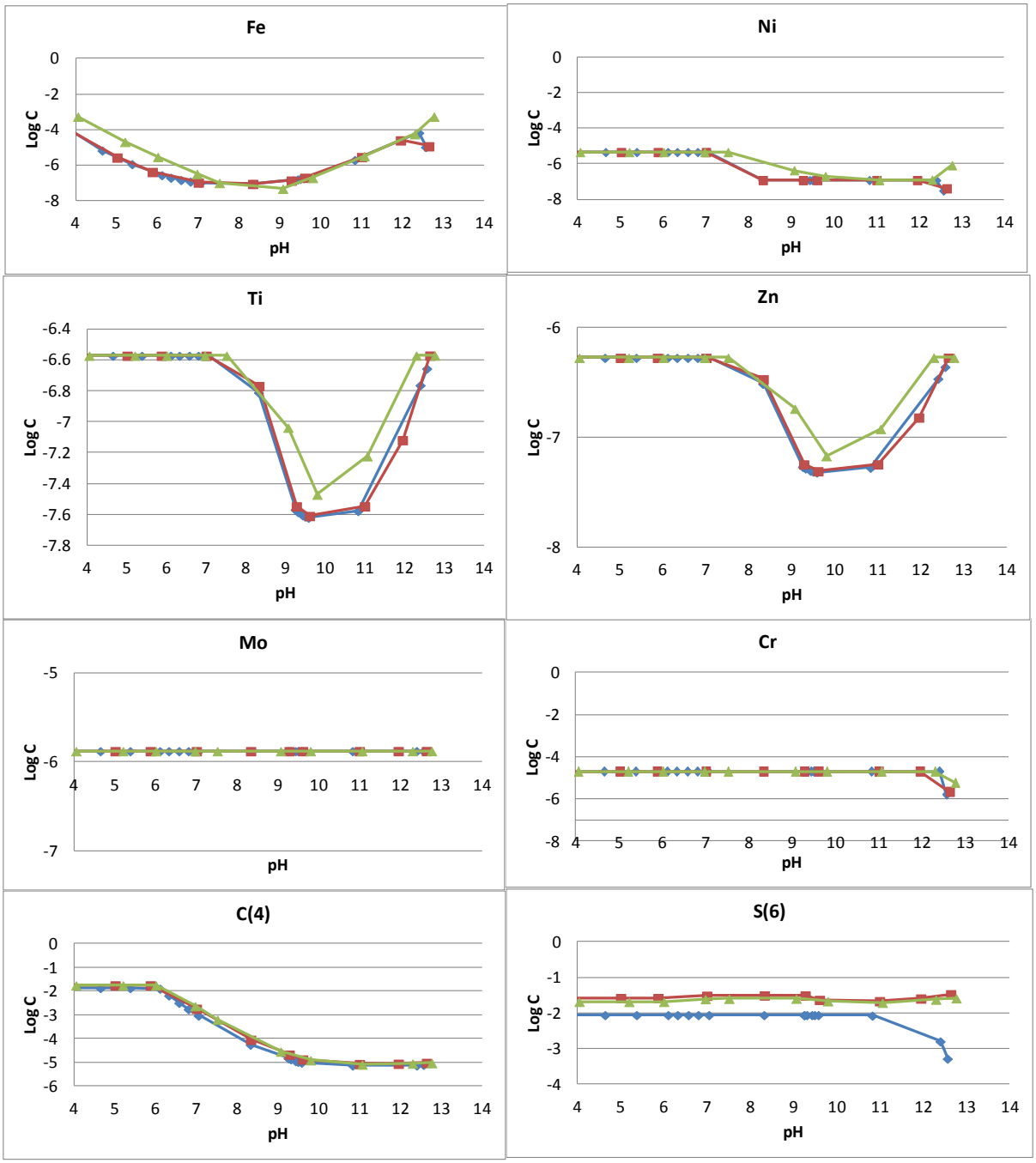

Figure 3.3b: Simulated Log C-pH diagrams for the release of major and minor elements from ANC of Secunda fly ash modeled with (i) demineralised water (DMW), (♦), (ii) combined brines, (■) and (iii) artificial sewage waste (ASW) organics in brines, (▲).

The Log C-pH diagrams for Figure 3.3(a and b) are discussed with respect to the elemental release for the Ca, Mg, Na, K, Li, Sr, S, Cl, Fe, Al, Si, Ni, Mo, Cr, and S as follows:

3.3.3.1 Calcium Log C-pH diagrams

From the results in Figure 3.3a, it can be noted that the release of the element Ca showed a limited increase with decrease with pH. The solubilisation in the three scenarios takes a similar trend, however, the fly ash-DMW system released more Ca at all pH levels than the other two which had almost the same release value at all the pH values. The higher soluble concentrations of Ca with decrease in pH might be coming from the dissolution of the various Ca-bearing mineral phases such as $Ca(OH)_2$, $CaSO_4$, CaO, gypsum, etc. Amongst the alkali metals, Ca showed the highest release as compared to Mg, Na, K and Li and other major and minor elements, in all the scenarios (with the exception of Na in ash-organics and brines scenarios which was slightly higher).

3.3.3.2 Magnesium Log C-pH diagrams

The release of Mg increases steadily between pH 12.8 and 9 for all the three modeled scenarios, with the release from the ash-ASW organics-brines system recording slightly higher order of magnitude than the other two. The presence of organics may have resulted to the formation of soluble Mg complexes with the organic ligands, thereby contributing to the overall soluble Mg concentration. Further decrease of pH from 9 to 4 did not cause much change in the solubility of Mg for all the scenarios as they all recorded same amounts of dissolved Mg.

3.3.3.3 Alkali Metals: Log C-pH diagrams

Na, K, and Li exhibited constant solubilisation which was independent of pH changes from all the scenarios. However Na and K release levels from ash-DMW scenario were lower than those of ash-organics-brines systems, which was expected as fresh ash was modeled to be having small quantities of Na and K existing as free ions coming from very soluble phases of possibly oxides or salts in the recipe and addition of brines must have increased the Na and K levels in the ANC model. The Ca, Mg, Na, K, and Li metals and their hydroxides and carbonates could be the major contributors of ANC for an alkaline buffer and therefore might offer an alkalinity buffer in a given ash disposal system. This phenomenon gives credence to the suggested possible applications of fly ash in providing necessary alkalinity, particularly for landfill biostabilization, anaerobic digestion and soil amendments among others [126] and possible acid mine drainage remediation which require alkalinity.

3.3.3.4 Trace/heavy elements: Log C-pH diagrams

For the heavy and trace metals in Figure 3.3b, (Cr, Zn, Ni, Al, Mo, Fe), all the scenarios showed similar trend in the levels of release with change in pH, with ash-ASW organics-brines scenario exhibiting slightly higher order of magnitude in some cases than those of the other scenarios. Complexation reactions with the organics may be attributed to this phenomenon and which increased solubilisation of the metals. For Cr, solubility increases at only very high pH between 12.8 and 12 and soluble concentration of Cr remain constant all the way to the lower pH values. Mo showed constant solubilisation just like the case of the Na, K and Li.

Two broad leaching behaviours as a function of pH were observed from the three fly ash-ASW organics-brines scenarios (i) leaching of Ca, Mg, Ni and Sr follows a cationic pattern where the concentration decreases monotonically as pH increases; (ii) leaching of Al, Fe, Ti and Zn follow an amphoteric pattern where the concentration increases at acidic and alkaline pH, although Al showed some anomaly from pH 11 where the concentration decreased with the increase in pH. Al showed an amphoteric pattern in which its release increased between pH 12.8 and 11 for all the scenarios and then decreased with decrease in pH down to neutral pH of 7. This could be due to solubility effect in which some precipitation of Al-complexes may occur which would reduce the amount of soluble Al in the leachate. The trend changed upon a decrease in pH so that the release of Al increased progressively as pH decreased. This was as a result of dissolution of Al complexes under the acidic conditions. The leaching of Al could also be controlled by amorphous forms of $Al(OH)_3$ for pH ranging between 6 and 9, and possibly by gibbsite ($Al(OH)_3(c)$) for pH higher than 9 as suggested by Lo and co-workers [126] and Mizutani and co-workers [127]. Ti, Fe and Ni release also showed a similar trend of amphoteric behaviour with pH changes. Their release decreased with a decrease in pH up to about pH 9.5 and then started to increase progressively up to pH 7 after which it remained constant with further decrease in pH. However a higher order of magnitude was recorded for the Fe released from the ash-ASW-brines scenario compared to the other two. Ni release was constant and of equal magnitude in all the three scenarios at pH lower than 7. Molybdenum also showed a relatively constant release throughout the pH range and the amount released from the three ash-ASW-brines scenario were the same, indicating the Mo release was pH independent.

Some consistency in the leaching behaviour for many elements was observed across the pH range, indicating that the release of elements was mainly solubility-controlled. The release of Si showed a general steady increase in the three scenarios with a decrease in pH between 13 and 11. However, the three scenarios had different orders of magnitude in the following order: ash-combined brines > ash-(ASW) organics-brines > ash-demineralised water (DMW). A slight decrease was registered for the ash-ASW organics and ash-combined brines up to pH 9.5 as the ash-DMW showed continued steady

increase up to that of pH value of 9.5. The three scenarios then showed steady state phenomenon with an equal order of magnitude but with a slight increase between pH 5 and 4. Molybdenum recorded a steady state with equal order of magnitude for the three modeled scenarios suggesting that the release of Mo was pH independent but could be influenced by other factors. For those elements that showed some discrepancy and inconsistency at a certain pH, such as Ni, Al and Si, other release-controlling mechanisms such as sorption, or solid-solution formation might not be ruled out even though they were not factored in by the model. In these simulations, hydroxide precipitations were assumed to be potential immobilization mechanisms for the metals [128]. The elements were also assumed to form soluble hydroxide complexes which contributed to increased release of some of the elemental concentration.

3.3.3.5 Anions: Log C-pH diagrams

The ash-DMW scenario showed the lowest levels of S(6) element release among the three modelled scenarios, with the initial levels at pH 12.8 registering about one and half orders of magnitude lower than the other two scenarios of ash-ASW organics and that of ash-combined brines systems. A progressive increase was registered between pH of 12.8 and 11 after which the concentration remained constant up to pH of 4. The two ash-ASW organics-brines scenario simulations gave a similar trend across the modeled pH range. However the ash-ASW organics-brines scenario showed slightly lower levels for S(6) release than that of the ash-brines scenario. The two scenarios exhibited a slight decrease in release levels of S(6) between pH values 12.8 and 9.5, followed by a slight increase at pH 9. The solubilisation was constant up to pH 7 then a slight decrease between pH 7 and 4.

The C(4) release showed a progressive increase with the decrease in pH up to 6 after which it remained constant for all the three scenarios. It showed almost a similar monotonic trend amongst the three modeled scenarios.

From the above modeling work, it was revealed that co-disposal of fly ash and brines does not show a significant difference in the leaching of elements (except Sr) compared to that of ash disposal without the brines and the organics in the brines. This would therefore indicate that the fly ash may not behave as a salt sink in ash dumps as originally thought at the onset of the main project and neither would the continued co-disposal of fly ash with brines have major impacts on the release of elements into the environment. However since the modeling did not take into account possible carbonation by atmospheric CO_2 (open system), more insights will be explored in future modeling. Further work will be done on the dynamic leaching modeling using columns so as to understand the reaction and transport mechanisms involved during the ash-brines interactions.

Much of the release chemistry of the elements discussed in **section 3.3.3** was closely related to the phase dissolution/precipitation and formation as the major controlling factors. This is articulated in **section 3.3.4** below which showed mineralogical transformations of the fly ash mixed with ASW organics and brines at various pH values during the ANC modeling.

3.3.4 Effect of artificial sewage waste (ASW) organics and combined brines on mineralogy of fly ash during acid neutralization capacity (ANC) modeling

The mineralogical transformations of fly ash after coming into contact with ASW organics and combined brines were studied using the simulation results of the modeling of fly ash mixed with ASW organics and combined brines. The simulation data were presented in the form of graphs given in Figure 3.4 showing mineral phase profiles of dissolution, precipitation and formation, at given pH values. Figure 3.5 represents the ANC simulation results of the ash-combined brines scenario. Considered in these two modeling scenarios were only those phases that showed significant quantitative changes at different pH values. These results supplement and give further insights into the release mechanisms and confirmation of certain phases as controlling the release of some of the elements discussed in **section 3.3.3**.

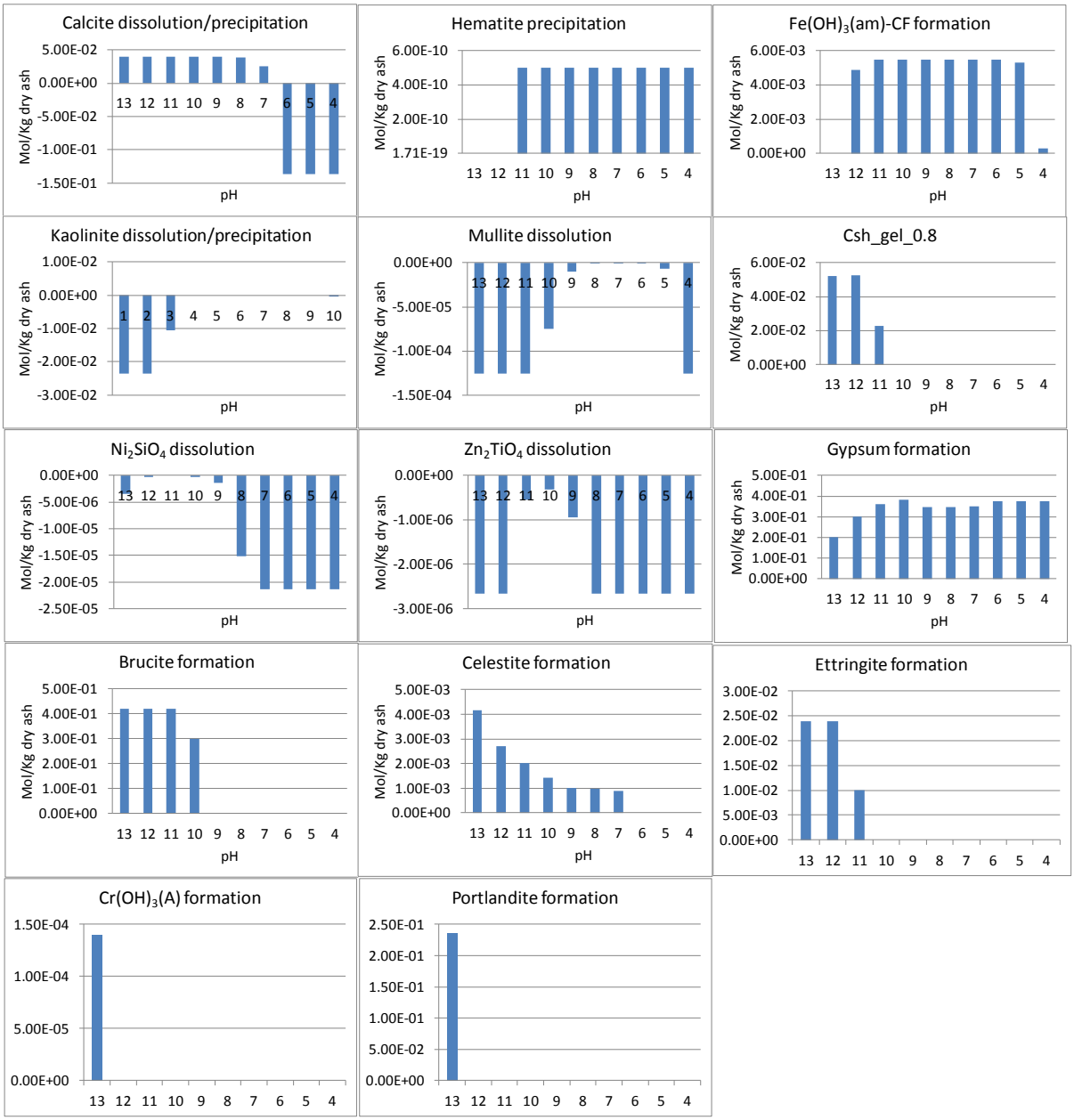

Figure 3.4: Mineralogical transformation based on ANC of fly ash with ASW organics-combined brines scenario: for only those phases that showed quantitative changes at different pH values. (Positive values indicate phase precipitation or new phase formation, negative values indicate phase dissolution).

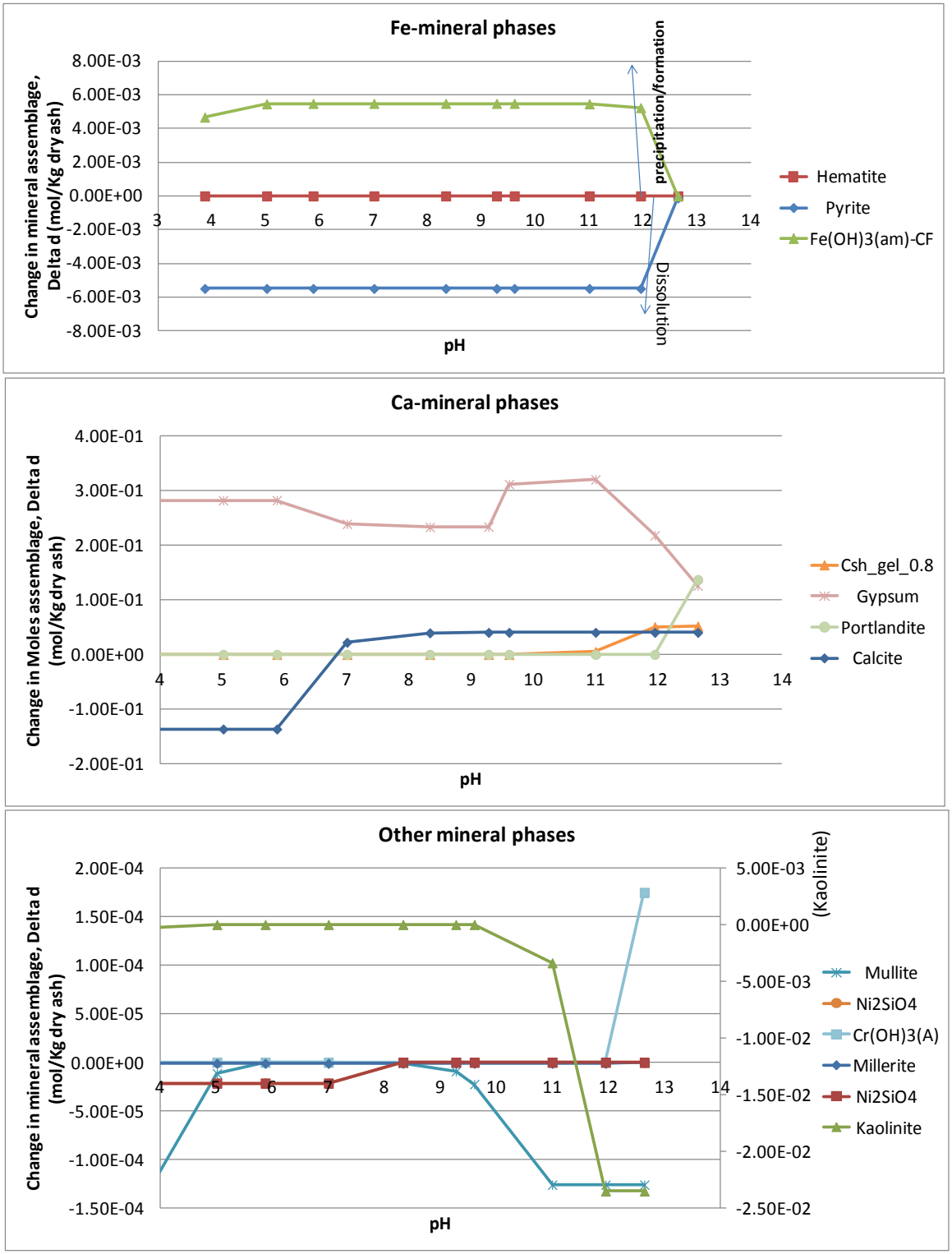

Figure 3.5: Change in mineral assemblages against pH during ANC of fly ash with combined brines only. (i.e. with no ASW organics). Positive delta values indicate precipitation and negative delta values indicate dissolution.

The mineralogical changes from the two scenarios of fly ash interactions with combined brines-ASW organics and fly ash with combined brines, (Figure 3.4 and Figure 3.5 respectively), were almost the same and showed similar trends for the majority of the mineral phases. The minerals in the original modeling ash recipe which showed dissolution of all the respective initial amounts across the pH range of 13 to 4 were not included in these graphs as their d_phase value was zero. Some of these mineral phases were anhydrite, $CaMoO_4$, $CaCrO_4$, lime, millerite, periclase, pyrite and $SrSiO_3$ that were originally present in the ash recipe. The total dissolution of these minerals would therefore be controlling the concentration of their constituent elements release during the ANC modeling previously discussed in **section 3.3.3**.

The results of the ANC simulation showing mineralogical changes are discussed and an attempt made to relate these changes to the release chemistry trends of the elements highlighted in Figure 3.3.

From Figures 3.4 and 3.5, the following observations were made and discussed.

Calcite ($CaCO_3$), and gypsum ($CaSO_4.2H_2O$): These two mineral phases showed complementary trends of dissolution and precipitation across the entire pH range (13 to 4). Dissolution of calcite resulted to precipitation of gypsum to almost the same extent. In the case of calcite almost equal amounts of calcite precipitated at higher pH values between 13 and 9 (4.03E-02 mol/Kg dry ash) whereas gypsum recorded an increased trend of formation within the same pH range (from about 0.2 to 0.35 mol/Kg dry ash). A higher amount of precipitated gypsum within the pH range of 13 and 8 was also augmented by the dissolution of other Ca-bearing minerals namely the Csh_gel_0.8 ($Ca_{0.8}SiO_{2.8}$:H_2O) and portlandite ($Ca(OH)_2$) at high pH levels. This is well captured in Figure 5. However between pH 9 and 7 the amount of calcite precipitating decreased with the decrease in pH, recording the lowest amount, 2.54E-02 mol/Kg dry ash at pH 7. At pH values lower than 7 calcite dissolved with an equal amount (1.36E-01 mol/Kg dry ash) across the pH range down to pH 4. Interestingly in same pH range, gypsum recorded a proportionally increased precipitation in both scenarios as shown in Figure 4 and 5. It should also be noted that the presence of the brines causes a general increase in the quantities of calcite and gypsum (either precipitated or dissolved). This means the dissolution of one of the controlled phases, that is, either the precipitation of calcite or gypsum or dissolution of either. This could explain the lack of a significant change in the trend of release levels of total Ca in Figure 3.3a (**section 3.3.3)**. Generally, the dissolution and precipitation mechanisms of calcite and gypsum play an important role in the release chemistry of their constituent elements, mainly Ca and C.

Kaolinite ($Al_2Si_2O_5(OH)_4$): The amounts of kaolinite that dissolved at high pH of 13 and 12, were equal, (2.35E-02 mol/Kg dry ash), but reduced at pH 11 (to 1.04E-02 mol/Kg dry ash). However negligibly small and equal amounts (5.00e-10 mol/Kg dry) of kaolinite were recorded at pH 10 and 5

followed by dissolution at pH 4 (3.12E-04 mol/Kg dry ash). The general negligible amounts of kaolinite dissolution and precipitation underscored the high stability of kaolinite under the normal environmental scenario. Kaolinite may be less controlled by physico-chemical factors and more controlled by mechanical forces, resulting partly from kaolinite's larger particle size and more irregular particle arrangement. Large overburden pressures also improve kaolinite's resistance to chemical damage [129].

Mullite ($Al_6Si_2O_{13}$): All the initial amounts (1.26E-04mol/Kg dry ash) dissolved at high pH values of 13 to 11, then the amount reduced progressively as the pH decreased to 6. Increasingly higher amounts were recorded at pH 5 and with a maximum amount recorded at pH value 4, an amount equal to that recorded at pH 13. This could be due to amphoteric nature of the mullite which augments the explanation given for the release chemistry of the Al and Si in **section 3.3.3**. The dissolution and precipitation mechanisms of mullite and kaolinite therefore play an important role in the release chemistry of their constituent elements, mainly Al and Si (**section 3.3.3**).

Ni_2SiO_4: For ash-organics-brines scenario, 3.40E-06 mol/Kg dry ash dissolved at pH 13. However, the dissolved amount was observed to reduce drastically at pH 12 such that at pH 11, no dissolution occurred (Figure 3.4). Interestingly, dissolution of this phase appeared again at pH 10 and the dissolved amount increased progressively with the decrease in pH down to 7 where the dissolved amount was 2.14E-05 mol/Kg dry ash. At pH 4, the entire initial amount dissolved. A similar trend was observed in the ash-brines scenario as shown in Figure 3.5 which also displayed the above mineralogical trends of Csh_gel_0.8, kaolinite, and mullite. The dissolution of Ni_2SiO_4 is expected to contribute to the observed release trends of Ni and Si elements in Figures 3.3a and 3.3b.

Zn_2TiO_4: The initial amounts dissolved completely at high pH 13 and 12. However the dissolved amount reduced progressively with the decrease in pH, down to pH 10 at which value an amount of 3.11E-07 mol/Kg dry ash dissolved. However a further decrease of pH from 10 to 8 recorded a progressive increase of phase dissolution amounts. A complete dissolution of the initial amount again occurred at pH 8 and below down to pH 4. Notably equal dissolved amounts at pH 13, 12 and 8 - 4 were observed. The amphoteric nature of Zn_2TiO_4 could attribute to this observed behaviour. The dissolution phenomena could explain the release chemistry trends for the Zn and Ti elements.

Hematite (Fe_2O_3): this phase showed negligible precipitation across the pH range 13 - 4. The lowest dissolved amount (1.71E-19 mol/Kg dry ash) was recorded at highest pH of 13. This low solubility behaviour is expected as depicted in the model results. At pH values lower than 12, equal amounts (5.00E-10 mol/Kg dry ash) were precipitated and a decrease in pH to 12 precipitates 5.00E-10 mol/Kg dry ash, an amount that was negligible and remained constant even at the rest of the lower pH values.

Neo-formed mineral phases: Some new phases were formed in the two modeled scenarios, as shown in Figures 3.4 and 3.5. These included $Fe(OH)_3$(am)-CF, brucite, celestite, Csh_gel_0.8, Ettringite, gypsum, portlandite and $Cr(OH)_3$(A). Most of the above secondary mineral phases could have been obtained by hydration of fly ashes under the different pH conditions which were confirmed from the XRD analytical work carried out by Gitari and co-workers [122] being part of the Phase I major ash-brine project work.

$Fe(OH)_3$(am)-CF: This was a new phase formed at pH 12 though in negligible amount of 4.90E-03 mol/Kg dry ash. The formed amount increased with a decrease in pH, up to a maximum amount of 5.50E-03 mol/Kg dry ash at pH 10. Below pH 10 down to 7, the same amount was recorded. Below pH value 7, the amounts formed decreased with the decrease in pH, with the lowest amount recorded as 3.09E-04 mol/Kg dry ash formed at pH 4. This behaviour was displayed by all the Fe-bearing minerals (hematite, pyrite and $Fe(OH)_3$(am)-CF) presented in Figure 3.5. The negligibly small amounts of hematite and the formation of $Fe(OH)_3$(am)-CF as a new phase would account for the decreased trends of Fe release, as discussed in **section 3.3.3**.

Portlandite ($Ca(OH)_2$), and $Cr(OH)_3$(A): The mineral phases formed only at high pH 13 recording 2.35E-01 and 1.39E-04 mol/Kg dry ash respectively. Brucite ($Mg(OH)_2$) formed maximum at pH 13, and a decrease in amount was recorded for each decrease in pH with the lowest value of 2.99E-01 mol/Kg dry ash at pH 10. Below pH 10, no brucite was formed. Celestite ($SrSO_4$) formed pH values 13 down to 7, and the amount decreased proportionally with the decrease in pH such that the maximum amount formed was recorded as 4.17E-03 mol/Kg dry ash at pH 13 and lowest as 8.8E-04 mol/Kg dry ash at pH 7. No celestite formation was recorded at pH less than 7. This showed that alkaline conditions favour celestite formation, Csh_gel_0.8 ($Ca_{0.8}SiO_{2.8}$:H_2O), brucite ($Mg(OH)_2$), portlandite ($Ca(OH)_2$) and $Cr(OH)_3$. Ettringite ($Ca_6Al_2(SO_4)_3(OH)_{12}$:$26H_2O$) formation only occurred at relatively higher pH values of 13, 12 and 11, with almost equal amounts formed at pH 12 and 11. Almost twice the amount of Csh_gel_0.8 phase to that of Ettringite was formed. Gypsum ($CaSO_4 \cdot 2H_2O$) formation occurred across the pH range 13 to 4 but showed a trend in which the amounts formed increased with the decrease in pH from 13 to 10, the latter recording the highest value of 3.83E-01 mol/Kg dry ash. A relatively lower amount of 3.46E-01 mol/Kg dry ash at pH 9, 8 and 7 was recorded. However, a higher amount of 3.76E-01 mol/Kg dry ash was recorded at pH values lower than 7. The neo-formation of these mineral phases could account for the trends observed showing decreased in release chemistry of their constituent elements at the above discussed pH values. Mg by brucite formation, Sr and S(6) by celestite, Ca, Al and S(6) by Ettringite, Ca and S(6) by gypsum and portlandite. The $Cr(OH)_3$(A) formation accounted for lowest release values at the highest pH of 13 as previously shown in Figure 3.3b. Some literature has suggested that Cr in leachates can be in equilibrium with amorphous or crystalline $Cr(OH)_3$ [130]. This trace element Cr

could also be associated with iron oxides and alumino-silicates, with the sorption-desorption chemistry taking a dominant role as discussed by Hareeparsad and co-workers [26], and Gitari and co-workers [122]. This therefore suggests that a possible combination of factors could be affecting the leaching of Cr, besides the pH and solubility controls.

Similar trends in the mineralogical and ANC simulation results for the two discussed scenarios were used as a pointer that ASW organics had no significant effects on the ANC of fly ash, in the subsequent discussions.

3.3.5 Effect of artificial sewage waste (ASW) organics and individual brines on mineralogy of fly ash under different acid neutralization (ANC) simulation scenarios

The results of simulation of fly ash with combined organics and brines captured a scenario that represented the normal occurrence in the environment. However there are times when the brines levels generated from the power stations do fluctuate at an individual element's level, a situation which would definitely affect the ANC and the leaching potential of the ash as well as the mineralogy of the ash. The extent to which the ANC is affected was studied based on simulation results previously presented in Figure 3.2. The effect on mineralogy was studied using the simulation results on mineral phase assemblages of the modelled scenarios for the ANC on ash and ASW organics in different individual brines. The latter included Mg^{2+}, Ca^{2+}, Na^{+}, CO_3^{2-}, SO_4^{2-}, and Cl^{-} brines as presented in Figure 3.6. Further supplementary information on phase assemblage simulation results on dissolution, precipitation and new phase formation is presented in **Appendix 1** (Tables A3 – A8) for ANC of fly ash with ASW organics and the individual brines. Most phases underwent total dissolution across the pH range 13 - 4. Some of these include anhydrite, $CaCrO_4$, $CaMoO_4$, lime, millerite, periclase and $SrSiO_3$ in all the individual brine scenarios. However there are some phases which showed variations in the mineral assemblages at particular pH values, with some even showing dissolution and precipitation at various pH values (e.g. kaolinite) whereas others showed no change at certain pH values. Kaolinite showed increased dissolution with increase in pH (with maximum dissolution values recorded at pH 12 and 13), although, negligibly small amounts were registered in all the brines.

Calcite showed precipitation within the pH range 13- 7 for ash and organic simulated with Ca, Mg Na and C(4) brines, all of which exhibited similar trends of equal amounts between pH 13 and 8 followed by a decrease down to pH 7. Dissolution of calcite was observed from pH 7 and below. A similar trend was observed for all other scenarios. Generally, equal amounts of calcite precipitated at pH

values above 7 in Mg^{2+}, Ca^{2+}, Na^{+} and CO_3^{2-} brines. No calcite precipitation was recorded in SO_4^{2-} and Cl^{-} brines. Below pH 7, an increasing calcite dissolution trend was registered with decrease in pH, and maximum dissolution generally taking place at pH values 4 and 5 in all brines.

From the original modeling ash recipe, anhydrite, $CaCrO_4$, $CaMoO_4$, lime, mullite, Ni_2SiO_4, periclase, $SrSiO_3$, Zn_2TiO_4 phases were some of the phases that showed dissolution characteristics across all the pH values between 13 and 4 as given in Figures 3.5. However, negligibly small levels of dissolution are exhibited for $CaMoO_4$, Ni_2SiO_4, and Zn_2TiO_4 in all the above scenarios, which controls the total concentration of their respective constituent elements as previously discussed in **section 3.3.3**.

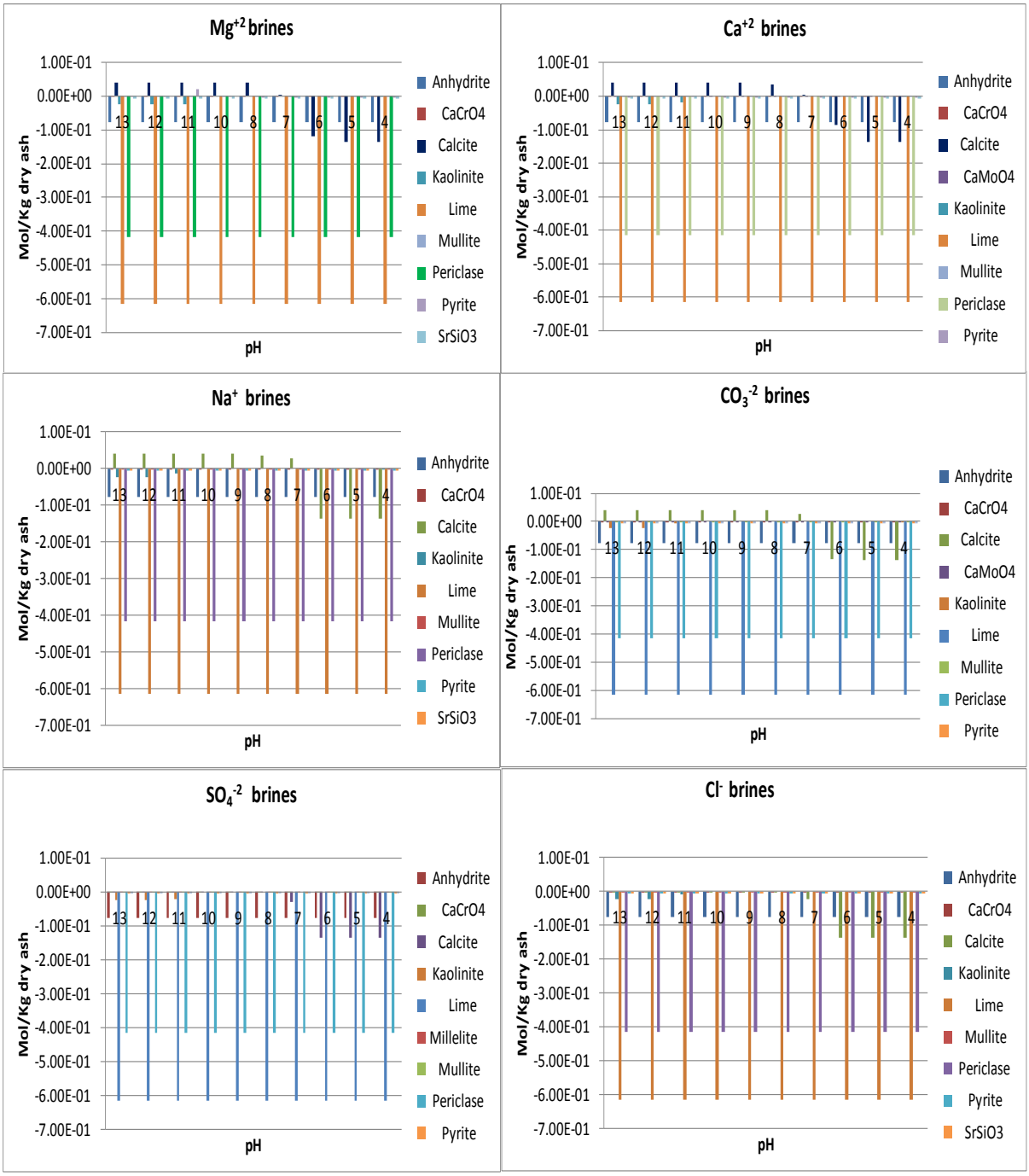

Figure 3.6: Phase assemblage graphs for ANC of ash-ASW organics interactions with individual brines (Mg^{2+}, Ca^{2+}, Na^{+}, CO_3^{2-}, SO_4^{2-} and Cl^{-}) for major mineral phases in the ash recipe. (Positive values indicate phase precipitation or new phase formation, negative values indicate phase dissolution). NB: Colors may not necessarily match for each of the mineral phases in the brines as generated.

Individual brines also caused the formation of new mineral phases (Figure 3.7) which were originally not present in the modelled fly ash recipe. Among these newly formed phases included $Fe(OH)_3$(am)-CF, brucite, Csh_gel_0.8, Ettringite, gypsum, portlandite, $Cr(OH)_3$(A), and celestite. Brucite was the predominating new phase in all the brines at pH values above 10 except for Ca^{2+} and SO_4^{2-} brines in which portlandite predominated only at pH 13. Gypsum predominated at pH values 10 and below, with similar quantitative trend in the three cationic brines and SO_4^{2-} brines. The highest amounts of gypsum were recorded with the Ca^{2+} brines. Gypsum formation was not recorded with CO_3^{2-} and Cl^- brines.

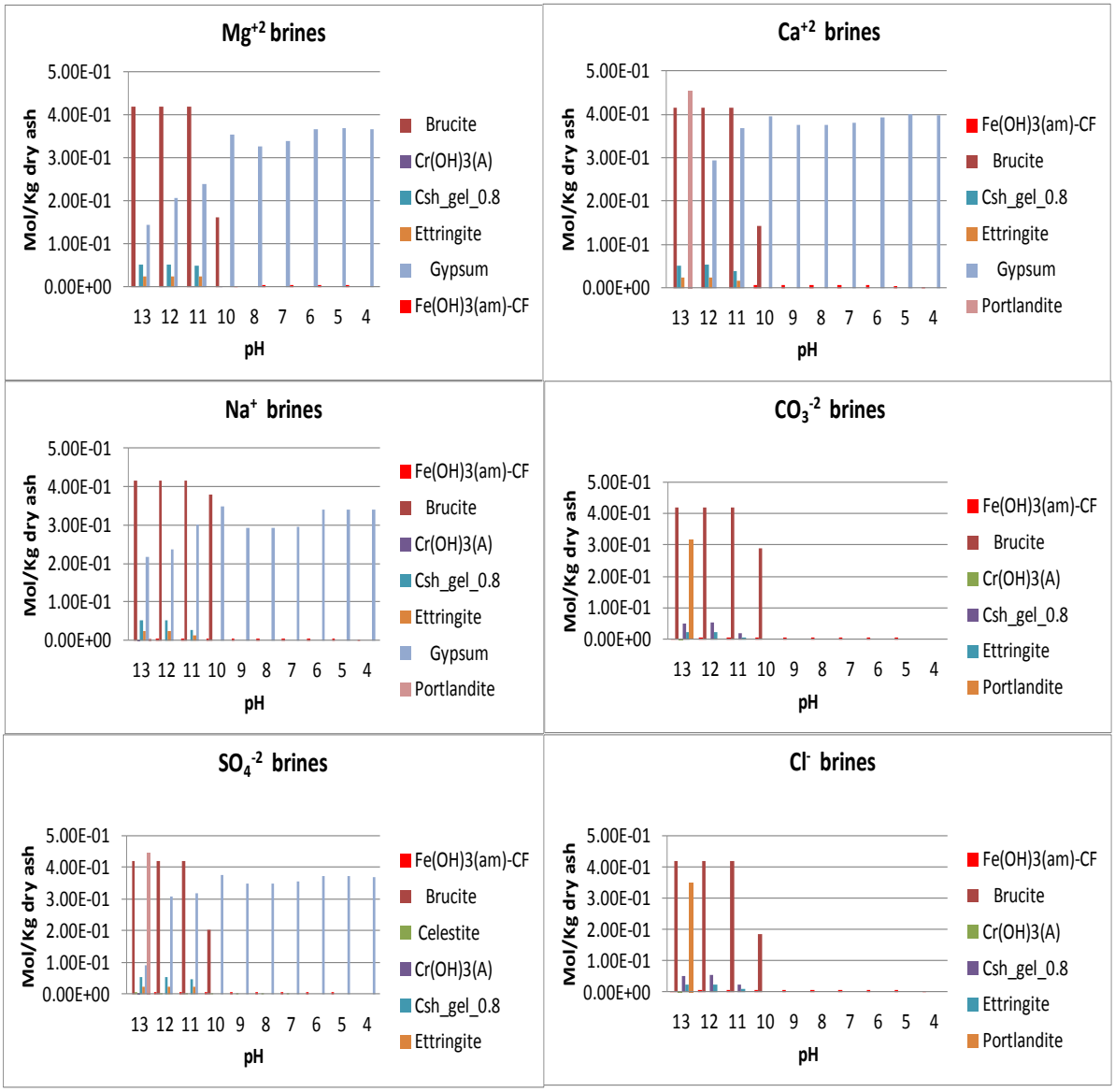

Figure 3.7: Newly formed phases from ANC of ash-ASW organics interactions with individual brines (Mg^{2+}, Ca^{2+}, Na^{+}, CO_3^{2-}, SO_4^{2-} and Cl^{-}). NB: Colors may not necessarily match for each of the mineral phases in the brines as generated.

To capture the dissolution/precipitation/formation characteristics of the mineral phases under different modelled scenarios relative to fly ash-DMW system as the reference, graphs for significant relative change in mineral assemblages, Rc_d[1], at given pH values were drawn and presented in Figure 3.8. Some of the minerals that showed observable relative change in mineral assemblages during ANC with various brines added include calcite, $CaMoO_4$, hematite, kaolinite, mullite, pyrite, $Fe(OH)_3$(am)-CF, portlandite, $Cr(OH)_3$(A), $ZnTiO_4$ and $NiSiO_4$. Figure 3.8 represents those mineral phases that showed relative changes in delta_delta values and hence all the mineral phases with no significant difference in their solubilities when in contact with ASW organics, brines or ASW organics and

brines, compared with that of ash-DMW scenario were not considered for discussion. The suggestion was that their solubility was comparably the same as that in the ash-DMW scenario. Generally, for $Rc\_d^1 > 0$, implies that the mineral phase dissolution/precipitation/formation is the number of times more than that in ash-DMW scenario. For $Rc\_d^1 = 0$, no significant difference in the mineral phase dissolution/precipitation/formation within the respective scenario compared to that in ash-DMW scenario and for $Rc\_d^1 < 0$, implies the mineral phase dissolution/precipitation/formation in that test scenario is equivalent to such number of times less than that in ash-DMW scenario. For instance, from Figure 3.8(a), calcite showed increased potential of precipitation at increased pH values between 7 and 13, by about 550 times more than that in ash-DMW scenario for all scenarios (except that of Cl^- and SO_4^{2-} brines in which it dissolved across the pH range).

The Rc-d^1 values for $CaMoO_4$, hematite, $Fe(OH)_3$(am)-CF and portlandite are too small to have a major impact on the overall mineralogical transformation of fly ash under various disposal scenarios. For mullite, Rc-d^1 values show higher solubilities but quantatively different from that of ash-DMW at the different pH values, as SO_4^{2-} brines showed the highest levels of mullite at pH 6 while Na^+ brines registered the highest levels at alkaline pH of 10. For kaolinite a very distinct difference was showed amongst the scenarios in which the order was kaolinite being more number of times soluble in all the scenarios than ash-DMW reference scenario; (Mg^{2+} > S(6) > Ca^{2+} > Na^+ > brines combined > Cl^- > CO_3^{2-}, all between pH 10 and 12.

The Rc-d^1 values for the mineral phases considered, suggest that the mineral phase transformation could be affected by the type and levels of brines with which fly ash could be co-disposed. Solubility of calcite showed higher solubility in the ash-ASW organics with SO_4^{2-} brines and Cl^- brines scenarios than in DMW, at pH 6 to 9 and 13, both scenarios exhibiting similar trends in the same pH range but differed quantitatively. All the other scenarios showed a similar trend like that of ANC of (ash-ASW organics- CO_3^{2-} brines), in which calcite dissolution showed reduced solubility in DMW with a decrease in pH between 13 to 8, more than in the scenario, and between pH 7 and 3 the dissolution proceeded to the same extent.

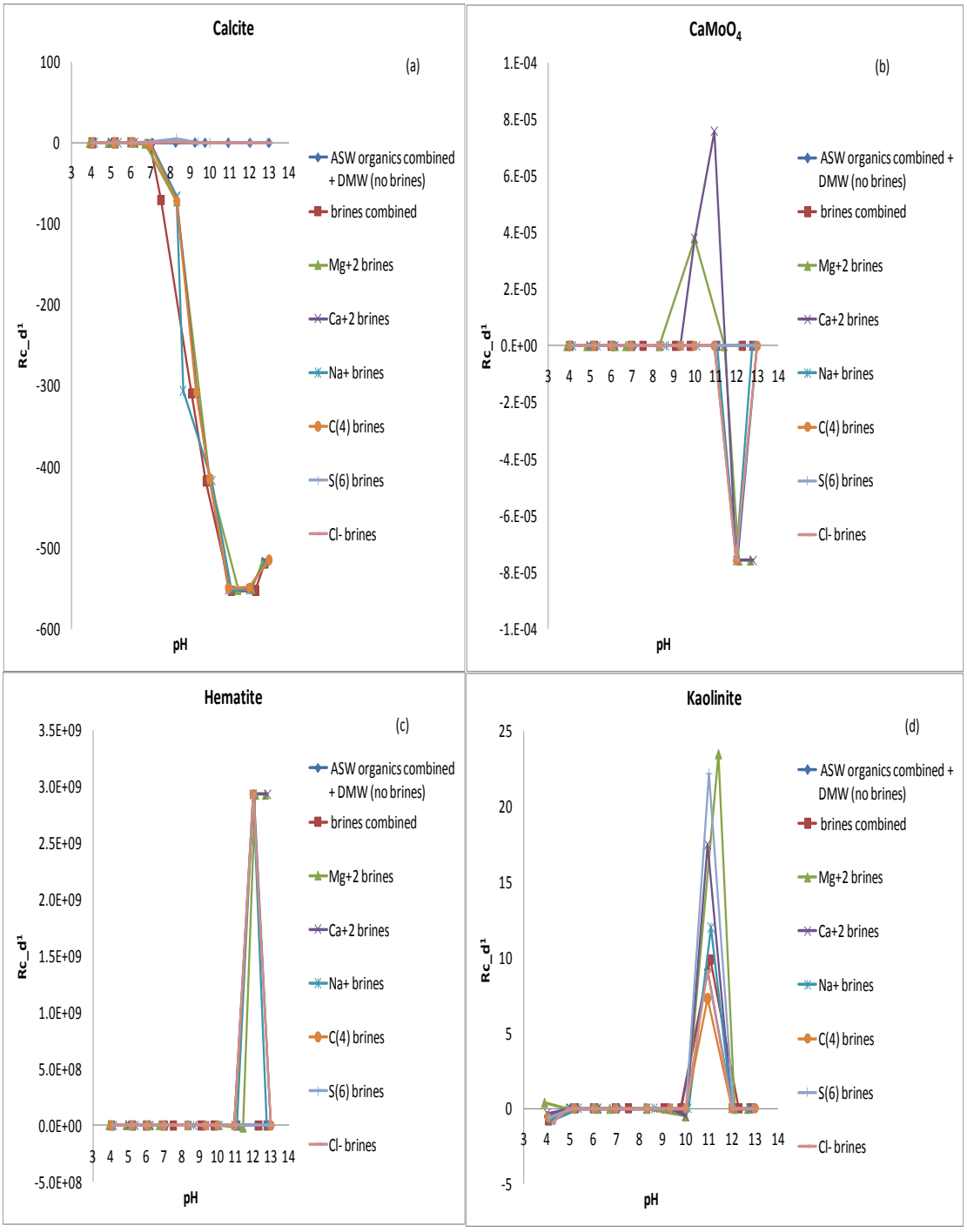
Calcite
(a)
100
0
-100
-200
-300
-400
-500
-600
3 4 5 6 7 8 9 10 11 12 13 14
Rc_d¹
pH
ASW organics combined + DMW (no brines)
brines combined
Mg+2 brines
Ca+2 brines
Na+ brines
C(4) brines
S(6) brines
Cl- brines
CaMoO4
(b)
1.E-04
8.E-05
6.E-05
4.E-05
2.E-05
0.E+00
-2.E-05
-4.E-05
-6.E-05
-8.E-05
-1.E-04
3 4 5 6 7 8 9 10 11 12 13 14
Rc_d¹
pH
ASW organics combined + DMW (no brines)
brines combined
Mg+2 brines
Ca+2 brines
Na+ brines
C(4) brines
S(6) brines
Cl- brines
Hematite
(c)
3.5E+09
3.0E+09
2.5E+09
2.0E+09
1.5E+09
1.0E+09
5.0E+08
0.0E+00
-5.0E+08
3 4 5 6 7 8 9 10 11 12 13 14
Rc_d¹
pH
ASW organics combined + DMW (no brines)
brines combined
Mg+2 brines
Ca+2 brines
Na+ brines
C(4) brines
S(6) brines
Cl- brines
Kaolinite
(d)
25
20
15
10
5
0
-5
3 4 5 6 7 8 9 10 11 12 13 14
Rc_d¹
pH
ASW organics combined + DMW (no brines)
brines combined
Mg+2 brines
Ca+2 brines
Na+ brines
C(4) brines
S(6) brines
Cl- brines

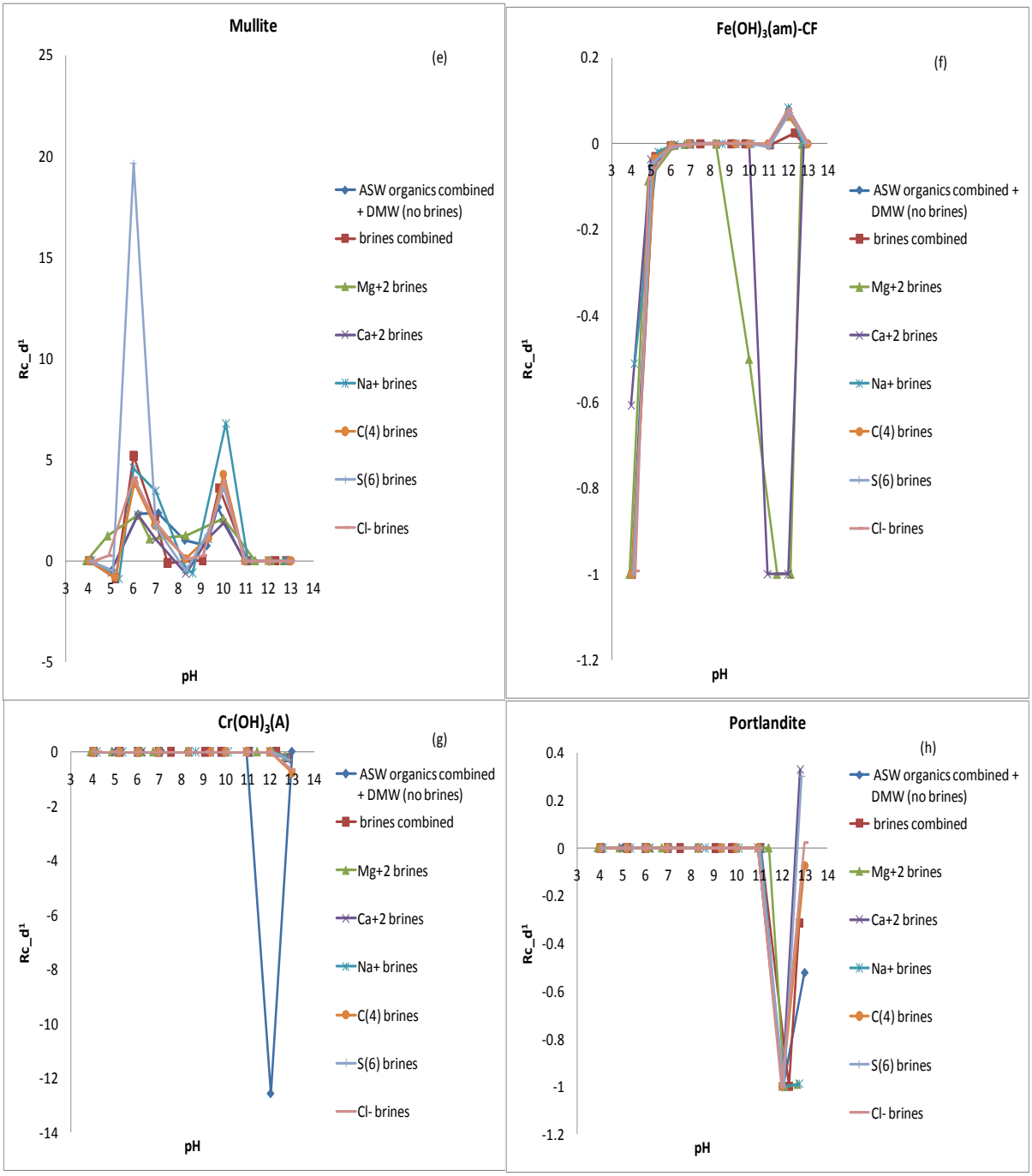
Mullite
(e)
Rc_d¹
pH
ASW organics combined + DMW (no brines)
brines combined
Mg+2 brines
Ca+2 brines
Na+ brines
C(4) brines
S(6) brines
Cl- brines
Fe(OH)3(am)-CF
(f)
Cr(OH)3(A)
(g)
Portlandite
(h)

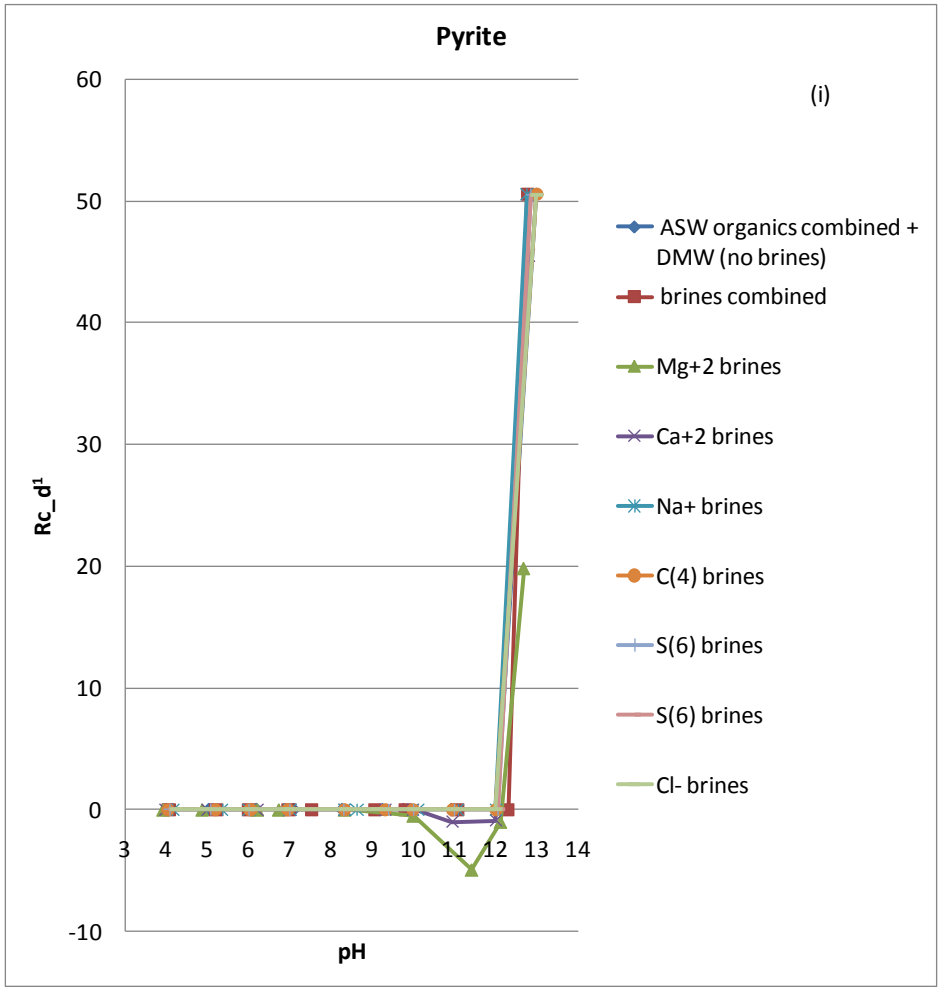

Figure 3.8: Graphs (a)-(i) for relative change in phase assemblages, Rc_d[1] against pH for mineral phases under different scenarios during ANC modeling of ash with ASW organics and individual brines. (ANC of ash with DMW was used as the reference scenario. Rc_d[1] is a ratio and hence has no units). NB: charges on ions given as per PHREEQC input/output nomenclature.

3.4 Conclusion

The batch leaching simulation results from hydrogeochemical modeling showed that mineral dissolution, precipitation and new phase formation during ash-organics-brines interactions was controlled by pH. The newly formed phases however remain in equilibrium with the ash-brines-organics mixture.

Each individual mineral phase dissolution/precipitation/formation system controls the concentration and speciation of the respective constituent elements as evidenced by the log C-pH diagrams obtained from the modeled scenarios. The ash-brines-organics interactions do exhibit and affect the mineralogical chemistry of fly ash. However the extent to which these interactions occur and their effect, varies from one scenario to another, and are dependent on the amounts and type of the constituent brine components. Organics do have a significant effect on dissolution characteristics of few minerals such as calcite, mullite, kaolinite, Ni_2SiO_4, and $SrSiO_3$. The effect is quantitatively conspicuous for calcite mineral phase and for the formation of some new phases such as $Fe(OH)_3$(am)-CF and portlandite. The extent to which the effect occurs is well captured by the use of relative change in mineral assemblage (Rc-d^1) graphs for each pH in each scenario relative to that in demineralised water. The behaviour of the organics could form some important concepts from which predictive solubility insights for mineral phases in ash-brines interactions could be established. Further modeling and characterization of the leaching behaviour by the use of columns will provide ample evidence to identify the major leaching processes of fly ash and give insights as to the predictive chemical behaviour of ash-brines interactions, release and transport. In the meantime, neutralization (pH) and chemical weathering govern the leaching reactions and control the release of major, minor and trace elements from fly ash, and are therefore considered to be the major leaching processes. The results demonstrated the versatility and application of PHREEQC modeling code in the study of equilibrium aqueous chemistry of ash-brines-organics interactions and the effect of the brines and organics in the brines co-disposed with fly ash. This work demonstrates how powerful geochemical modeling can be in that from the simulation results, we are able to describe the underlying mechanisms involved in the ash-brines interaction, elemental-release controlling factors, all of which increase the ability to make relevant decisions that appertains to the ash-brines disposal systems. The leaching levels of elements from fly ash either with water only or mixed with brines showed no significance difference and in some instances the use of brines led to reduction in some total released elements which would therefore point to the validity of possible continued co-disposal of ash and brines from the coal utility plants. It should however be noted that models may not be perfect although they have been able to reasonably describe leaching processes in the ash-organics-brines scenarios. The present work supports and augments previous experimental studies in which chemical and mineralogical transformations (and slight variations in chemical compositions of

disposed fly ashes in contact with brines and water) occur. However the extent to which the continued co-disposal of the ash and brines occur may possibly alter engineering properties of some fly ash, either favourably for its utilization, or negatively. This is an area that needs further study.

Acknowledgements

Mbugua J.M is grateful for project funding by the Pollution Research Group (PRG) at the University of KwaZulu Natal (UKZN) and tuition fee exemption by the UKZN. The Kenya Polytechnic University College for granting him study leave and supplementary support during the study period. The authors appreciate the laboratory experimental data by Dr Wilson Gitari and Prof Leslie Petrik of the University of Western Cape for availing the experimental data in Phase I, used for model calibration during the initial stages.

CHAPTER 4

REACTIVE-TRANSPORT MODELING OF FLY ASH-WATER-BRINES INTERACTIONS FROM LABORATORY-SCALE COLUMN STUDIES

John M. Mbugua[1]*, J. Catherine Ngila[1,2], Andrew Kindness[1], Chris Buckley[3], Molla Demlie[4] and Shameer Hareeparsad[5]

[1] University of KwaZulu-Natal, School of Chemistry and Physics, Westville Campus, Private Bag X54001, Durban 4000, South Africa

[2] University of Johannesburg, Department of Applied Chemistry, P.O Box 17011, Doornfontein, Johannesburg 2028, South Africa

[3] University of KwaZulu-Natal, Pollution Research Group, Howard College Campus, Durban 4041, South Africa

[4] University of KwaZulu-Natal, Department of Geological Sciences, Westville Campus, Durban 4000, South Africa

[5] Sasol Synfuels (Pty) Ltd, Environmental Sciences and Engineering Research and Development, Secunda, Mpumalanga 2302, South Africa

*Corresponding author: jmmwai@gmail.com, Tel: +27312601498; +27799228187

Abstract

Dynamic leaching tests are important studies that provide more insights into time-dependent leaching mechanisms of any given solid waste. Hydrogeochemical modeling using PHREEQC was applied for column modeling of two ash recipes and brines generated from South African coal utility plants, Sasol and Eskom. The modeling results were part of a larger ash-brine study aimed at acquiring knowledge on (i) quantification and characterization of the products formed when ash is in contact with water-brines in different scenarios, (ii) the mineralogical changes associated with water-brine-ash interactions over time, (iii) species concentration, (iv) leaching and transport controlling factors. The column modeling was successfully identified and quantified as important reactive mineralogical phases controlling major, minor and trace elements' release. The pH of the solution was found to be a very important controlling factor in leaching chemistry. The highest mineralogical transformation took place in the first 10 days of ash contact with either water or brines, and within 0.1 m from the column inflow. Many of the major and trace elements (Ca, Mg, Na, K, Sr, S(6), Fe, are leached

easily into water systems and their concentration fronts were high at the beginning (within the first 10 days) upon contact with the liquid phase. However, their concentration decreased with time until a steady state was reached. Modeling results also revealed that geochemical reactions taking place during ash-water-brine interactions does affect the porosity of the ash, whereas the leaching processes lead to increased porosity.

Besides supporting experimental data, modeling results gave predictive insights on leaching of elements which may directly impact on the environment, particularly ground water. These predictions will help develop scenarios and offer potential guide for future sustainable waste management practices as a way of addressing the co-disposal of brines within inland ash dams and heaps.

Keywords: Brines, Column modeling, Fly ash, Metal speciation, Mineral phases, PHREEQC, Porosity, Water pollution,

4.1 Introduction

Leaching is considered as one of the risks in ash disposal facilities to ground water systems, and whose quantification in Eskom and Sasol coal utility plants in South Africa, was the ultimate goal of this study. Both batch and dynamic leaching studies are important as they complement each other in terms of the diverse information of interest they provide. Chapter 3 of this Thesis covered the batch leaching modeling aspect of ash-brines interactions. Batch leaching experiments, performed over short durations are simple tests useful for determining the intrinsic properties of the solid waste with respect to one or several controlled parameters [131]. Batch tests can give valid information concerning the influence of various parameters, such as pH value, liquid/solid ratio, elution agent and elution time on the mobilisation of inorganic contaminants. However, a major disadvantage of all batch experiments is that they only represent a snapshot of the leaching history of the material investigated.

This chapter will therefore address the column modeling as part of dynamic leaching studies for both Secunda and Tutuka ash disposal systems using PHREEQC. Results from column modeling studies are useful in enhancing further understanding of long term time-dependent leaching mechanisms and the impact on ground water pollution. They also aid in quantification of release rates and also useful for the extrapolation of laboratory results to site conditions of various characteristics such as varying solution/solid ratios, cyclic infiltration, site specific geometry [89, 93, 121, 132, 133]. They involve modeling of the reactive and transport mechanisms of a given system. Reactive-transport modeling is an emerging research field within some hydrogeochemical modeling tools. It aims at achieving a time-dependent, quantitative, and ultimately predictive treatment of chemical transformations and mass transfers within the porous heterogeneous ash-water-brines system. Reactive-transport models (RTMs) provide platforms for testing concepts and hypotheses, and for integrating new experimental, observational, and theoretical knowledge about geochemical, biological and transport processes. Through numerical computation and simulation, RTMs provide most valuable diagnostic and prognostic tools available for elucidating the inherently complex dynamics of natural and engineered environments [134, 135]. Furthermore, they bridge the gap between fundamental, process-oriented research and applied research in the fields of operational modeling, environmental engineering and global change.

Fresh ash has more components than weathered ash and leaches more [122]. Leaching kinetics, acid neutralization capacity (ANC) and brines speciation all geared towards understanding the products of the ash-brines interactions (new recipe formed after weathering) and thus mass balance important.

Modeling of the mineralogical changes associated with the interaction of brines-water and fly ash during their co-disposal has been documented as part of the larger ash-brine project work [10, 11, 13,

15, 29, 122, 136-138]. The intermediate and final products from these interactions of brines-water and fly ash were quantatively reported together with the geochemical reactions associated with such interactions. Reactive transport modeling is a potentially valuable instrument to identify and describe the dynamic leaching processes of contaminants from waste materials which act as the source term, as well as further their rate of transport in soil and groundwater. This may form a basis for the development of realistic regulatory limits [96]. Sufficient understanding is required of the geochemical and mass transfer processes that control the leaching of contaminants in a percolation regime. This will therefore form the basis of our column modeling, aimed at determining the leaching and transport mechanism during fly ash-water and brine interactions. Reactive transport modeling using various codes has attracted great interest to earth scientists and engineers concerned with problems involving the evolution of the subsurface geochemical environment in response to coupled chemical and solute transport processes. This will include contaminant hydrologists interested in the transport of metals and dissolved organic compounds through an aquifer and how these substances interact with the local aquifer geochemistry. Reactive transport models allow the contaminant hydrologists, geologists, (hydrogeochemists) or soil scientists to view chemically reactive aqueous systems in soil or rock as dynamic rather than static systems. Purely static models limit the scope of questions to be answered such as time-dependent release of elements from solid wastes, the systems composition and speciation, reactions involved, and changes in phase assemblages. With a dynamic model, more information such as the appropriate boundary conditions, what materials are flowing into and out of the system are revealed, as well as time scales that the solid phases are transformed.

Within the set out scope, dynamic column leaching modeling was therefore undertaken in order to provide the linkage between changes in the ash chemistry and the transport properties of the fly ash from Secunda and Tutuka coal utility plants. Understanding these properties is important for accurate predictions of the fate and transport of contaminants by using numerical models. Modeling results have been used routinely in risk assessment, remedial designs, and regulatory decisions related to ground water contamination [139].

Even though large uncertainties are associated with the modeling results, a reactive-transport model is the only systematic method available to estimate the time dependency of the loads and fate of major and trace elements. In a complex ash-brine disposal system, these elements are leached and transported across the ash dump and as a result there is need to assess the sensitivity of the load estimate to various chemical and physical processes.

This study therefore seeks to demonstrate the application of PHREEQC as an analytical-hydrogeochemical tool in predicting the interaction of water and brines with fly ash during their co-disposal of waste from two major coal utility plants in South Africa, Sasol and Eskom. Conceptual

models were developed and relevant parameters involved were used as the inputs for the PHREEQC code using a modified Lawrence and Livermore National Laboratory (LLNL) database. Time-dependent release, transport and fate of the related mobile species were investigated. Modeling reactive transport in fly ash-brines-water disposal systems with a view to quantify and characterize the products formed and transport mechanisms involved was the focus of this study.

4.2 Methodology and hydrogeochemical modeling tools

In this section, some important highlights of the modeled fly ash and brines are provided while detailed description of the column parameters and its discretization are given. Description of the coupled geochemical-transport modeling and data input used in the model are also detailed in subsequent subsection, followed by the simulated data output presentation.

4.2.1 Fly ash modeling recipes and brines

Fly ash samples were collected from Secunda (Sasol) and Tutuka (Eskom) coal-utility plants in South Africa and from where the modeling ash recipes were derived and modified as adopted from Hareeparsad and co-workers [26], and Gitari and co-workers [122]. Experimental data were based on the mineralogical and chemical characterization of the fresh fly ashes and the brines carried out by Ojo [19] and Gitari and co-workers [122]. These were previously presented in Tables 3.1 and 3.2 in **chapter 3** of this thesis. The characterized brines incorporated in the model from Secunda and Tutuka are also given by Table 3.3 also in **chapter 3**. (NB: For the purposes of flow of this thesis, it was deemed unnecessary to reproduce Tables 3.1, 3.2 and 3.3 in subsequent chapters; however they shall be included in the separate manuscripts at the stage of submission for publication).

4.2.2 Column parameters and discretization

The column experimental parameters were adopted from the work of Ojo [19] and Hareeparsad and co-workers [26]. Other column parameters and hydraulic property calculations were performed in programmed spreadsheets by MS EXCEL and formed part of the input column and hydraulic parameters in PHREEQC code. Flux-type boundary conditions (also known as third type or Cauchy boundary condition) were employed. Closed-system conditions were applied which prevented, or at least minimised, CO_2 and other atmospheric gases uptake. The dynamic leaching test was made at

constant temperature (20 ˚C). A general description of PHREEQC input KEYWORDS and parameters used for transport modeling are presented in an example given in **Appendix 2** (Figure A1). In this study PHREEQC input file for Tutuka ash heap modeling with brine is given in **Appendix 3** (table A9).

The one dimensional (1D) column was discretized and defined by a series of cells (number of cells is given as *cells*), each of which has the same pore volume. Lengths are defined for each cell and the time step (*time step*) gives the time necessary for a pore volume of water to move through each cell. Thus, the velocity of water in each cell is determined by the length of the cell divided by the time step. The numbers of pore volumes of filling solution that are moved through the column are given by (*shifts* / *cells*) and the total time of the simulation is calculated as (*shifts* x *time steps).* The column length may not necessarily be discretized into equal cell lengths. At each shift, advection is simulated by moving solution *cells-1* to cell *cells*, solution *cells-2* to cell *cells-1*, and so on, until solution 0 (the infilling solution demineralised water or brine) is moved to cell 1 (upwind scheme). With flux-type boundary conditions (also known as third type or Cauchy boundary condition), the dispersion steps follow the advective shift. With Dirichlet boundary conditions, (also known as the first type or concentration constant boundary condition) the dispersion step and the advective shift are alternated. After each advective shift and dispersion step, kinetic reactions and chemical equilibria are calculated. The moles of pure phases and the compositions of the exchange assemblage, surface assemblage, gas phase, solid-solution assemblage, and kinetic reactants in each cell are updated after each chemical equilibration [99]. The column geometry and hydraulic parameters, and column discretization and transport parameters are presented in Tables 4.1 and 4.2 respectively.

Table 4.1: Column parameters and hydraulic properties for Secunda and Tutuka ash columns as calculated by MS EXCEL

symbol	definition	Secunda	Tutuka	units
ρ_w	density of water	1.000	1.000	g/cm^3
% H_2O	Moisture content of fly ash due to wet packing	17.300	20.000	%
m_c	Weight of empty Column	642.560	642.560	g
$m_c + m_{w\text{-}ash}$	Weight of Column + wet fly ash	1718.290	1718.290	g
$m_{w\text{-}ash}$	Weight of wet fly ash only	1075.730	1875.000	g
m_{H2O}	mass of water	186.101	375.000	g
$m_{d\text{-}ash}$	Dry weight of fly ash before leaching=(100 - % of H_2O)*$m_{w\text{-}ash}$	889.629	1500.000	g
$m_{w\text{-}ash\text{-}l}$	Dry weight of fly ash after leaching	859.190	859.190	g
$m_{leached}$	leached amounts	30.439	640.810	g
$\%m_{leached}$	% leached	3.422	42.721	%
d	diameter of column	6.000	6.000	cm
H	Column height	30.000	35.000	cm
h	height of compacted ash in column	25.000	30.000	cm
r	column radius	3.000	3.000	cm
V	column total volume (includes voidage)	706.858	848.230	cm^3
Vo	pore water volume of column(A*h*ε)	186.101	375.000	cm^3
PV=V/Vo	pore volumes	3.798	2.262	
Q	flow rate	0.003	0.003	cm^3/s
ε	porosity	0.263	0.442	
A	cross-sectional area	28.274	28.274	cm^2
i	hydraulic gradient=Q/KA	0.781	0.781	
v	pole water flow velocity(Q/εA)	0.000	0.000	cm/s
D	Darcy flow velocity	0.000	0.000	cm/s
K	Hydraulic conductivity	0.000	0.000	cm/s
t	total time (duration of simulated experiment)	7.78E+06	7.78E+06	s
ρ_b	bulk density of wet ash=$m_{w\text{-}ash}/V_{w\text{-}ash}$	1.522	2.210	g/cm^3
ρ	dry ash density	1.708	3.170	g/cm^3
Kd	distribution coefficient	5.780	5.000	
R	Retardation, R = (1 + dq/dc)=1+Kd	6.780	6.000	
q	concentration in the solid (mol/L of pore water)			mol/L
c	solute concentration (mol/L)			mol/L
D_L	Hydrodynamic dispersion coefficient	0.000	0.000	m^2/s
α_L	longitudinal dispersitivity	0.005	0.005	m
L/S	L/S=leachate volume/mass of dry ash=(ε/ρ).V/Vo)	0.585	0.315	L water / Kg dry ash
1 y	year	3.15E+07	3.15E+07	s

Table 4.2: Calculated column discretization parameters for PHRREQC transport input

Column Discretization (symbols)	Description	Secunda	Tutuka	units
Kd	normalized distribution coefficient = q/c = ρb/ε	5.0728	5.0728	
R	Retardation = 1+q/c = 1+ Kd	6.0728	6.0728	
mixf	mixing factor between two consecutive cells :Δx<			
	mixf >0, if Ncell > Totx/αL*[(1-1/R)/2)], integer			
	For mixf > 0, if Δx< [α_L2R] / (R-1): Δx<	1.20E-02	1.20E-02	m
	and N_{cell} = >	20	20	cells
v	pole water flow velocity(Q/εA)			
Δx	cell length	0.0125	0.0125	m
α_L	dispersitivity	0.005	0.005	m
Tot x	total column length or flowline	0.2500	0.25	m
N_{cell}	number of cells = Tot x/Δx	20	20	cells
Tot t	total time of injection or simulation	7776000	7776000	s
Δtv	for maximal value of Δt: = Δx , hence Δt < Δx/v (integer value)	2792	4688	s
timesteps	timesteps (=Tot t/Δt = Nshifts, integer value): Phreeqc input	3000	2000	shifts
Δt	Tot t/Nshifts: Phreeqc input	2592	3888	s

4.2.3 Coupled geochemical-transport modeling and data input

The coupled geochemical-transport model takes into account the physicochemical and transport phenomena in the fly ash material packed in a column of known geometrical dimensions and eluted with either demineralised water or brines as leaching solutions. PHREEQC code [14] was used and which was originally designed to model chemical reactions in natural waters of given compositions in open or closed batch systems. However, a newer version of PHREEQC (version 2.15.0) has the capability of also solving the mass balance equations (also referred to as advective-dispersive transport equation) in one dimensional (1D) flow domain for each of the components in the water composition. The resulting model is quite powerful and is capable of simulating a large variety of geochemical problems. In the PHREEQC simulation, the ash is modelled as a collection of pure mineral phases which come to equilibrium with the demineralized water or brine liquid phases. Modified LLNL database was used for all the simulations which involved inorganics (mineral phases and brines).

To couple the chemical model and the transport model, PHREEQC uses the split operator approach in which the code solves the model using the methods of Newton–Raphson algorithm for the equilibrium equations and the finite differences method (explicit scheme) for the transport equations (advection and diffusion) [14]. Our chemical model describes the mineralogical phases and the chemical reactions occurring in the ash-water and ash-brines systems. From the experimental data and by using PHREEQC coupled with the database LLNL, it was possible to identify the mineralogical phases expected to control the release of the target elements. The chemical model was developed through a three steps methodology described by Tiruta-Barna [27] and Hareeparsad and co-workers [26]. The advective-dispersive transport capabilities of PHREEQC are derived from a formulation of 1D, advective-dispersive transport presented by Appelo and Postma [99] and Parkhurst and Appelo [14].

Two cases each involving two modeling scenarios were carried out for Secunda and Tutuka fly ash recipes: Case (i) in which Secunda and Tutuka ash column modeling was run with demineralised water (DMW), and case (ii) in which Secunda and Tutuka ash column modeling was run with brines. In case (i), the DMW was to mimic the dynamic fly ash-water interactions that occur when fly ash is subjected to rainwater although a closed system as well as local equilibrium assumption were incorporated in the column model. Local equilibrium hypothesis was considered as it assumes that a system can be viewed as composed of subsystems where the rules of equilibrium thermodynamics apply, (equilibrium constant, K, in solution chemistry models are based on local equilbrium assumption).Under the laboratory-scale conditions, a closed system was imposed in order to minimise the effect of atmospheric CO_2 and other gases such as O_2 which could subject the modeled scenario extraneous and also redox conditions. Related work by Nyambura *and co-workers* [140] on carbonation using brine showed higher degree of calcite formation compared to the ultra-pure water carbonated residues. Input parameters for Secunda and Tutuka ash recipes were similar except that the ash composition differed quantitatively for the mineral phases previously given by Tables 1 and 2. The infilling solution was demineralised water at default conditions of temperature (20^oC), pH (7) and electron activity (pe, 4). The solution in the column was modeled to be containing mobile cations of alkali metals of Na, K and Li in small quantities (0.010, 0.002 and 0.004 mol/L originally in the fly ashes) respectively. For case (ii), similar input parameters to case (i) were applied but only differed in the infilling solution in which brine replaced DMW. In all the scenarios, some column parameters and hydraulic property calculations were done by an MS EXCEL spreadsheet program, part of it given in Table 7. Column discretization and transport parameters were also calculated and given in Table 8 and then input in the PHREEQC code under the TRANSPORT keyword. Dispersitivity value of 0.005 m was adopted from Appelo and Postma [99] as obtained from field experiments for porous media which closely resembled that of fly ash. This was based on the assumption that mechanical dispersion occurred in the column as the inflow liquid moved at rates that are both greater and less

than the average pore velocity due to heterogeneities at various column levels. Fly ash is assumed to be porous and heterogeneous and as a result the mixing of fluids that have different solute concentrations occur which tend to dilute the solute concentrations. Third-type or Cauchy flux boundary conditions (flux flux) were used for both ends of the 1D column. Previous ash-brine project work [10, 11, 13, 15, 19, 29, 122] provided relevant experimental data for acid neutralization capacity, (ANC), ash and brines characterisation, column dynamic leaching data, water flux and composition data, porosity and permeability data and conceptual model of brines flow in the ash heaps. All this data was useful in the modeling as part of the initial inputs and modeling conditions. The flow rates, the volumes of the leachates and the specific solid/liquid (S/L ratio) were imposed at a laboratory scale.

4.2.4 PHREEQC data output and presentation

PHREEQC simulations generate enormous amount of data depending on the specific interests and objectives of the modeller, among which the most significant simulation results are the pH and the elemental total concentrations in the leachate [141], as well as the mineralogical changes. Output data from the simulations were presented in the form of MS EXCEL spreadsheets and relevant graphs drawn which captured important properties and parametric changes in physico-geochemical-relationships from the simulations for both water and brine. Some of these profiles included:

- pH versus distance at different times (or pore volumes)
- Total elemental concentration (soluble components) versus pore volumes
- Total elemental concentration (soluble components) versus time
- Moles of mineral phase remaining versus time (or pore volumes) at breakthrough volumes
- Moles of mineral phase remaining versus distance
- Change of moles of mineral phase versus distance at different pore volumes or time
- Comparison of elemental concentration at outflow position
- Changes of mineral composition versus time in different positions
- Mineral molar volume calculations
- Changes of mineral volumes at distance with time

- Changes of porosity versus time in different positions

Some of the column simulation results of both Secunda and Tutuka fly ashes under all the scenarios are discussed in the following **section 4.3**.

4.3 Results and Discussion

Results for the different scenarios modeled were presented side by side for ease of reference and comparison in the interpretation and discussion. Some important observations from the simulation results have been highlighted which formed the basis for the overall conclusions.

The graphs drawn from the data generated from the simulations for both Secunda and Tutuka ash recipes under the different scenarios mentioned are presented in the following **sections 4.3.1** to **4.3.7**.

4.3.1 pH changes along the column distance at different time

The results for pH changes along the column distance at different days (or pore volumes) were presented by Figure 4.1. The pH trend for both Secunda and Tutuka ash recipes with water were similar and equally so was the trend between fly ash-brine models for the two ash recipes. Initial pore chemistry reflected the pH values of the ash recipes (about 12.6) before the interactions commenced. The same trend recorded in pH confirms similar mineralogy associated with the two ash recipes, only differing quantitatively. Large pH variation was observed between the influent point and 0.05 m of the column for up to 90 days during which time pH fluctuations were registered for different days along the column. This could be due to the equilibration reactions taking place when fly ash comes into contact with the water. At 0.05 m the pH drops from 12.6 to 10.4 after which it remains constant until 54 d after and then it starts to fall reaching 9.7 after 90 days. These changes in pH are an indication of the chemistry that is occurring at the point of first contact with water and also brines, resulting to dissolution of certain mineral phases that form leachates of lower pH values and which move down the column advectively. The pH front changes for different days for the first column distance of between 0.05 m and 0.25 m was observed. Between this column distance, there must be some chemistry occurring since a small decrease (2 or 3) in pH value over time can increase the solubility and decrease the adsorption of metals by many orders of magnitude. If the pH decreases over time, the concentration of metals in the leachate is expected to increase over time as well. Same trend of pH along the column was observed for both ash recipes with brines.

These results illustrated the distinctive general chemistry of the ash recipes used in the model under different scenarios, with ash-brine systems exhibiting marked but similar trends between the two ash recipes but at different pore volumes.

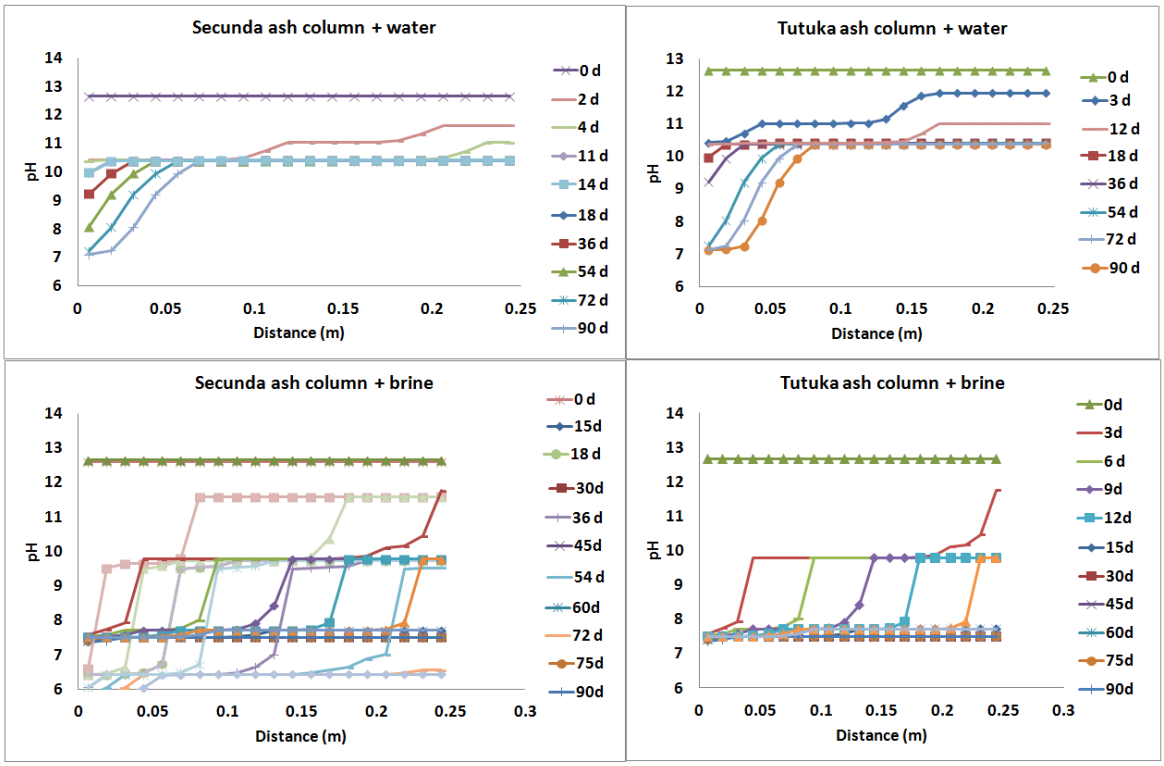

Figure 4.1: The pH versus column distance at different days for Secunda and Tutuka ash-demineralized water and brines scenarios. (NB. d stands for days in all subsequent graphs in this chapter)

Evolution of pH along the column for different pore volumes at break through volumes was presented in Figure 4.2. The initial pH value of about 12.6 for the four ash columns reflects the pH values of the fly ash which shows to be highly alkaline. The first 10 pore volumes result in a sharp decrease of pH value of Tutuka ash, the one with brines recording the lowest value of 9.7 and with water pH value of 11. Same trend was also registered with Secunda ash. The sharp decrease could be due to precipitation of the alkaline-causing species and possible sorption of some species (e.g. CaO, and MgO) that were initially responsible for the alkalinity of the solution during the equilibration period. The pH for Tutuka ash with water stabilises for a while at 11 (at 15 pore volumes) after which it drops to 10.5 after which it remains constant up to 90 days (150 pore volumes) like that of Secunda with water. Both Secunda and Tutuka ash recipes showed similar trend in pH variation with pore volumes, but only differing in pH values at same pore volumes when interacting with brines. Fly ash-brines

interaction results in marked change in pH over time, the initial alkaline pH of fly ash leachate with brine was lowered upon weathering to a final pH of about 6.5 for Secunda ash and 7.5 for Tutuka ash in 150 pore volumes. The difference could be attributed to the quantitative variations in the modeled ash recipes and different levels of brine constituents emanating from each of the coal utility plants of Sasol and Eskom.

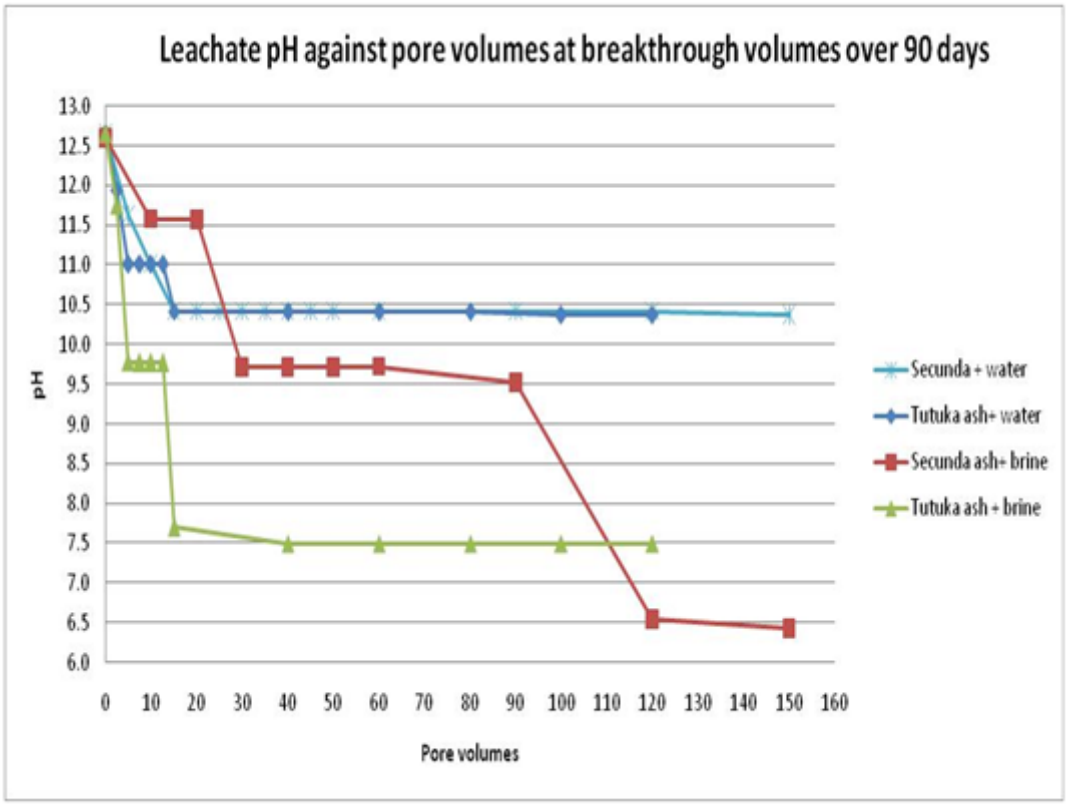

Figure 4.2: The pH of leachates against pore volumes at breakthrough volumes over 90 days for Secunda and Tutuka ash-water-brines scenarios (NB: pore volumes has no units as it is a ratio)

4.3.2 Change of total elemental concentration (soluble components in leachate) with pore volumes and pH

The variation of the total elemental concentrations in the leachate against pH and the pore volumes were plotted and presented in Figures 4.3a - 4.3d. The simulation results showed that the first 20 pore volumes were significant and did cause marked change in the concentration of elements in the leachate in all modeled scenarios. This would be a good pointer that important reactions that result to leaching and transport mechanisms were taking place as a result of the ash-demineralized water or ash-brine interactions in the columns. The graphs show a general trend of rapid decline in the concentration of major and minor elements in the first 20 pore volumes, which may indicate flushing out of the elements in solution as soon as the leaching started. For some elements like Na, K, and Li, the results suggest that their soluble salts are on the surfaces of ash particles which get flushed as leaching progresses [12]. After the 20 pore volume, high concentration was recorded within which equilibration took place. For some elements like Na and S(6) small quantities continued being released even after flushing which may suggest some flushing of these elements not just at the surfaces but also in the ash matrices. The release pattern of Cr and Mo was similar to that of Na, K, and Li though comparably very low in amounts. Increase in the concentration of Mg in Tutuka in the first 10 pore volumes could indicate steady dissolution of Mg-bearing mineral phases in the fly ash. Brucite ($Mg(OH)_2$) formation was predicted as the controlling factor for the concentration of Mg in the leachate. Dissolution and precipitation reactions were therefore the main controlling factors for most of the elements concentration. Further increase between 15 and 20 pore volume occurred and may be attributed to some minor fractions of Mg present in the slowly dissolving glassy phase in the case of Tutuka. For Al and Si they recorded initial increase in concentrations in both fly ashes due to possible dissolution of amorphous aluminosilicates and silica present in fly ashes. The pH is also an important controlling factor as the decrease in pH affected some elements concentration like C, Al, Si, Ni, and Cr in all the scenarios. However adsorption and ion exchange mechanisms may also apply to some elements such as Ni considering the trend is not consistent like the other elements.

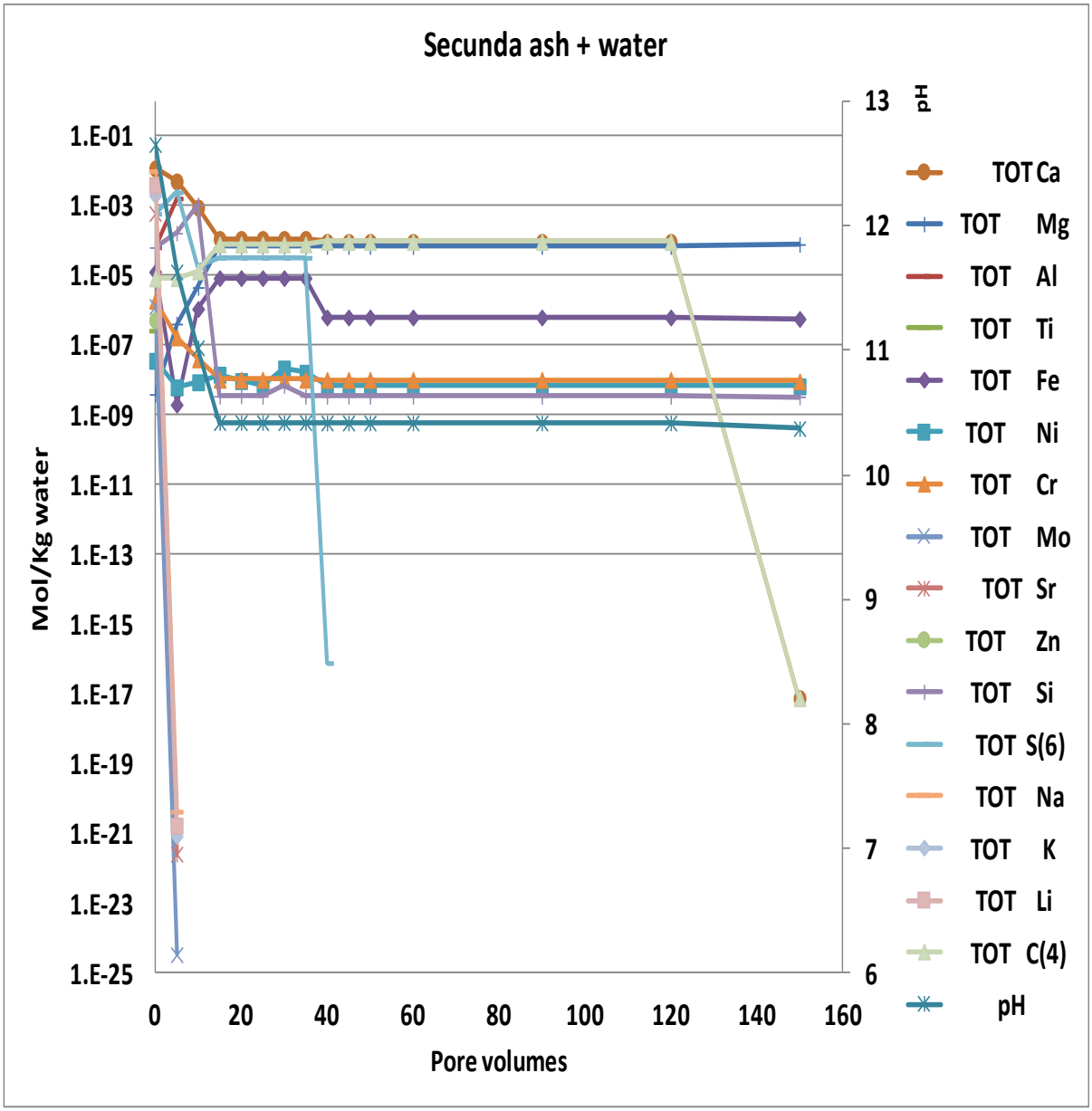

Figure 4.3a: Total elemental concentration against pore volumes and pH for column models for Secunda ash with water

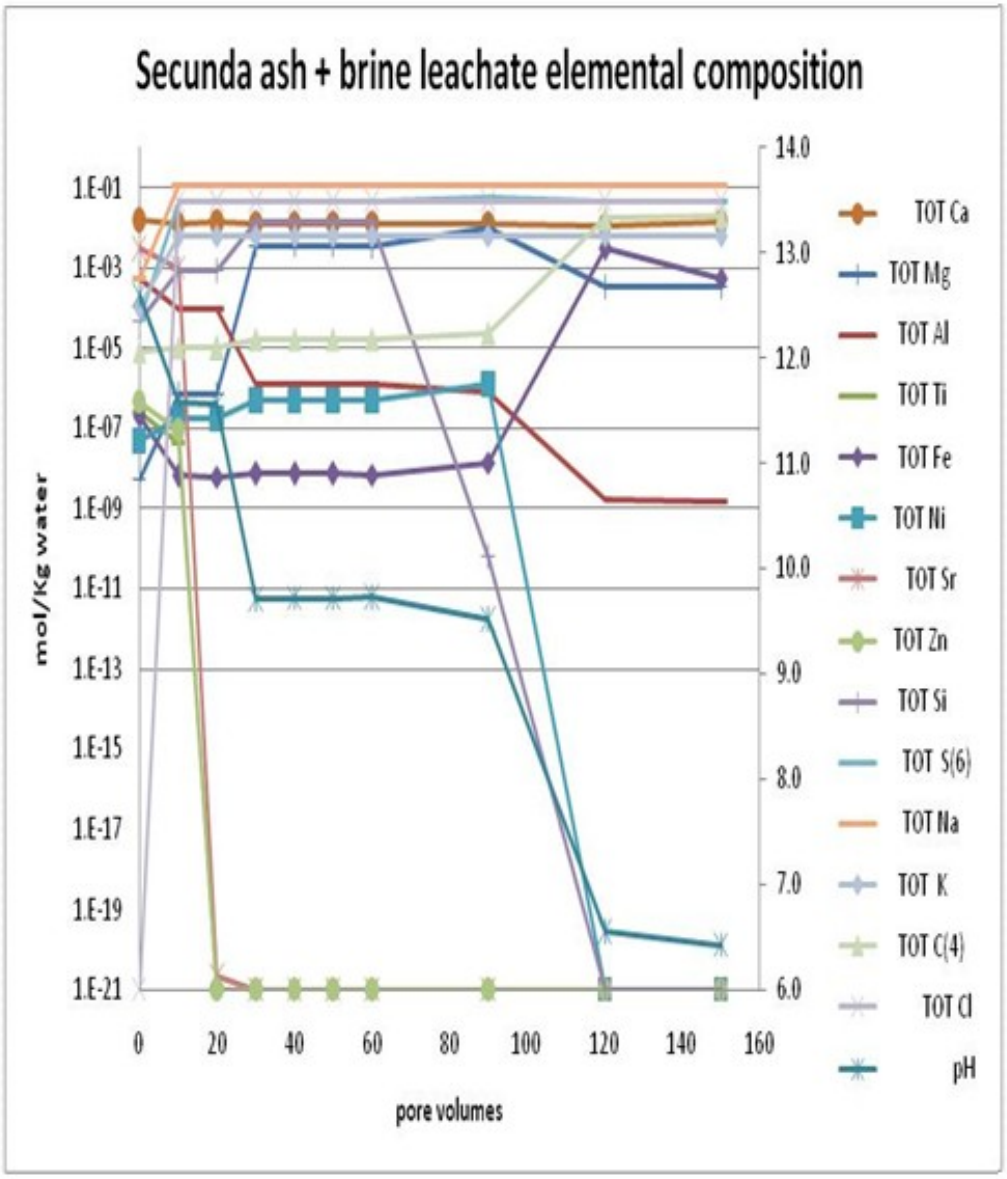

Figure 4.3b: Total elemental concentration against pore volumes and pH for column models for Secunda ash with brine

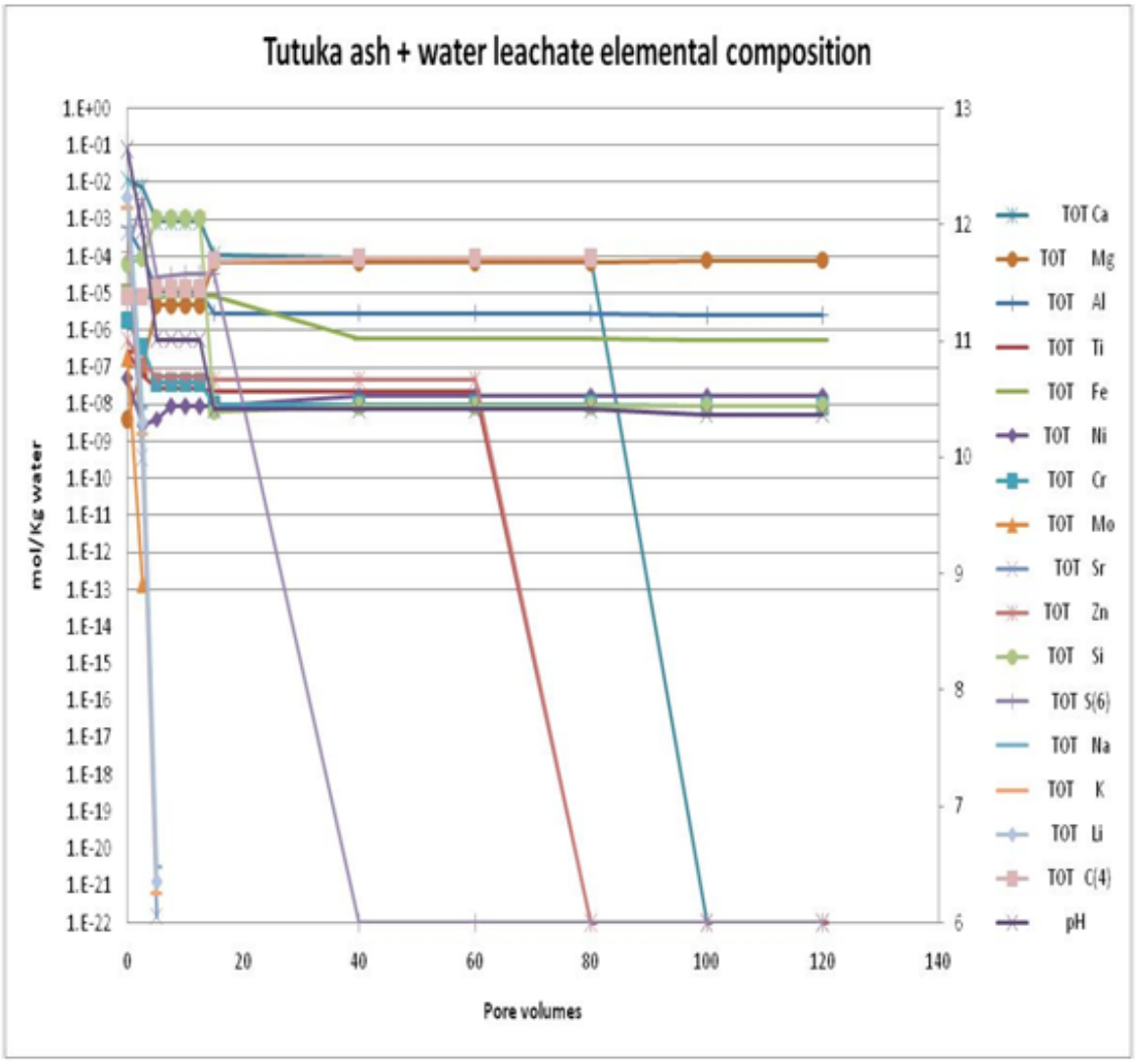

Figure 4.3c: Total elemental concentration against pore volumes and pH for column models for Tutuka ash with water

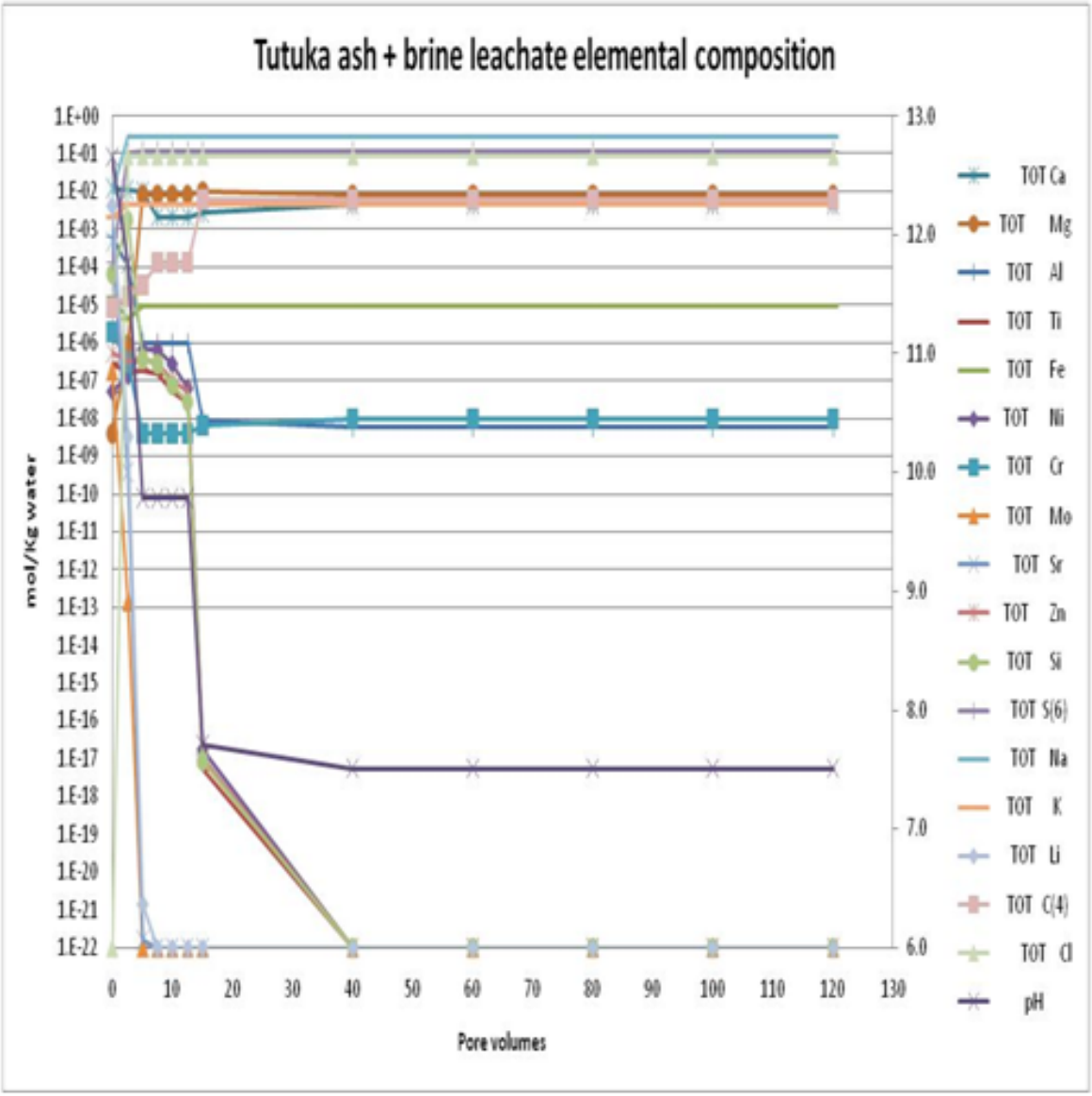

Figure 4.3d: Total elemental concentration against pore volumes and pH for column models for Tutuka ash with brine

4.3.3 Total elemental concentration of major and trace elements versus distance and pH after 90 days

Column simulations results gave the breakthrough curves given by Figures 4.4a and 4.4b. The results are those of Secunda and Tutuka fly ash interactions with water (Figure 4.4a) and brines (Figure 4.4b) along a column after 90 days. Both ash-water scenarios (for Secunda and Tutuka) showed similar trends for individual elemental concentrations in the leachate after the 90 days but only differ in quantities and magnitude of change. The major and trace elements considered were as listed in Figure 4.4a. The highest change in concentrations of the elements in the leachate was recorded between column distance of 0.05 m and 0.1 m, except Fe which exhibited the change about 0.125 m for Tutuka ash-demineralized water column model. In the case of the two ash recipes with brines (Figure 4.4b), some of these elements were eluted at constant concentration along the column. These elements were Ca, Mg, S(VI), Na, K and C. The element Fe increases in concentration progressively up to about 0.075 m of the column after which it levels up to a constant value up to the end of the column as shown in Figure 4.4b. In these figures also, Al was shown to have its concentration being pH-controlled as it showed a decrease in concentration within the first 0.05 m of the column as the pH increased within this distance.

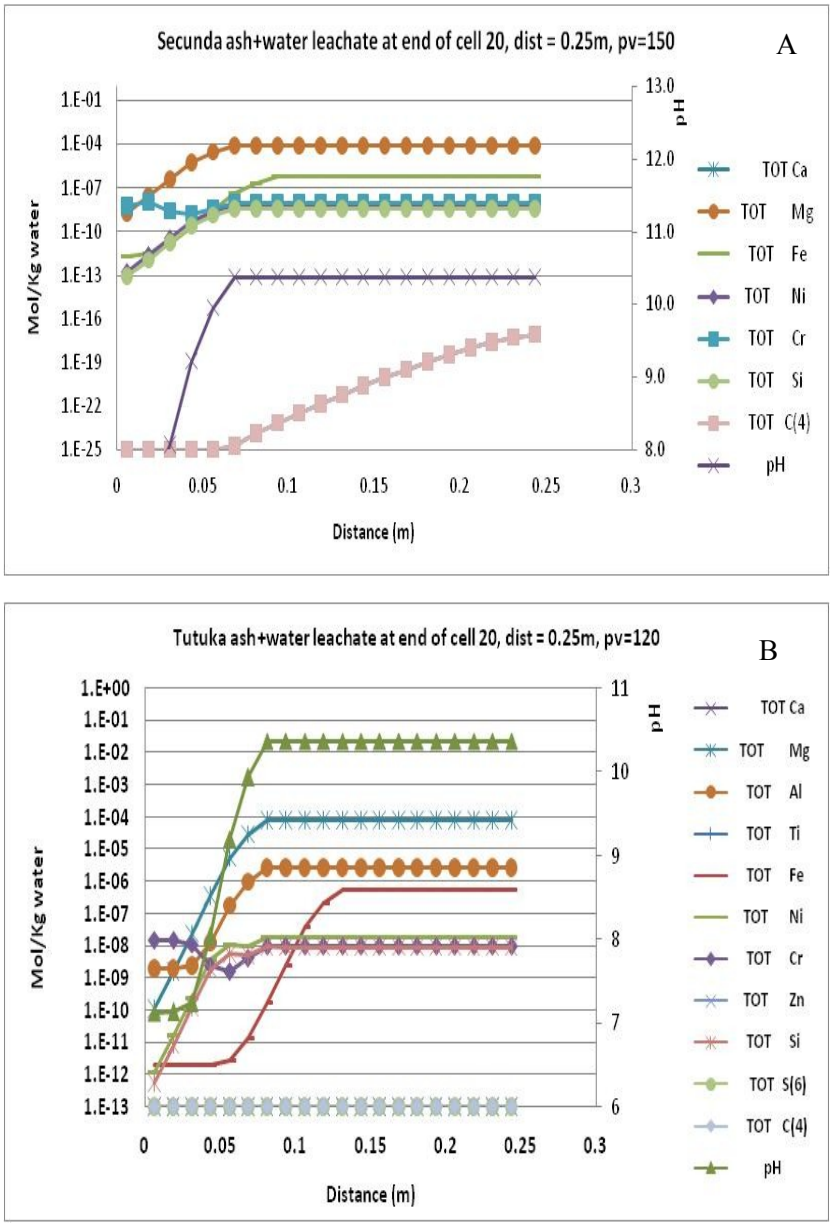

Figure 4.4a: Total elemental concentrations along the column distance after 90 days for major and trace elements for: (A) Secunda ash-water and (B) Tutuka ash-water

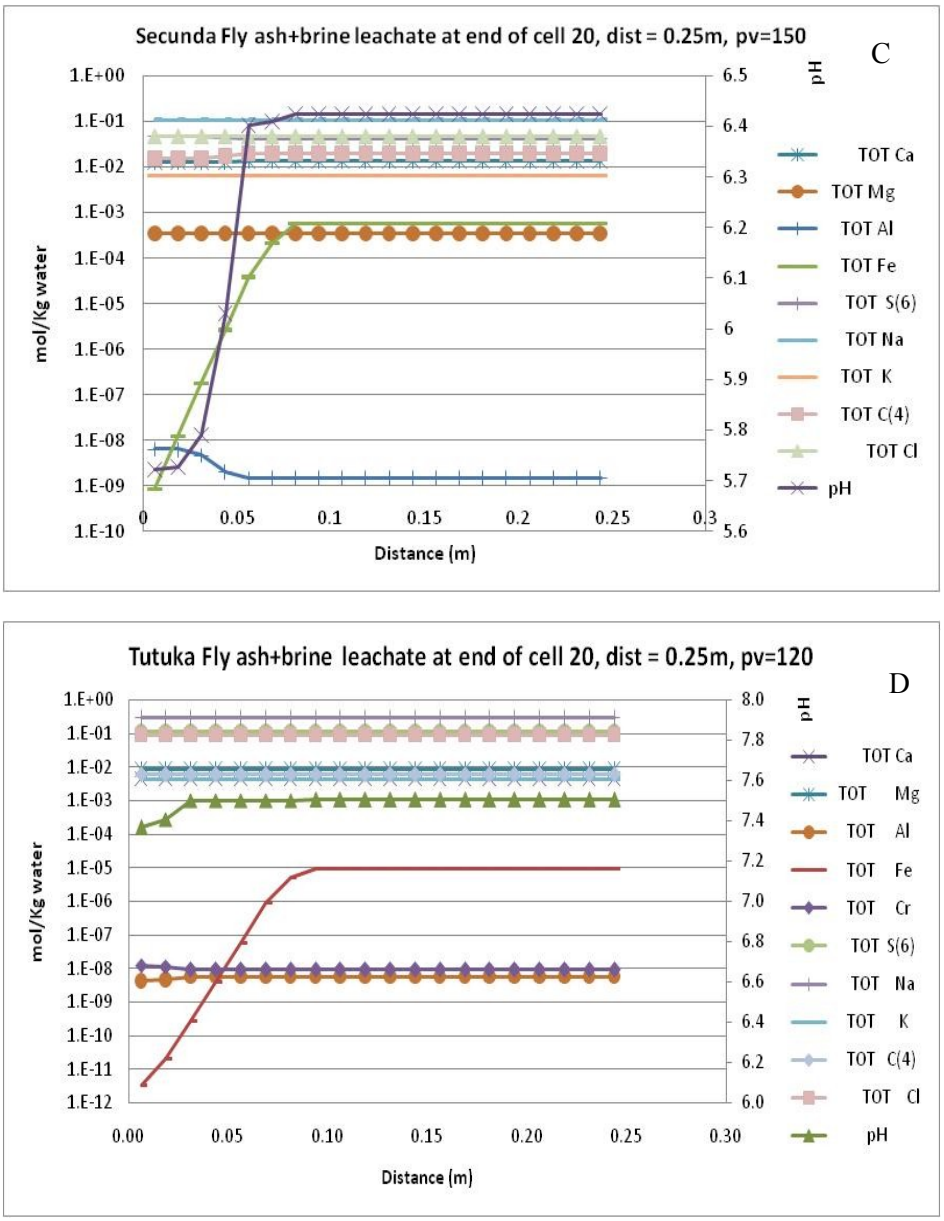

Figure 4.4b: Total elemental concentrations along the column distance after 90 days for major and trace elements for: (C) Secunda ash-brine and (D) Tutuka ash-brine

The profiles for total elemental concentrations along the column distance at different times for individual elements were presented in Figures 4.5a – 4.5j. The profiles were for Secunda and Tutuka fly ash recipes with water and brines.

From Figure 4.5a, initial Ca concentrations (at 0 day) were the highest all through the column distance. The concentration fronts for each particular day were low at near the inflow point but increased down gradient for the case of the ash-water interactions. This would be an indication of the solubility of Ca-bearing minerals undergoing dissolution when in contact with the pore water. Concentration decreases on interaction of ash with water and brines. However, the initial days (0-9 days) of interactions registered relatively higher concentrations for Ca near the point of inflow compared to the rest part of the columns. Individual elements show moving concentration fronts along the down gradient column distance. The concentration fronts trend observed in the ash-water and ash-brine interaction down gradient in different days is a clear pointer of the mobility mechanism likely taking place for the control of the Ca concentration within a given level. By knowing how much of a given species is present in the leachate after a given number of days (time), one can use this information to predict future scenarios. The trend of release of Ca, especially in the Secunda leachate, could indicate the dissolution of sparingly soluble mineral phases after the soluble Ca-containing salts have been flushed out of the system. The initial increase in the concentrations of Ca could be caused by the dissolution of readily soluble, Ca-rich phases such as CaO and $CaSO_4$. On the other hand, the lowering of the concentrations of Ca could be as a result of precipitation of new Ca-rich mineral phases in the ash-water system such as Csh_gel_0.8, portlandite, anhydrite and gypsum. These simulation results are in agreement with what was observed from the column experimental results from UWC by Ojo and co-workers [29] as outlined in **section 1.1.1**.

For the purposes of capturing and interpretation of the data for each graph depicting concentration fronts for each element for given days, the column distance was divided into three zones: the zone closest to the inlet (0 – 0.1 m), the middle zone (0.1 – 0.17 m) and the zone closest to the outlet of the column (0.17 -0.25 m).

Generally, all the elements featured in these graphs Figures 4.5(a-j) exhibited concentration fronts which were relatively higher at the zone closest to the inlet of the column particularly in the ash-water interaction scenarios. This applied for Ca, Mg, Fe, Ni, Si, S(6), C, in which high concentration fronts were observed at the zone closest to the inlet and as the fronts moved down gradient the fronts were reduced. However, Cr, Al, behaved differently. Their initial concentration fronts were all high while they were lower at the zone closet to the column inlet, increased slightly higher at the middle zone after which the lower days exhibited higher concentration fronts. These simulation results were in agreement with the general experimental results highlighted in **section 1.1.1.** in which the upflow

column leaching test showed that the initial leachates from the fly ashes contained high concentrations of species such as Ca, Mg, Na, K, S, and Sr which decreased as the leaching continued until steady states were reached. The Fe, Mn, Se, As, Cu, Pb, Mo and Cr concentrations were also high at the beginning of the leaching test before decreasing over time [6, 10].

The other elements like Mo, Zn, Sr, Li, exhibited concentration fronts for between 0 and 9 days and their concentrations were too small to be considered significant as shown in Figure 4.5j. Sodium and potassium behaved conservatively like chlorine in that they showed no significant variation[142] in all the simulated days. These elements were not observed in Secunda and Tutuka ash-water column system or were of negligibly small amounts in the subsequent days.

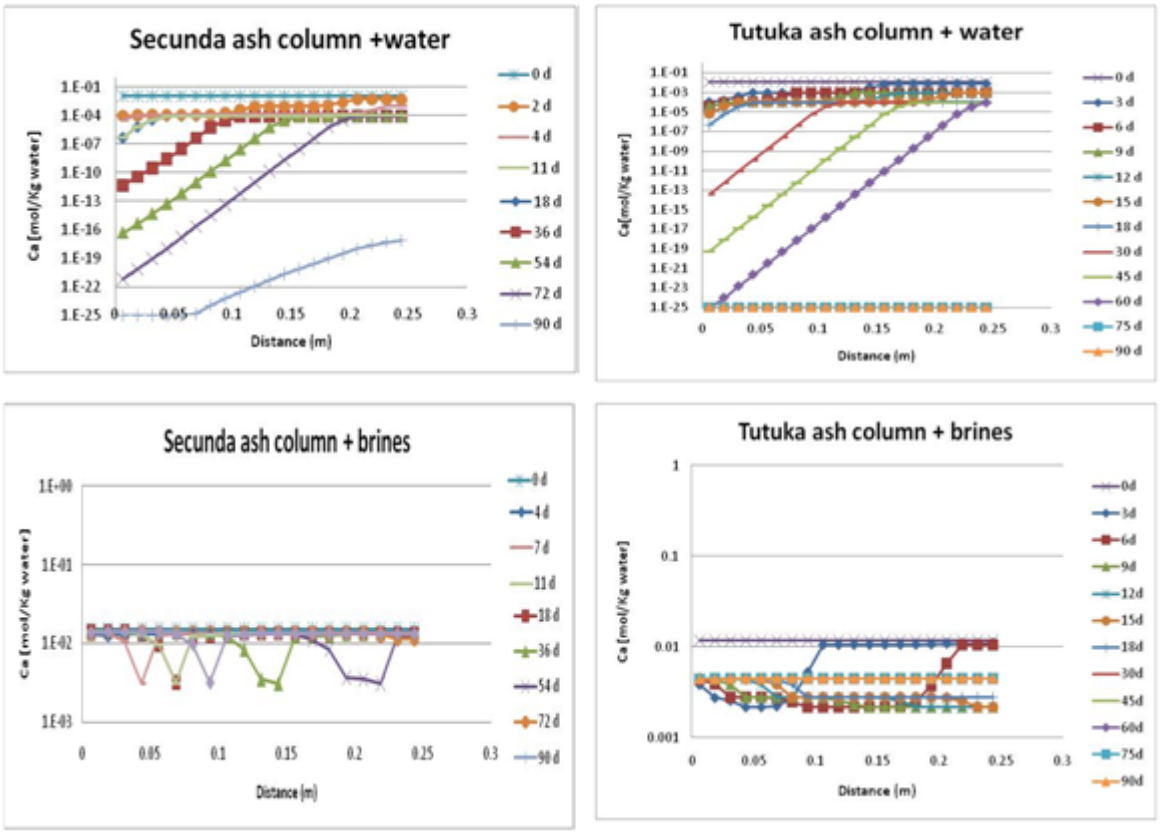

Figure 4.5a: Total elemental concentrations along the vertical column distance at different times for calcium (Ca) for Secunda and Tutuka ash with demineralized water and brines

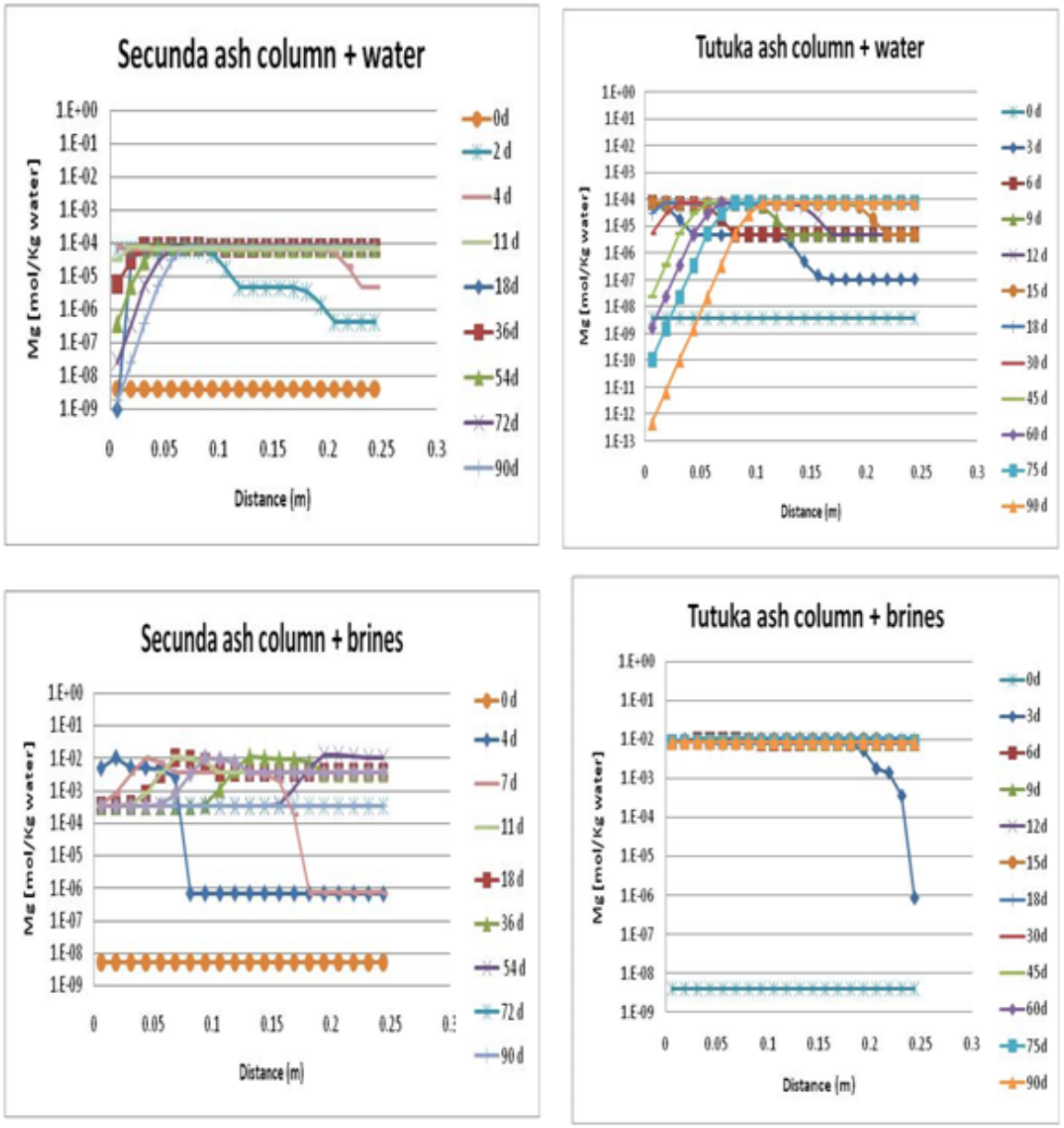

Figure 4.5b: Total elemental concentrations along the vertical column distance at different times for magnesium (Mg) for Secunda and Tutuka ash with demineralized water and brines

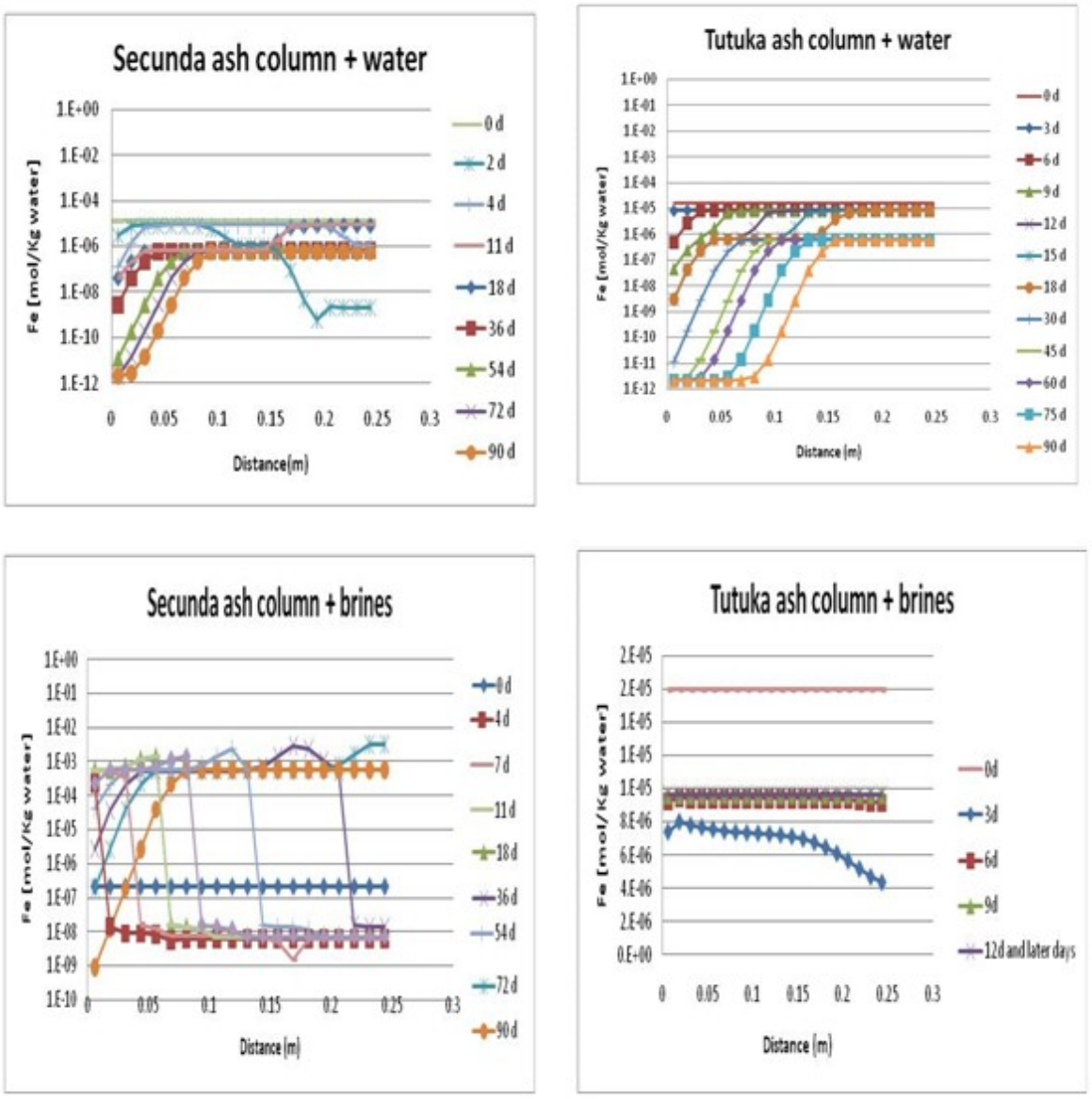

Figure 4.5c: Total elemental concentrations along the vertical column distance at different times for iron (Fe) for Secunda and Tutuka ash with demineralized water and brines

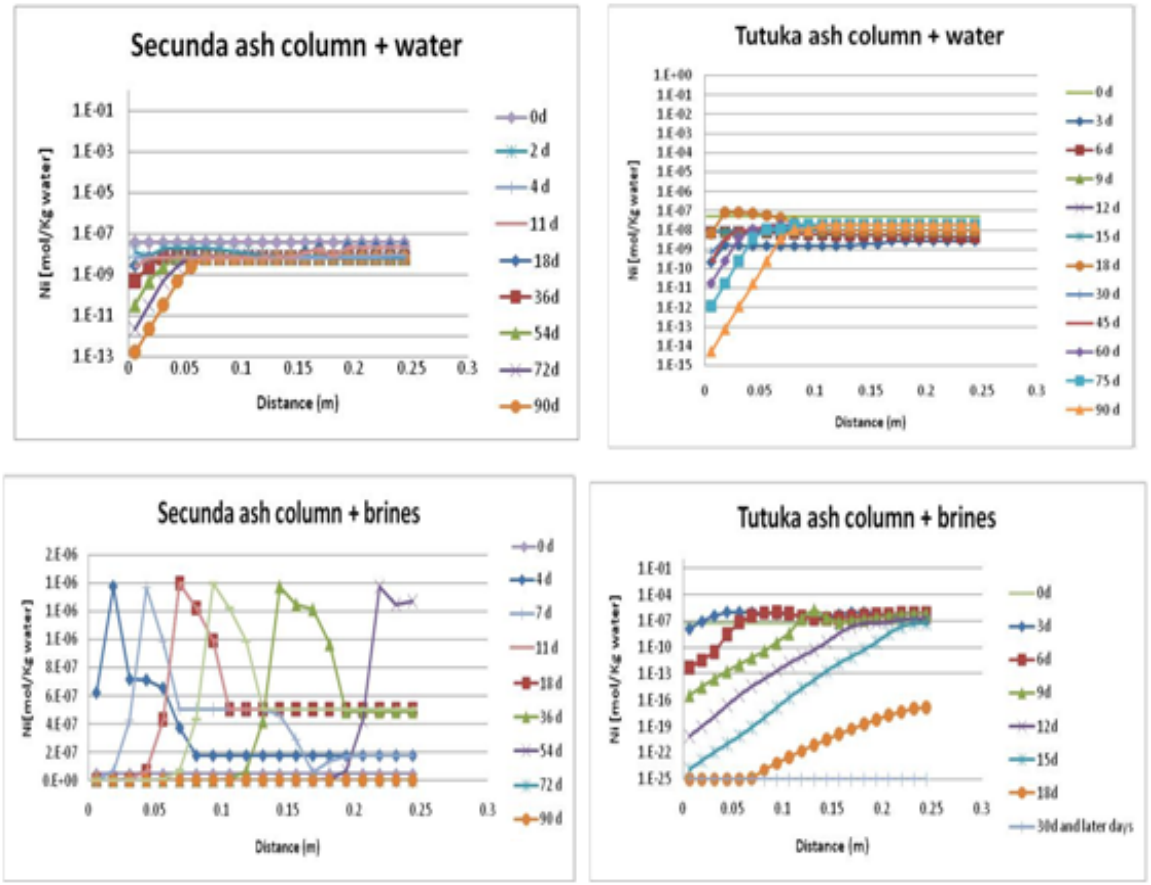

Figure 4.5d: Total elemental concentrations along the vertical column distance at different times for nickel (Ni) for Secunda and Tutuka ash with demineralized water and brines

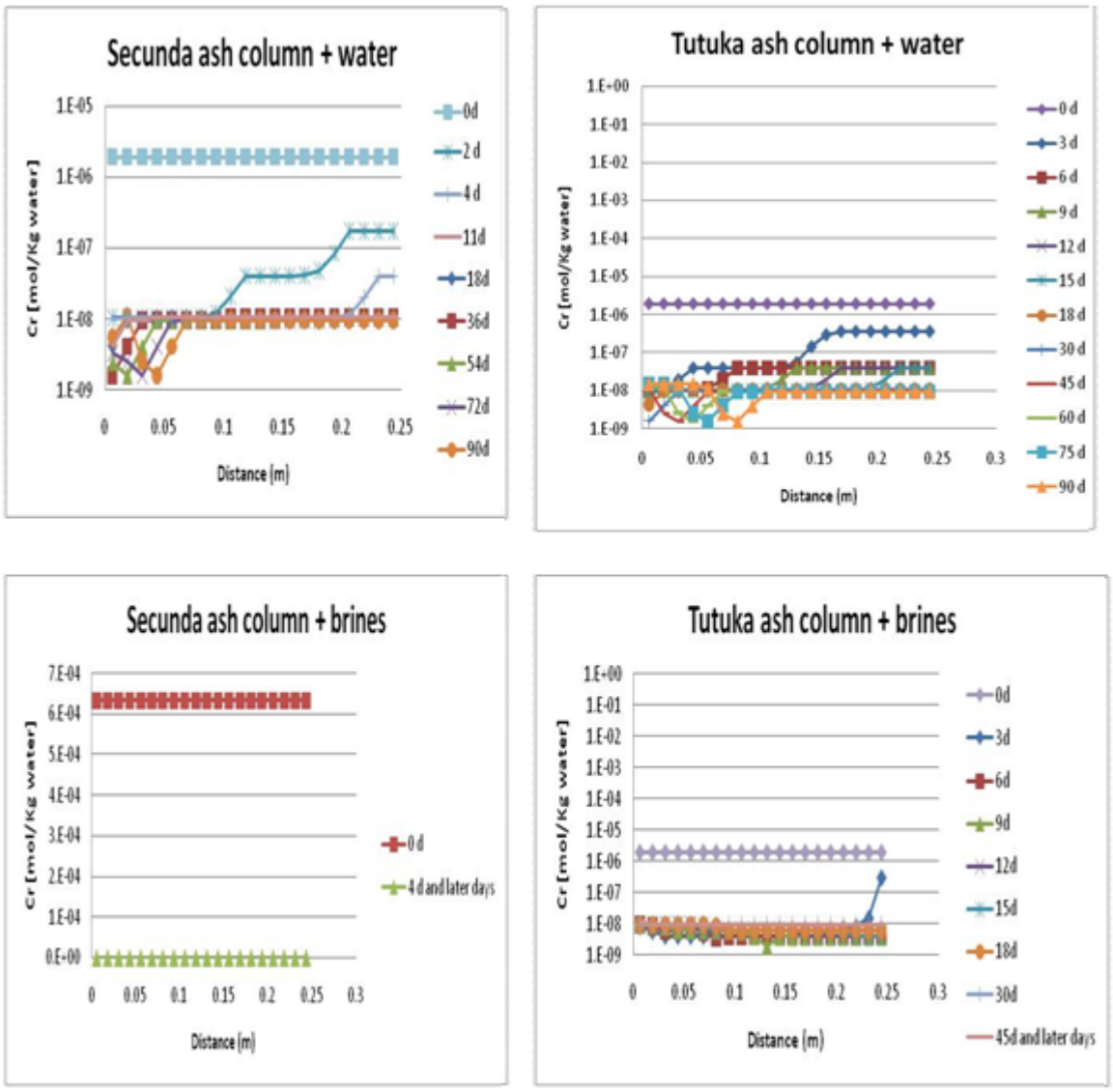

Figure 4.5e: Total elemental concentrations along the vertical column distance at different times for chromium (Cr) for Secunda and Tutuka ash with demineralized water and brines

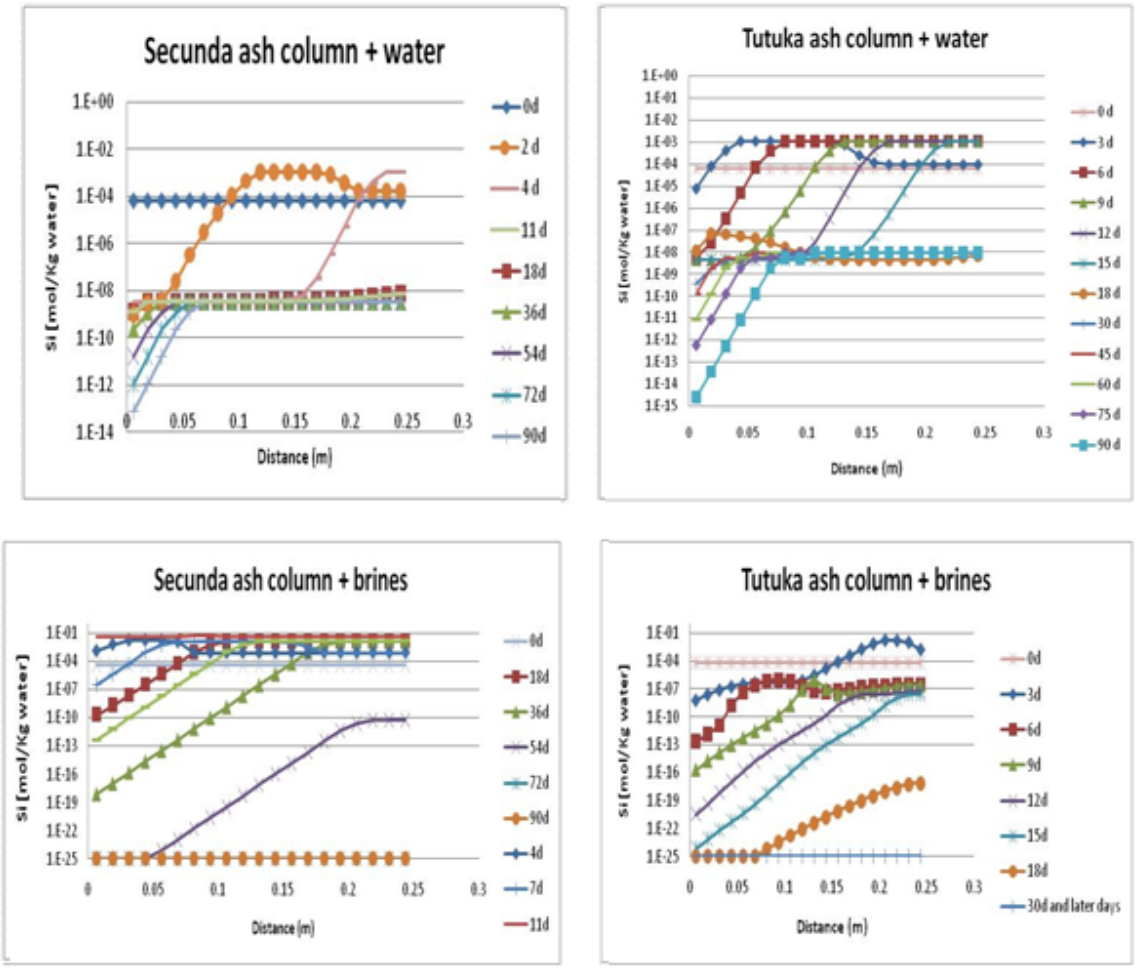

Figure 4.5f: Total elemental concentrations along the vertical column distance at different times for silicon (Si) for Secunda and Tutuka ash with demineralized water and brines

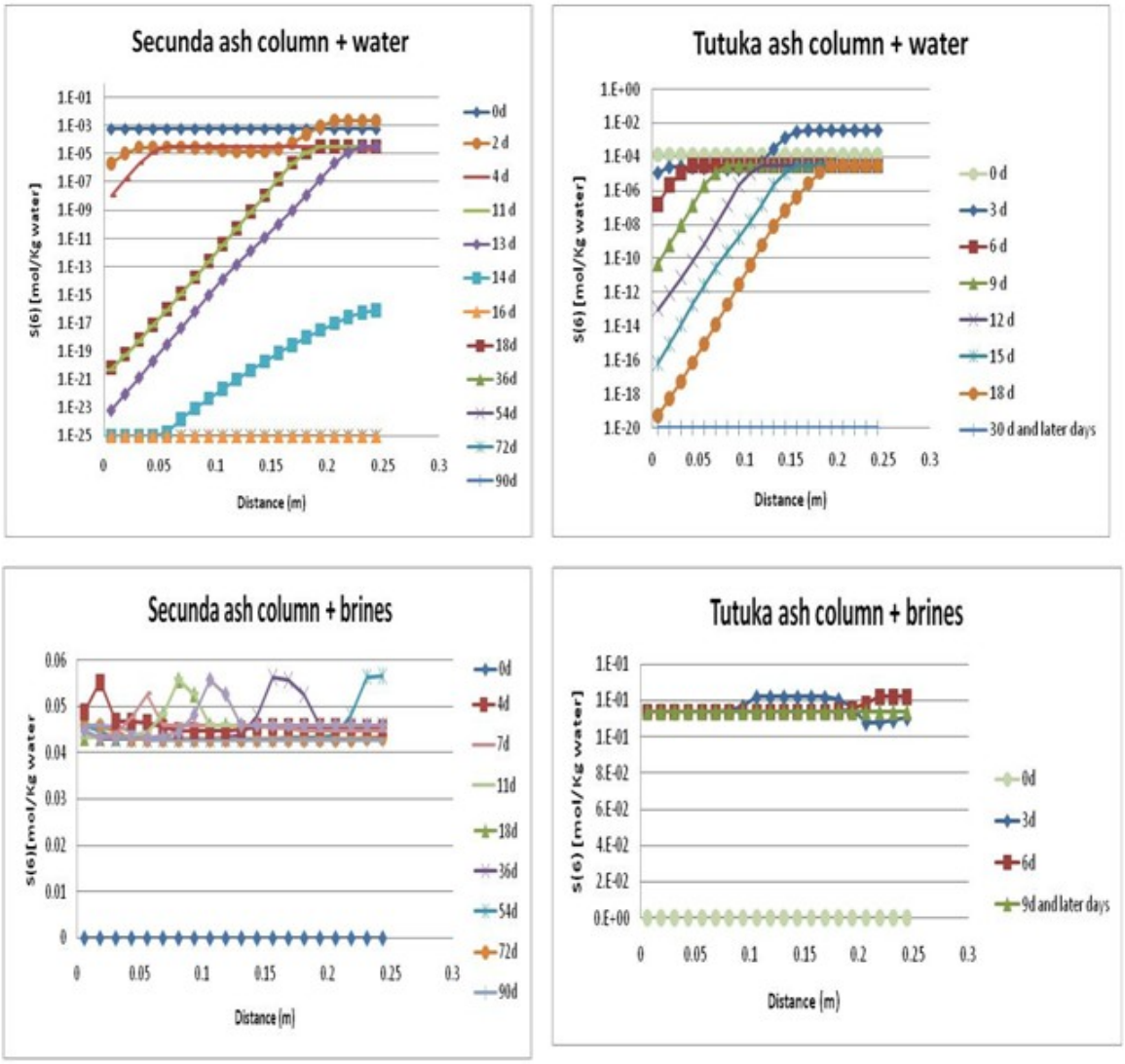

Figure 4.5g: Total elemental concentrations along the vertical column distance at different times for sulphur (S(6)) for Secunda and Tutuka ash with demineralized water and brines

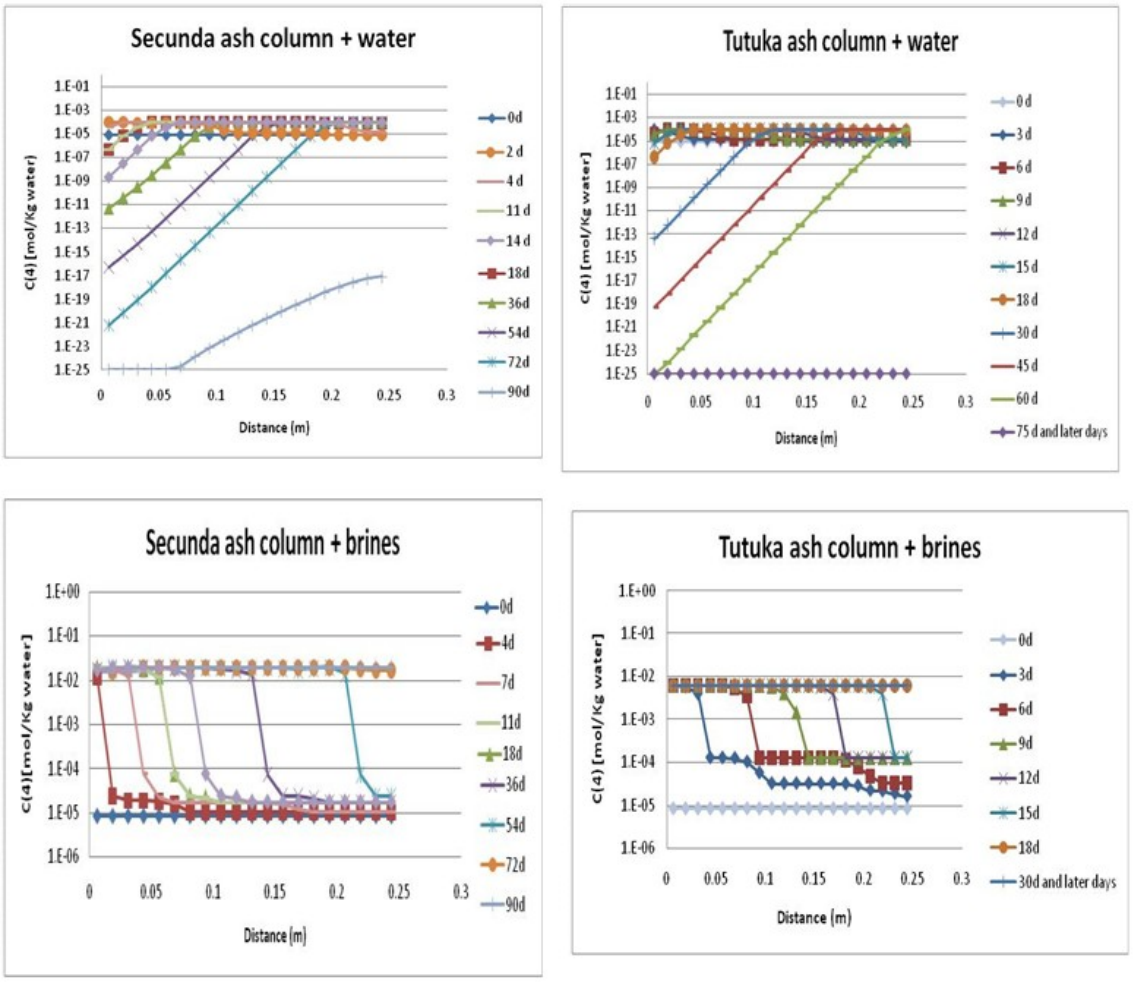

Figure 4.5h: Total elemental concentrations along the vertical column distance at different times for carbon (C(4)) for Secunda and Tutuka ash with demineralized water and brines

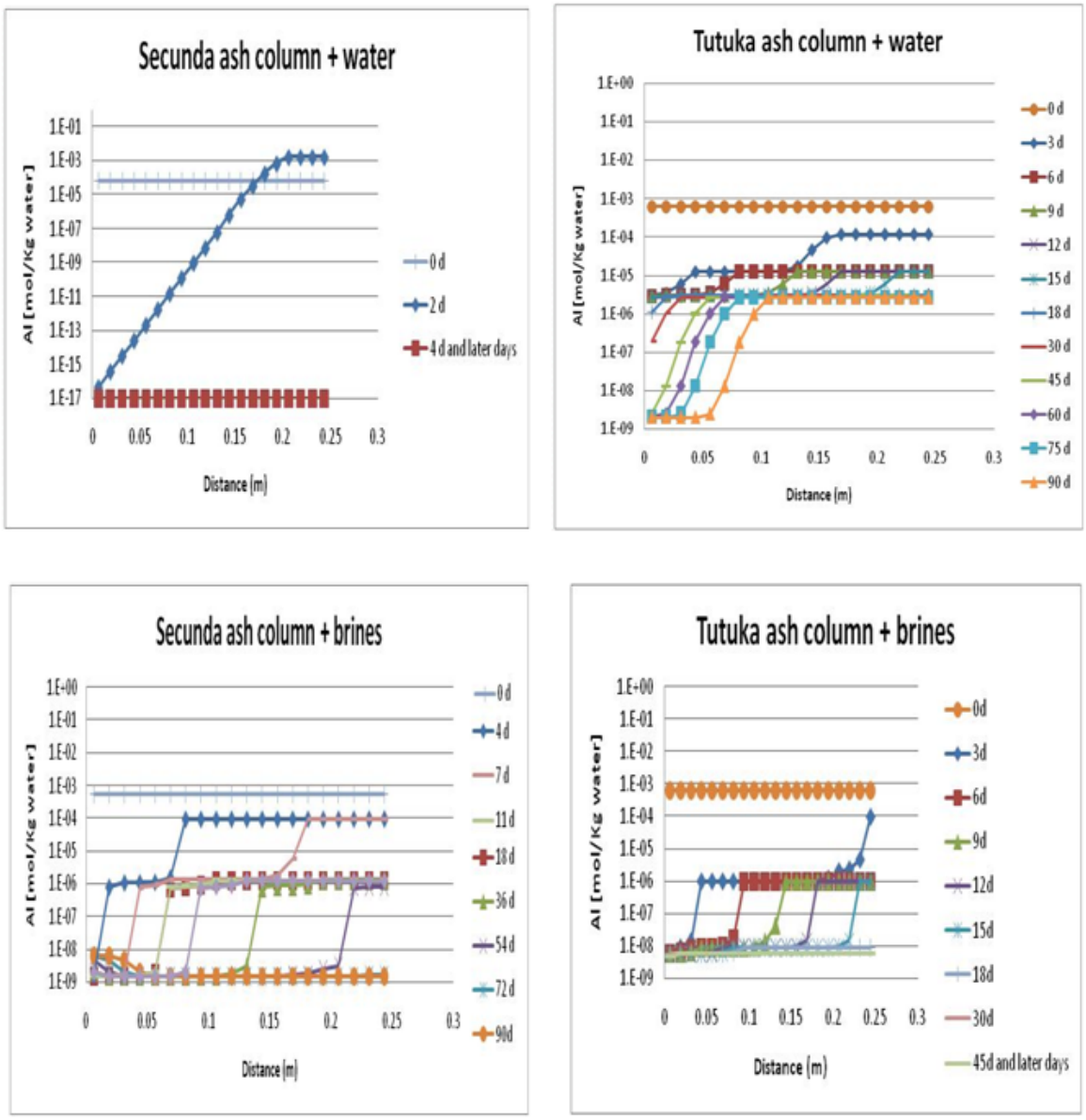

Figure 4.5i: Total elemental concentrations along the vertical column distance at different times for aluminium (Al) for Secunda and Tutuka ash with demineralized water and brines

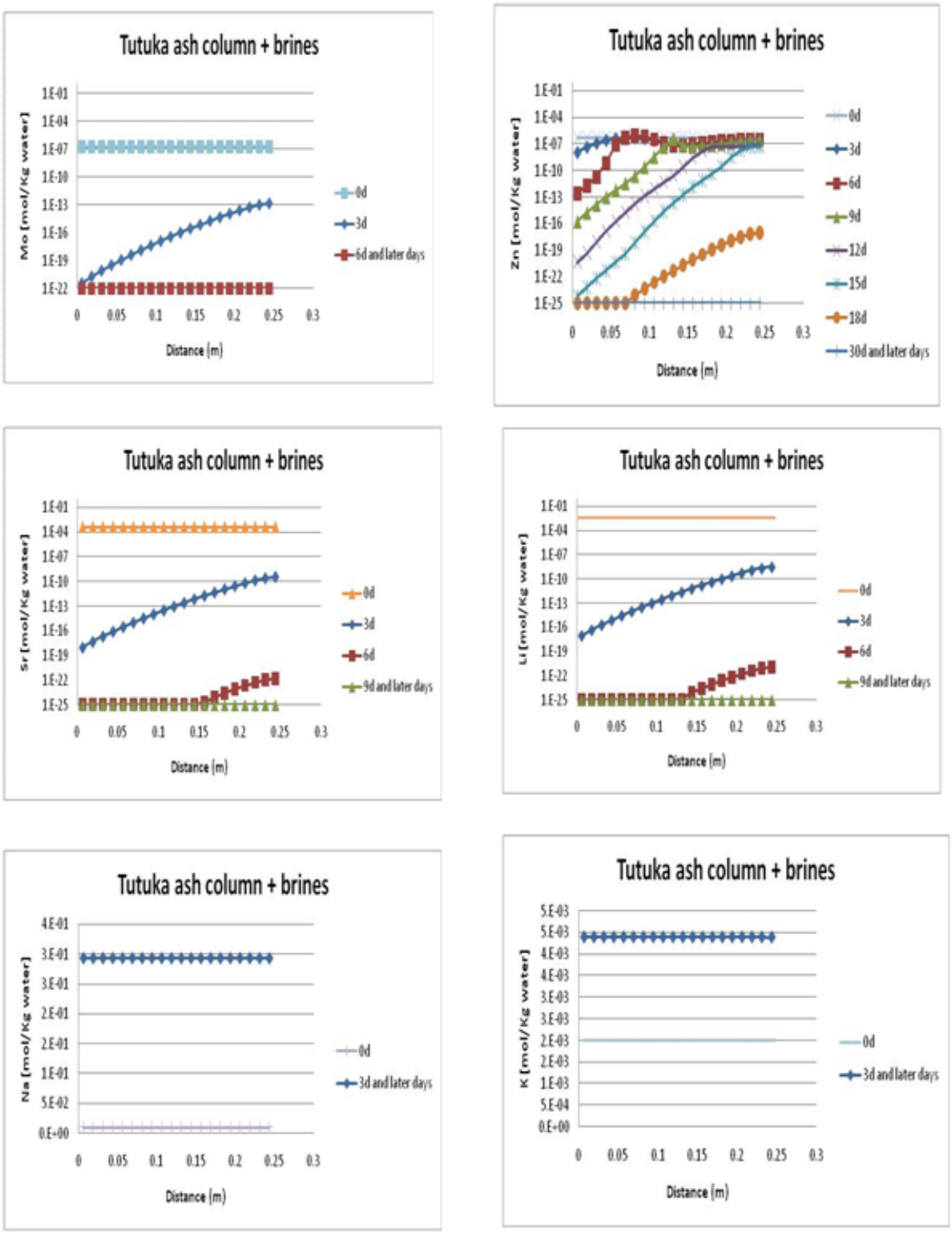

Figure 4.5j: Total elemental concentrations along the vertical column distance at different times for the elements: Na, K, Li, Sr, Zn, Mo for Secunda and Tutuka ash with demineralized water and brines

4.3.4 Major mineral phases present versus time at breakthrough volumes over 90 days

Figures 4.6a and 4.6b show the amount of mineral phases present over 90 days period after each breakthrough volume (at cell 20, last cell considered in column discretization) for Secunda and Tutuka fly ashes either modeled with water or brines. Generally same minerals that show marked changes in amounts over the 90-days period of dynamic leaching were recorded in both fly ashes, except in the case of millerite which was only present in Secunda fly ash. More supplementary results on mineralogy on column modeling are given in **Appendix 4** (Tables A2 - A4). Minerals such as brucite, Csh_gel_0.8 and Ettringite showed sharp decrease in amounts in the first five days of contact with water and brines as the pH value dropped from 12.6 to about 10.5 for Secunda with water, 11.2 for Tutuka with water, 11.8 for Secunda with brine and 10.0 for Tutuka with brines. The reduction in amounts of these minerals was as a result of dissolution reactions at the time of equilibration during the first 3-4 days of contact with brines and water and which was highly pH-controlled.

Generally most of the mineral phases got dissolved within the first 30 days except calcite and hematite whose amount remain constant at about 0.068 and 0.03 moles respectively in Tutuka. The amount of calcite present remained fairly constant until after 70 days in the case of Secunda ash with water and 45 days for Tutuka ash with water where a decrease to depletion was recorded within the next almost 20 days. The dissolution of calcite accounts for the marked increase of the concentrations of Ca and S(VI) in the leachate after between 40 and 90 days. However the amounts were not sufficient enough to cause oversaturation of gypsum for it to precipitate.

In the case of ash-brines scenario, calcite initial amounts remained constant for the first 50 days (Secunda) and about 18 days (Tutuka) after which the amount increased in both ash-brine systems, recording about 1.8 moles/kg water after 70 days and the about 2.2 moles /kg water after 90 days (Secunda), and constant amount of about 0.065 moles/kg water of calcite. The increased amounts could be attributed to the presence of Ca and S(VI) in the brines which cause precipitation of the calcite. At the initial stages of ash-brine interaction, gypsum is precipitated as the brines provide sufficient amounts of Ca and S(VI) to make gypsum oversaturated and hence precipitates as depicted in Figure 4.6b for Secunda and Tutuka ash-brine systems. Further Ca in solution is availed by the dissolution of Csh_gel_0.8 particularly after about 35 days in Secunda and after 5 days for Tutuka ash-brine scenarios. Csh_gel_0.8 mineral also responded to changes in pH, by taking the same trend as pH and showing dissolution for the first 4 days, remains almost constant up to 15 days and then get depleted at the 18th day. The formation of ettringite in the first 5 days and then dissolving in the Secunda ash-brine system may have been controlled by the Csh_gel_0.8 mineralogical changes in the initial 10 days in which it dissolved for the first 4 days, remained constant up to about 8 days and then

started precipitating to reach a total of about 1.25 moles in 10 days. This amount remained constant until about 38 days upon which dissolution took place to depletion after 55 days, between which period it had some control on the precipitation of gypsum.

The respective initial amounts of hematite were constant throughout the 90 days for all Secunda and Tutuka modeled systems. Most of the other mineral phases may have dissolved or were present in negligible amounts over the 90 days period.

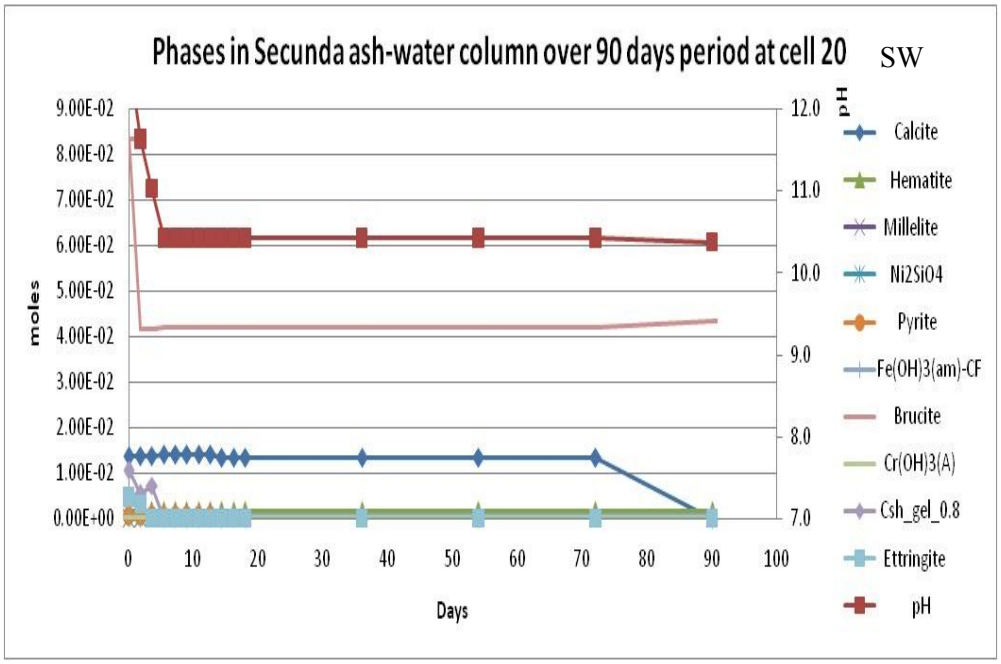

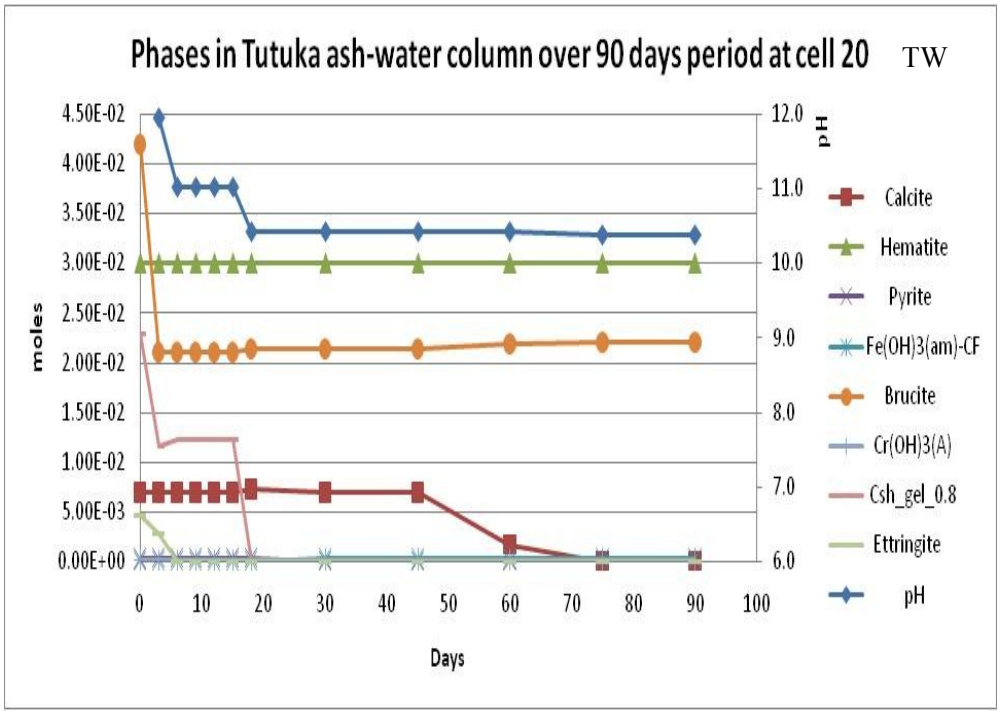

Figure 4.6a: Amount of mineral phases present over a 90-days period after each breakthrough volume for Secunda and Tutuka ash-brine columns: SW-Secunda ash and water, TW-Tutuka ash and water; (NB. Legend symbols different)

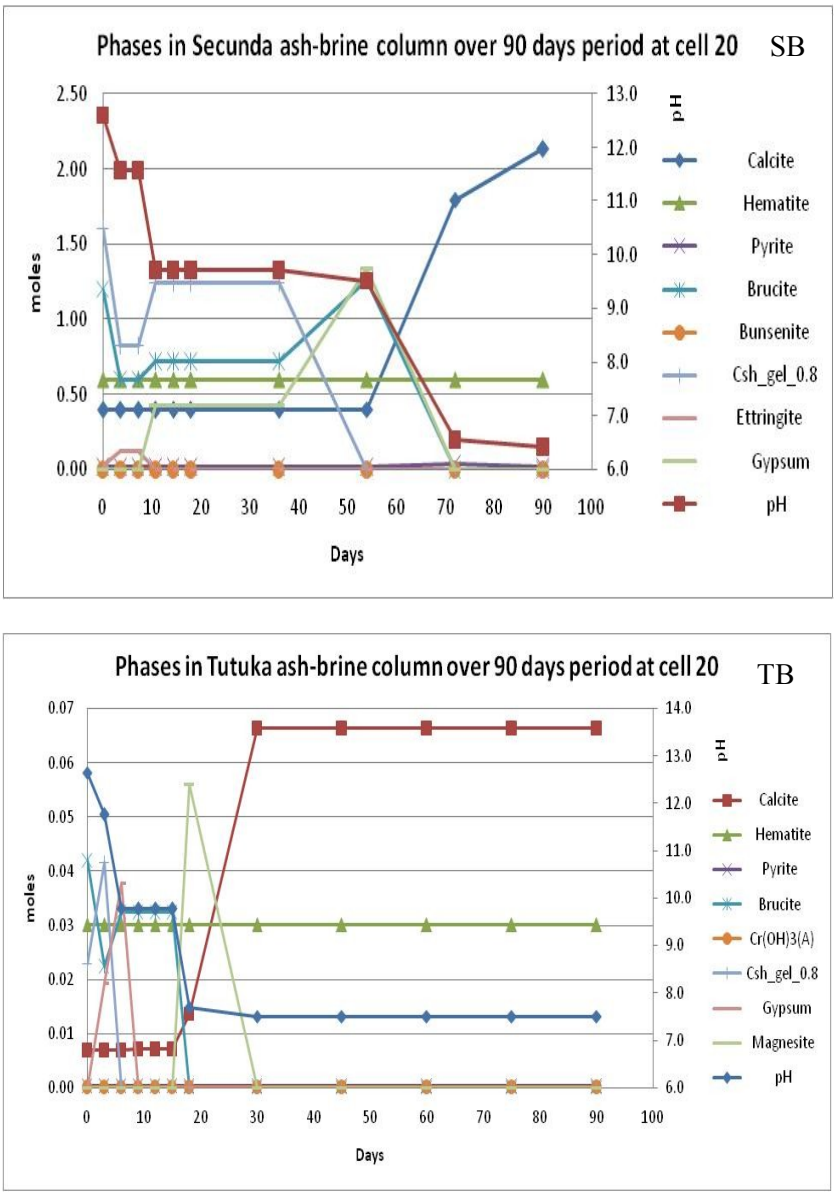

Figure 4.6b: Amount of mineral phases present over a 90-days period after each breakthrough volume for Secunda and Tutuka ash-brine columns: SB- Secunda ash and brine, TB-Tutuka ash and brine; (NB. Legend symbols different)

4.3.5 Moles of mineral phases present versus distance along the column at end of simulated time (90 days).

The results of the mineral phase amounts along the column distance during the 90 days simulation were jointly presented in Figures 4.7a and 4.7b while Figure 4.8 captured the individual mineral phases. Secunda and Tutuka ash-water systems showed that the major mineral phases remaining after 90 days were hematite, nickel silicate, amorphous hydrous ferric oxide (HFO), amorphous chrome and brucite. Hematite amounts remained constant at all column positions whereas between 0.07 m and 0.15 m a general increase of brucite and amorphous HFO was recorded. Amorphous chrome showed no significant change in Secunda ash-water system but with Tutuka, its neoformed phase occurred at about 0.02 m (though very small amounts) and same amounts remained up to the end of the column. From the Secunda and Tutuka ash-water model, brucite formed at a point closer to the column inflow for Secunda compared to that of Tutuka.

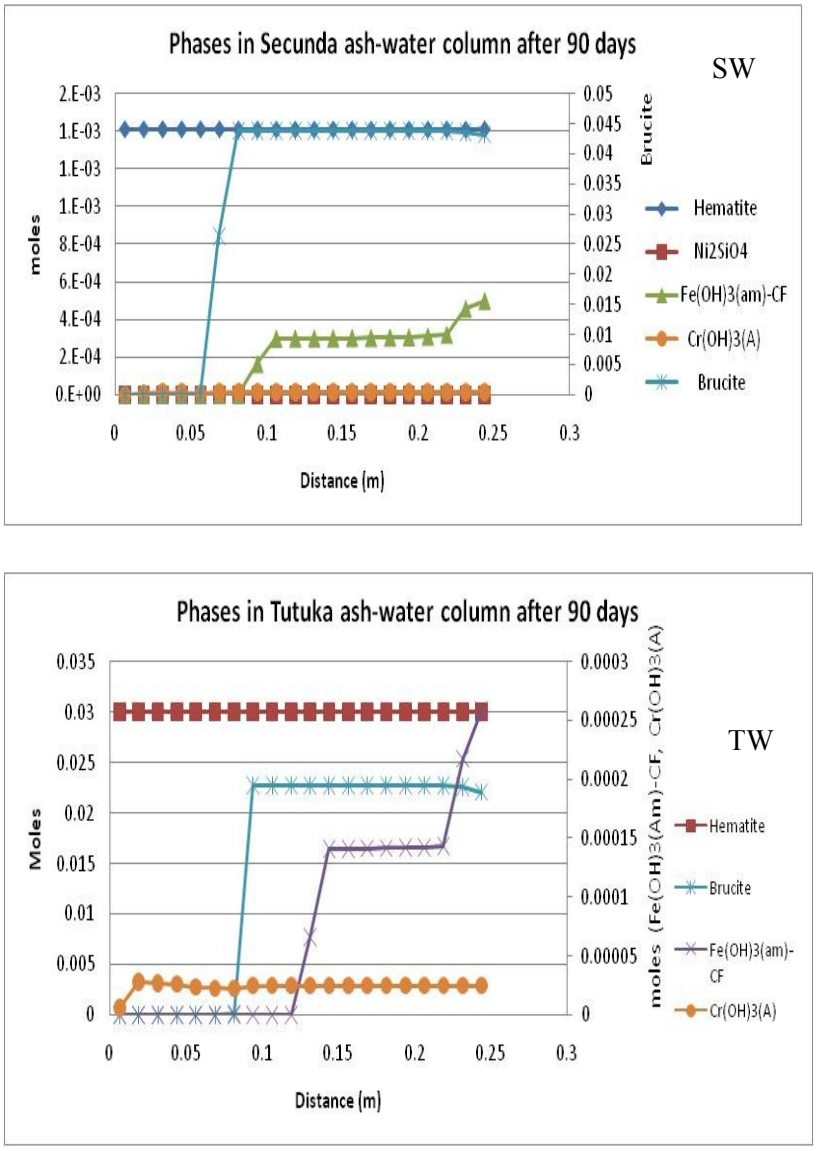

Figure 4.7a: Amount of mineral phases remaining along the column after 90-days ash-brine dynamic interaction for Secunda and Tutuka ash columns: SW-Secunda ash and water, TW-Tutuka ash and water (NB. Legend symbols different)

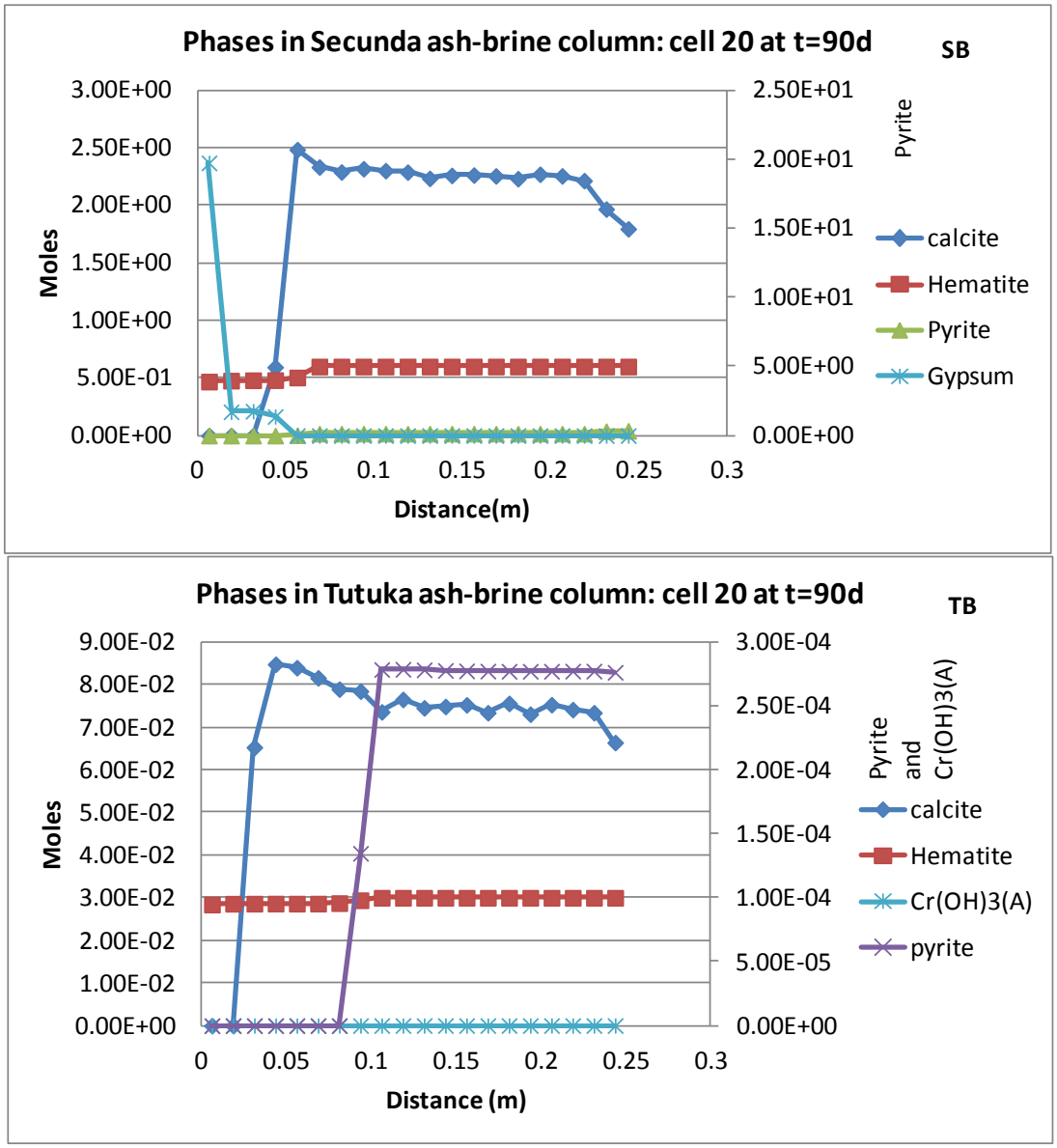

Figure 4.7b: Amount of mineral phases remaining along the column after 90-days ash-brine dynamic interaction for Secunda and Tutuka ash columns: SB- Secunda ash and brine, TB-Tutuka ash and brine (NB. Legend symbols different)

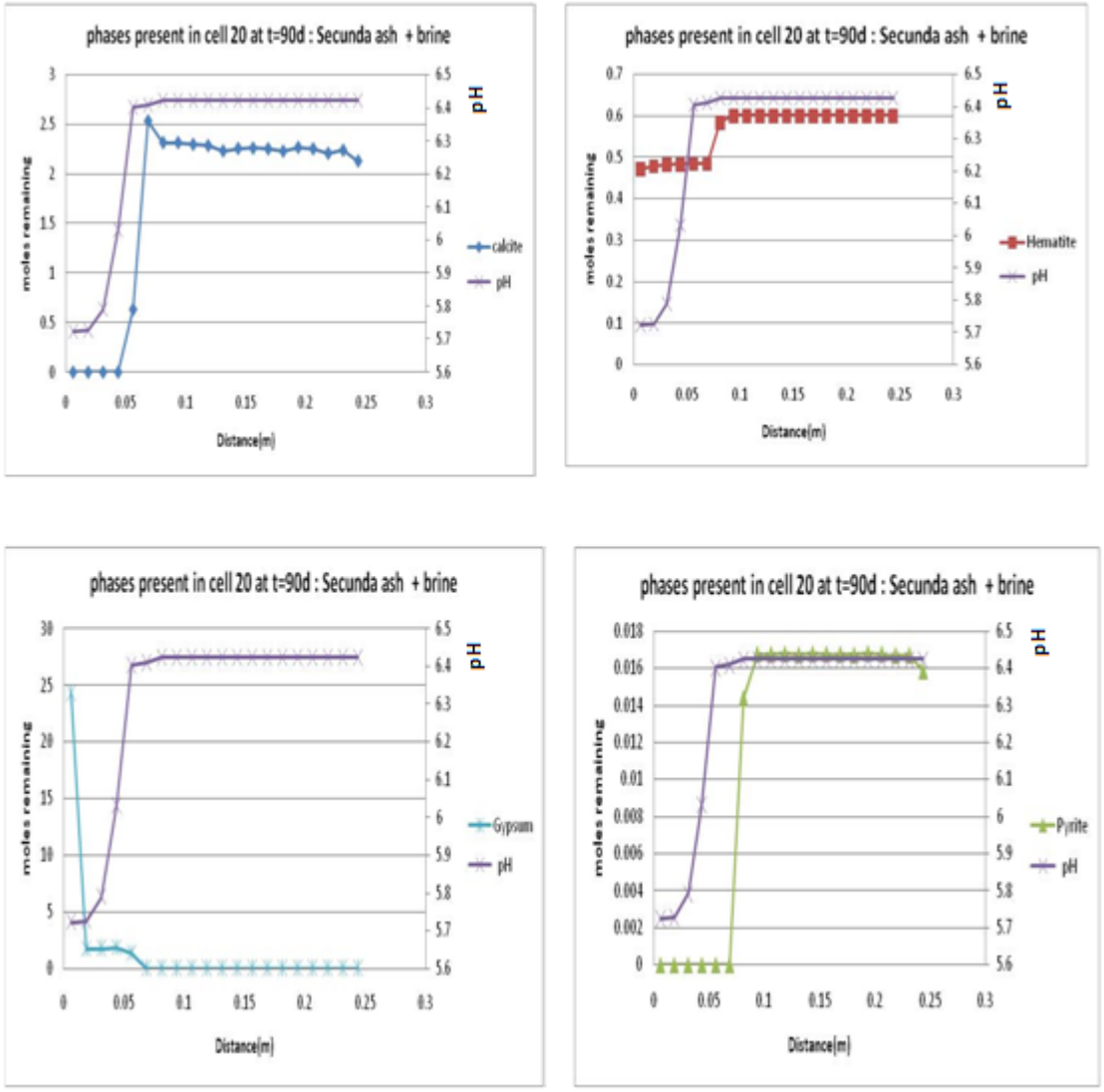

Figure 4.8: Moles of mineral phases present and pH versus vertical column distance after 90 days

From Figure 4.8, it can be seen clearly that calcite started being formed at 0.05 m and the amount increased rapidly to about 2.5 moles/kg water after which slight fluctuations within 2 and 2.5 moles were recorded up to the end of the column after 90 days. While calcite is precipitating and thus increasing in amount at this column distance, gypsum amounts are decreasing, implying dissolution of the mineral is taking place during the Secunda ash-brine system. After about 0.075 m all the gypsum will have dissolved while the precipitation reaction of calcite will have reached a steady state, thereby amount present remaining constant up to the column outflow position.

4.3.6 Quantitative change of mineral phases versus distance at last pore volumes (or at end of simulation time)

Figures 4.9 and 4.10 describe the mineral phase changes after the 90 days simulation for the two fly ashes (Secunda and Tutuka) with water and brines respectively. For the fly ash with water simulations, brucite was the only mineral that showed significant change in phase amounts which occurred just after 0.05 m from the column inflow position. Dissolution took place at pH value of 10.5 for both fly ash-water scenarios. From Figure 4.10, the calcite dissolution took place at 0.05 m as gypsum precipitated at pH value of 6.4 after which a steady pH was achieved, confirming the precipitation-dissolution of calcite and gypsum was pH controlled. Precipitation of calcite was recorded at 0.075 m after which no change in amounts was observed. Dissolution of hematite was also recorded but in very small amounts at pH value of 5.9 (Secunda) and 7.3 (Tutuka) about 0.1 m from the column inflow.

Generally hematite, $Cr(OH)_3(A)$, $Fe(OH)_3(am)$-CF and brucite show some quantifiable though very small changes in moles for fly ash with brines simulations. The mole changes in brucite and $Cr(OH)_3(A)$ were pH-controlled and took place between 0.05 and 0.1 m from the column inflow.

Some significant changes in moles of mineral phases were recorded for the minerals hematite, pyrite and calcite, gypsum and $Cr(OH)_3(A)$, in Secunda and Tutuka ash-brine column models. Dissolution of hematite, pyrite and calcite took place at between 0.05 and 0.1 m from the column inflow at pH value of 6.4 while gypsum precipitated at about 0.05 m at the same pH for Secunda ash-brine column model. Similar trend was observed for the Tutuka ash-brine column model. The significant changes in moles of mineral phases confirmed the effect of brines in mineralogical changes of fly ashes. Many of the other mineral phases underwent dissolution and some were of very small quantities whose change in amount was considered insignificant.

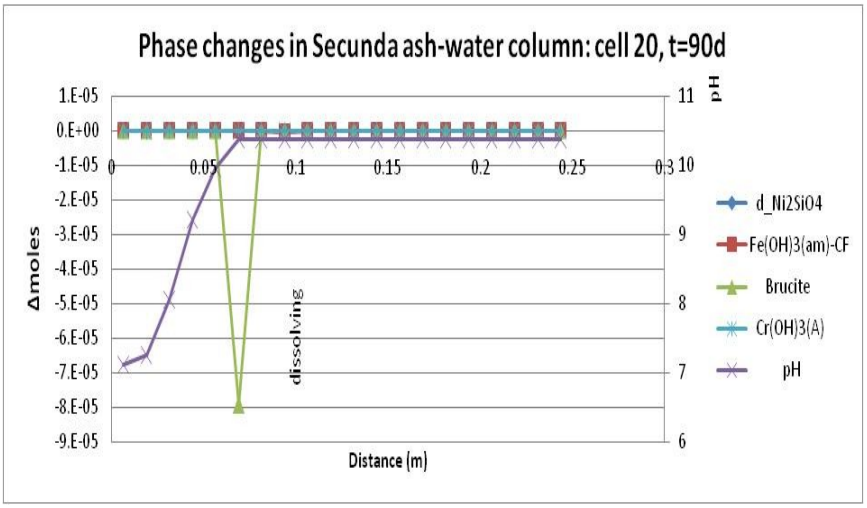

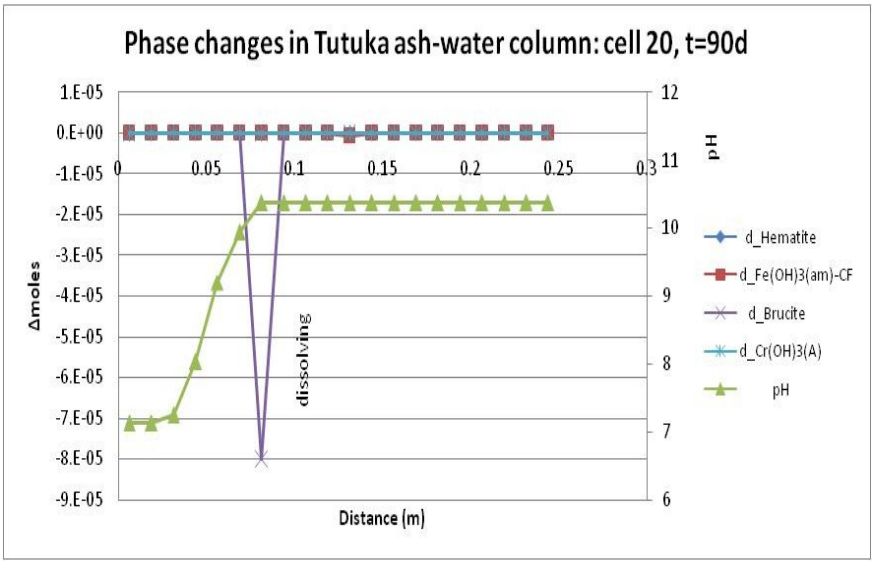

Figure 4.9: Amount of change of mineral phases along the column after 90-days ash-water dynamic interaction for Secunda and Tutuka ash columns

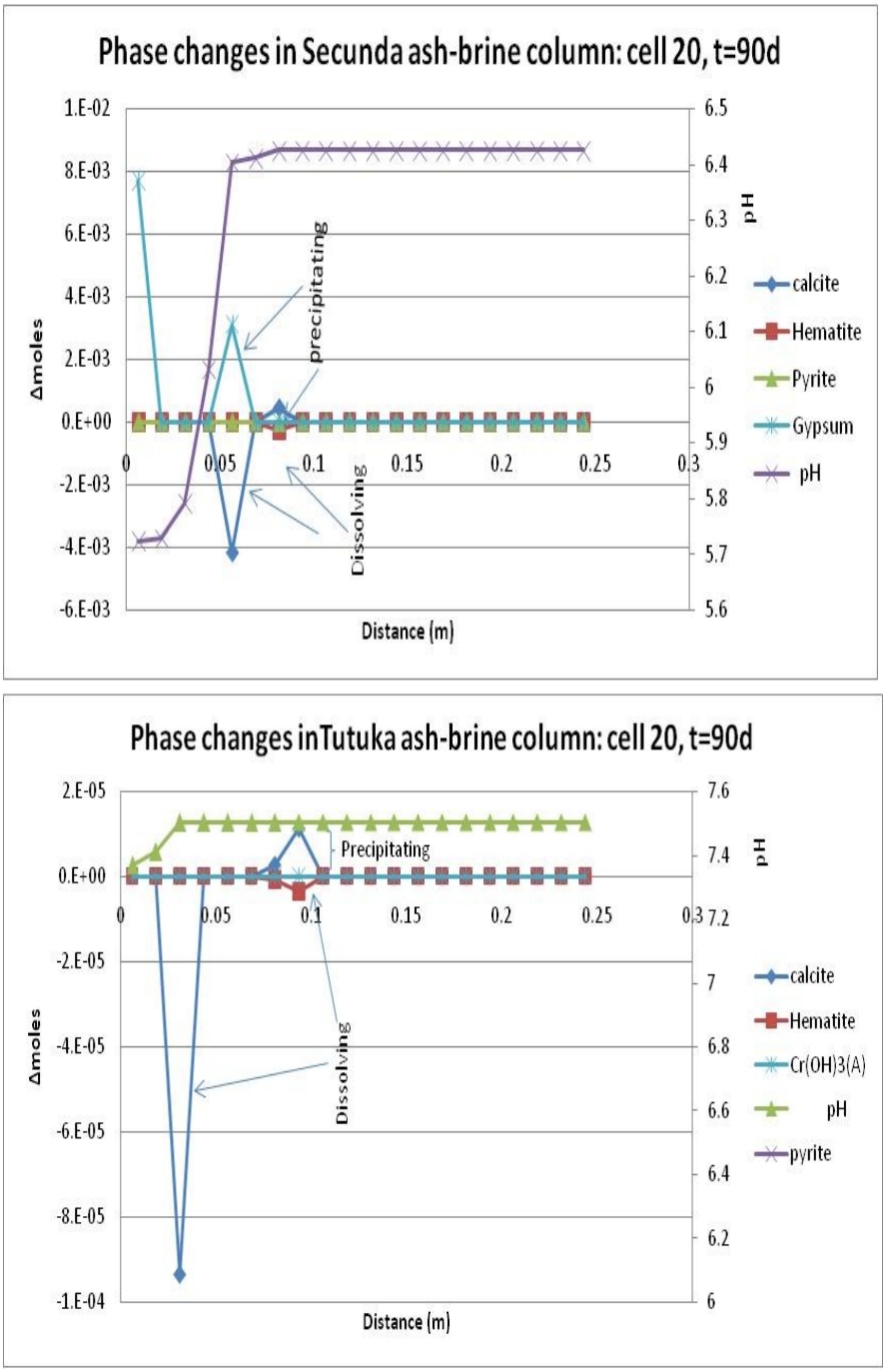

Figure 4.10: Amount of change of mineral phases along the column after 90-days ash-brine dynamic interaction for Secunda and Tutuka ash columns (negative changes in moles show dissolution, positive change show precipitation)

4.3.7 Effect of geochemical reactions on porosity

As a step towards determining the effect of geochemical reactions on porosity of the fly ash under different scenarios, molar volume calculations were carried out in a spreadsheet format as given in Table 4.3. The density of each of the mineral phases was literature-searched and reported (references were give as superscripts against the density values in the table) and from the molar volume of the mineral phase, its mineral fraction (Vm) was also determined.

In our modeling work, Secunda ash recipe with brine was used as the case study that would give insights as to the effects of the various geochemical reactions have on the porosity of the fly ash as it interacted with the water/brines systems. The porosity effects were based on the following mineral phases: anhydrite, calcite, hematite, kaolinite, lime, mullite, periclase, pyrite and $SrSiO_3$ which contribute significantly towards the volume fraction of the heterogeneous fly ash recipe. The rest of the modeled mineral phases in the recipe contribute negligible volume fractions as shown from the Table 4.3.

Table 4.3: Calculated molar volumes, initial volume, and volume fractions of mineral phases for Secunda ash recipe: Vm-mineral volume fraction. (Superscript references a, b, c, d and e against density values: a[143], b[144], c[145]), d[146], e[147]).

Mineral phase	Amount (Moles)	Molar mass (g/mole)	density (g/cm^3)	molar volume (cm^3/mol)	initial mineral vol (cm^3/L)	Vm
$Al(OH)_3$(mC)	0.00E+00	78.00	2.42[a]	32.23	0.00000	0.00000
Anhydrite	7.66E-03	136.14	2.97[a]	45.84	0.35093	0.09260
Brucite	0.00E+00	58.32	2.39[a]	24.40	0.00000	0.00000
Bunsenite	0.00E+00	74.69	6.60[a]	11.32	0.00000	0.00000
$CaCrO_4$	1.96E-05	156.07	3.12[a]	50.02	0.00098	0.00026
Calcite	1.36E-02	100.09	2.71[a]	36.93	0.50403	0.13300
$CaMoO_4$	1.32E-06	200.01	4.20[a]	47.62	0.00006	0.00002
Celestite	0.00E+00	183.68	3.95[a]	46.50	0.00000	0.00000
$Cr(OH)_3$(A)	0.00E+00	103.02	2.65[b]	38.87	0.00000	0.00000
Csh_gel_0.8	0.00E+00	173.52	3.24[a]	53.55	0.00000	0.00000
Ettringite	0.00E+00	1255.09	1.80[a]	697.27	0.00000	0.00000
$Fe(OH)_3$(am)-CF	0.00E+00	106.87	2.46[c]	43.48	0.00000	0.00000
Gypsum	0.00E+00	172.17	2.30[a]	74.86	0.00000	0.00000
Hematite	1.41E-03	159.69	5.30[a]	30.13	0.04251	0.01122
Kaolinite	2.35E-03	258.16	2.60[a]	99.29	0.23334	0.06157
Lime	6.15E-02	56.08	3.35[a]	16.76	1.03136	0.27214
Magnesite	0.00E+00	84.31	3.00[a]	28.10	0.00000	0.00000
Millelite	1.16E-07	90.76	5.50[a]	16.50	0.00000	0.00000
Mullite	1.26E-05	426.05	3.05[a]	139.69	0.00176	0.00046
$Ni(OH)_2$	0.00E+00	92.71	4.10[d]	22.61	0.00000	0.00000
Ni_2SiO_4	2.14E-06	209.47	2.62[e]	79.95	0.00000	0.00000
$NiCO_3$	0.00E+00	118.70	2.60[d]	45.65	0.00000	0.00000
Periclase	4.16E-02	40.30	3.78[a]	10.66	0.44391	0.11713
Portlandite	0.00E+00	74.09	2.23[a]	33.23	0.00000	0.00000
Pyrite	5.50E-04	87.91	5.01[a]	17.55	0.00965	0.00255
SiO_2(am)	0.00E+00	60.08	2.01[a]	29.89	0.00000	0.00000
$Sr(OH)_2$	0.00E+00	121.63	3.63[d]	33.55	0.00000	0.00000
$SrSiO_3$	6.09E-04	163.70	2.90[a]	56.45	0.03436	0.00907
Zn_2TiO_4	2.67E-07	242.68	5.10[a]	47.58	0.00001	0.00000
				Total initial mineral vol (ΣVs)=(cm^3/L sol)	2.65290	0.70000
NB. References				ε, Porosity =	0.30000	
a	http://webmineral.com/data/			ΣVm = total mineral fraction =	0.70000	0.70000
b	www.claisse.info/2010%20papers/l7.pdf			ΣVt= total minerals volume		
c	astronomy.nmsu.edu/jlevans/seminarSpr07/koppetal2002.pdf			Vv = Vt-Vs = void volume		
d	en.wikipedia.org/wiki/Nickel(II)_hydroxide			ΣVm + ε = 1		
e	https://www.u-cursos.cl/ingenieria/2008/2/GL4A1/1/.../23321			ΣVs/ΣVt=ΣVm		

Porosity changes against pore volumes and pH of Secunda ash and brine were presented in Figure 4.11. The porosity of the fly ash increased sharply during the first 30 pore volumes. This was also the period in which fast geochemical reactions were taking place as evidenced by the sharp decrease in the pH from 12.4 to about 9, and equilibrium trying to be attained. Between pore volumes of 30 and 60, the porosity remains constant at about 0.835, within which period the pH also remained constant at about 9. Sharp increase in porosity to about 0.91 was then recorded between pore volume of 60 and 90. During the leaching process of a solid material, the concentration of the chemical species present in the interstitial solution is expected to decrease. The chemical equilibrium initially established is then upset. The more soluble mineral phases in the fly ash dissolve successively in order to restore the equilibrium. Therefore, further leaching results in an increase in porosity due to the dissolution of mineral phases. Modification of the transport properties of the fly ash in the column would therefore be taking place in turn. From pore volume 90 downwards, a decrease of porosity was recorded, as the pH values further reduced to about 6. Though some dissolution of mineral phases was still occurring, the formation of neo-formed phases or precipitation previously given in Figures 4.7 through 4.10; (e.g. hematite, $Fe(OH)_3$(am)-CF, pyrite, calcite, brucite, $Cr(OH)_3$(A) and gypsum) could attribute the decrease in the porosity which could have interfered with the flow rates in the column. This in fact could explain why there was some clogging of the column during the experimental work by Hareeparsad and co-workers. Geochemical reactions do therefore affect the mineralogy of the fly ash and consequently may affect the porosity of the fly ash. Modeling porosity evolution within mixing regions of fly ash-brine interactions (during reactive transport) may have important applications in several environmental and engineering problems. This information could give some useful insights in making certain engineering decisions on possible improvement on the reuse of fly ash in the road construction industry.

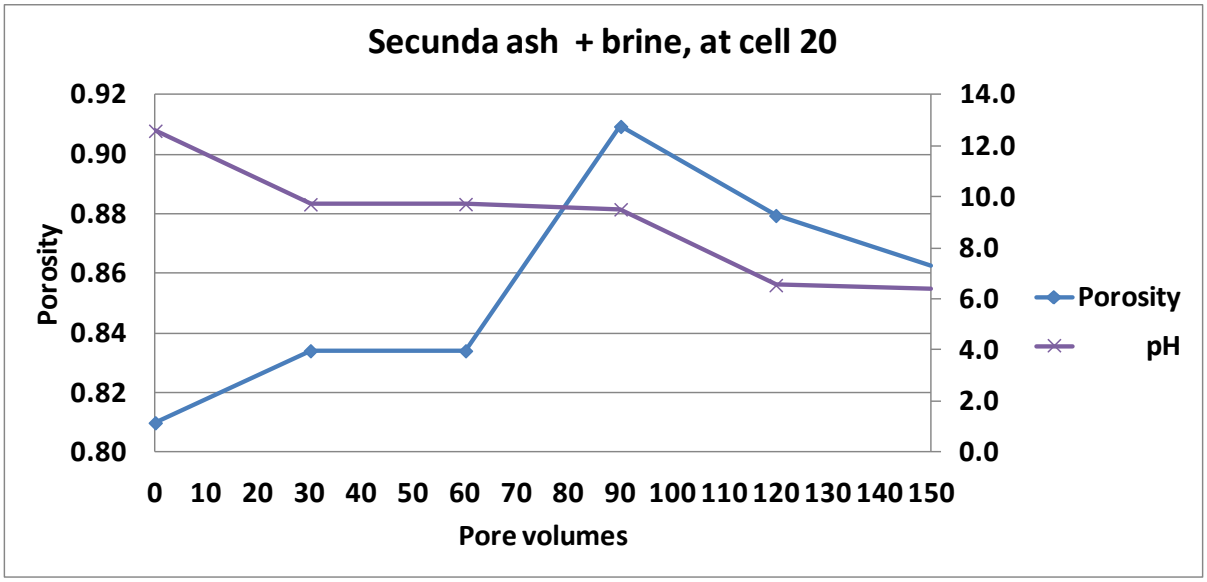

Figure 4.11: Porosity changes against pore volumes and pH of Secunda ash and brine

4.4 Conclusion

This paper has presented the dynamic-leaching modeling results of two South African fly ash recipes subjected to water and brines. Column modeling was successfully done and revealed information on the time-dependent leaching and transport chemistry of the species in ash-water and ash-brine interactions. The model demonstrated identification and quantification of reactive mineralogical phases controlling the element release. The pH of the solution was found to be an important controlling factor in leaching chemistry. This is because it determines the surface charge of the fly ash, and the degree of ionization and speciation of the elements in solution. The interactions between the charged ions in solution and the surface of fly ash particles contribute to the release of species into solution. Alteration of the geochemistry of fly ash is effected during the ash-water or ash-brine interaction over time. Some minerals are dissolved, others are precipitated while some new phases (secondary phases) are likely to be formed during the interactions. The highest mineralogical transformation took place in the first 10 days of ash contact with either water or brines, and within 0.1 m from the column inflow. The mineralogical transformations are caused by the many and complex geochemical reactions in fly ash-water-brines systems. These geochemical reactions that involve dissolution and precipitation of mineral phases do affect the porosity of the fly ash. This information could give some useful insights in making certain engineering decisions on possible improvement on the reuse of fly ash in the road construction industry.

Many of the major and trace elements (Ca, Mg, Na, K, Sr, S(VI), Fe, are leached easily and their concentration fronts are high at the beginning (within the first 10 days) upon contact with the liquid phase, but their concentration decrease with time until a steady state was reached. The leaching was also influenced by the change in the pH. When comparing the mineralogical results from the leached residue with those in the original mineral sample, there are indications that the mineral differences in the residue minerals indicated different dissolution kinetics of the minerals containing similar cations or anions and which govern the solution behaviour of those cations. Similar results were also obtained from the UWC column experiment as documented in their previous report [29]. Qualitatively, these results have served to support experimental work carried out by the collaborating institution, UWC. Leach column modeling undertaken has successfully provided the linkage between changes in the ash chemistry and the transport properties of the ash.

Further model validation and improvement will be carried out as the dynamic leaching models incorporated equilibrium reactions, speciation, and dissolution and precipitation reactions only. Owing to inadequate experimental data, ionic exchange and sorption/surface complexation modeling was deliberately not included in our modeling. Ion exchange and sorption reactions may lead to an additional attenuation or release of major cations and heavy metals. However, site-specific ion exchange or sorption parameters (like of the iron-oxide and Csh-gel mineral phases), which would justify the quantitative description of these reactions, were not available. This may form part of the future work to be undertaken for model modification and improvement.

Acknowledgements

The funding of the project by the Pollution Research Group (PRG) of UKZN and the remission of fees by UKZN is gratefully acknowledged. The authors would also like to thank the University of Western Cape through Dr Gitari for availing the experimental data. The first author also acknowledges The Kenya Polytechnic University College for granting him study leave and supplementary support during the study period.

CHAPTER 5

APPLICATION OF HYDROGEOCHEMICAL MODELING IN SIMULATING THE TRANSPORTATION OF ELEMENTS IN FLY ASH HEAP UNDER DIFFERENT DISPOSAL SYSTEMS IN SOUTH AFRICA

John M. Mbugua[1]*, J. Catherine Ngila[1,2], Andrew Kindness[1], Chris Buckley[3], Molla Demlie[4] and Shameer Hareeparsad[5]

[1] University of KwaZulu-Natal, School of Chemistry and Physics, Westville Campus, Private Bag X54001, Durban 4000, South Africa

[2] University of Johannesburg, Department of Department of Applied Chemistry, P.O Box 17011, Doornfontein, Johannesburg 2028, South Africa

[3] University of KwaZulu-Natal, Pollution Research Group, Howard College Campus, Durban 4041, South Africa

[4] University of KwaZulu-Natal, Department of Geological Sciences, Westville Campus, Durban 4000, South Africa

[5] Sasol Synfuels (Pty) Ltd, Environmental Sciences and Engineering Research and Development, Secunda, Mpumalanga 2302, South Africa

*Corresponding author: **jmmwai@gmail.com,** Tel: +27312601498; +27799228187

Abstract

Ash heap modeling of South African fly ash from Tutuka using PHREEQC was carried out and the duration of transportation projected for 20 years based on two disposal scenarios, namely; irrigation of ash with rainwater, and irrigation with brines. The hydrogeochemical modeling code was applied in the study which gave insights into the speciation, release and transport of elements from the water and brines-fly ash long term interactions. Tutuka ash-water heap model showed a general sharp decrease of total elemental concentrations released during the first 2.5 years simulation as the pH value dropped from 12.6 to 8.7, after which it remained constant and their concentration remained constant up to 20 years. The elements showing this trend included Ca, Mg, Al, Fe, Sr, Zn, Na, K, Li and C(4). Generally, brines caused sharp increase in released concentration of the elements Ca, Mg, S(6) and C(4) for the first 3 years of heap irrigation whereas with water irrigation an opposite trend was

observed in which the elemental concentrations decreased. The geochemical modeling revealed the possible controlling parameters and demonstrated the evolution of the fly ash geochemistry under a range of possible conditions and time scale. Generally therefore, the modeled leachate quality results revealed that many elements are mobile and move through the ash heap in a progressive leaching pathway. Qualitatively, the ash heap modeling results corroborated with the column experimental data and cores analysis work carried out by the collaborating institution, University of Western Cape (UWC) in which species such as Sr, Mg, Al, Na, K, Ca, Ti, Cr, and SO_4^{2-} show a similar general trend in each of the different Tutuka cores at a specific depth profile, being highly weathered in the top layers of the cores and accumulating at about 6-10 m down the core profile. The Na, Mg, K, Ca and SO_4^{2-} trends closely resemble each other indicating that these species could be present as soluble sulphate salts and these elements exhibited high mobility down the ash heap. The elements Fe, Zn, Ni and Ti were generally present in low concentrations in pore waters of the ash core samples. The model could therefore be used to support experimental work and provided reasonable leachate quality from the modeled Tutuka ash heap. Overall, the ash heap modeling enhanced the understanding of the ash-brines interactions and demonstrated that leachate composition is determined by the following factors; (i) the mass flows from the pores of fly ash, (ii) the surface dissolution of the mineral phases, (iii) the various chemical reactions involved during the ash-brine and ash-water interactions, (iv) the interactions with a gas phase (atmospheric CO_2), (v) the composition of the initial fly ash, and (vi) by the leachate flow and hydrodynamics as captured in the conceptual model. Further model validation is recommended with lysimeters to quantatively compare the simulated results against the experimental data and improve on the model.

Keywords: ash heap, brines, coupled transport modeling, leachate quality, mineralogical changes

5.1 Introduction

Fly ash heaps and dams are potential long-term sources of contamination to surface-water sources and groundwater systems due to their possible enrichment in major and trace elements relative to normal geological materials [148]. This may occur if they are released into the environment in sufficient amounts, and therefore a long-standing need to assess the release and mobilization of elements that result from weathering of fly ash, is important. Geochemical reactions and the mineralogical changes that occur between fly ash components and the chemical species in the brine solutions have been reported as part of the larger collaborative ash-brine project work [10, 11, 13, 15, 29, 122, 136-138]. The interactions between the various species in the fly ash and the brine may result either in neoformed phases (as secondary phases) or in dissolution of the primary phases. The speciation, release, transport and fate of the released mobile elements were investigated. Modeling reactive transport in fly ash-water-brines systems with a view to quantify and characterize the products formed and transport mechanisms involved has been the focus of our study. Prediction of the leachate quality when fly ash heap is subjected to brines and water irrigation was carried out using PHREEQC as the modeling tool.

Reactive-transport modeling as an emerging research field, aims at a comprehensive, quantitative, and ultimately predictive treatment of chemical transformations and mass transfers within the earth system. The field of modern geosciences is one of the fields in which reactive-transport models have had significant contribution. In their work, Regnier and co-workers [134] noted that reactive-transport models (RTMs) provide platforms for testing concepts and hypotheses, and for integrating new experimental, observational, and theoretical knowledge about geochemical, biological and transport processes. Through numerical computation and simulation, RTMs provide the most valuable diagnostic and prognostic tools available for elucidating the inherently complex dynamics of natural and engineered environments such as our ash heap scenario. Furthermore, RTMs bridge the gap between fundamental, process-oriented research and applied research in the fields of operational modeling, environmental engineering and global change. Reactive-transport models are a recent development and modelers do not have a large body of work from which to draw. The combined capability to model flow, transport, and chemical reactions provides a systematic approach for studying ground-water processes [149]. For a process-based interpretation of test results and their translation to field situations, sufficient understanding is required of the geochemical and mass transfer processes that control the leaching of contaminants in a percolation regime. This understanding will form the basis of our ash heap modeling in order to determine the leaching and transport mechanism during fly ash-water and fly ash-brine interactions as well as the quality of the leachates.

Even though large uncertainties are associated with the modeling results [92, 109, 133-135], a reactive-transport model is the only systematic method available to estimate the time dependency of the loads and fate of major and trace elements in a complex ash-brine disposal system transported down an ash heap and to assess the sensitivity of the load estimate to various chemical and physical processes.

This study therefore seeks to model the Tutuka ash heap and demonstrate the application of PHREEQC as an analytical-hydrogeochemical tool in predicting the interaction of water and brines respectively, with fly ash during their co-disposal from Eskom coal-utility plant, Tutuka.

5.2 Modeling methodology

A description of a one-dimensional advective-dispersive-reactive-transport model which is used to simulate transport of various elements down gradient of an ash heap disposal beds at Tutuka disposal facilities is presented. Model definitions include geometry and boundary conditions, initial conditions, and selection of chemical reactions. Conceptual models were developed and mechanisms involved were used as the input parameters for the PHREEQC program using a modified Lawrence and Livermore National Laboratory (LLNL) database for inorganics. A description of the conceptual model and the PHREEQC input data code used for the simulations are provided in the subsequent sections 5.2.1 and 5.2.2 respectively. Both fly ash-water and fly ash-brine models had common input parameters except the infilling solutions. The fly ash-water model had water equilibrated with atmospheric CO_2 and O_2 gases where as the fly ash-brine model had the infilling solution of brines whose composition was as given in the ash-brine interim reports [136, 137]. The results for both systems are presented in a combined format and given in **section 5.3**.

Previous ash-brine project work [10, 11, 13, 15, 19, 29, 122, 136-138] provided relevant experimental data for acid neutralization capacity, (ANC), ash and brines characterisation, column dynamic leaching data, water flux and composition data, porosity and permeability data and conceptual model of brines flow in the heaps, all of which were used for the modeling as part of the initial modeling conditions. The flow rates, the volumes of the leachates and the specific solid/liquid (S/L ratio) were imposed at the laboratory scale.

5.2.1 Conceptual model

Initial conceptual model of Tutuka ash heap entailed capturing the wet disposal method involving irrigating the heap with water to mimic rainwater as well as irrigation with brines as a method for co-disposal of ash and brines. The Tutuka fly ash composition and that of brines were as given in [26, 136, 137] and the water was equilibrated with atmospheric CO_2 and O_2 gases. In our model a heap height of 12 m was considered. For simplicity we will consider the ash heap as a 12 m column which is cylindrical in section and represents an element of volume within the heap. The column was discretized into 10 cells of equal lengths (1.2 m each) with 4000 shifts and a time step of 157680 seconds. It was assumed that there was no diffusion (diffusion coefficient = 0) while a dispersitivity of 0.8 m was imposed as adapted from Appelo and Postma estimates [99]; the general trend is that macrodispersivity is about 10% of the travelled distance. These assumptions and estimates which gave a more realistic and reasonable values of pH and total elemental concentrations which compared well with some results of the core samples obtained from the UWC ash brine report [29]. Bulk density of fly ash (2.21 g/cm^3) and UWC's hydraulic data was adapted in the model in which Darcy flow rate of 0.0002 cm/s and hydraulic conductivity of 0.00015 cm/s were used in the model. Porosity of 0.3 and flow rate of 2 ml/min was also used. The above parameters notwithstanding, the reality however on the ground is usually different in the way the ash heap is designed. A basement layer of about between 10-20 m high is usually established after which a track is built on this raised mound. Subsequent mound is constructed on the first, adding up to a total height of about 20 m. Fresh ash was considered for the model which therefore dictated the initial conditions for the model. A single layer approach was considered as opposed to the two layer approach which presents complicating factors with respect to the weathering patterns. Cation exchange reactions were incorporated in the model from UWC data on cation exchange as given by [29]. Effects of soil and plant growth were not factored into the construction of a conceptual site model. Runoff from the site was considered minimal and therefore inconsequential. Water balance on the fly ash dump irrigated with water or brines can be visualised in Figure 5.1 as adapted from the ash-brine report [150].

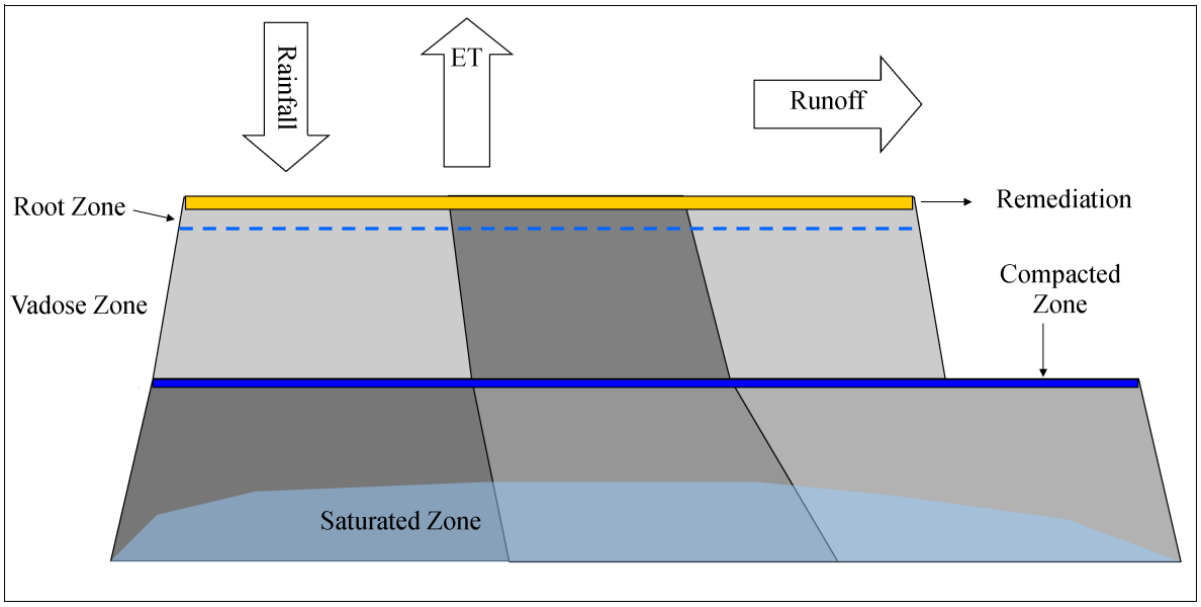

Figure 5.1: Conceptual model of Tutuka ash heap adapted from [150]

The figure illustrates the root (where vegetation growth occurs for remediation purposes), vadose, compacted, as well as the saturated zones of an ash heap. Accounting for the water balance considers the amount of rainfall, water percolating through the stated zones of the ash heap, surface runoff and evapotranspiration (ET).

5.2.2 Input parameters

The fly ash mineral phases and brine composition were as given in preceding ash-brine project work [26, 136, 137]. Additional aspects are the incorporation of atmospheric air (O_2 and CO_2 gases at fugacity values of $10^{-3.5}$ and 10^{-7} respectively) in equilibrium with the fly ash and also ion exchange as per the UWC cation exchange capacity data [29]. Third-type or Cauchy flux boundary conditions (flux flux) were used for both ends of the 1D model. Other parameters are as described in the conceptual model in **section 5.2.1**.

5.3 Results and Discussion

Simulation data obtained in this study showed predicted release and mobility of major and trace elements in fly ash heaps subjected to rainwater irrigation and another scenario subjected to brine irrigation. This ultimately gave the quality of the leachate down the modeled ash heap. Important physico-geochemical changes occurring during the weathering of fly ash-water-brine systems were captured in the representative profiles from the simulated data.

5.3.1 pH – depth profile of the ash heap at different times

The variation of pH against the Tutuka ash heap depth (of 11.4 m) over the simulation time of 20 years irrigated with water and brine is given by Figure 5.2. For the ash heap-water scenario, the pH dropped from 13 to between 8 and 8.8 after 2.5 years at the ash heap depth of 1 m. The pH was then observed to increase slightly to a maximum of 8.8 at a depth of 1 - 4 m down gradient and remained constant at 8.8 for the first 2.5 years. This could be interpreted to be the depth at which the greatest weathering of fly ash was taking place. Under such weathering conditions (described in the conceptual model in section 5.2.1), the fly ash mineral phases were undergoing transformation in which neutralization reactions were taking place as a result of acidic rain (due to atmospheric CO_2) interacting with alkaline fly ash. Similar pH-depth profiles were recorded for the subsequent years (5, 7.5 and 20 years) with negligibly small differences in the pH values at various ash heap depths as shown in Figure 5.2. For the ash heap-brines scenario, a similar trend was observed as that of the fly ash heap-water scenario, although pH values dropped to 7.7 at 2 m after 2.5 years. There after the pH increased slightly at subsequent depths to pH 8 at the depth of 5 m down gradient and remained constant up to 20 years. The results compared well with the UWC cores data analysis in which the lowest pH of the pore water was observed at the top layer 0.55 – 3.00 m and immediately after the water level [29] as highlighted in **section 1.1.1**. This observation indicates that the greatest weathering of the fly ash had occurred at the top layer of the ash heap (0.55- 4 m) upon contact with water or brine. Below this depth of 4 m, the pH of the pore fluid was persistent for the rest of the subsequent years. After depth of about 4 m, pH was maintained around 7.5 to 8 for ash irrigated with brine and at about 9 for ash irrigated with rainwater. This means that the high pH of Tutuka ash gets lowered with time due to weathering, resulting to self regulating of the ash-brine-water system.

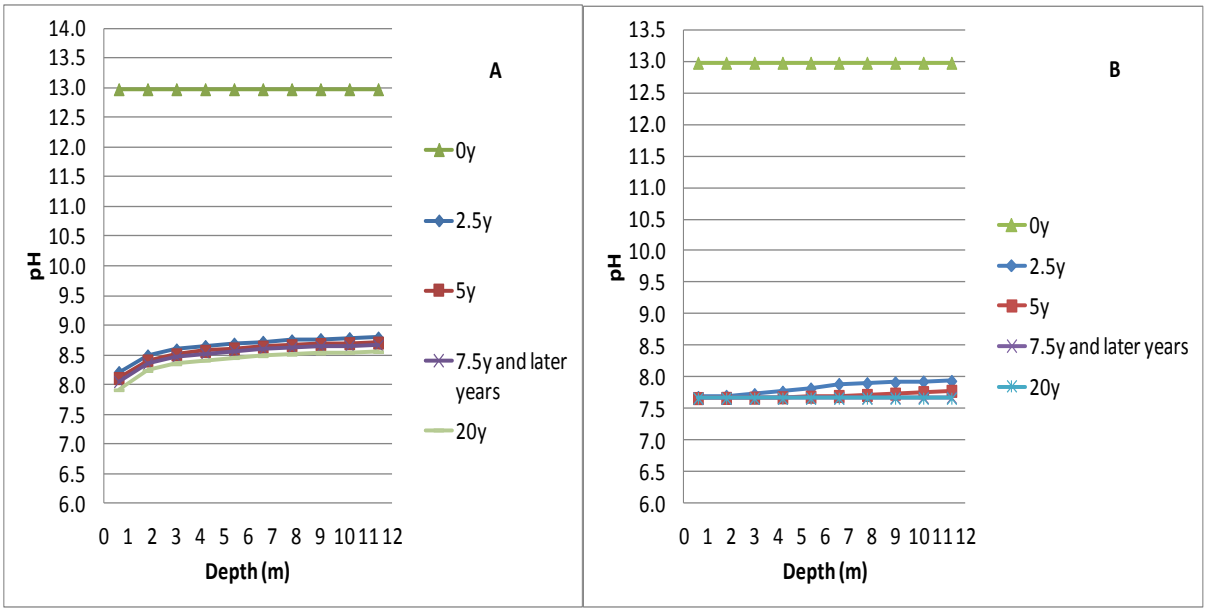

Figure 5.2: Graph showing variation of pH against the Tutuka ash heap depth for varying number of years of irrigation with: (A) water, and (B) brine. (0y, 2.5y…..20y indicate 0 to 20 years).

5.3.2 Total elemental concentrations against ash heap depth after 20 years for Tutuka ash heap with water and with brine irrigation

The simulation results for the total elemental concentration down gradient the two modeled ash heap scenarios are presented in Figure 5.3. Further supplementary results on elemental concentrations are given in **Appendix 5** (Figure A5). The following observations can be noted from each of the modeled scenarios.

5.3.2.1 Ash heap irrigated with water

(i) Zinc (Zn) and Aluminium (Al) concentrations increased between 0.55 and 2 m depth. Below this depth their respective concentrations remained constant. In the case of Al, it is considered to be a conservative element in coal ash [81, 151] hence its concentration was not expected to change. The amounts in the leachate were however relatively small, indicating much of the elemental content had not been leached before the 20 years. The leaching pattern of Zn and Al could be deduced as adsorption controlled. In this type of leaching pattern (adsorption-controlled release) the concentration of metals in pore fluid continually changes, because the metal concentrations in the solid and liquid phase are controlled by the partition coefficients. Adsorption-controlled release corresponds to an

equilibrium condition where desorption occurs instantaneously. Leaching could also have occurred through chemical dissolution of the respective element-containing mineral phases from the fly ash-water interactions, followed by precipitation or adsorption onto particles [81].

(ii) The concentrations of the rest of the major and minor elements (Ca, Mg, Fe Sr, Na, Li, K and C) did not show any significant variation down gradient of the ash heap irrigated with water. The amounts are however within a range of 1- 4 orders of magnitude lower than those of the ash heap irrigated with brines (for Zn it was lowered by 1 order of magnitude, C and Sr lowered by about 3, Na, K, Li by about 4, whereas Fe was lowered by 5 and Mg about 9 orders of magnitude).

5.3.2.2 Ash heap irrigated with brine

(i) Iron (Fe) showed slight increase in concentration for 1-2 m down gradient while Sr and Zn showed steady increase up to 11.4 m in both ash heaps. This could be due to slow dissolution of minerals associated with these elements (Hematite, Pyrite for Fe, $SrSiO_3$ for Sr and Zn_2TiO_4 for Zn) down gradient or possible desorption of the elements taking place.

(ii) The concentrations of the rest of the major and minor elements were constant down gradient the ash heap. This may suggest that the release pattern for metals from the fly ash heap-water scenario and that of ash heap with brine appeared to be adsorption-controlled. Concentrations of most of the elements were in higher orders of magnitude in leachate collected from the fly ash heap irrigated with brine than those from ash heap with water.

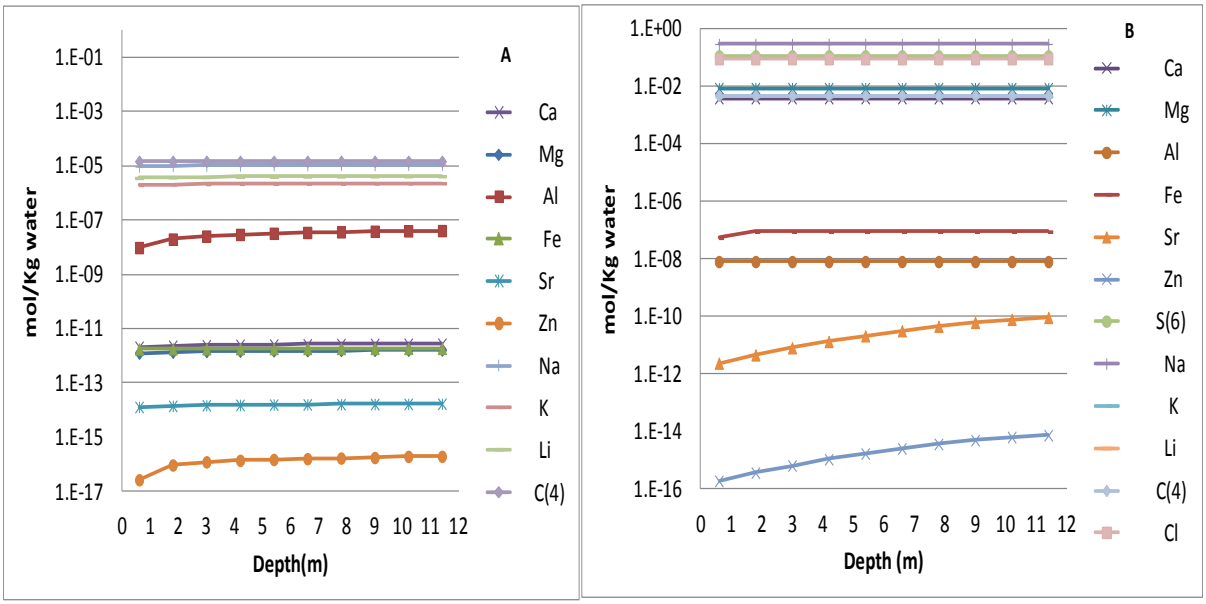

Figure 5.3: Total elemental concentrations in leachates after 20 years against the depth down the ash heap irrigated with: (A) water, and (B) brine; (NB. Legend symbols different for A and B)

5.3.3 Mineralogical changes against time and pH after ash heap irrigation with brine over a 20-year period

The quantitative mineralogical changes occurring down gradient the ash heap scenarios against pH and time are presented in Figure 5.4. The mineral phases that showed significant change in the fly ash-brine heap over 20 years of brine irrigation were calcite, hematite, $Fe(OH)_3$(am)-CF and magnesite. However amounts of $Fe(OH)_3$(am)-CF were negligibly small throughout the years. Any other minerals particularly the silicon based minerals such as mullite and quartz were assumed to have undergone insignificant chemical changes but got flushed down gradient the ash heap. (This could also explain why not much quantitative mineralogical data was obtained from the ash heap irrigated with water). For the ash heap irrigated with brines, the amount of calcite decreased in the first 3 years, as the pH value decreased from 13 to 8 then followed by a sharp increase in amounts occurring up to 5 years. This showed the dissolution and precipitation of calcite was pH-controlled. This variation of the mineral calcite could explain the variation of the Ca metal concentration in the leachate over the years. A slight decrease in calcite was recorded up to about 8 years within which the pH also showed some slight decrease and then remained constant up to 20 years. Hematite amount remained constant over the 20 years while magnesite was formed as a new phase up to 2.5 years after which it dissolved progressively up to 5 years and then got depleted.

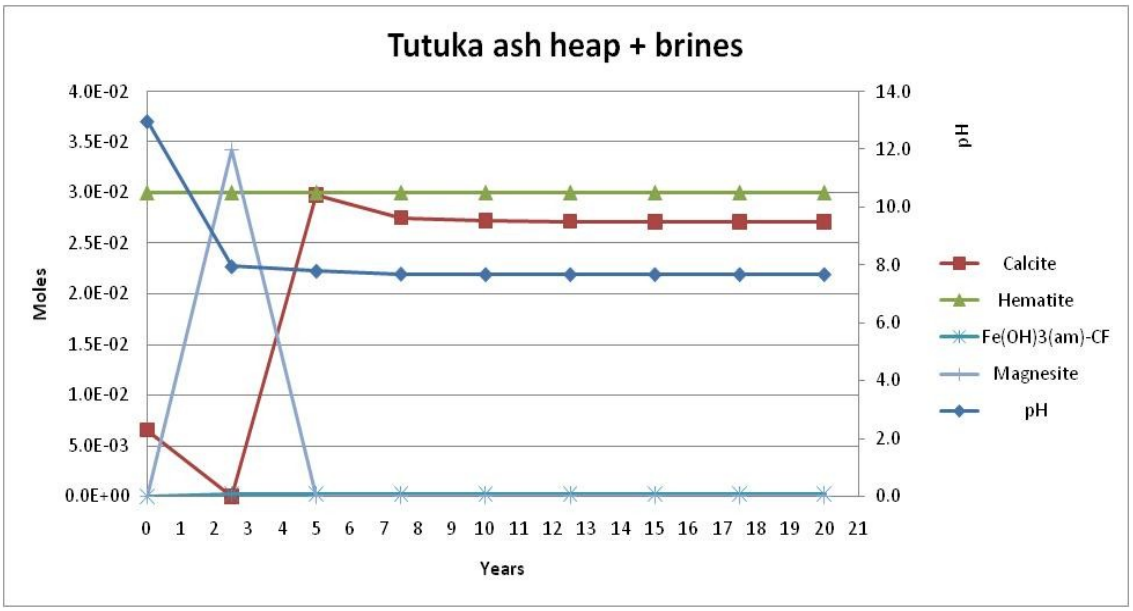

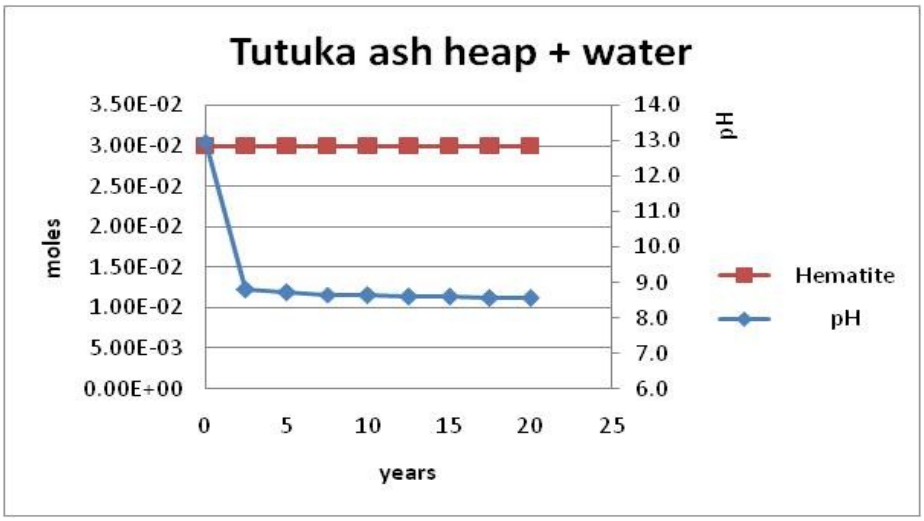

Figure 5.4: Major mineral phases present against time and pH after ash heap irrigation with brine and water over a 20-year period

5.3.4 Comparison of total elemental concentrations at outflow position over time between ash heap with brines and that with water

Generally, brines caused sharp increase in concentrations (mol/Kg of water) of the elements Ca, Mg, S(6) and C(4) for the first 3 years of heap irrigation (Figure 5.5) whereas with water irrigation an opposite trend was observed in which the elemental concentrations decreased. The increased trend is due to the brine composition which contains most of these elements and hence causes elevated concentrations. With both brine and water irrigation systems, a reduction in elemental concentration in the leachate was registered for Al and Fe. This could be due to precipitation and adsorption of these elements down gradient of ash heap. After 3 years the amounts remained constant up to 20 years for all elements. A general sharp decrease of the element's concentration for Sr, Zn, Na, K and Li was recorded for ash heap-water scenario for the first 3 years, but with brines, Sr, Na and K showed slight increase for the first 3 years due to flushing and then a progressive decrease up to 20 years. Zn showed a steady decrease in concentration. This sharp decrease in concentration of the elements could be due to flushing of the dissolved elements down gradient whereas for Zn some precipitation or possible adsorption could be occurring down gradient of the ash heap. These results show that concentration of metals in leachate was controlled not only by solubility but other factors such as adsorption and precipitation processes.

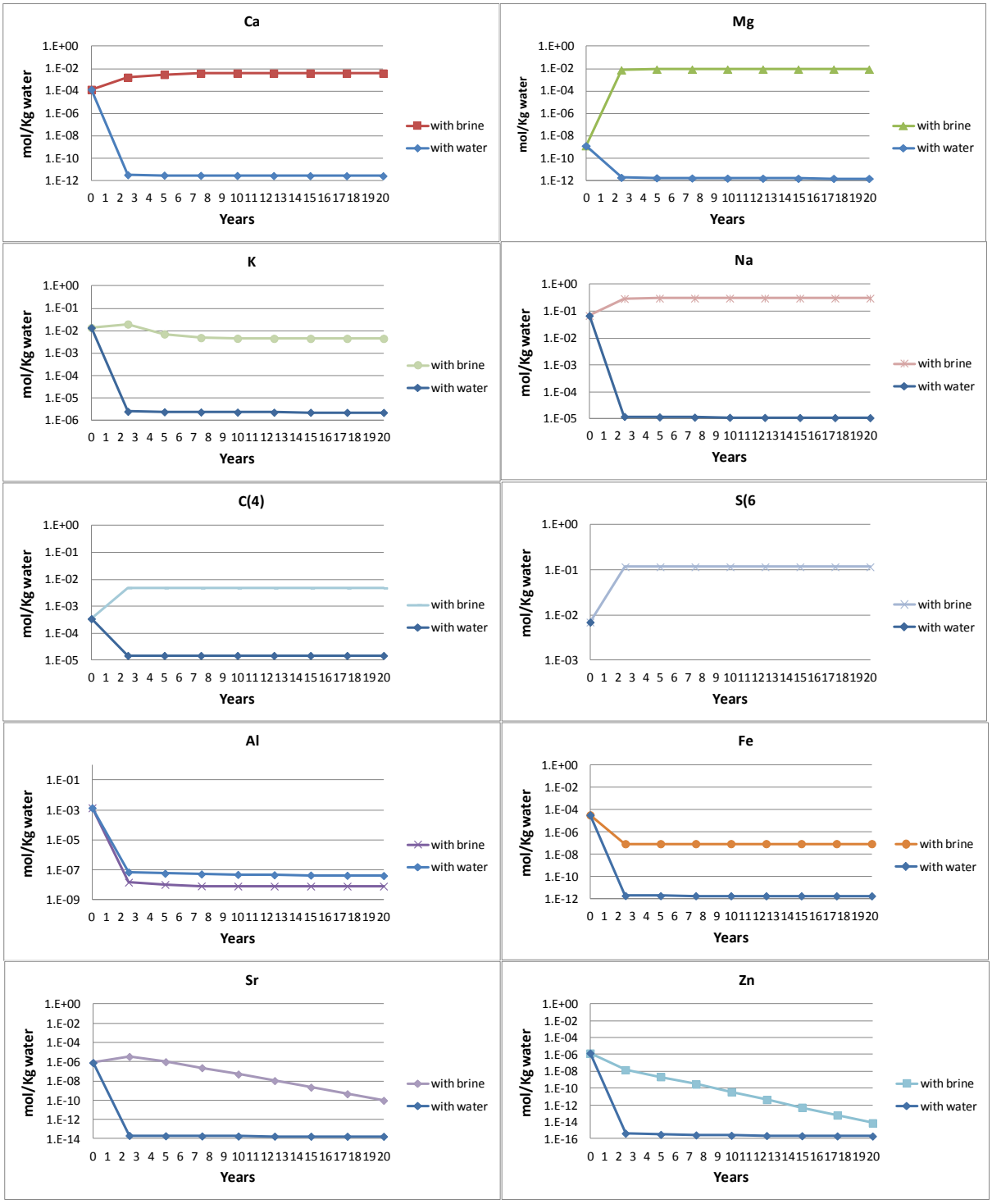

Figure 5.5: Comparison of total major and minor elements released from ash heap irrigated with rainwater and that irrigated with brines over a period of 20 years. (Leachate quality at 11.4 m depth of the ash heap in both scenarios).

5.3.5 Total elemental concentration of major and trace elements versus depth and pH for the two scenarios

The results of the modeled fly ash heap irrigated with water were presented in Figure 5.6 and those of the ash heap irrigation with brine were presented in Figure 5.7. In order to interpret the results obtained, the following information must be noted for the two modeled scenarios.

5.3.5.1 Fly ash heap irrigated with water

i) At zero (0) years: There is no contact between fly ash and water hence the elemental concentrations represented in Figure 5.6 are those in the fresh fly ash down gradient the 11.4 m ash heap. Irrigation of the ash heap with water caused a general decrease of elemental concentration to lower levels than the initial amounts in the ash heap. This is a clear indication that over time the fly ash-water interactions resulted in leaching of the major and minor elements down gradient the ash heap.

ii) After 2.5 years, when the ash and the rain water have interacted, the concentration of most of the elements Ca, Mg, Na, Fe, Sr, K, Li, C and Cl showed insignificant changes down gradient of the ash heap and implied resistance to weathering. The concentration of these elements in the subsequent years (5, 7.5, 10, 12.5 and 20 years) showed the same trend down gradient the ash heap as shown by the superimposition of the respective profiles on each other.

iii) The elements Al and Zn showed some increased concentration vertically down the ash heap in the first 2 m of the inflow position of ash depth. After the 2 m depth the concentration remained constant throughout the rest of the ash heap depth of 11.4 m. The trend was the same vertically down gradient of the ash heap after each of the modeled years (2.5, 5, 7.5, 10, 12.5, 15, 17.5 and 20 years).

5.3.5.2 Fly ash heap irrigated with brine

i) At zero (0) years: There is no contact between fly ash and brine hence the elemental concentrations represented are those in the fresh fly ash down gradient of the 11.4 m ash heap. Irrigation of the ash heap with brines caused the elevation of the elemental concentration levels above the initial amounts.

ii) After 2.5 years, when the ash and the brine solution have interacted, the concentration of the elements Na, Fe, Al, Cl, C and S showed no significant changes down gradient the ash heap and which showed some conservative behaviour. The concentration of these elements in the subsequent years (5, 7.5, 10, 12.5 and 20 years) showed the same trend down gradient the ash heap as shown by the superimposition of the respective profiles on each other (Figure 5.7). Some elements namely, Ca, Mg, Sr, Zn, Li, K, showed some significant variations of concentration vertically down the ash heap at different depths. Calcium (Ca) and Mg concentration remained constant up to a depth of 4 m and then a gradual decrease followed up to a depth of 11.4 m. The elements Sr, Zn, Li, and K showed a progressive increase of concentration vertically down gradient after each of the modeled years (2.5, 5, 7.5, 10, 12.5, 15, 17.5 and 20 years).

iii) After the first 2 m closer to the inflow position of the ash heap the concentration of the elements Ca, Mg, Fe , Zn, Sr, K and C(4) decreased after 2.5 years and there after remained constant up to the outflow position when ash heap was irrigated with water. The same trend was observed for the subsequent years. This shows that a lot of the geochemical reactions and leaching chemistry occurred during the initial 2.5 years after fly ash contact with brines. Transformational processes of the mineral phases leading to precipitation could be attributed by the decrease in the elemental concentrations. This could also be due to flushing of the elements particularly the very soluble ones such as K and Sr as well as possible precipitation reactions that could have taken place.

iv) Zn showed some distinct profiles for each of the years simulated as depicted in Figure 5.7. At about 1 m the concentration reduced after which there was a steady increase of the concentrations down gradient up to 11.4 m. For each of the subsequent years this trend was maintained but at different lower concentrations. Similar trend was recorded for Sr, Li and K though with quantatively different amounts. The same trend was observed for these elements at 1 m down gradient up to 2.5 years. The concentration then increased after 2.5 years and then remained constant up to 11.4 m down gradient. For the rest of the subsequent years the same trend was observed down gradient the ash heap.

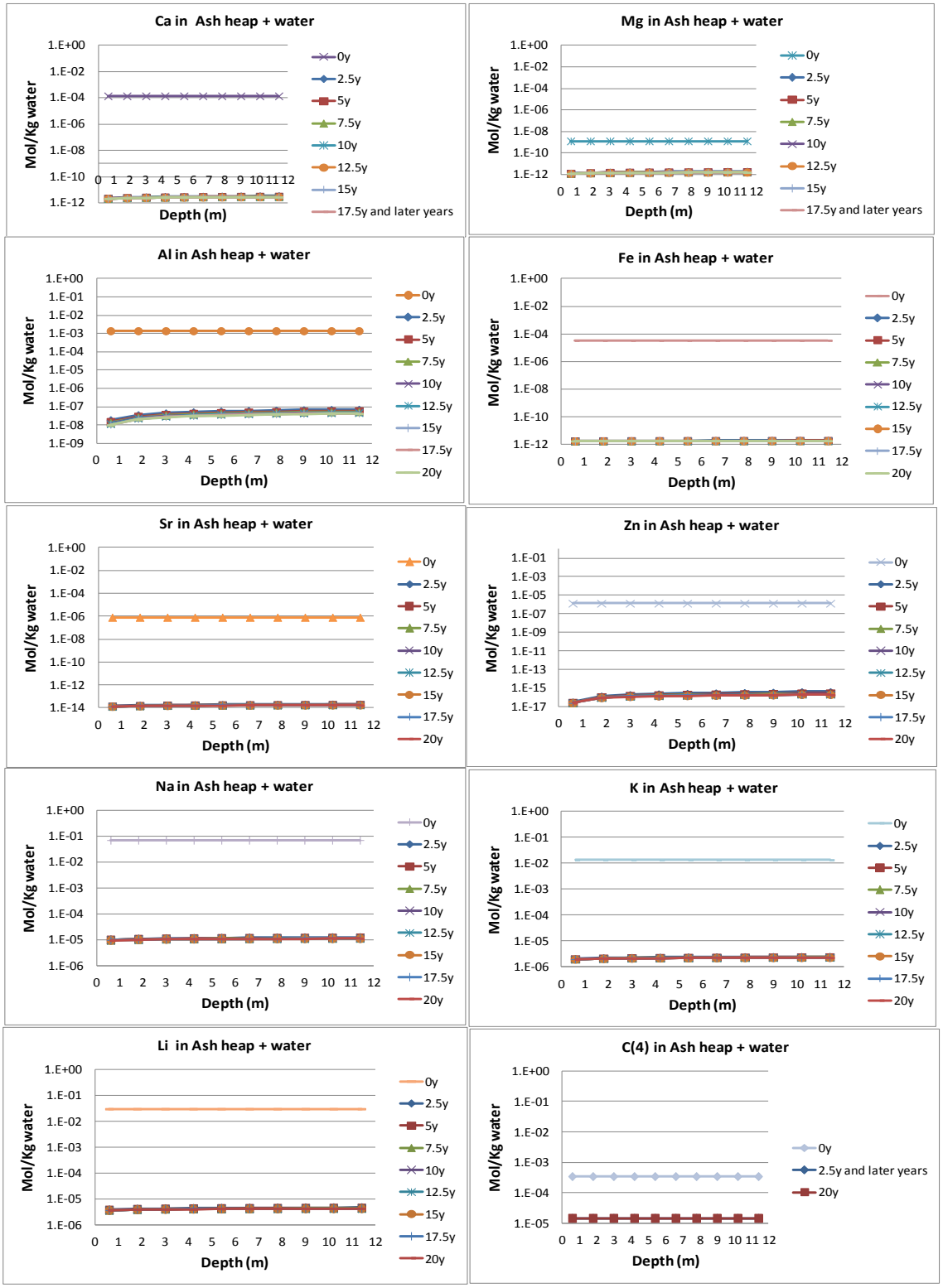

Figure 5.6: Total elemental concentration of major and minor elements in the leachate, against the depth at certain years of ash heap irrigation with water

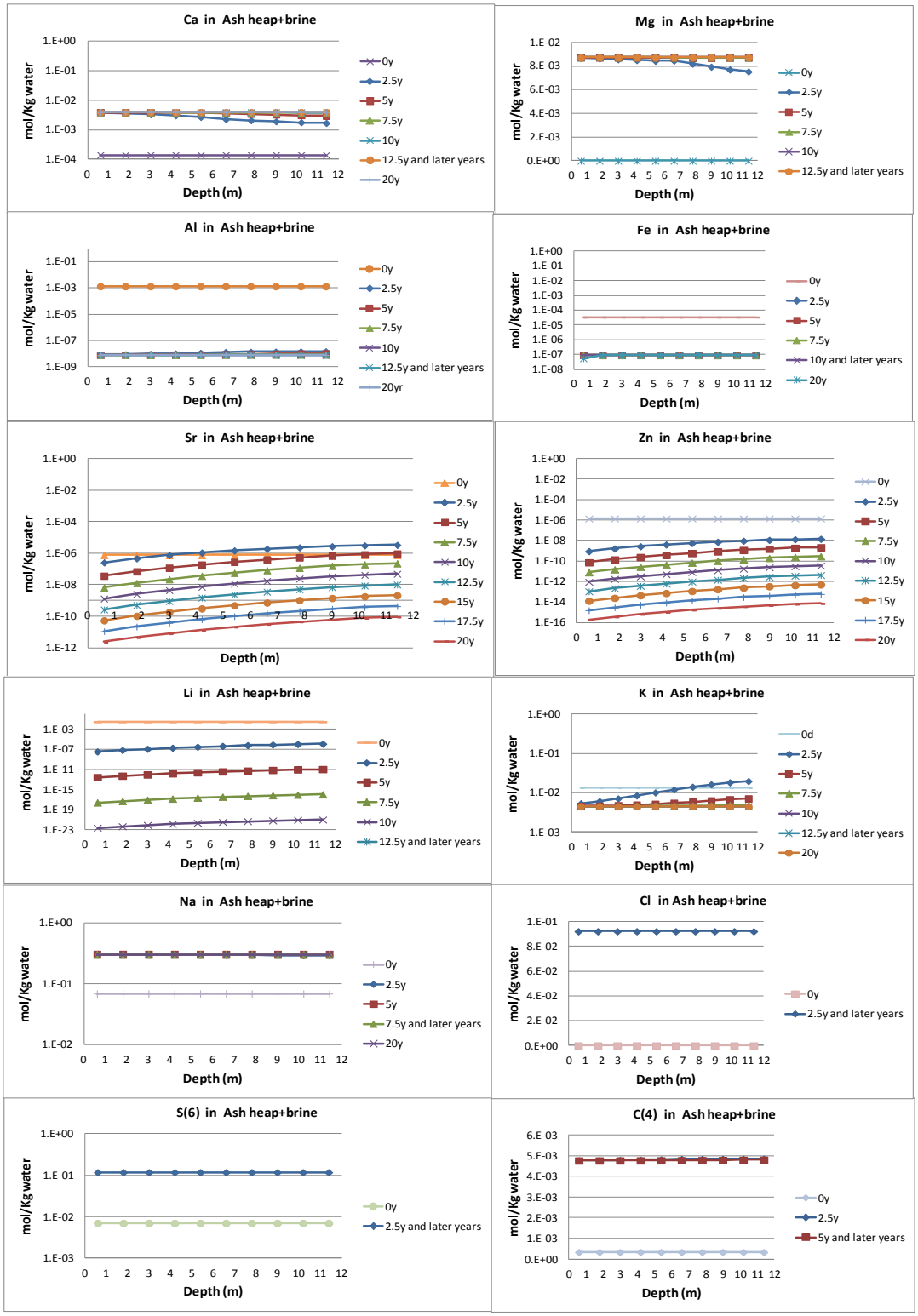

Figure 5.7: Total elemental concentration of major and minor elements in leachate against the depth, at certain years of ash heap irrigation with brine

5.4 Conclusion

Simulations of reactive transport were performed for a period of 20 years of seepage by rain water and brines irrigation into the ash heap. Because this is a forward model, the modeling results are predictions of the future and cannot be compared to field data 'per se'. However attempts have been made to have the modeling conditions and parameters as close as possible to the field disposal site conditions as described by the conceptual model.

The modeling results revealed that the weathering of ash either irrigated with rainwater or with brine is pH dependent. Initial high pH causes dissolution of some mineral phases that are amphoteric such as Al and Zn. When comparing the mineralogical results from the leached residue with those in the original mineral sample, the mineral differences in the residue minerals indicate different dissolution kinetics of the minerals containing similar cations or anions and which govern the solution behaviour of those cations.

Between the ash heap depth of 1 and 3 m, the pH value dropped from 13 to between 8 and 8.8 after 5 years and remained constant up to 20 years at 8.5 down gradient. Similar trend was observed with brines but the pH values dropped to 7.7 at 2 m after 2.5 years, then the pH increased slightly at subsequent depths to pH 8 from 5 m down gradient and remained constant for all years up to 20 years. The model results were in agreement with the UWC cores data analysis in which lowest pH of the pore water was observed at the top layer 0.55-3 m and immediately after the water level. This observation indicated that the greatest weathering of the fly ash occurred at the top layer (0.55-3 m) and upon making contact with water (at the point of saturation down the ash heap) [29].

Tutuka ash-water heap model showed a general sharp decrease of total elemental concentrations that occurred during the first 2.5 years as the pH value dropped from 12.6 to 8.7, after which it remained constant and their concentration remained constant up to 20 years. The elements showing this trend included Ca, Mg, Al, Fe, Sr, Zn, Na, K, Li and C(4). The sharp decrease in the elemental concentration could be due to flushing of these elements when ash was irrigated with rainwater. For the ash heap irrigated with brines, the first 3 years showed marked changes in elemental concentration as the pH dropped from 12.6 to 7.8 after which it remained constant up to 20 years. Among the elements that showed increased amounts within the first 3 years were Ca, Mg, C(4), Na, Sr and K, after which the concentrations remained constant. This sharp increase could be due to dissolution of the various element-related minerals as the ash was irrigated with brines. The Cl amounts were also high within the first 2.5 years since extra amounts got added from the brines even though the ash exhibited conservative behaviour after the 2.5 years.

Overall, the ash heap modeling enhanced the understanding of the ash-brines interactions and demonstrated that leachate composition is determined by the following factors; (i) the mass flows from the pores of fly ash, (ii) the surface dissolution of the mineral phases, (iii) the various chemical reactions involved during the ash-brine and ash-water interactions, (iv) the interactions with a gas phase (atmospheric CO_2), (v) the composition of the initial fly ash, and (vi) by the leachate flow and hydrodynamics as captured in the conceptual model. These findings from the modeling work went further to support the works of Schiopu and co-workers [141]. The release patterns of the major and minor elements from the ash-water and ash-brine interactions were deduced to be a possible combination of solubility control, adsorption-desorption, precipitation and chemical exchange processes [20, 127, 148, 152, 153].

When comparing the mineralogical results from the leached residue with those in the original modeled ash recipe, the mineral differences in the ash residue exhibited in Tutuka ash heap indicate different dissolution kinetics of the minerals containing similar cations or anions and which govern the solution behaviour of those ions. This means that as much as the leaching takes a particular dissolution pathway, down gradient the ash heap, the dissolution of the mineral phases in the fly ash is also a function of time. The modeling studies have demonstrated that reaction kinetics is important in governing chemical exchanges for depth scales up to 11.4 m for a period of 20 years ash weathering under different scenarios. Future research should focus on incorporation of sorption chemistry in the model and further validation by use of field data.

Acknowledgements

Mbugua J.M is grateful for project funding by the Pollution Research Group (PRG) at the University of KwaZulu Natal (UKZN) and tuition fee exemption by the UKZN. The Kenya Polytechnic University College for granting him study leave and supplementary support during the study period. The authors acknowledge the contribution by Dr Wilson Gitari, Prof Leslie Petrik and Ojo O. Fatoba of the University of Western Cape for availing the laboratory experimental data in Phase I, used for model calibration during the initial stages.

CHAPTER 6

GENERAL CONCLUSIONS AND RECOMMENDATIONS

6.1 General conclusions

The focus areas of the study were (i) hydrogeochemical modeling of the chemical speciation of brines, (ii) the leaching chemistry of the fly ash under different disposal conditions (i.e. with water and brines), (iii) modeling of equilibrium aqueous chemistry of ash-brines-organics interactions, (iv) modeling of kinetic and transport mechanisms associated with interactions of water and brines with fly ash during their disposal, (v) mineralogical transformations associated with intermediate and final products, and (vi) long term prediction of leachate quality by modeling the ash heap under different disposal conditions. These were achieved progressively by first learning and gaining competency in the PHREEQC program, modeling the batch reactions (acid neutralization capacity of fly ash with water and with brines), modeling the dynamic leaching using columns, and then followed by modeling the ash heap.

The effect of organics and brines on the metal leaching and acid neutralization capacity (ANC) of fly ash was successfully studied by static/batch leaching modeling. The results revealed that mineral dissolution, precipitation and new phase formation during ash-organics-brines interactions (and by extension weathering of ash either irrigated with rainwater or with brine in ash heap) occurred and that the processes were pH-controlled. The newly formed phases however remain in equilibrium with the ash-brines-organics mixture. Each individual mineral phase dissolution/precipitation/formation system controls the concentration and speciation of the respective constituent elements as evidenced by the log C-pH diagrams obtained from the modeled scenarios.

The ash-brines-organics interactions do exhibit and affect the mineralogical chemistry of fly ash. However the extent to which these interactions occur and their effect, varies from one scenario to another, and are dependent on the amounts and type of the constituent brine components.

Organics do have significant effect on dissolution characteristics of few minerals such as calcite ($CaCO_3$), mullite ($Al_6Si_2O_{13}$), Kaolinite ($Al_2Si_2O_5(OH)_4$), Ni_2SiO_4, and $SrSiO_3$. The effect is quantitatively conspicuous for calcite mineral phase and for the formation of some new phases such as $Fe(OH)_3$(am)-CF and portlandite ($Ca(OH)_2$) .

Hydrogeochemical modeling further revealed that neutralization and chemical weathering govern the leaching reactions and control the release of major, minor and trace elements from fly ash, and are therefore considered to be the major leaching processes.

The leaching levels of elements from fly ash either with water only or mixed with brines generally showed no significant difference. However, in some instances the use of brines led to some reduction in the total released elements. These observations point to possible continued co-disposal of ash and brines from the coal utility plants. It should however be noted that models may not be perfect although they have been able to reasonably describe leaching processes in the ash-organics-brines scenarios. Column modeling was successfully done and revealed information on the time-dependent leaching and transport chemistry of the species in ash-water and ash-brine interactions. The simulation results demonstrated identification and quantification of reactive mineralogical phases controlling the element release. Alteration of the geochemistry of fly ash was shown to be effected during the ash-water or ash-brine interaction over time. Interaction of fly ashes with water and brines result in mineralogical alterations of the original fresh ash through dissolution and precipitation. Part of the mineralogical transformation also involved formation of new phases that were not originally present in the ash recipe. The largest mineralogical transformation took place in the first 10 days of ash contact with either water or brines, and within 0.1 m from the column inflow. The mineralogical transformations are caused by the many and complex geochemical reactions in fly ash-water-brines systems.

The modeling results obtained in this study supports and augments previous experimental studies in which chemical and mineralogical transformations (and slight variations in chemical compositions of disposed fly ashes in contact with brines and water) have been reported to occur.

The geochemical reactions that involve dissolution and precipitation of mineral phases do affect the porosity of the fly ash. Precipitation and new-phase formation caused a decrease in porosity while dissolution led to increased porosity of fly ash. This information could give some useful insights in making certain engineering decisions on possible improvement on the reuse of fly ash in the road construction industry. In this study, the potential of modeling tools to support experimental leaching studies were successfully demonstrated. The modeling results corroborated well with the experimental results obtained from Petrik and co-workers (at the University of Western Cape, UWC) as documented in their ash-brine report. The model was also able to predict long term leaching and mobility of elements and ultimately the quality of leachate. The ash heap modeling results were also in agreement with the UWC cores data analysis in which the lowest pH of the pore water was observed at the top layer 0.55 - 3 m and immediately after the water level. The observation indicated that the greatest weathering of the fly ash occurred at the top layer (0.55 - 3 m) and after making contact with water.

Overall, the ash heap modeling study enhanced the understanding of the ash-brines interactions and demonstrated that leachate composition is determined by the following factors; (i) the mass flows

from the pores of fly ash, (ii) the surface dissolution of the mineral phases, (iii) the various chemical reactions involved during the ash-brine and ash-water interactions, (iv) the interactions with a gas phase (atmospheric CO_2), and (v) by the leachate flow and hydrodynamics as captured in the conceptual model. The findings from the modeling work went further to support the works of Schiopu and co-workers [141]. The release patterns of the major and minor elements from the ash-water and ash-brine interactions were deduced to be a possible combination of solubility control, adsorption-desorption, precipitation and chemical exchange processes. However, adsorption-desorption aspects were not captured in this model as the study focused on solubility control and chemical exchange processes.

The results demonstrated the versatility and application of PHREEQC modeling code in the study of equilibrium aqueous chemistry of ash-brines-organics interactions and the effect of the brines and organics in the brines co-disposed with fly ash. The findings of this study did address the key research questions adequately as outlined in **Chapter 1**, (section 1.2) of this thesis.

It can therefore be concluded that indeed, hydrogeochemical modeling of fly ash-brines interactions provided better understanding of the speciation, release and transport of multi elements, and that the modeling study was sufficient to support experimental data and engineering decisions towards sustainable fly ash-brines waste management. Even though PHREEQC modeling may be said to have some inherent limitations, it is an important tool that can indicate the trends of chemical reactions and the plausible dissolution/precipitation reactions in an ash-water and ash-brine systems.

6.2 Recommendations

The batch and dynamic (column and ash heap) leaching models used in this study incorporated equilibrium reactions, speciation, ionic exchange, dissolution and precipitation reactions. However, the ash-brine modeling research was not exhaustive due to certain limitations. Owing to inadequate (insufficient) experimental data, the ionic exchange and sorption/surface complexation processes were deliberately not included in our modeling study. It is noted that ion exchange and sorption reactions may lead to an additional attenuation or release of major cations and heavy metals. However, site-specific ion exchange or sorption parameters (such as those of iron-oxide mineral phases), which would otherwise justify the quantitative description of these reactions, were not available.

In view of the above limitations, further work should be undertaken to allow model modification and improvement. Further validation and modification of the model could be achieved by use of lysimeter data which could not be carried out as this was outside the scope of the PhD work. The main reason for omitting this aspect was that the lysimeters could not be commissioned on time by the Sasol-Eskom project management and this led to revision of PhD project objectives.

Another area that needs further investigation is the extent to which the continued co-disposal of the ash and brines occur. This may possibly alter engineering properties of some fly ash, either favourably for its utilization, or negatively.

Thus the following is a list of recommendations for further study:

I. Further validation of the model by use of lysimeter data

II. Compare PHREEQC results with lysimeter results.

III. Predict lysimeter performance

IV. Improvement of the model by incorporating and modeling sorption chemistry (ion exchange and surface complexation aspects)

V. Incorporate the kinetics in the model

VI. Obtain and collate historical rain and evaporation data

References

1. ACI Education Bulletin E3-01, C.E.-. ed. *Cementitious Materials for Concrete: Materials for Concrete Construction*. ed. A.C.I. (ACI). 2001, American Concrete Institute (ACI). 25.
2. Lehmann, P., Berchtold, M., Ahrenholz, B., Tölked, J., Kaestnera, A., Krafczykd, M., Flühlera, H., Künschc, H. R., *Impact of geometrical properties on permeability and fluid phase distribution in porous media.* Advances in Water Resources, 2008. **31**(9): p. 1188-1204.
3. van Breukelen, B.M., Appelo, C. A. J., Olsthoorn, T. N., *Hydrogeochemical transport modeling of 24 years of Rhine water infiltration in the dunes of the Amsterdam Water Supply.* Journal of Hydrology, 1998. **209**(14): p. 281-296.
4. Jacques, D., Šimůnek, J., Mallants, D., van Genuchten, M. T., *Modelling coupled water flow, solute transport and geochemical reactions affecting heavy metal migration in a podzol soil.* Geoderma, 2008. **145**(3-4): p. 449-461.
5. Eskom. *ESKOM Annual Report, 2009, http://www.eskom.co.za/annreport09/annreport09/,*. 2009, [cited 2011 October 2011].
6. Roux, T., Gericke, G., Buckley, C., Petrik, L., Hareeparsad, S., Menghistu, M., *Towards the Development of Sustainable Salt Sinks: Fundamental Studies on the Co-Disposal of Brines in Inland Ash Dams* in *Executive Summary Report*. 2007, Sasol Technology: Secunda, South Africa.
7. Golden, D.M., *Water Pollution Arising from Solid Waste (Coal, Fly Ash, Slag) Disposal, and Measures to Prevent Water Pollution* Water Science and Technology, 1981. **15** p. 1-10.
8. Adriano, D.C., Page, A.L., Elseewi, A.A., Chang, A.C., Straughan, I., *Utilization and disposal of fly ash and other coal residues in terrestrial ecosystems: A Review.* J Environ Qual 1980. **9**: p. 333-344.
9. Carlson, C.L., Adriano, D.C, *Enviromental impacts of coal combustion residues* Journal of Enviromental Quality, 1993. **22**: p. 227-247.
10. Petrik, L., Gitari, W., Etchebers, O., Kumar Vadapalli V., Nel, J., Fatoba, O., Nyamihingura, A., Antonie, M., *Towards the Development of Sustainable Salt Sinks* in *3rd Interim Progress Report.* 2007, University of the Western Cape (UWC).
11. Petrik, L., Gitari, W. M., Nel, J., Fatoba, O., Nyamihingura, A., Akinyemi, S. A., *Towards the Development of Sustainable Salt Sinks*, in *Fundamental Studies on the Co-Disposal of Brines within Inland Ash Dams*. 2009, University of the Western Cape: Western Cape. p. 55.
12. Gitari, W.M., *Evaluation of the Leachate Chemistry and Contaminants Attenuation in Acid Mine Drainage by Fly Ash and its derivatives*, in *Department of Chemistry*. 2006, University of the Western Cape: Cape Town. p. 385.
13. Gitari, M.W., Ojo F.O, Nyamihingura, A., Petrik, L.F., Vadapalli, V.R.K., Nel, J., October, A., Dlamini, L., Gericke, G., Mahlaba, J.S. , *Chemical Weathering In A Dry Ash Dump: An Insight From Physicochemical and Mineralogical Analysis Of Drilled Cores*, in *World of coal Ash (WOCA) Conference*. 2009, WOCA: Lexington. p. 23.
14. Parkhurst, D.L., and Appelo, C.A.J., *User's guide to PHREEQC (Version 2)--a computer program for speciation, batch-reaction, one-dimensional transport, and inverse geochemical calculations* U.S. Geological Survey Water-Resources Investigations Report, 1999: p. 99-4259, 312
15. Ojo, F.O., *Chemical Compositions and Leaching behaviour of some South African Fly Ashes*, in *Chemistry*. 2007, University of Western Cape: Western Cape. p. 216.
16. Langenkamp, H., Part, P., *Organic Contaminants in Sewage Sludge for Agricultural Use*. 2001, European Commission Joint Research Centre Institute for Environment and Sustainability Soil and Waste Unit. p. 73.
17. Leet, W.A., Lee, F.S-C, Gandy, R., Cronauer, D.C., *The Organic/Mineral Interaction in Coal Liquefaction Bottoms*, Amoco Oil Corporation: Naperville.

18. Pérez-López, R., Cama, J., Miguel N., José, A.C., Saaltink, M.W., *Attenuation of pyrite oxidation with a fly ash pre-barrier: Reactive transport modelling of column experiments.* Applied Geochemistry, 2009. **24**(9): p. 1712-1723.
19. Ojo, O.F., *Chemical interactions and mobility of species in fly ash-brine co-disposal systems*, in *Department of Chemistry University of the Western Cape*. 2010, (PhD Thesis), University of the Western Cape: Western Cape.
20. Shoham-Fridera, E., Shelefb, G., Kressa, N., *Chemical changes in different types of coal ash during prolonged, large scale, contact with seawater.* Waste Management 2003. **23**: p. 10.
21. Yeheyis, M.B., Shang, J.Q., Yanful, E.K. , *Long-term evaluation of coal fly ash and mine tailings co-placement: A site-specific study.* Journal of Environmental Management 2009. **91**: p. 237-244.
22. Mahlaba, J.S., Kearsley, E.P., Kruger, R.A., Pretorius, P.C., *Evaluation of workability and strength development of fly ash pastes prepared with industrial brines rich in and Cl- to expand brine utilisation.* Minerals Engineering, 2011. **24**(10): p. 1077-1081.
23. Soong, Y., Fauth, D. L., Howard, B. H., Jones, J. R., Harrison, D. K., Goodman, A. L., Gray, M. L., Frommell, E. A., *CO2 sequestration with brine solution and fly ashes.* Energy Conversion and Management, 2006. **47**(13-14): p. 1676-1685.
24. B. Ligia, R.Z., J. Mehu, *Assessment of the multi-scale leaching behaviour of compacted coal fly ash.* Journal of hazardous materials 2006. **137**: p. 1466-1478.
25. Schiopu, N., Tiruta-Barna, L., Jayr, E., Méhu, J., Moszkowicz, P., *Modelling and simulation of concrete leaching under outdoor exposure conditions.* Science of The Total Environment, 2009. **407**(5): p. 1613-1630.
26. Hareeparsad, S., Tiruta-Barna, L., Brouckaert, C.J., Buckley, C.A., *Quantitative geochemical modelling using leaching tests: Application for coal ashes produced by two South African thermal processes.* Journal of Hazardous Materials, 2010. **186**(2-3): p. 1163-1173.
27. Tiruta-Barna, L., Rakotoarisoa, Z., Méhu, J., *Assessment of the multi-scale leaching behaviour of compacted coal fly ash.* Journal of Hazardous Materials, 2006. **137**(3): p. 1466-1478.
28. Stumm, W., Morgan, J.J., *Aquatic Chemistry*. third ed. , ed. Inc. 1996, New York: John Wiley & Sons.
29. Petrik, L., Gitari, W. M., Nel, J., Ojo, O.F., Nyamihingura, A., Akinyemi S. A., *Towards the Development of Sustainable Salt Sinks: Fundamental Studies on the Co-Disposal of Brines within Inland Ash Dams*, in *Sasol-Eskom Phase Two 4th Quarter Interim Report 2009*. 2009, University of the Western Cape: Western Cape. p. 179.
30. Wadley, S., Buckley, C.A. (1997) *Chemical Speciation Self-Study Work Manual*., 560
31. Bethke, C.M., *The question of uniqueness in geochemical modeling.* Geochim. Cosmoschim. Acta., 1992. **56**: p. 4315-4320.
32. Feuerborn, H.J., *Coal ash utilisation over the world and in Europe*, in *Workshop on Environmental and Health Aspects of Coal Ash Utilization International workshop*. 2005, European Coal Combustion Products Association e.V.: Tel-Aviv, Israel. p. 5.
33. Sasol (2005) *Unlocking the Potential Wealth of Coal: Introducing Sasol's Unique Coal-to-Liquids Technology*. P. 6
34. Kolbe, J.L., Lee, L.S., Jafvert, C.T., Murarka, I.P. *Use of Alkaline Coal ASh for Reclamation of a Former Strip Mine*. in *World of Coal Ash (WOCA) Conference*. 2011. Denver, USA.
35. Jankowski, J., Ward, C., French, D., Groves, S., *Mobility of trace elements from selected Australian fly ashes and its potential impact on aquatic ecosystems.* Fuel 2006. **85**: p. 243-256.
36. Eskom. *ESKOM Annual Report 2001: http://www.eskom.co.za/annreport02/profile.htm,*. 2001 [cited 2012 January 2012].
37. Matjie, R.H., Ginster, M., Alphen, C.V., Sobieck, A. *Detailed Characterisation of Sasol Ashes*. in *World of Coal Ash (WOCA)*. 2005. Lexington, Kentucky, USA: WOCA.
38. Kruger, R.A., *South African Coal Ash Association*, P. communication, Editor. 2002: Johannesburg.

39. Singh, G. *Environmental Issues With Best Management Practices of Responsible Mining*. in *20th National Convention of Mining Engineers*. 2009. Neyveli Local Centre, India.
40. Koukouzas, N., Wardb, C.R., Papanikolaou, D., Li, Z., Ketikidis, C., *Quantitative evaluation of minerals in fly ashes of biomass, coal and biomass–coal mixture derived from circulating fluidised bed combustion technology.* Journal of Hazardous Materials 2009. **169**: p. 100-107.
41. Naik, T.R., Singh, S.S., *Fly Ash Generation And Utilization - An Overview*, in *Recent Trend in Fly Ash Utilization*. 1993, Center for By-Products Utilization, India: Milwaukee. p. 32.
42. EURELECTRIC, Union of the Electricity Industry, *Fly Ash from Coal Fired Power Plants: A Non-Hazardous Material*. 2000, Union of the Electricity Industry - EURELECTRIC: Brussels. p. 20.
43. Ferguson, G., *Use of self-cementing fly ashes as a soil stabilization agent.* Fly ash for Soil Improvement, Geotechnical Special Publication, 1993. **36**: p. 15.
44. Berry, E.E., Hemmings, R.T., Cornelius, B.J., *Mechanisms of hydration reactions in high volume fly ash pastes and mortars.* Cement and Concrete Composites, 1990. **12**(4): p. 253-261.
45. Mehta, P.K., *Influence of fly ash characteristics on the strength of portland-fly ash mixtures.* Cement and Concrete Research, 1985. **15**(4): p. 669-674.
46. Mlambo, T.K., Doucet, F.J., van der Merwe, E.M., Altermann, W., Atanasova, M., Kruger, R.A., *The Injection of Fly ash Slurries in Deep Geological Reseavoirs for Improved Reservoir Integrity and Safe CO2 Sequestration*, in *World of Coal Ash (WOCA) conference*. 2011, WOCA: Denver, USA. p. 6.
47. Muriithi , G.N., Gitari, M.W., Petrik, L.F. *Brine Remediation Using Fly Ash and Accelerated Carbonation*. in *International Mine Water Conference*. 2009. Pretoria.
48. Ramesh, A. and J.A. Kozinski, *Rearrangements in metals environment of inorganic particles during combustion and solidification.* Combustion and Flame, 2001. **125**(1): p. 920-930.
49. American Society for Testing and Materials, A., *Standard speciation for fly ash and raw or calcined natural pozzolan for use as a mineral admixture in Portland cement concrete.* , in *Annual Book of ASTM Standards*. 1993, ASTM: Philadelphia.
50. Mahlaba, J.S., Kearsley, E.P., Kruger, R.A., *Effect of fly ash characteristics on the behaviour of pastes prepared under varied brine conditions.* Minerals Engineering. **24**(8): p. 923-929.
51. Adriano, D.C., Page, A.L., Elseewi, A.A., Chang, A.C., Straughan I., *Utilization and disposal of fly ash and other coal residues in terrestrial ecosystems: A Review.* J Environ Qual 1980. **9**: p. 333-344.
52. Carlson, C.L, Adriano, D.C., *Enviromental impacts of coal combustion residues* Journal of Enviromental Quality, 1993. **22**: p. 227-247.
53. Ichikawa, K., Otaka, M., Watanabe, H., Inumaru, J., *Study on Coal & Coal Ash Properties and the Modeling Technique of Mineral Particle Behavior in the Gasifier.* Nihon Kikai Gakkai Nenji Taikai Koen Ronbunshu(2000) 2000. **4**: p. 365-366.
54. Mueller, M., Willenborg, W., Hilpert, K., And Singheiser, L. , *Structural dependence of alkali oxide activity in coal ash slags.* VII International Conference on Molten Slags Fluxes and Salts, The South African Institute of Mining and Metallurgy., 2004.
55. Mahlaba, J.S., Kearsley, E.P., Kruger, R.A., *Physical, chemical and mineralogical characterisation of hydraulically disposed fine coal ash from SASOL Synfuels.* Fuel, 2011. **90**(7): p. 2491-2500.
56. Koukouzas, N., Hämäläinen, J., Papanikolaou, D., Tourunen, A., Jäntti, T., *Mineralogical and elemental composition of fly ash from pilot scale fluidised bed combustion of lignite, bituminous coal, wood chips and their blends.* Fuel, 2007. **86**(14): p. 2186-2193.
57. Feuerborn, H.J., *Coal Combustion Products in Europe-an update on Production and Utilization, Standardisation and Regulation*, in *World of Coal Ash (WOCA)*. 2011, WOCA: Denver. p. 18.
58. Ginster, M., Matjie, R., *Beneficial Utilization of Sasol Coal Gasification Ash*, in *World of Coal ASh (WOCA)*. 2005, WOCA: Lexington, Kentucky, USA. p. 5.

59. Bone, B.D., Barnard, L H., Boardman, D.I., Carey, P.J., Hills, C.D., Jones, H.M., MacLeod, C.L., Tyrer, M., *Review of scientific literature on the use of stabilisation/solidification for the treatment of contaminated soil, solid waste and sludges*. 2004, Environment Agency,UK: Bristol. p. 343.
60. Sasol (2009) *Managing the challenge of water scarcity*. Sasol Sustainability Report 2009
61. Eskom (2010) *Eskom Annual Report 2010*. http://financialresults.co.za/2010/eskom_ar2010/eskom_abriged-ar2010/index.html, 52
62. Olebogeng I, M., Martin Ginster, Ratale H. Matjie and Karl-Heinz J. Riedel, *Leachate Characteristics of Ash from a Laboratory-Scale Brine Encapsulation Simulation Process.* 2007 World of Coal Ash (WOCA), 2007.
63. WaterWorld (2011) *Water treatment process provides ultrapure, condensate water at one of world's largest coal power plants*. p. 2
64. Jeevaratnam, E.G., Pretorius, C.P. " *Ash as a sustainable salt sink for Secunda Complex*. 2003, Sasol Technology R&D Gate B document.: Johannesburg.
65. Mahlaba, J.S., *Evaluation of Paste Technology to Co-Dispose of Ash and Brines at Sasol Synfuels Complex*, in *Faculty of Engineering and the Built Environment*. 2006, University of the Witwatersrand: Johannesburg. p. 144.
66. Moller, N., Weare J. H. , *Enhanced Geothermal Systems Research and Development: Models of Subsurface Chemical Processes Affecting Fluid Flow*. 2008, University of California: San Diego. p. 48.
67. Glater, J., Cohen, Y., *Brine Disposal from Land Based Membrane Desalination Plants: A Critical Assessment*. 2003, Polymer and Separations Research Laboratory, University of California,: Los Angeles. p. 16.
68. Mahlaba, S.J.a.P., P. C. ". *Exploring Paste Technology as a Codisposal Option for Fly Ash and Brines. Proc, Paste 2006*. in *9th International Seminar on Paste and Thickened Tailings*. 2006. Limerick, Ireland
69. Mehari, T.M., *Development of a Numerical Model for Unsaturated/ Saturated Hydraulics in Ash/Brine Systems*, in *Department of Geohydrology*. 2010, University of the Free State: Bloemfontein. p. 141.
70. Cara, S., Carcangiu, G., Massidda, L., Meloni, P., Sanna, U., Tamanini, M., *Assessment of pozzolanic potential in lime-water systems of raw and calcined kaolinic clays from the Donnigazza Mine (Sardinia-Italy).* Applied Clay Science, 2006. **33**(1): p. 66-72.
71. Pedro, A., C.G., Eduardo, P.M., Jesus, P.J., Goumans, J.M., Senden, G.J., van der Sloot, H.A., *Engineering properties of the coal ashes stored in the "Valdeserrana" Lagoon. Andorra power plant (Spain)*, in *Studies in Environmental Science*. 1997, Elsevier. p. 167-173.
72. Hodgson, F.I.D., Krantz, R.M. , *Investigation into groundwater quality deterioration in the olifants river catchment above the Loskop Dam with specialized investigation in the Witbank dam sub-catchment.* . 1998, Water Research Commission Pretoria.
73. Vítková, M., Ettler, V., ebek O., Mihaljevi, M., *Metal-contaminant leaching from lead smelter fly ash using pH-stat experiments.* Mineralogical Magazine, 2008. **72** (1): p. 521-524.
74. Nikolaj, K.J.L., Jette, B.H., Margareta, W., Ann-Marie, F., Ole, H., *Influence of critical test conditions on the results of pH-dependent leaching tests*. 2002, Nordtest: Espoo. p. 104.
75. Lewin, K., *Leaching tests for waste compliance and characterisation: recent practical experiences; Harmonization of Leaching/Extraction Tests for Environmental Risk Assessment.* Science of The Total Environment 1996. **178**(1-3): p. 85-94.
76. Hjelmar, O., *Leachate from land disposal of coal fly ash.* Waste Management & Research, 1990. **8**(6): p. 429-449.
77. Egemen, E., Yurteri, C., *Regulatory Leaching Tests For Fly Ash: A Case Study.* Waste Management & Research, 1996. **14**(1): p. 43-50.
78. Fallman, A.M., Aurell, B., *Leaching tests for environmental assessment of inorganic subtances in wastes, Sweden.* The Science of the Total environment, 1996. **178**: p. 71-84.

79. Hans, V.S., Andre, V.Z., Rob, C., Ole H. *Harmonisation of leaching test methods in support of EU regulations controlling the beneficial use of industrial slag in construction*. in *2nd International Slag Valorisation Symposium* 2011. Leuven.
80. Cen-European Prestandard Env 12920, *Characterisation Of Waste–Methodology for the Determination of the Leaching Behaviour of Waste Under Specified Conditions*. ENV 12920: 1997 - Texte trilingue - Publication CEN novembre 1997 - draft revision 1, 1997: p. 19
81. Shoham-Frider, E., Shelef, G., Kress, N. *Chemical changes in different types of coal ash during prolonged, large scale, contact with seawater.* Waste Management, 2003. **23**(2): p. 125-134.
82. Hesbach, P., Kim, A., Abel, A., Lamey, S., *Serial batch leaching procedure for characterization of coal fly ash.* Environmental Monitoring and Assessment, 2010. **168**(1): p. 523-545.
83. Hesbach, P., Beck, M., Eick, M., Daniels, W.L., Burgers, C., Greiner, A., Hassett, D. , *Inter-laboratory Comparison of Leaching Methods*, in *World of Coal Ash, April 11-15, 2005*. 2005: Lexington, KY.
84. van der Sloot, H.A., Heasman, L., Quevauviller, P., *Chapter 12: Standardization of leaching/extraction tests*, in *Studies in Environmental Science*. 1997, Elsevier. p. 227-238.
85. prEN14405, *Leaching behaviour test – Up-flow percolation test - Horizontal standard.* . 2003.
86. van der Sloot, H.A., *Quick techniques for evaluating the leaching properties of waste materials: their relation to decisions on utilization and disposal.* TrAC Trends in Analytical Chemistry, 1998. **17**(5): p. 298-310.
87. NEN 7345, *Determination of leaching from monolithic construction materials and waste materials by means of a diffusion test*. October, 1994.
88. NEN 7343, *Leaching characteristics of solid (earth and stony) building and waste materials. Leaching tests. Determination of the leaching of inorganic constituents from granular materials with the column test*, N.N. Institute, Editor. 1995.
89. De Windt, L., R. Badreddine, and V. Lagneau, *Long-term reactive transport modelling of stabilized/solidified waste: from dynamic leaching tests to disposal scenarios.* Journal of Hazardous Materials, 2007. **139**(3): p. 529-536.
90. Hage, J.L.T. and E. Mulder, *Preliminary assessment of three new European leaching tests.* Waste Management, 2004. **24**(2): p. 165-172.
91. Tiruta-Barna, L., *Using PHREEQC for modelling and simulation of dynamic leaching tests and scenarios* Journal of Hazardous Materials, 2008. **157**(2-3): p. 525-533.
92. Ligia, T., Apichat, I., Radu, B., *Long-term prediction of the leaching behavior of pollutants from solidified wastes* Advances in Environmental Research 2004. **8**(3-4): p. 697-711.
93. Ligia, B., Zolalaina, R., Mehu, J., *Assessment of the multi-scale leaching behaviour of compacted coal fly ash.* Journal of hazardous materials 2006. **137**: p. 1466-1478.
94. Garavaglia, R., Caramuscio, P. . *Coal fly-ash leaching behaviour and solubility controlling solids*. in *Proceedings of the Environmental Aspects of Construction with Waste Materials* 1994: Elsevier Science.
95. Council, N.R., *Ground Water Models-Scientific and Regulatory Applications*, N.R. Council, Editor. 1990, National Academic press: Washington D.C. p. 303.
96. Zhu, C., Anderson, G., *Environmental Applications of Geochemical Modeling*. 2002, Cambridge: Cambridge University Press.
97. Rabadjieva, D., Tepavitcharova, S.,Todorov, T., Dassenakis, M., Paraskevopoulou, V. Petrov, M. *Thermodynamic Modeling of Inorganic Chemical Speciation in River Waters Affected by Mine Water Discharges*. in *PROMITHEAS-2,* . 2008. Athens (Greece).
98. Bundschuh, J., Zilberbrand, M., ed. *Geochemical Modeling of Groundwater, Vadose and Geothermal Systems*. Multiphysics Modeling, ed. M. Modeling. Vol. 5. 2011, CRC Press. 332.
99. Appelo, C.A.J., Postma, D, *Geochemistry, Groundwater and Pollution*. 2 ed. 2005, Amsterdam: A.A Balkema Publishers.

100. Pitzer, K.S., ed. *Theory - Ion interaction approach*. Activity Coefficients in Electrolyte Solutions, ed. R.M. Pytkowitcz. Vol. 1. 1979, CRC Press, Inc. : Boca Raton, Florida. pp. 157-208.
101. Crawford, J., *Geochemical Modelling – A Review of Current Capabilities and Future Directions*. 1999, Swedish Environmental Protection Agency: Stockholm, Sweden. p. 42.
102. Twardowska, I. and J. Szczepanska, *Solid waste: terminological and long-term environmental risk assessment problems exemplified in a power plant fly ash study.* Science of The Total Environment, 2002. **285**(1â€“3): p. 29-51.
103. van der Lee, J. and L. De Windt, *Present state and future directions of modeling of geochemistry in hydrogeological systems.* Journal of Contaminant Hydrology, 2001. **47**(2-4): p. 265-282.
104. Yeh, G.T. and V.S. Tripathi, *A critical evaluation of recent developments in hydrogeochemical transport models of reactive multichemical components.* Water Resour. Res., 1989. **25**(1): p. 93-108.
105. Brown, K.P. and E.Z. Hosseinipour, *Modeling speciation, transport and transformation of metals from mine wastes.* Ecological Modelling, 1991. **57**(1-2): p. 65-89.
106. Jinying, Y., Luis, M., Ivars, N., *Neutralizing processes in leaching of solid waste: Modeling of interactions between solid waste and strong acid* Journal of Environmental Science and Health, Part A 1998. **33**: p. 923 - 950.
107. Zhang, F., Yeh, G.T., Parker, J.C., Jardine, P.M., Brooks, S.C., Pace, M.N., Kim, Y.J., Watson, D.B., *A reaction-based paradigm to model reactive chemical transport in groundwater with general kinetic and equilibrium reactions.* Journal of Contaminant Hydrology, 2007. **92**(1-2): p. 10-32.
108. Zhang, F., Yeh, G.T., Parker, J.C., Jardine, P.M., *A reaction-based river/stream water quality model: Model development and numerical schemes.* Journal of Hydrology, 2008. **348**(3-4): p. 496-509.
109. Phanikumar, M.S. and J.T. McGuire, *A multi-species reactive transport model to estimate biogeochemical rates based on single-well pushâ€“pull test data.* Computers & Geosciences. **36**(8): p. 997-1004.
110. Samper, J., Zheng, L., Fernández, A.M., Montenegro, L., *Inverse modeling of multicomponent reactive transport through single and dual porosity media.* Journal of Contaminant Hydrology 2008. **98**: p. 115-127.
111. Lensing, H.J., M. Vogt, and B. Herrling, *Modeling of biologically mediated redox processes in the subsurface.* Journal of Hydrology, 1994. **159**(1-4): p. 125-143.
112. Parkhurst, D.L., *PHREEQC vs MinTEQ*, in *http://wwwbrr.cr.usgs.gov/projects/GWC_coupled/phreeqc/mail/msg00625.html*. 2003.
113. Wadley, S., Buckley, C.A. , *Chemical Speciation Self-Study Work Manual*. 1997. p. 560.
114. Bethke, C.M., Yeakel, S. (2011) *The Geochemist's Workbench User's Guides, Version 9.0.* . Aqueous Solutions LLC.
115. Aqueous-Solutions-LLC. *The Geochemist's Workbench® version 9.0*. 2012 [cited 2012 May 2012]; Available from: http://www.gwb.com/gwb.htm.
116. Parkhurst, D.L., Kipp, K.L., Charlton, S.R. , *PHAST Version 2-A program for simulating groundwater flow, solute transport, and multicomponent geochemical reactions*, in *U.S. Geological Survey Techniques and Methods 6-A35,* . 2010, USGS. p. 235
117. Dzombak, D.A., Morel, F. M. M., *Surface complexation modeling: hydrous ferric oxide*. null. 1990. null.
118. USGS. *Features not documented in WRIR 99-4295* "Revisions and Bug Fixes", 2011 [cited 2011 October 2011]; http://wwwbrr.cr.usgs.gov/projects/GWC_coupled/phreeqc/RELEASE.5570.TXT.
119. Muluken, B.Y., Julie, Q.S., Ernest, K.Y., *Long-term evaluation of coal fly ash and mine tailings co-placement: A site-specific study.* Journal of Environmental Management 2009. **91** p. 237-244.

120. Adriano, D.C., Page, A.L., Chang, A.C., Elseewi, A.A., *Cadmium availability to Sudan grass ongrown on soils amended with sewage sludge and fly ash.* Journal of Environmental Quality, 1982. **1**: p. 197-203.
121. Van der Sloot, H.A., Van Zomeren, A., Dijkstra, J.J., Hoede, D., Scharff, H., *Modeling of the source term for a predominantly inorganic waste landfill using data obtained from laboratory-scale testing, lysimeter studies and pilot scale monitoring*, in *56th Fachtagung "Stoffbewertung und Gewasserrokologie"*. 2002: Munchen. p. 20.
122. Gitari, W.M., Fatoba, O.O., Petrik, L. F., Vadapalli, V.R.K. , *Leaching characteristics of selected South African fly ashes: Effect of pH on the release of major and trace species.* Journal of Environmental Science and Health 2009. **44**(Part A): p. 206-220.
123. Melchior, C.D., Bassett, R.L *Chemical Modeling of Aqueous Systems II*. ACS Symposium series, ed. A.C. Society. Vol. 416. 1990, California: American Chemical Society. 556.
124. Appelo, C.A.J., Postma, D. , *Geochemistry, groundwater and pollution*. 2nd ed. 2005, Amsterdam: A.A Balema Publishers. 649.
125. Benjamin, M.M., *Water Chemistry*. 1st ed. McGraw-Hill Series in Water Resources and Environmental Engineering. Vol. 1. 2002, New York: McGraw-Hill. 668.
126. Lo, H.M., Liao, Y.L., *The metal-leaching and acid-neutralizing capacity of MSW incinerator ash co-disposed with MSW in landfill sites.* Journal of Hazardous Materials, 2007. **142**(1-2): p. 512-519.
127. Mizutani, S., Yoshida, T., Sakai, S., Takatsuki, H., *Release of metals from MSW I fly ash and availability in alkali condition.* Waste Management, 1996. **16**(5-6): p. 537-544.
128. Parka, J., Batchelorb, B., *A multi-component numerical leach model coupled with a general chemical speciation code.* Water Research, 2002. **36** p. 11129. Coles, C.A., Yong, R.N., *Aspects of kaolinite characterization and retention of Pb and Cd.* Applied Clay Science 2002. **22**: p. 39- 45.
130. Cho, H., Oh, D., Kim, K. , *A study on removal characteristics of heavy metals from aqueous solution by fly ash.* J. Hazard. Mater., 2005. **B127**: p. 187-195.
131. De Windt, L. and R. Badreddine, *Modelling of long-term dynamic leaching tests applied to solidified/stabilised waste.* Waste Management, 2007. **27**(11): p. 1638-1647.
132. Nicoleta S, T.-B.L., Emmanuel J, Jacques M, Pierre M., *Modeling and Simulation of Concrete leaching under outdoor exposure conditions.* Science of theTotal Environment, 2008. **407**(2009): p. 1613-1630.
133. Baranger, P., Azaroual, M., Freyssinet, P., Lanini, S., Piantone, P., *Weathering of a MSW bottom ash heap: a modelling approach.* Waste Management, 2002. **22**(2): p. 173-179.
134. Regnier, P., Jourabchi, P., Slomp, C.P. , *Reactive-Transport modeling as a technique for understanding coupled biogeochemical processes in surface and subsurface environments.* Netherlands Journal of Geosciences / Geologie en Mijnbouw 2003. **82**(1): p. 5-18.
135. Douglas, C.C., Ronald, M., Pearson, C., Hurcomb, D., *Mineral Dissolution and Dam Seepage Chemistry-The Bureau of Reclamation Experience*. 2007, U.S. Department of the Interior - Bureau of Reclamation - Technical Service Center: Denver p. 26.
136. Mbugua, J.M., Ngila, J. C., Kindness, A., Buckley, C., Demlie, M., *Hydrogeochemical modeling of fly ash co-disposed with brines and organics: Effects of Organics and Brines on ANC of coal Ash*, in *Towards The Development Of Sustainable Salt Sinks: Fundamental Studies On The Co-Disposal Of Brines Within Inland Ash Dams (Sasol-Eskom Ash-Brine Project- 2009 Q3&4 Quarterly Interim report, Phase 2)*. 2009, University of KwaZulu-Natal (UKZN): Durban (South Africa). p. 33.
137. Mbugua, J.M., Ngila, J. C., Kindness, A., Buckley, C., Demlie, M., *Hydrogeochemical modeling of fly ash co-disposed with brines and organics: Column and ash heap modeling of Secunda and Tutuka fly ashes and the effect of brines on the leaching chemistry of fly ashes*, in *Towards The Development Of Sustainable Salt Sinks: Fundamental Studies On The Co-Disposal Of Brines Within Inland Ash Dams (Sasol-Eskom Ash-Brine Project-2010 Q1-4 Interim report, Phase 2)*. 2010, University of KwaZulu-Natal (UKZN): Durban (South Africa). p. 108.

138. Fatoba, O.O., Petrik, L.F., Gitari, W.M., Iwuoha, E.I., *Fly ash-brine interactions: Removal of major and trace elements from brine.* Journal of Environmental Science and Health, Part A, 2011. **46**(14): p. 1648-1666.
139. Zhu, C., Burden, D.S *Mineralogical compositions of aquifer matrix as necessary initial conditions in reactive contaminant transport models.* Journal of Contaminant Hydrology 2001. **51**: p. 145-161.
140. Nyambura, M.G., Mugera, G.W., Felicia, P.L., Gathura, N.P., *Carbonation of brine impacted fractionated coal fly ash: implications for CO2 sequestration.* J Environ Manage 2011. **92**(3): p. 655-664.
141. Schiopu, N., Tiruta-Barna, L., Jayr, E., Méhu, J., Moszkowicz, P., *Modelling and simulation of concrete leaching under outdoor exposure conditions.* Science of The Total Environment, 2009. **407**(5): p. 1613-1630.
142. Quinby-Hunt, M.S., Wilde, P., *Modeling of Dissolved Elements in Sea Water.* Ocean Science and Engineering 1986-87. **11** (3&4): p. 153-251.
143. http://webmineral.com/data, *Mineralogy Database*. 2009, http://webmineral.com/.
144. Kourti, I., Rani, D.A., Boccaccini, A.R., Cheeseman, C.R. . *Geopolymers From DC plasma Treated APC Residues, Metakaolin, and GGBFS*. in *Second International Conference on Sustainable Construction Materials and Technologies*. 2010. Ancona, Italy.
145. Kopp, R.E., Humayun, M., *Kinetic model of carbonate dissolution in Martian meteorite ALH84001.* Geochimica et Cosmochimica Acta, 2003. **Vol. 67**(o. 17): p. 10.
146. en.wikipedia.org/wiki/ (2010) *Nickel(II) hydroxide, Nickel(II) carbonate*.
147. https://www.u-cursos.cl/ingenieria/2008/2/GL4A1/1/.../23321 (2008) *GL4A1-1 Introduction to Environmental Geology, 2008, Spring Semester*.
148. Donahoe, R.J., *Secondary mineral formation in coal combustion byproduct disposal facilities: implications for trace element sequestration.* Geological Society, London, Special Publications, 2004. **236**(1): p. 641-658.
149. Parkhurst, D.L., Stollenwerk, K.G., Colman, J.A., *Reactive-Transport Simulation of Phosphorus in the Sewage Plume at the Massachusetts Military Reservation Cape Cod, Massachusetts*. 2003, Water-Resources Investigations Report Massachusetts. p. 40.
150. Steyl, G., Nel, J.M., van der Merwe, C., Gomo, M., Teboho, S., Leketa, K. , *ESKOM-SASOL PHASE II Sustainable Salt Sinks*, in *Deliverable 1: Inception Report*. 2010, University of the Free State: Bloemfontein. p. 63.
151. Katz, G.E., Berkowitz, B., Guadagnini, A., Saaltink, M.W., *Experimental and modeling investigation of multicomponent reactive transport in porous media.* Journal of Contaminant Hydrology, 2011. **120-121**(0): p. 27-44.
152. Ph. Freyssinet, P.P., M. Azaroual, Y. Itard, B. Clozel-Leloup, D. Guyonnet and J. C. Baubron, *Chemical changes and leachate mass balance of municipal solid waste bottom ash submitted to weathering* Waste Management, 2002. **22**(2): p. 159-172.
153. Mendoza, T., Hernández, O.A., Abundis, M., Nestor, J.M, *Geochemistry of leachates from the El Fraile sulfide tailings piles in Taxco, Guerrero, southern Mexico.* Environmental Geochemistry and Health, 2006. **28**(3): p. 243-255.

APPENDICES

Appendix 1: Input file and tables of supplementary results for acid neutralization capacity (ANC) of Secunda and Tutuka fly ashes with brines and organics

Table A1: Input file for ANC of fly ash with ASW organics and combined brines.

```
SOLUTION_MASTER_SPECIES
    Ni              Ni+2              0     Ni               58.69
    Ti              Ti(OH)4           0     Ti               47.88
    Si              H4SiO4            0     Si               28.0855
    Cl              Cl-               0     Cl               35.4527
SOLUTION_SPECIES
Ni+2 = Ni+2
    log_k     0
Ti(OH)4 = Ti(OH)4
    log_k     0
2H2O + SiO2 = H4SiO4
    log_k     -2.7
2H+ + H2SiO4-2 = SiO2 + 2H2O
    log_k     22.96
H2O + 0.01e- = H2O-0.01
    log_k     -9
Cl- =  Cl-
    log_k     0
    delta_h   -39.933 kcal
SOLUTION 1 with DMW, organic sewage recipe and brines combined
    temp      20
    pH        7 charge
    pe        4
    redox     pe
    units     mol/l
    density   1
    Li        0.0002
    Na        0.108689913
    K         0.006611507
    Acetate   0.5 mMol/l
    Glycine   0.5 mMol/l
    Tartarate 0.25 mMol/l
```

```
    Glutamate 0.2 mMol/l
    Salicylate 0.155 mMol/l
    Phthalate 0.125 mMol/l
    Mg        0.000339
    C(4)      0.004
    S(6)      0.045431058
    Cl        0.046388599
    -water    1 # kg



REACTION 1 ANC with NO3-
    NO3-       1
    0  0.046  0.085  0.12  0.174  0.175  0.177
    0.179  0.202  0.208  0.212  0.218 moles

SELECTED_OUTPUT
    -file                ANC Secunda Sept2009 ash +ASW + Combined brines JMM
    -reset               false
    -ph                  true
    -pe                  true
    -totals              Ca  Mg  Al  Ti  Fe  Ni  Cr
                         Mo  Sr  Zn  Si  S(6)  Na  K
                         Li  Phthalate  Acetate  Glycine  Salicylate  Tartarate  Glutamate
                         C(4)  Cl
    -molalities          Ca(Acetate)+  Ca(Glutamate)  Ca(Glycine)+  Ca(Phthalate)
                         Ca(Salicylate)  Ca(Tartarate)  Ca+2  CaCO3
                         CaH(Glutamate)+  CaH(Glycine)+2  CaH(Phthalate)+  CaH(Salicylate)+
                         CaH(Tartarate)+  CaHCO3+  CaNO3+  CaOH+
                         CaSO4  Mg(Acetate)+  Mg(Glutamate)  Mg(Glycine)+
                         Mg(Phthalate)  Mg(Salicylate)  Mg(Tartarate)  Mg+2
                         MgCO3  MgH(Salicylate)+  MgHCO3+  MgOH+
                         MgSO4  Al(OH)4-  FeSO4  MoO4-2
                         Sr+2  SrHCO3+  SrNO3+  SrOH+
                         SrSO4  SiO2  H2SiO4-2  H3SiO4-
                         H4SiO4  Na(Acetate)  Na(Phthalate)-  Na(Tartarate)-
                         Na+  NaCO3-  NaCrO4-  NaH(Tartarate)
                         NaHCO3  NaSO4-  K(Tartarate)-  K+
```

```
                        KSO4-  Li+  LiSO4-  SO4-2
                        CO3-2  HCO3-  Cl-  Acetate-
                        Phthalate-2  Glycine-  Glutamate-2  Salicylate-2
                        Tartarate-2  H(Acetate)  H(Glutamate)-  H(Glycine)
                        H(Phthalate)-  H(Salicylate)-  H(Tartarate)-  H2(Glutamate)
                        H2(Glycine)+  H2(Phthalate)  H2(Salicylate)  H2(Tartarate)
                        H3(Glutamate)+  H2CO3
    -equilibrium_phases  Anhydrite  CaCrO4  Calcite  CaMoO4
                        Hematite  Kaolinite  Lime  Millerite
                        mullite  Ni2SiO4  Periclase  Pyrite
                        SrSiO3  Zn2TiO4  Fe(OH)3(am)-CF  Brucite
                        Al(OH)3(mC)  Bunsenite  Celestite  Cr(OH)3(A)
                        Csh_gel_0.8  Ettringite  Gypsum  Magnesite
                        Ni(OH)2  NiCO3  Portlandite  SiO2(am)
                        Sr(OH)2  Zn(OH)2(gamma)
PHASES
Cu(OH)2
    Cu(OH)2 + 2H+ = Cu+2 + 2H2O
    log_k     8.64
Csh_gel_0.8
    Ca0.8SiO2.8:H2O + 1.6H+ = 0.8Ca+2 + 1.8H2O + SiO2
    log_k     11.08
Csh_gel_1.1
    Ca1.1SiO3.1:H2O + 2.2H+ = 1.1Ca+2 + 2.1H2O + SiO2
    log_k     16.72
CSH_1.4
    Ca1.4SiO3.4:0.90H2O + 2.8H+ = 1.4Ca+2 + 2.3H2O + SiO2
    log_k     23.74
Csh_gel_1.8
    Ca1.8SiO3.8:H2O + 3.6H+ = 1.8Ca+2 + 2.8H2O + SiO2
    log_k     32.7
CuCrO4
    CuCrO4 = CrO4-2 + Cu+2
    log_k     -5.4754
MgCrO4
    MgCrO4 = CrO4-2 + Mg+2
    log_k     5.3801
CaCrO4
```

```
    CaCrO4 = Ca2+ + CrO42-
    log_k     -2.2657
CaMoO4
    CaMoO4 = Ca2+ + MoO42-
    log_k     -7.94
BaMoO4
    BaMoO4 = Ba2+ + MoO42-
    log_k     -7.42
BaCrO4
    BaCrO4 = Ba2+ + CrO42-
    log_k     -9.6681
BaCr0.23S0.77O4
    Ba(CrO4)0.23(SO4)0.77 = Ba2+ + 0.23CrO42- + 0.77SO42-
    log_k     -10.13
BaCr0.04S0.96O4
    BaCr0.04S0.96O4 = Ba2+ + 0.04CrO42- + 0.96SO42-
    log_k     -9.79
Cr(OH)3(A)
    Cr(OH)3 + H+ = Cr(OH)2+ + H2O
    log_k     -0.75
Cr(OH)3(C)
    Cr(OH)3 + H+ = Cr(OH)2+ + H2O
    log_k     1.7005
Cr-Ettringite
    Ca6Al2(CrO4)3(OH)12:26H2O + 12H+ = 2Al+3 + 6Ca2+ + 3CrO42- + 38H2O
    log_k     53
Cr-hydrocalumite
    Ca4Al2CrO10:15H2O + 12H+ = 2Al+3 + 4Ca2+ + CrO42- + 21H2O
    log_k     71.02
Magnesiochromite
    MgCr2O4 + 8H+ = 2Cr+3 + 4H2O + Mg2+
    log_k     21.693
mullite
    Al6Si2O13 + 18H+ = 6Al+3 + 9H2O + 2SiO2
    log_k     45.41
Ca-Monosulfoaluminate
    Ca4Al2O6(SO4):12H2O + 12H+ = 2Al+3 + 4Ca2+ + 18H2O + SO42-
    log_k     73.37
```

```
Friedel-salt
    Ca4Al2Cl2O6:10H2O + 12H+ = 2Al+3 + 4Ca2+ + 2Cl- + 16H2O
    log_k     74.95
Ca3Al2(OH)12-cement
    Ca3Al2(OH)12 + 12H+ = 2Al+3 + 3Ca2+ + 12H2O
    log_k     80.33
Al(OH)3(mC)
    Al(OH)3 + 3H+ = Al+3 + 3H2O
    log_k     9.35
Ettringite
    Ca6Al2(SO4)3(OH)12:26H2O + 12H+ = 2Al+3 + 6Ca2+ + 38H2O + 3SO42-
    log_k     62.5362
Fe(OH)3(am)-CF
    Fe(OH)3 + 3H+ = Fe+3 + 3H2O
    log_k     4.9156
Millerite
    NiS + H+ = HS- + Ni2+
    log_k     -8.0345
Ni2SiO4
    Ni2SiO4 + 4H+ = 2H2O + 2Ni2+ + SiO2
    log_k     14.3416
SiO2(am)
    SiO2 + 2H2O = H4SiO4
    log_k     -2.7
Sr(OH)2
    Sr(OH)2 + 2H+ = 2H2O + Sr2+
    log_k     27.5229
SrSiO3
    SrSiO3 + 2H+ = H2O + SiO2 + Sr2+
    log_k     14.8438
Zn2TiO4
    Zn2TiO4 + 4H+ = Ti(OH)4 + 2Zn2+
    log_k     12.3273
Chalcedony
    SiO2 = SiO2
    log_k     -3.7281
Chrysotile
    Mg3Si2O5(OH)4 + 6H+ = 5H2O + 3Mg2+ + 2SiO2
```

```
    log_k     31.1254
Cristobalite(alpha)
    SiO2 = SiO2
    log_k     -3.4488
Cristobalite(beta)
    SiO2 = SiO2
    log_k     -3.0053
Greenalite
    Fe3Si2O5(OH)4 + 6H+ = 3Fe+2 + 5H2O + 2SiO2
    log_k     22.6701
Kaolinite
    Al2Si2O5(OH)4 + 6H+ = 2Al+3 + 5H2O + 2SiO2
    log_k     6.8101
Quartz
    SiO2 = SiO2
    log_k     -3.9993
Sepiolite
    Mg4Si6O15(OH)2:6H2O + 8H+ = 11H2O + 4Mg+2 + 6SiO2
    log_k     30.4439
Uraninite
    UO2 + 4H+ = 2H2O + U+4
    log_k     -3.49
    delta_h   -18.63 kcal
EQUILIBRIUM_PHASES 1
    Al(OH)3(mC) 0 0
    Anhydrite 0 0.007655828
    Brucite   0 0
    Bunsenite 0 0
    CaCrO4    0 1.96e-005
    Calcite   0 0.013647571
    CaMoO4    0 1.32e-006
    Celestite 0 0
    Cr(OH)3(A) 0 0
    Csh_gel_0.8 0 0
    Ettringite 0 0
    Fe(OH)3(am)-CF 0 0
    Gypsum    0 0
    Hematite  0 0.001410907 dissolve_only
```

```
    Kaolinite 0 0.00235 dissolve_only
    Lime      0 0.061520593
    Magnesite 0 0
    Millerite  0 1.16e-007 dissolve_only
    mullite   0 1.26e-005 dissolve_only
    Ni(OH)2   0 0
    Ni2SiO4   0 2.14e-006 dissolve_only
    NiCO3     0 0
    Periclase 0 0.041633259
    Portlandite 0 0
    Pyrite    0 0.000549869
    SiO2(am)  0 0
    Sr(OH)2   0 0
    SrSiO3    0 0.000608628 dissolve_only
    Zn(OH)2(gamma) 0 0
    Zn2TiO4   0 2.67e-007 dissolve_only
KNOBS
    -iterations            200
    -convergence_tolerance 1e-008
    -tolerance             1e-015
    -step_size             100
    -pe_step_size          10
END
```

Table A2: Input parameters for the brines from Secunda and Tutuka coal-utility plants in different modeling scenarios (Concentrations in mol/L)

PHREEQC input of brines scenarios in ANC			
	Elements	**SECUNDA**	**TUTUKA**
Mg^{+2} addition PHREEQC SOLUTION Input			
	Mg	3.39E-04	8.38E-03
	C(4)	4.00E-03	6.00E-03
	S(6)	4.54E-02	1.11E-01
	Cl	4.64E-02	8.83E-02
Na^{+} addition PHREEQC SOLUTION Input			
	Na	1.08E-01	2.87E-01
	C(4)	4.00E-03	6.00E-03
	S(6)	4.54E-02	1.11E-01
	Cl	4.64E-02	8.83E-02
Ca^{+2} addition PHREEQC SOLUTION Input			
	Ca	2.05E-02	4.30E-03
	C(4)	4.00E-03	6.00E-03
	S(6)	4.54E-02	1.11E-01
	Cl	4.64E-02	8.83E-02
$SO4^{-2}$ addition PHREEQC SOLUTION Input			
	S(6)	4.54E-02	1.11E-01
	Ca	2.05E-02	4.30E-03
	Mg	3.39E-04	8.38E-03
	K	6.51E-03	4.30E-03
	Na	1.08E-01	2.87E-01
Cl^{-} addition PHREEQC SOLUTION Input			
	Cl	4.64E-02	8.83E-02
	Ca	2.05E-02	4.30E-03
	Mg	3.39E-04	8.38E-03
	K	6.51E-03	4.30E-03
	Na	1.08E-01	2.87E-01
$CO3^{-2}$ addition PHREEQC SOLUTION Input			
	C(4)	4.00E-03	6.00E-03
	Ca	2.05E-02	4.30E-03
	Mg	3.39E-04	8.38E-03
	K	6.61E-03	4.30E-03
	Na	1.08E-01	2.87E-01

Table A3: Dissolution, precipitation and phase formation delta data for ANC on ash+ASWorganics + Mg^{2+} brines

Dissolution, precipitation and phase formationdelta data for the Secunda Sept 2009 ash recipe with ASW organics + Mg Brines (Moles/Kg dry ash)									
delta, $d_{ash + ASW org + Mg brines}$									
pH	13	12	11	10	8	7	6	5	4
d_Anhydrite	-7.66E-02	-7.66E-02	-7.66E-02	-7.66E-02	-7.66E-02	-7.66E-02	-7.66E-02	-7.66E-02	-7.66E-02
d_CaCrO4	-1.96E-04	-1.96E-04	-1.96E-04	-1.96E-04	-1.96E-04	-1.96E-04	-1.96E-04	-1.96E-04	-1.96E-04
d_Calcite	4.02E-02	4.02E-02	4.02E-02	4.01E-02	3.93E-02	1.14E-03	-1.19E-01	-1.36E-01	-1.36E-01
d_CaMoO4	-1.32E-05	-1.32E-05	-1.32E-05	-1.32E-05	-1.32E-05	-1.32E-05	-1.32E-05	-1.32E-05	-1.32E-05
d_Kaolinite	-2.35E-02	-2.35E-02	-2.35E-02	2.50E-10	5.00E-10	5.00E-10	5.00E-10	5.00E-10	-1.95E-03
d_Lime	-6.15E-01	-6.15E-01	-6.15E-01	-6.15E-01	-6.15E-01	-6.15E-01	-6.15E-01	-6.15E-01	-6.15E-01
d_Mullite	-1.26E-04	-1.26E-04	-1.26E-04	-5.01E-05	-1.85E-06	-8.33E-08	-1.18E-07	-1.06E-04	-1.26E-04
d_Ni2SiO4	-3.33E-06	-3.13E-07	-4.84E-08	-3.57E-07	-6.14E-06	-2.14E-05	-2.14E-05	-2.14E-05	-2.14E-05
d_Periclase	-4.16E-01	-4.16E-01	-4.16E-01	-4.16E-01	-4.16E-01	-4.16E-01	-4.16E-01	-4.16E-01	-4.16E-01
d_Pyrite	-2.22E-03	-4.92E-06	2.16E-02	-2.77E-03	-5.50E-03	-5.50E-03	-5.50E-03	-5.50E-03	-5.50E-03
d_SrSiO3	-6.09E-03	-6.09E-03	-6.09E-03	-6.09E-03	-6.09E-03	-6.09E-03	-6.09E-03	-6.09E-03	-6.09E-03
d_Zn2TiO4	-2.67E-06	-2.67E-06	-1.89E-06	-3.64E-07	-2.67E-06	-2.67E-06	-2.67E-06	-2.67E-06	-2.67E-06
d_Fe(OH)3(am)-CF	0.00E+00	0.00E+00	0.00E+00	2.75E-03	5.50E-03	5.49E-03	5.48E-03	4.99E-03	0.00E+00
d_Brucite	4.20E-01	4.20E-01	4.20E-01	1.63E-01	0.00E+00	0.00E+00	0.00E+00	0.00E+00	0.00E+00
d_Celestite	3.44E-03	3.77E-03	3.98E-03	3.27E-03	2.99E-03	2.72E-03	1.81E-03	1.65E-03	1.61E-03
d_Cr(OH)3(A)	1.48E-04	1.84E-04	1.94E-04	9.80E-05	0.00E+00	0.00E+00	0.00E+00	0.00E+00	0.00E+00
d_Csh_gel_0.8	5.25E-02	5.21E-02	5.03E-02	0.00E+00	0.00E+00	0.00E+00	0.00E+00	0.00E+00	0.00E+00
d_Ettringite	2.39E-02	2.39E-02	2.37E-02	0.00E+00	0.00E+00	0.00E+00	0.00E+00	0.00E+00	0.00E+00
d_Gypsum	1.43E-01	2.08E-01	2.40E-01	3.54E-01	3.28E-01	3.39E-01	3.66E-01	3.70E-01	3.67E-01
d_Portlandite	2.90E-03	0.00E+00	0.00E+00	0.00E+00	0.00E+00	0.00E+00	0.00E+00	0.00E+00	0.00E+00
Color codes:		Dissolves		precipitate		No effect		new phase formed	

Table A4: Dissolution, precipitation and phase formation delta data for ANC on ash+ASWorganics + Ca^{2+} brines

Dissolution, precipitation and phase formationdelta data for the Secunda Sept 2009 ash recipe with ASW organics + Ca Brines (Moles/Kg dry ash)										
delta, $d_{ash + ASW org+ Ca brines}$										
pH	13	12	11	10	9	8	7	6	5	4
d_Anhydrite	-7.66E-02	-7.66E-02	-7.66E-02	-7.66E-02	-7.66E-02	-7.66E-02	-7.66E-02	-7.66E-02	-7.66E-02	-7.66E-02
d_CaCrO4	-1.96E-04	-1.96E-04	-1.96E-04	-1.96E-04	-1.96E-04	-1.96E-04	-1.96E-04	-1.96E-04	-1.96E-04	-1.96E-04
d_Calcite	4.02E-02	4.02E-02	4.02E-02	4.02E-02	4.01E-02	3.62E-02	4.64E-03	-8.64E-02	-1.36E-01	-1.36E-01
d_CaMoO4	-1.32E-05	-1.32E-05	-1.32E-05	-1.32E-05	-1.32E-05	-1.32E-05	-1.32E-05	-1.32E-05	-1.32E-05	-1.32E-05
d_Kaolinite	-2.35E-02	-2.35E-02	-1.77E-02	2.50E-10	5.00E-10	5.00E-10	5.00E-10	5.00E-10	5.00E-10	-9.08E-04
d_Lime	-6.15E-01	-6.15E-01	-6.15E-01	-6.15E-01	-6.15E-01	-6.15E-01	-6.15E-01	-6.15E-01	-6.15E-01	-6.15E-01
d_Mullite	-1.26E-04	-1.26E-04	-1.26E-04	-4.66E-05	-1.98E-05	-3.03E-07	-8.24E-08	-1.18E-07	-2.02E-05	-1.26E-04
d_Ni2SiO4	-4.01E-06	-1.04E-06	0.00E+00	-2.26E-07	-6.47E-07	-2.14E-05	-2.14E-05	-2.14E-05	-2.14E-05	-2.14E-05
d_Periclase	-4.16E-01	-4.16E-01	-4.16E-01	-4.16E-01	-4.16E-01	-4.16E-01	-4.16E-01	-4.16E-01	-4.16E-01	-4.16E-01
d_Pyrite	-4.96E-03	-4.55E-04	-4.56E-05	-5.50E-03	-5.50E-03	-5.50E-03	-5.50E-03	-5.50E-03	-5.50E-03	-5.50E-03
d_SrSiO3	-6.09E-03	-6.09E-03	-6.09E-03	-6.09E-03	-6.09E-03	-6.09E-03	-6.09E-03	-6.09E-03	-6.09E-03	-6.09E-03
d_Zn2TiO4	-2.67E-06	-2.67E-06	-4.46E-07	-3.53E-07	-5.60E-07	-2.67E-06	-2.67E-06	-2.67E-06	-2.67E-06	-2.67E-06
d_Fe(OH)3(am)-CF	0.00E+00	0.00E+00	0.00E+00	5.50E-03	5.50E-03	5.50E-03	5.49E-03	5.48E-03	5.26E-03	1.34E-03
d_Brucite	4.16E-01	4.16E-01	4.16E-01	1.44E-01	0.00E+00	0.00E+00	0.00E+00	0.00E+00	0.00E+00	0.00E+00
d_Celestite	3.90E-03	2.76E-03	2.75E-03	1.62E-03	1.41E-03	1.37E-03	1.11E-03	3.31E-04	0.00E+00	0.00E+00
d_Cr(OH)3(A)	1.30E-04	1.75E-04	1.95E-04	0.00E+00	0.00E+00	0.00E+00	0.00E+00	0.00E+00	0.00E+00	0.00E+00
d_Csh_gel_0.8	5.22E-02	5.26E-02	3.79E-02	0.00E+00	0.00E+00	0.00E+00	0.00E+00	0.00E+00	0.00E+00	0.00E+00
d_Ettringite	2.39E-02	2.39E-02	1.75E-02	0.00E+00	0.00E+00	0.00E+00	0.00E+00	0.00E+00	0.00E+00	0.00E+00
d_Gypsum	0.00E+00	2.94E-01	3.68E-01	3.96E-01	3.77E-01	3.77E-01	3.82E-01	3.94E-01	4.00E-01	3.99E-01
d_Portlandite	4.56E-01	0.00E+00	0.00E+00	0.00E+00	0.00E+00	0.00E+00	0.00E+00	0.00E+00	0.00E+00	0.00E+00
Color codes:		Dissolves		precipitate		No effect		new phase formed		

Table A5: Dissolution, precipitation and phase formation delta data for ANC on ash+ASWorganics + Na^+ brines

Dissolution, precipitation and phase formationdelta data for the Secunda Sept 2009 ash recipe with ASW organics + Na Brines (Moles/Kg dry ash)										
delta, $d_{ash + ASW org+ Na brines}$										
pH	13	12	11	10	9	8	7	6	5	4
d_Anhydrite	-7.66E-02	-7.66E-02	-7.66E-02	-7.66E-02	-7.66E-02	-7.66E-02	-7.66E-02	-7.66E-02	-7.66E-02	-7.66E-02
d_CaCrO4	-1.96E-04	-1.96E-04	-1.96E-04	-1.96E-04	-1.96E-04	-1.96E-04	-1.96E-04	-1.96E-04	-1.96E-04	-1.96E-04
d_Calcite	4.03E-02	4.03E-02	4.03E-02	4.03E-02	3.98E-02	3.64E-02	2.75E-02	-1.36E-01	-1.36E-01	-1.36E-01
d_CaMoO4	-1.32E-05	-1.32E-05	-1.32E-05	-1.32E-05	-1.32E-05	-1.32E-05	-1.32E-05	-1.32E-05	-1.32E-05	-1.32E-05
d_Kaolinite	-2.35E-02	-2.35E-02	-1.25E-02	5.00E-10	5.00E-10	5.00E-10	5.00E-10	5.00E-10	5.00E-10	-2.69E-04
d_Lime	-6.15E-01	-6.15E-01	-6.15E-01	-6.15E-01	-6.15E-01	-6.15E-01	-6.15E-01	-6.15E-01	-6.15E-01	-6.15E-01
d_Millelite	-1.16E-06	-1.16E-06	-1.16E-06	-1.16E-06	-1.16E-06	-1.16E-06	-1.16E-06	-1.16E-06	-1.16E-06	-1.16E-06
d_Mullite	-1.26E-04	-1.26E-04	-1.26E-04	-1.26E-04	-3.88E-06	-4.74E-07	-1.78E-07	-2.02E-07	-4.65E-06	-1.26E-04
d_Ni2SiO4	-3.26E-06	0.00E+00	0.00E+00	-2.06E-07	-3.43E-06	-2.14E-05	-2.14E-05	-2.14E-05	-2.14E-05	-2.14E-05
d_Periclase	-4.16E-01	-4.16E-01	-4.16E-01	-4.16E-01	-4.16E-01	-4.16E-01	-4.16E-01	-4.16E-01	-4.16E-01	-4.16E-01
d_Pyrite	-5.50E-03	-5.50E-03	-5.50E-03	-5.50E-03	-5.50E-03	-5.50E-03	-5.50E-03	-5.50E-03	-5.50E-03	-5.50E-03
d_SrSiO3	-6.09E-03	-6.09E-03	-6.09E-03	-6.09E-03	-6.09E-03	-6.09E-03	-6.09E-03	-6.09E-03	-6.09E-03	-6.09E-03
d_Zn2TiO4	-2.67E-06	-2.67E-06	-6.10E-07	-2.78E-07	-1.99E-06	-2.67E-06	-2.67E-06	-2.67E-06	-2.67E-06	-2.67E-06
d_Fe(OH)3(am)-CF	0.00E+00	5.22E-03	5.46E-03	5.49E-03	5.50E-03	5.50E-03	5.50E-03	5.47E-03	5.36E-03	1.67E-03
d_Brucite	4.16E-01	4.16E-01	4.16E-01	3.80E-01	0.00E+00	0.00E+00	0.00E+00	0.00E+00	0.00E+00	0.00E+00
d_Celestite	4.09E-03	3.99E-03	3.64E-03	3.20E-03	2.57E-03	2.55E-03	2.49E-03	1.29E-03	1.28E-03	1.26E-03
d_Cr(OH)3(A)	1.41E-04	0.00E+00	0.00E+00	0.00E+00	0.00E+00	0.00E+00	0.00E+00	0.00E+00	0.00E+00	0.00E+00
d_Csh_gel_0.8	5.24E-02	5.15E-02	2.58E-02	0.00E+00	0.00E+00	0.00E+00	0.00E+00	0.00E+00	0.00E+00	0.00E+00
d_Ettringite	2.39E-02	2.39E-02	1.19E-02	0.00E+00	0.00E+00	0.00E+00	0.00E+00	0.00E+00	0.00E+00	0.00E+00
d_Gypsum	2.16E-01	2.38E-01	3.01E-01	3.50E-01	2.92E-01	2.93E-01	2.96E-01	3.41E-01	3.41E-01	3.40E-01
d_Portlandite	3.67E-03	0.00E+00	0.00E+00	0.00E+00	0.00E+00	0.00E+00	0.00E+00	0.00E+00	0.00E+00	0.00E+00
Color codes:		Dissolves		precipitate		No effect		new phase formed		

Table A6: Dissolution, precipitation and phase formation delta data for ANC on ash+ASWorganics + CO_3^{2-} brines

Dissolution, precipitation and phase formationdelta data for the Secunda Sept 2009 ash recipe with ASW organics + CO3 Brines (Moles/Kg dry ash)										
delta, $d_{ash + ASW org+ CO3 brines}$										
pH	13	12	11	10	9	8	7	6	5	4
d_Anhydrite	-7.66E-02	-7.66E-02	-7.66E-02	-7.66E-02	-7.66E-02	-7.66E-02	-7.66E-02	-7.66E-02	-7.66E-02	-7.66E-02
d_CaCrO4	-1.96E-04	-1.96E-04	-1.96E-04	-1.96E-04	-1.96E-04	-1.96E-04	-1.96E-04	-1.96E-04	-1.96E-04	-1.96E-04
d_Calcite	4.00E-02	4.01E-02	4.01E-02	4.01E-02	4.00E-02	3.90E-02	2.74E-02	-1.34E-01	-1.36E-01	-1.36E-01
d_CaMoO4	-1.32E-05	-1.32E-05	-1.32E-05	-1.32E-05	-1.32E-05	-1.32E-05	-1.32E-05	-1.32E-05	-1.32E-05	-1.32E-05
d_Hematite	1.71E-19	5.00E-10	5.00E-10	5.00E-10	5.00E-10	5.00E-10	5.00E-10	5.00E-10	5.00E-10	5.00E-10
d_Kaolinite	-2.35E-02	-2.35E-02	-7.95E-03	5.00E-10	5.00E-10	5.00E-10	5.00E-10	5.00E-10	5.00E-10	-5.30E-04
d_Lime	-6.15E-01	-6.15E-01	-6.15E-01	-6.15E-01	-6.15E-01	-6.15E-01	-6.15E-01	-6.15E-01	-6.15E-01	-6.15E-01
d_Millelite	-1.16E-06	-1.16E-06	-1.16E-06	-1.16E-06	-1.16E-06	-1.16E-06	-1.16E-06	-1.16E-06	-1.16E-06	-1.16E-06
d_Mullite	-1.26E-04	-1.26E-04	-1.26E-04	-8.53E-05	-2.03E-05	-9.01E-07	-1.10E-07	-1.75E-07	-9.43E-06	-1.26E-04
d_Ni2SiO4	-4.67E-06	-2.62E-07	0.00E+00	0.00E+00	-2.63E-07	-1.01E-05	-2.14E-05	-2.14E-05	-2.14E-05	-2.14E-05
d_Periclase	-4.16E-01	-4.16E-01	-4.16E-01	-4.16E-01	-4.16E-01	-4.16E-01	-4.16E-01	-4.16E-01	-4.16E-01	-4.16E-01
d_Pyrite	-5.50E-03	-5.50E-03	-5.50E-03	-5.50E-03	-5.50E-03	-5.50E-03	-5.50E-03	-5.50E-03	-5.50E-03	-5.50E-03
d_SrSiO3	-5.37E-03	-6.09E-03	-6.09E-03	-6.09E-03	-6.09E-03	-6.09E-03	-6.09E-03	-6.09E-03	-6.09E-03	-6.09E-03
d_Zn2TiO4	-2.67E-06	-2.53E-06	-5.52E-07	-2.79E-07	-4.90E-07	-2.67E-06	-2.67E-06	-2.67E-06	-2.67E-06	-2.67E-06
d_Fe(OH)3(am)-CF	2.26E-03	5.12E-03	5.47E-03	5.50E-03	5.50E-03	5.50E-03	5.50E-03	5.47E-03	5.28E-03	0.00E+00
d_Brucite	4.20E-01	4.20E-01	4.19E-01	2.88E-01	0.00E+00	0.00E+00	0.00E+00	0.00E+00	0.00E+00	0.00E+00
d_Cr(OH)3(A)	4.10E-05	0.00E+00	0.00E+00	0.00E+00	0.00E+00	0.00E+00	0.00E+00	0.00E+00	0.00E+00	0.00E+00
d_Csh_gel_0.8	5.09E-02	5.24E-02	1.91E-02	0.00E+00	0.00E+00	0.00E+00	0.00E+00	0.00E+00	0.00E+00	0.00E+00
d_Ettringite	2.32E-02	2.37E-02	7.31E-03	0.00E+00	0.00E+00	0.00E+00	0.00E+00	0.00E+00	0.00E+00	0.00E+00
d_Portlandite	3.17E-01	0.00E+00	0.00E+00	0.00E+00	0.00E+00	0.00E+00	0.00E+00	0.00E+00	0.00E+00	0.00E+00
Color codes:		Dissolves		precipitate		No effect		new phase formed		

Table A7: Dissolution, precipitation and phase formation delta data for ANC on ash+ASWorganics + SO_4^{2-} brines

Dissolution, precipitation and phase formationdelta data for the Secunda Sept 2009 ash recipe with ASW organics + SO4 Brines (Moles/Kg dry ash)										
delta, $d_{ash + ASW org+ SO4 brines}$										
pH	13	12	11	10	9	8	7	6	5	4
d_Anhydrite	-7.66E-02	-7.66E-02	-7.66E-02	-7.66E-02	-7.66E-02	-7.66E-02	-7.66E-02	-7.66E-02	-7.66E-02	-7.66E-02
d_CaCrO4	-1.96E-04	-1.96E-04	-1.96E-04	-1.96E-04	-1.96E-04	-1.96E-04	-1.96E-04	-1.96E-04	-1.96E-04	-1.96E-04
d_Calcite	-1.15E-04	-7.23E-05	-7.24E-05	-1.07E-04	-1.54E-04	-3.55E-03	-3.01E-02	-1.36E-01	-1.36E-01	-1.36E-01
d_CaMoO4	-1.32E-05	-1.32E-05	-1.32E-05	-1.32E-05	-1.32E-05	-1.32E-05	-1.32E-05	-1.32E-05	-1.32E-05	-1.32E-05
d_Kaolinite	-2.35E-02	-2.35E-02	-2.23E-02	5.00E-10	5.00E-10	5.00E-10	5.00E-10	5.00E-10	5.00E-10	-4.99E-04
d_Lime	-6.15E-01	-6.15E-01	-6.15E-01	-6.15E-01	-6.15E-01	-6.15E-01	-6.15E-01	-6.15E-01	-6.15E-01	-6.15E-01
d_Millelite	-1.16E-06	-1.16E-06	-1.16E-06	-1.16E-06	-1.16E-06	-1.16E-06	-1.16E-06	-1.16E-06	-1.16E-06	-1.16E-06
d_Mullite	-1.26E-04	-1.26E-04	-1.26E-04	-7.48E-05	-2.43E-05	-3.98E-07	-1.07E-07	-7.47E-07	-2.38E-05	-1.26E-04
d_Ni2SiO4	-4.31E-06	0.00E+00	0.00E+00	-1.34E-07	-4.08E-07	-2.14E-05	-2.14E-05	-2.14E-05	-2.14E-05	-2.14E-05
d_Periclase	-4.16E-01	-4.16E-01	-4.16E-01	-4.16E-01	-4.16E-01	-4.16E-01	-4.16E-01	-4.16E-01	-4.16E-01	-4.16E-01
d_Pyrite	-5.50E-03	-5.50E-03	-5.50E-03	-5.50E-03	-5.50E-03	-5.50E-03	-5.50E-03	-5.50E-03	-5.50E-03	-5.50E-03
d_SrSiO3	-6.09E-03	-6.09E-03	-6.09E-03	-6.09E-03	-6.09E-03	-6.09E-03	-6.09E-03	-6.09E-03	-6.09E-03	-6.09E-03
d_Zn2TiO4	-2.67E-06	-2.67E-06	-9.24E-07	-3.13E-07	-4.74E-07	-2.67E-06	-2.67E-06	-2.67E-06	-2.67E-06	-2.67E-06
d_Fe(OH)3(am)-CF	0.00E+00	5.17E-03	5.44E-03	5.50E-03	5.50E-03	5.50E-03	5.49E-03	5.45E-03	5.21E-03	0.00E+00
d_Brucite	4.20E-01	4.20E-01	4.19E-01	2.03E-01	0.00E+00	0.00E+00	0.00E+00	0.00E+00	0.00E+00	0.00E+00
d_Celestite	4.68E-03	2.24E-03	2.08E-03	8.53E-04	5.62E-04	5.35E-04	3.15E-04	0.00E+00	0.00E+00	0.00E+00
d_Cr(OH)3(A)	1.26E-04	0.00E+00	0.00E+00	0.00E+00	0.00E+00	0.00E+00	0.00E+00	0.00E+00	0.00E+00	0.00E+00
d_Csh_gel_0.8	5.20E-02	5.22E-02	4.75E-02	0.00E+00	0.00E+00	0.00E+00	0.00E+00	0.00E+00	0.00E+00	0.00E+00
d_Ettringite	2.39E-02	2.39E-02	2.22E-02	0.00E+00	0.00E+00	0.00E+00	0.00E+00	0.00E+00	0.00E+00	0.00E+00
d_Gypsum	8.97E-02	3.07E-01	3.17E-01	3.74E-01	3.49E-01	3.49E-01	3.54E-01	3.70E-01	3.71E-01	3.70E-01
d_Portlandite	4.46E-01	0.00E+00	0.00E+00	0.00E+00	0.00E+00	0.00E+00	0.00E+00	0.00E+00	0.00E+00	0.00E+00
Color codes:		Dissolves		precipitate		No effect		new phase formed		

Table A8: Dissolution, precipitation and phase formation delta data for ANC on ash+ASWorganics + Cl^- brines

Dissolution, precipitation and phase formationdelta data for the Secunda Sept 2009 ash recipe with ASW organics + Cl Brines (Moles/Kg dry ash)										
delta, $d_{ash + ASW org+ Cl brines}$										
pH	13	12	11	10	9	8	7	6	5	4
d_Anhydrite	-7.66E-02	-7.66E-02	-7.66E-02	-7.66E-02	-7.66E-02	-7.66E-02	-7.66E-02	-7.66E-02	-7.66E-02	-7.66E-02
d_CaCrO4	-1.96E-04	-1.96E-04	-1.96E-04	-1.96E-04	-1.96E-04	-1.96E-04	-1.96E-04	-1.96E-04	-1.96E-04	-1.96E-04
d_Calcite	-1.02E-04	-6.26E-05	-6.21E-05	-8.95E-05	-1.56E-04	-1.48E-03	-2.29E-02	-1.36E-01	-1.36E-01	-1.36E-01
d_CaMoO4	-1.32E-05	-1.32E-05	-1.32E-05	-1.32E-05	-1.32E-05	-1.32E-05	-1.32E-05	-1.32E-05	-1.32E-05	-1.32E-05
d_Kaolinite	-2.35E-02	-2.35E-02	-9.70E-03	5.00E-10	5.00E-10	5.00E-10	5.00E-10	5.00E-10	5.00E-10	5.00E-10
d_Lime	-6.15E-01	-6.15E-01	-6.15E-01	-6.15E-01	-6.15E-01	-6.15E-01	-6.15E-01	-6.15E-01	-6.15E-01	-6.15E-01
d_Millelite	-1.16E-06	-1.16E-06	-1.16E-06	-1.16E-06	-1.16E-06	-1.16E-06	-1.16E-06	-1.16E-06	-1.16E-06	-1.16E-06
d_Mullite	-1.26E-04	-1.26E-04	-1.26E-04	-7.97E-05	-1.19E-05	-8.97E-07	-1.16E-07	-1.86E-07	-6.03E-05	-1.26E-04
d_Ni2SiO4	-3.43E-06	0.00E+00	0.00E+00	0.00E+00	-5.96E-07	-1.37E-05	-2.14E-05	-2.14E-05	-2.14E-05	-2.14E-05
d_Periclase	-4.16E-01	-4.16E-01	-4.16E-01	-4.16E-01	-4.16E-01	-4.16E-01	-4.16E-01	-4.16E-01	-4.16E-01	-4.16E-01
d_Pyrite	-5.50E-03	-5.50E-03	-5.50E-03	-5.50E-03	-5.50E-03	-5.50E-03	-5.50E-03	-5.50E-03	-5.50E-03	-5.50E-03
d_SrSiO3	-6.09E-03	-6.09E-03	-6.09E-03	-6.09E-03	-6.09E-03	-6.09E-03	-6.09E-03	-6.09E-03	-6.09E-03	-6.09E-03
d_Zn2TiO4	-2.67E-06	-2.67E-06	-5.50E-07	-3.05E-07	-7.21E-07	-2.67E-06	-2.67E-06	-2.67E-06	-2.67E-06	-2.67E-06
d_Fe(OH)3(am)-CF	2.26E-03	5.21E-03	5.47E-03	5.50E-03	5.50E-03	5.50E-03	5.49E-03	5.47E-03	5.02E-03	2.28E-05
d_Brucite	4.20E-01	4.20E-01	4.19E-01	1.85E-01	0.00E+00	0.00E+00	0.00E+00	0.00E+00	0.00E+00	0.00E+00
d_Cr(OH)3(A)	5.88E-05	0.00E+00	0.00E+00	0.00E+00	0.00E+00	0.00E+00	0.00E+00	0.00E+00	0.00E+00	0.00E+00
d_Csh_gel_0.8	5.22E-02	5.26E-02	2.27E-02	0.00E+00	0.00E+00	0.00E+00	0.00E+00	0.00E+00	0.00E+00	0.00E+00
d_Ettringite	2.36E-02	2.38E-02	9.05E-03	0.00E+00	0.00E+00	0.00E+00	0.00E+00	0.00E+00	0.00E+00	0.00E+00
d_Portlandite	3.51E-01	0.00E+00	0.00E+00	0.00E+00	0.00E+00	0.00E+00	0.00E+00	0.00E+00	0.00E+00	0.00E+00
Color codes:		Dissolves		precipitate		No effect		new phase formed		

Appendix 2: PHREEQC input KEYWORDS and parameters description for transport modeling

A general description of transport modeling concepts with PHREEQC is given by the following input file (Figure A2) which was derived from one of the many case studies handled in the course of PHREEQC exercises. In the input data description the words in block letters are called KEYWORDS data blocks. The symbol # denotes any writing after it is just but a description and not part of the executable program. An attempt has been made to define and clarify some of the input parameters in this case as representative of the other cases that follow in order to give an overview of the concepts and meanings encountered in PHREEQC ADR-transport modeling either in column or ash heap modeling.

This describes the database used in the simulation and its location: in our case LLNL.

```
DATABASE C:\Users\user\Desktop\Llnl.txt
TITLE Infiltration of rainwater in equilibrium with atmosphere through acid mine drainage
tailings and underlying aquifer
```

This gives the title of the simulation

```
SOLUTION 0
    temp      25
    pH        7
    pe        4
    redox     pe
    units     mmol/kgw
    density   1
    -water    1 # kg

EQUILIBRIUM_PHASES 0 atmospheric O2 and CO2
    CO2(g)    -3.5 10
    O2(g)     -0.7 10
    Pyrite    0 0.01
SAVE solution 0
END
SOLUTION 1-2
    temp      25
    pH        7
    pe        4
    redox     pe
    units     mmol/kgw
    density   1
    -water    1 # kg
EQUILIBRIUM_PHASES 1-2
    Pyrite    0 1
SOLUTION 3-10
    temp      25
    pH        7
    pe        4
    redox     pe
    units     mmol/kgw
    density   1
    -water    1 # kg
EQUILIBRIUM_PHASES 3-10
    Calcite   0 1
    Kaolinite 0 1
    Gypsum    0 0
    Goethite  0 0
```

- The keyword SOLUTION 0 denotes the infilling solution which is rainwater mimicked as pure water (density of 1 g/cm^3) at default conditions of temperature, pH, pe, and no redox couple adopted. Default units are mmol/kg water and this water is in constant contact with atmospheric O_2 and CO_2 in equilibrium with 0.01moles of pyrite to ensure full oxidation of pyrite.
- EQUILBRIUM_PHASES 0 keyword denotes phases that are to be in equilibrium with the infilling solution components. For each solid phase, log *saturation index* followed by the amounts in *moles* are shown. Large number of moles (default 10) assures saturation. For gases, fugacity was set at $10^{-3.5}$ Atm for CO_2, and for O_2 it was $10^{-0.7}$ Atm and 10moles for each gas.

- SOLUTION 1-2: Solution in column cells1-2 (water at) and in equilibrium with pyrite in those cells.
- Solution in cells 3-10 is pure water at default conditions and equilibrated with 1 mole each of calcite and kaolinite. Gypsum and goethite are allowed to precipitate from solution if it becomes saturated as they are assigned saturation index of 0 and are absent in solution initially.(moles = 0)

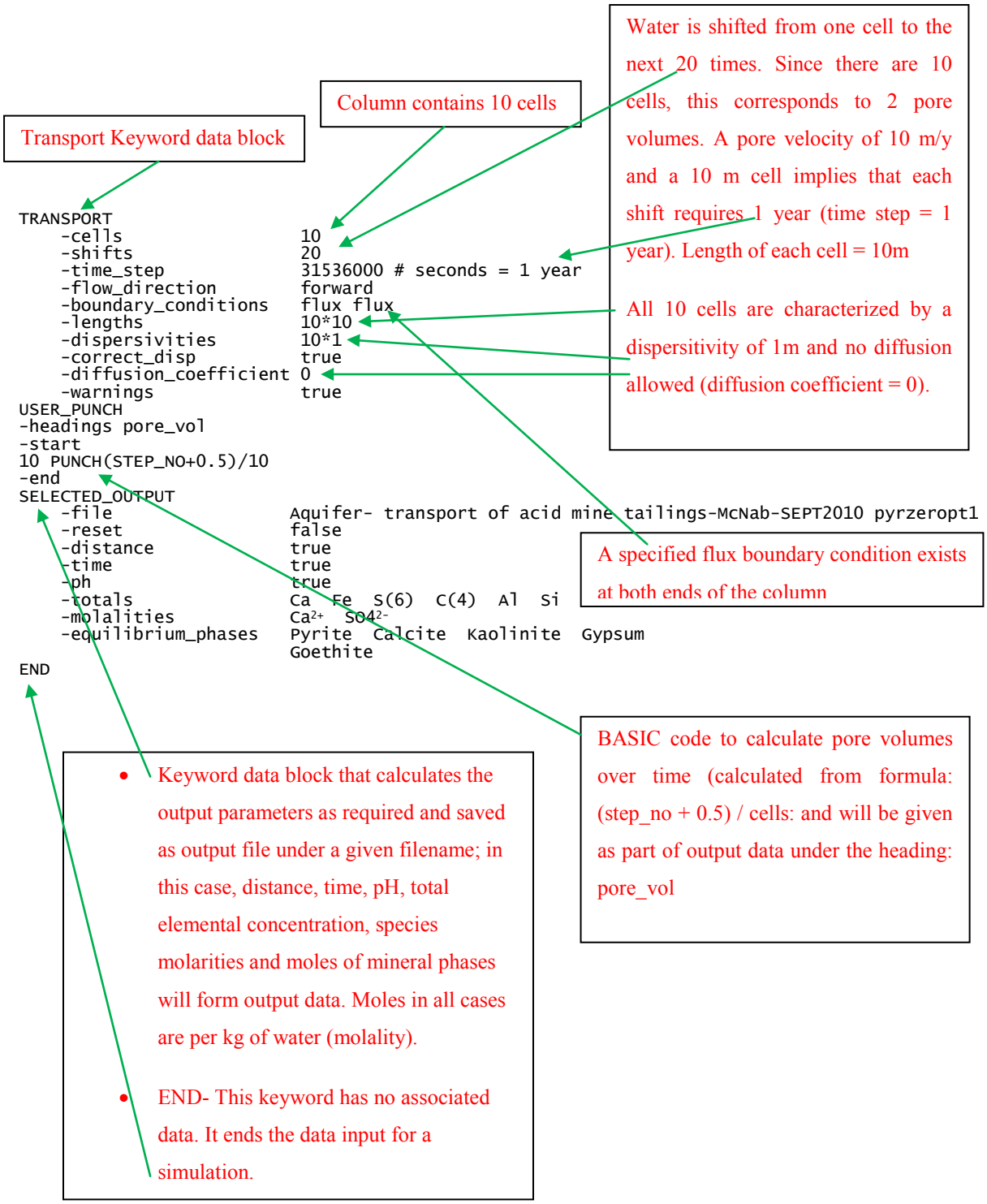

Figure A1: PHREEQC input transport KEYWORDS and parameters description

Appendix 3: Tutuka ash heap modeling with brine

Table A9: PHREEQC input for Tutuka ash heap modeling with brine

```
DATABASE C:\Users\user\Desktop\Llnl.txt
TITLE Tutuka ash heap modeling with brine- JMM 20yrs
SOLUTION_MASTER_SPECIES
    Si            SiO2            0     Si              28.0855
SOLUTION_SPECIES
2H2O + SiO2 = H4SiO4
    log_k     -2.7
2H+ + H2SiO4-2 = SiO2 + 2H2O
    log_k     22.96
PHASES
Cu(OH)2
    Cu(OH)2 + 2H+ = Cu+2 + 2H2O
    log_k     8.64
Csh_gel_0.8
    Ca0.8SiO2.8:H2O + 1.6H+ = 0.8Ca+2 + 1.8H2O + SiO2
    log_k     11.08
Csh_gel_1.1
    Ca1.1SiO3.1:H2O + 2.2H+ = 1.1Ca+2 + 2.1H2O + SiO2
    log_k     16.72
CSH_1.4
    Ca1.4SiO3.4:0.90H2O + 2.8H+ = 1.4Ca+2 + 2.3H2O + SiO2
    log_k     23.74
Csh_gel_1.8
    Ca1.8SiO3.8:H2O + 3.6H+ = 1.8Ca+2 + 2.8H2O + SiO2
    log_k     32.7
CuCrO4
    CuCrO4 = CrO4-2 + Cu+2
    log_k     -5.4754
MgCrO4
    MgCrO4 = CrO4-2 + Mg+2
    log_k     5.3801
CaCrO4
    CaCrO4 = Ca+2 + CrO4-2
```

log_k -2.2657

CaMoO4

CaMoO4 = Ca^{2+} + $MoO4^{2-}$

log_k -7.94

BaMoO4

BaMoO4 = Ba^{2+} + $MoO4^{2-}$

log_k -7.42

BaCrO4

BaCrO4 = Ba^{2+} + $CrO4^{2-}$

log_k -9.6681

BaCr0.23S0.77O4

Ba(CrO4)0.23(SO4)0.77 = Ba^{2+} + 0.23$CrO4^{2-}$ + 0.77$SO4^{2-}$

log_k -10.13

BaCr0.04S0.96O4

BaCr0.04S0.96O4 = Ba^{2+} + 0.04$CrO4^{2-}$ + 0.96$SO4^{2-}$

log_k -9.79

Cr(OH)3(A)

Cr(OH)3 + H+ = Cr(OH)2+ + H2O

log_k -0.75

Cr(OH)3(C)

Cr(OH)3 + H+ = Cr(OH)2+ + H2O

log_k 1.7005

Cr-Ettringite

Ca6Al2(CrO4)3(OH)12:26H2O + 12H+ = 2Al+3 + 6Ca^{2+} + 3$CrO4^{2-}$ + 38H2O

log_k 53

Cr-hydrocalumite

Ca4Al2CrO10:15H2O + 12H+ = 2Al+3 + 4Ca^{2+} + $CrO4^{2-}$ + 21H2O

log_k 71.02

Magnesiochromite

MgCr2O4 + 8H+ = 2Cr+3 + 4H2O + Mg^{2+}

log_k 21.693

mullite

Al6Si2O13 + 18H+ = 6Al+3 + 9H2O + 2SiO2

log_k 45.41

Ca-Monosulfoaluminate

Ca4Al2O6(SO4):12H2O + 12H+ = 2Al+3 + 4Ca^{2+} + 18H2O + $SO4^{2-}$

log_k 73.37

Friedel-salt

```
    Ca4Al2Cl2O6:10H2O + 12H+ = 2Al+3 + 4Ca2+ + 2Cl- + 16H2O
    log_k     74.95
Ca3Al2(OH)12-cement
    Ca3Al2(OH)12 + 12H+ = 2Al+3 + 3Ca2+ + 12H2O
    log_k     80.33
Millerite
    NiS + H+ = HS- + Ni2+
    log_k     -8.0345
Ni2SiO4
    Ni2SiO4 + 4H+ = 2H2O + 2Ni2+ + SiO2
    log_k     14.3416
SiO2(am)
    SiO2 + 2H2O = H4SiO4
    log_k     -2.7
Sr(OH)2
    Sr(OH)2 + 2H+ = 2H2O + Sr2+
    log_k     27.5229
SrSiO3
    SrSiO3 + 2H+ = H2O + SiO2 + Sr2+
    log_k     14.8438
Zn2TiO4
    Zn2TiO4 + 4H+ = Ti(OH)4 + 2Zn2+
    log_k     12.3273
SOLUTION 0 Infillling solution-brine
    temp      20
    pH        7.36
    pe        4
    redox     pe
    units     mol/l
    density   1
    Na        0.293
    Mg        0.00856
    K         0.00439
    Ca        0.0044
    Cl        0.0902
    S(6)      0.114 charge
    C(4)      0.006
    -water    1 # kg
```

```
EQUILIBRIUM_PHASES 0 Atmospheric O2 and CO2
    CO2(g)    -3.5 10
    O2(g)     -0.7 10
SAVE solution 0
SAVE equilibrium_phases 0
END
SOLUTION 1-10 Initial solution for column
    temp      20
    pH        7 charge
    pe        4
    redox     pe
    units     mol/l
    density   1
    Li        0.004
    Na        0.01
    K         0.002
    -water    1 # kg
EQUILIBRIUM_PHASES 1-10 Tutuka ash recipe
    Al(OH)3(mC) 0 0
    Anhydrite 0 0.0069
    Brucite   0 0
    Bunsenite 0 0
    CaCrO4    0 3e-005
    Calcite   0 0.0069
    CaMoO4    0 1.8e-007
    Celestite 0 0
    Cr(OH)3(A) 0 0
    CSH_1.4   0 0 dissolve_only
    Csh_gel_0.8 0 0
    Csh_gel_1.1 0 0 dissolve_only
    Csh_gel_1.8 0 0 dissolve_only
    Diaspore  0 0
    Ettringite 0 0
    Fe(OH)3(am)-CF 0 0
    Gypsum    0 0
    Hematite  0 0.03 dissolve_only
    Kaolinite 0 0.000532 dissolve_only
    Lime      0 0.0441
```

```
    Magnesite 0 0
    Millerite 0 0 dissolve_only
    mullite   0 0.005 dissolve_only
    Ni(OH)2   0 0
    Ni2SiO4   0 3e-006 dissolve_only
    NiCO3     0 0
    Periclase 0 0.021
    Portlandite 0 0
    Pyrite    0 0.0003 dissolve_only
    SiO2(am)  0 0
    Sr(OH)2   0 0
    SrSiO3    0 0.000459 dissolve_only
    Zincite   0 0
    Zn(OH)2(gamma) 0 0
    Zn2TiO4   0 2e-006 dissolve_only
EXCHANGE 1-10
    X       5.022
    -equilibrate with solution 1
SAVE solution 1-10
SAVE equilibrium_phases 1-10
SAVE exchange 1-10
TRANSPORT
    -cells                  10
    -shifts                 4000
    -time_step              157680 # seconds
    -flow_direction         forward
    -boundary_conditions    flux flux
    -lengths                10*1.2
    -dispersivities         10*0.8
    -correct_disp           true
    -diffusion_coefficient 0
    -punch_frequency        500
    -warnings               true
SELECTED_OUTPUT
    -file                 Mbugua-Tutuka ash heap modeling with brine 3rd SEPT2010 20yrs
    -user_punch           true
    -reset                false
    -distance             true
```

```
    -time                true
    -ph                  true
    -totals              Ca  Mg  Al  Ti  Fe  Ni  Cr
                         Mo  Sr  Zn  Si  S(6)  Na  K
                         Li  C(4)  Cl
    -molalities          Ca+2  CaCO3  CaHCO3+  CaNO3+
                         CaOH+  CaSO4  Mg+2  MgCO3
                         MgHCO3+  MgSO4  FeSO4  MoO4-2
                         Sr+2  SrNO3+  SrOH+  SrSO4
                         SiO2  Na+  NaCO3-  NaHCO3
                         NaSO4-  K+  KSO4-  Li+
                         LiSO4-  SO4-2  CO3-2  HCO3-
    -equilibrium_phases  Anhydrite  CaCrO4  Calcite  CaMoO4
                         Hematite  Kaolinite  Lime  Millerite
                         mullite  Ni2SiO4  Periclase  Pyrite
                         Zn2TiO4  Fe(OH)3(am)-CF  Brucite  Al(OH)3(mC)
                         Bunsenite  Celestite  Cr(OH)3(A)  Csh_gel_0.8
                         Ettringite  Gypsum  Magnesite  Ni(OH)2
                         NiCO3  Portlandite  SiO2(am)  Sr(OH)2
                         SrSiO3  Zn(OH)2(gamma)
    -saturation_indices  Anhydrite  CaCrO4  Calcite  CaMoO4
                         Hematite  Kaolinite  Lime  Millerite
                         mullite  Ni2SiO4  Periclase  Pyrite
                         Zn2TiO4  Fe(OH)3(am)-CF  Brucite  Al(OH)3(mC)
                         Bunsenite  Celestite  Cr(OH)3(A)  Csh_gel_0.8
                         Ettringite  Gypsum  Magnesite  Ni(OH)2
                         NiCO3  Portlandite  SiO2(am)  Sr(OH)2
                         SrSiO3  Zn(OH)2(gamma)
USER_PUNCH
-headings pore_vol
-start
10 PUNCH(STEP_NO+0.5)/10
-end
END
```

Appendix 4: Change of moles of mineral phases versus distance at last pore volumes (or at end of simulation time) for column modeling

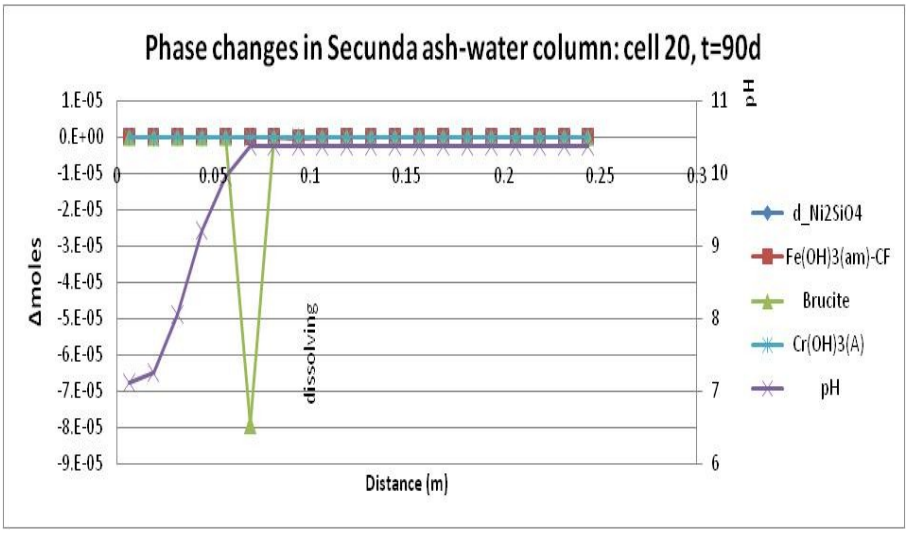

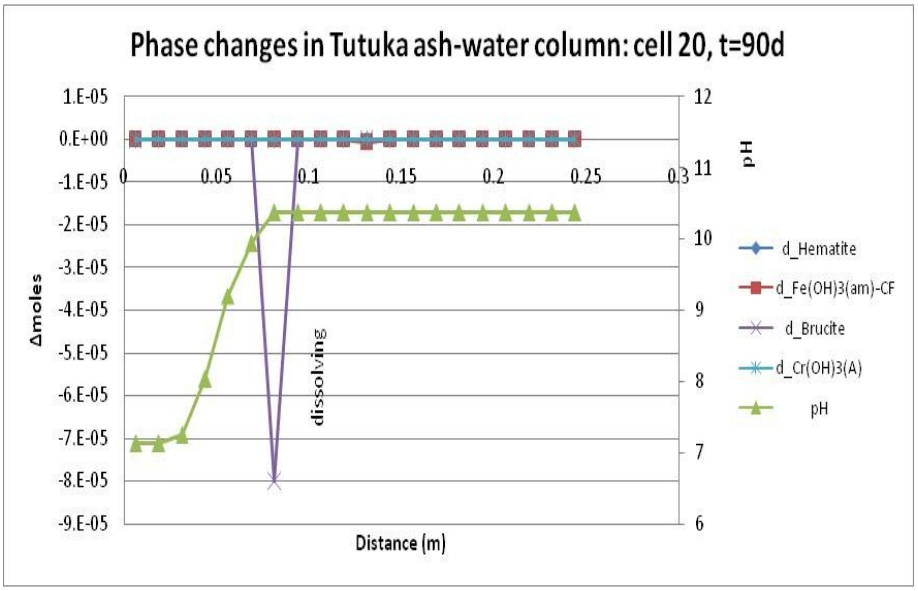

Figure A2: Amount of change of mineral phases along the column after 90-days ash-water dynamic interaction for Secunda and Tutuka ash columns

From Figure A2, brucite was the only mineral that showed significant change in phase amounts which occurred just after 0.05 m from the column inflow position. Dissolution took place at pH value of 10.5 for both ash-water scenarios.

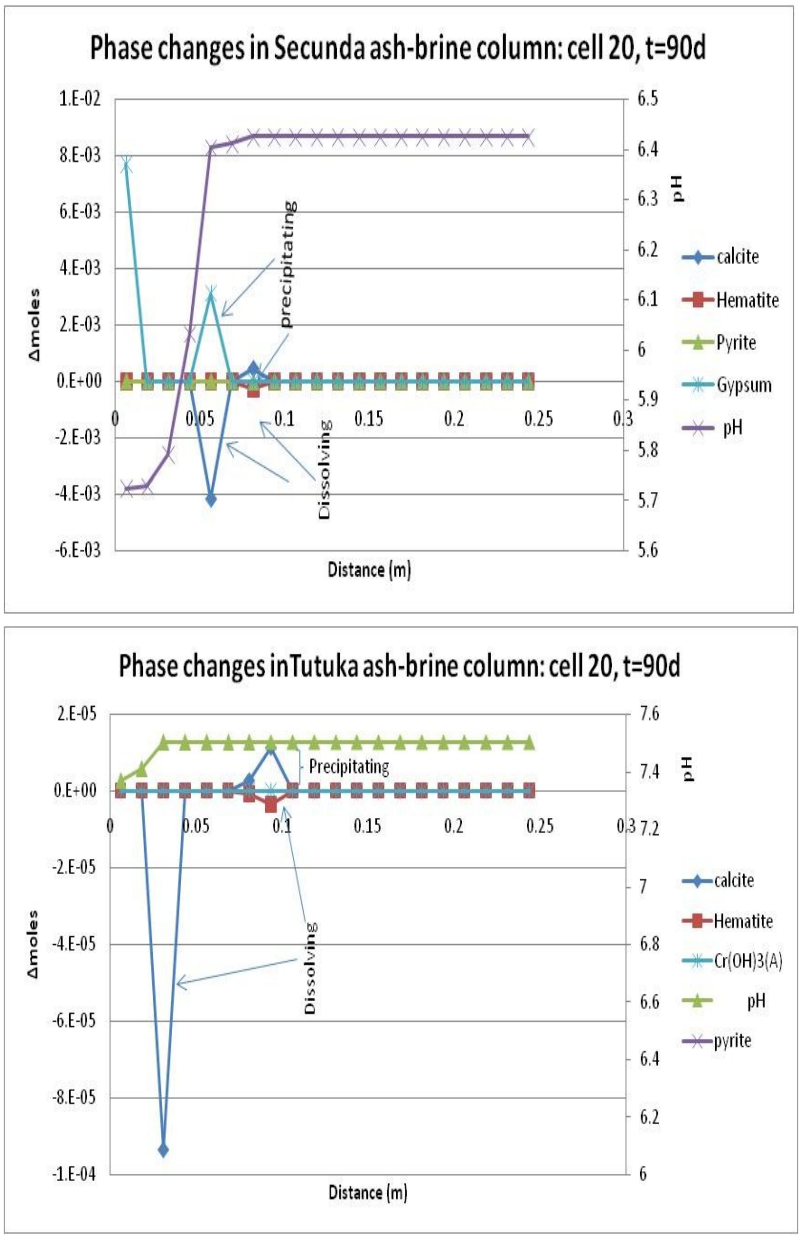

Figure A3: Amount of change of mineral phases along the column after 90-days ash-brine dynamic interaction for Secunda and Tutuka ash columns (negative changes in moles show dissolution, positive change show precipitation)

From Figure A3, the calcite dissolution took place at 0.05 m as gypsum precipitated at pH value of 6.4 after which a steady pH was achieved, confirming the precipitation-dissolution of calcite and gypsum was pH controlled. Precipitation of calcite was recorded at 0.075 m after which no change in amounts was observed. Similar trend was observed in the two ash-brine model scenarios. Dissolution of hematite was also recorded but in very small amounts at pH value of 5.9 (Secunda) and 7.3 (Tutuka) about 0.1 m from the column inflow.

The above mineral phase changes are well captured in the following individual mineral graphs under the different scenarios, Figure A4.

TW

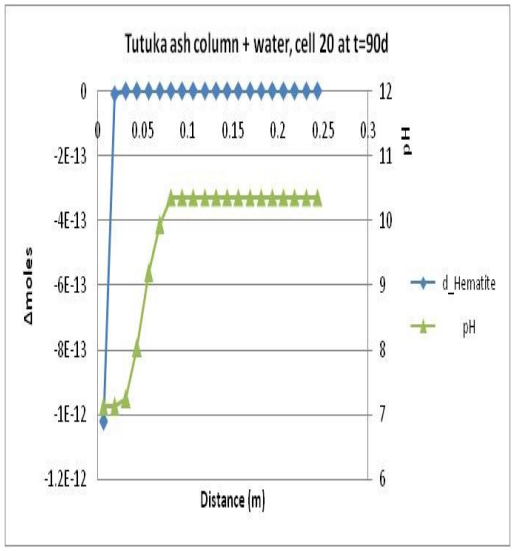
Tutuka ash column + water, cell 20 at t=90d
Amoles
pH
Distance (m)
d_Hematite
pH

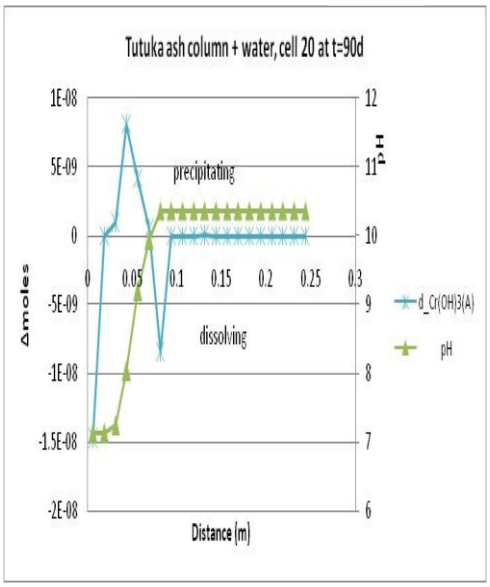
Tutuka ash column + water, cell 20 at t=90d
precipitating
dissolving
Amoles
pH
Distance (m)
d_Cr(OH)3(A)
pH

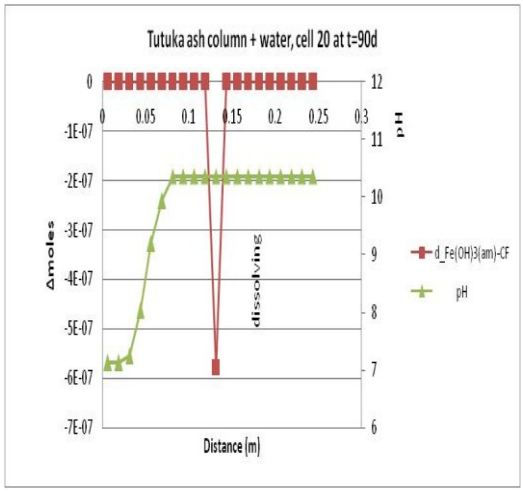
Tutuka ash column + water, cell 20 at t=90d
dissolving
Amoles
pH
Distance (m)
d_Fe(OH)3(am)-CF
pH

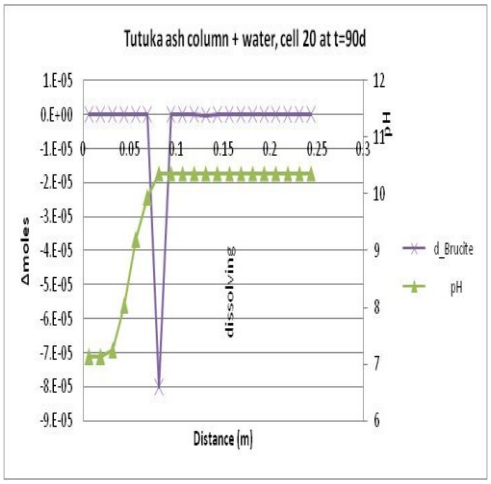
Tutuka ash column + water, cell 20 at t=90d
dissolving
Amoles
pH
Distance (m)
d_Brucite
pH

SW

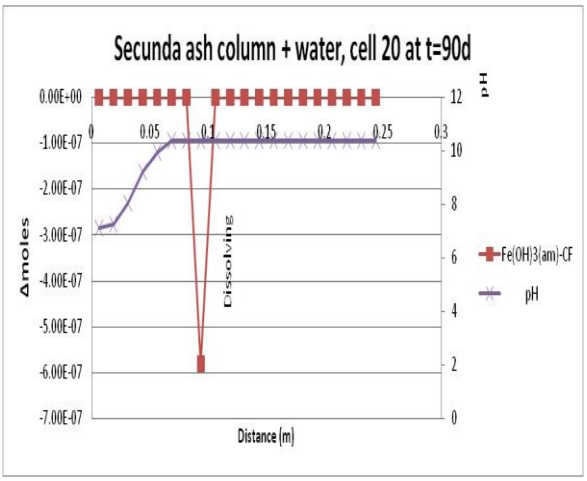
Secunda ash column + water, cell 20 at t=90d
Amoles
pH
Distance (m)
Dissolving
Fe(OH)3(am)-CF
pH

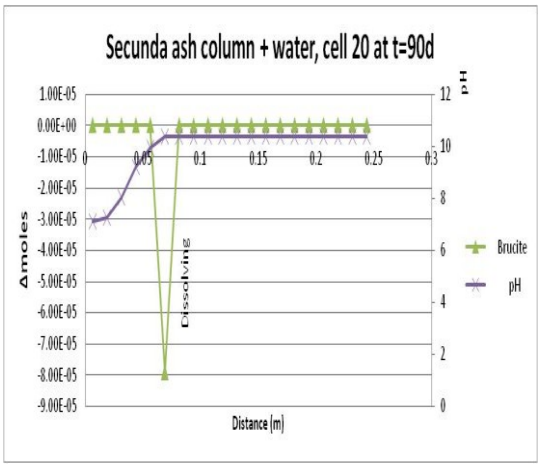
Secunda ash column + water, cell 20 at t=90d
Amoles
pH
Distance (m)
Dissolving
Brucite
pH

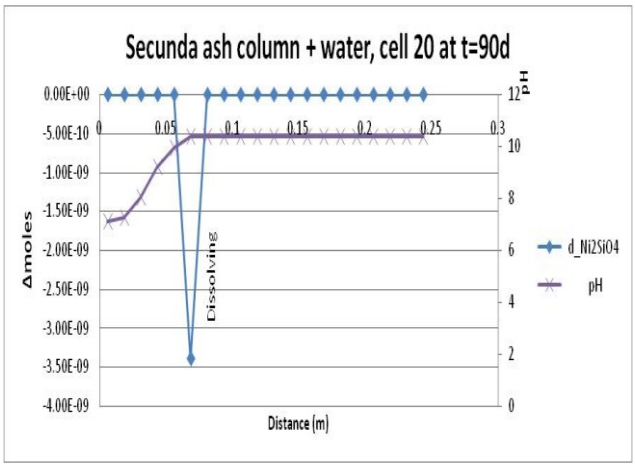
Secunda ash column + water, cell 20 at t=90d
Amoles
pH
Distance (m)
Dissolving
d_Ni2SiO4
pH

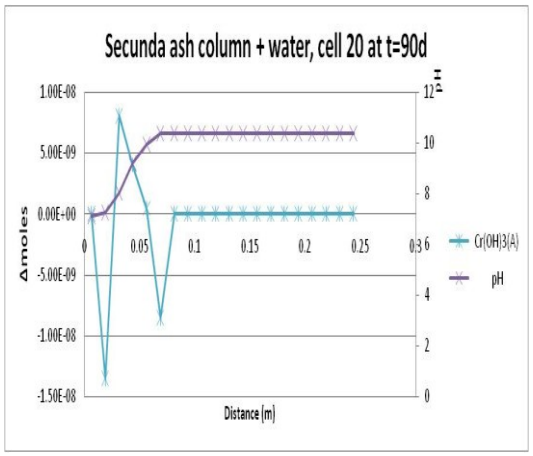
Secunda ash column + water, cell 20 at t=90d
Amoles
pH
Distance (m)
Cr(OH)3(A)
pH

SB

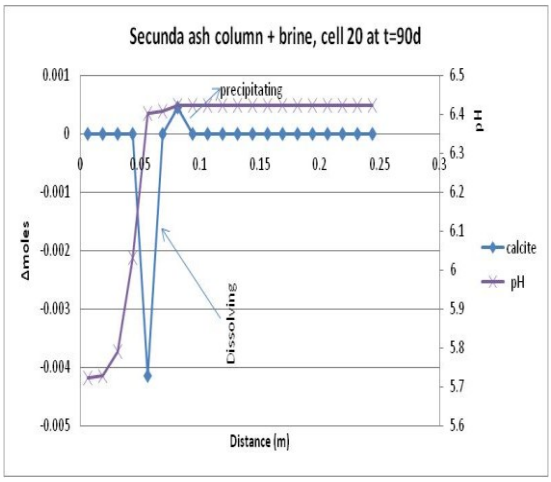
Secunda ash column + brine, cell 20 at t=90d
precipitating
Dissolving
calcite
pH
Δmoles
pH
Distance (m)

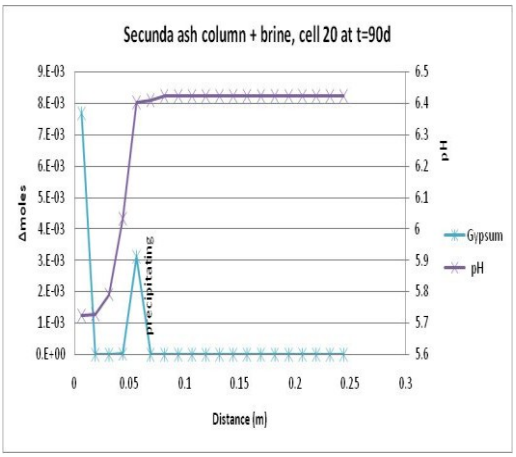
Secunda ash column + brine, cell 20 at t=90d
precipitating
Gypsum
pH
Δmoles
pH
Distance (m)

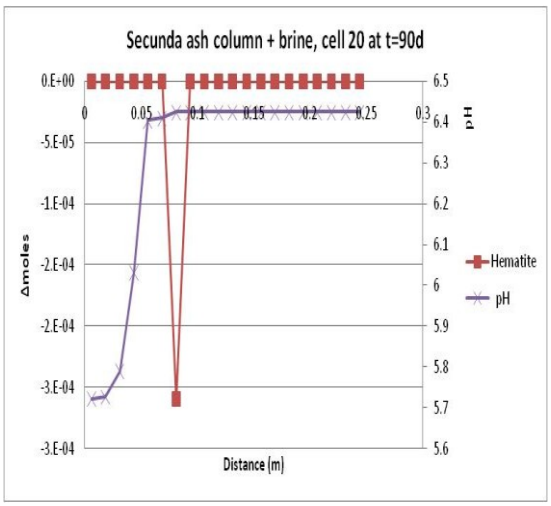
Secunda ash column + brine, cell 20 at t=90d
Hematite
pH
Δmoles
pH
Distance (m)

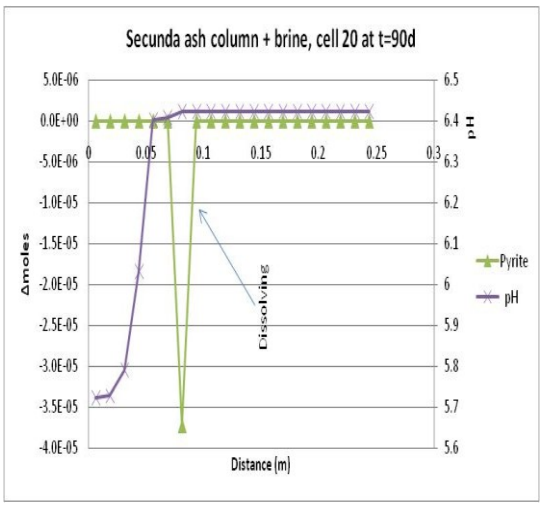
Secunda ash column + brine, cell 20 at t=90d
Dissolving
Pyrite
pH
Δmoles
pH
Distance (m)

TB

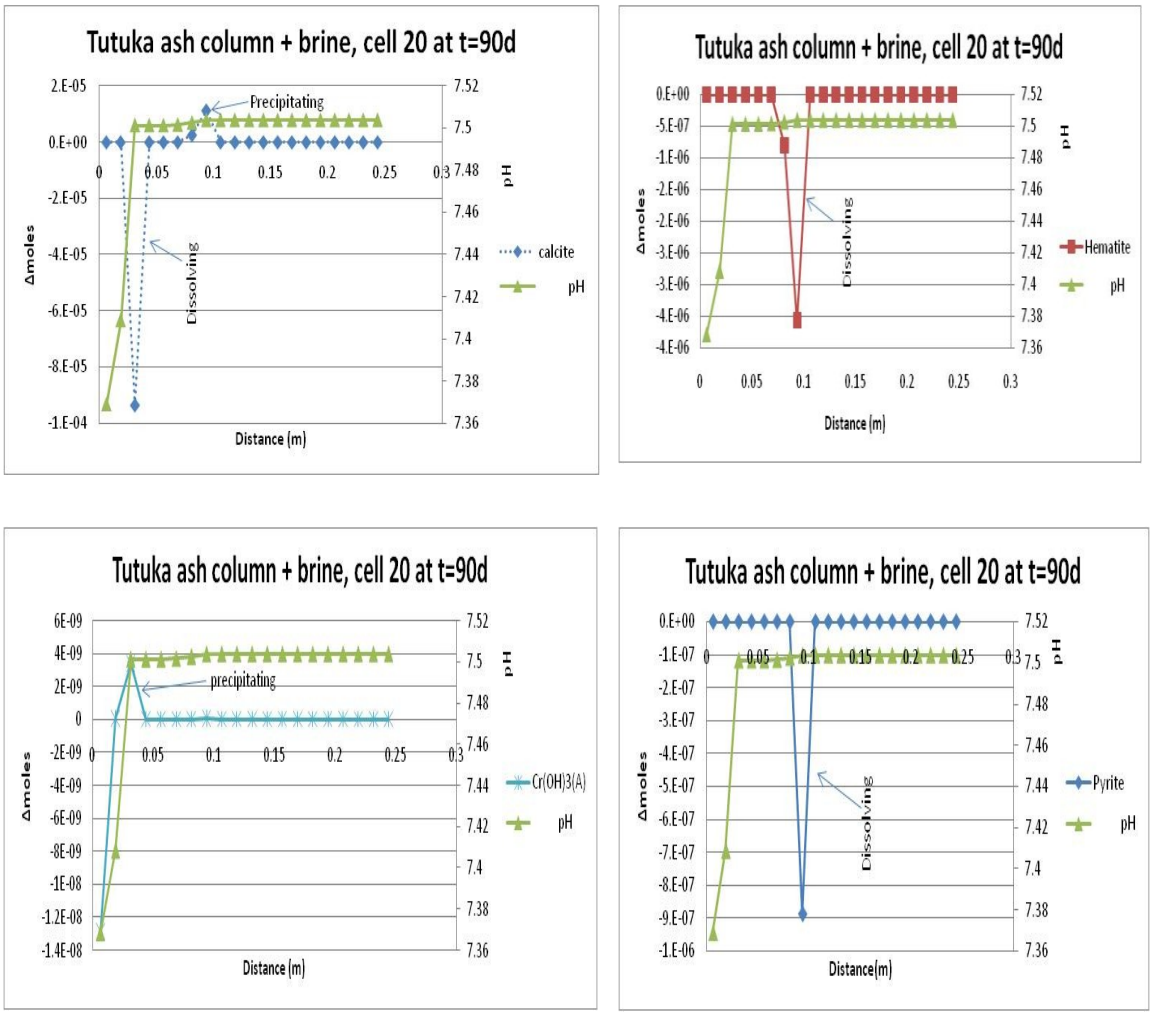

Figure A4: Mole changes of some mineral phases along the column at cell 20 after 90 days for Tutuka ash-brine column: SW-Secunda ash and water, TW-Tutuka ash and water, SB- Secunda ash and brine, TB-Tutuka ash and brine

Figures A4 (TW) and A4 (SW) show individual mineral phase changes after 90 days along the column distance for Secunda and Tutuka ash-water models. Generally hematite, $Cr(OH)_3(A)$, $Fe(OH)_3(am)$-CF and brucite show some quantifiable though very small changes in moles. The mole changes in brucite and $Cr(OH)_3(A)$ were pH-controlled and took place between 0.05 and 0.1 m from the column inflow.

From Figure A4 (TB) and A4 (SB) marked changes in moles amount of mineral phases were recorded for the minerals hematite, pyrite and calcite, gypsum and $Cr(OH)_3(A)$, in Secunda and Tutuka ash-brine column models. Dissolution of hematite, pyrite and calcite took place at between 0.05 and

0.1 m from the column inflow at pH value of 6.4 while gypsum precipitated at about 0.05 m at the same pH for Secunda ash-brine column model. Similar trend was observed for the Tutuka ash-brine column model. Many of the other mineral phases underwent dissolution and some were of very small quantities whose change in amount was considered insignificant.

Appendix 5: Total elemental concentrations of leachates at break through volumes over a 20-year period of ash heap weathering irrigated with water and brines

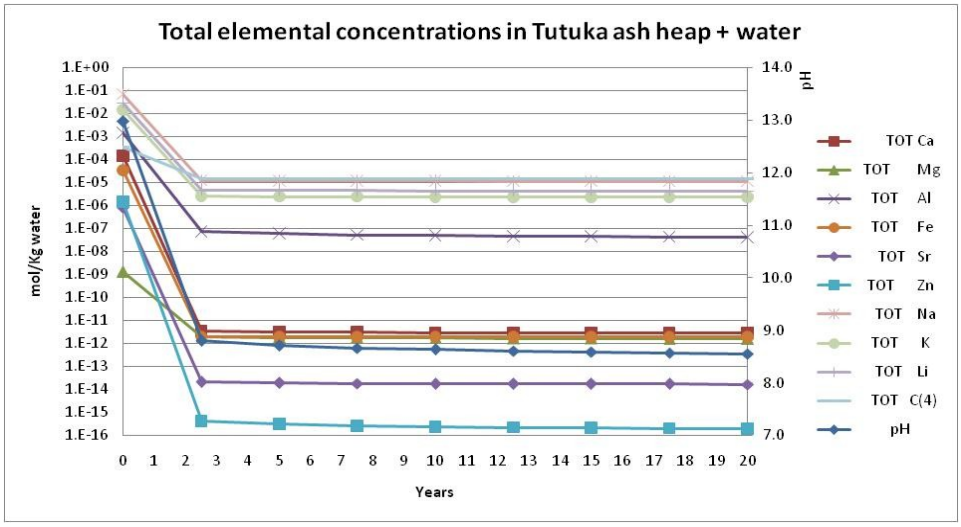

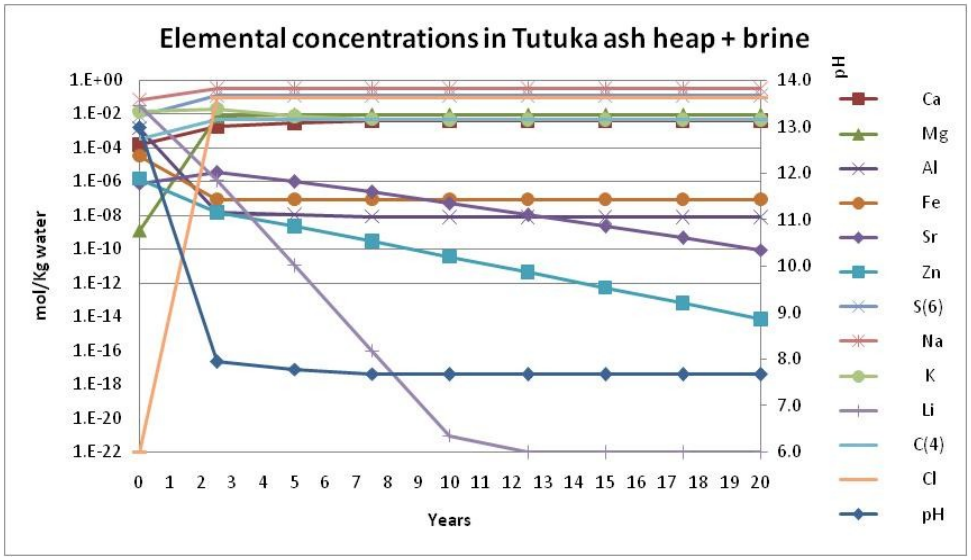

Figure A5: Total elemental concentrations against time in Tutuka ash heap with water and with brine irrigation

Appendix 6: Analytical data for Batch ANC tests carried out on Secunda and Tutuka fly ashes (UWC Data) from [6] and [10, 11])

Table A10: Concentrations (mmol/L) of species leached out of Secunda fly ash as a function of pH

	12.48		11.29		10.68		9.58		8.78		7.25		5.83		4.77
	ave	sdv	ave	sdv	ave	sdv	ave	sdv	ave	sdv	ave	sdv	ave	sdv	ave
Ca	21.674	0.0812	49.94	0.2646	60.404	0.1411	72.779	0.1764	77.595	0.494	82.972	0.3	88.448	0.1764	106.81
Mg	0.0015	2E-05	0.009	6E-05	0.0509	0.001	14.214	0.1542	18.959	0.1687	22.801	0.244	25.664	0.0524	31.158
Na	0.3203	0.0039	0.32	0.0022	0.3516	0.0036	0.3791	0.0015	0.4021	0.0053	0.4209	0.007	0.4543	0.0043	0.396
K	0.0435	0.0004	0.04	0.0004	0.0464	0.0005	0.0472	0.0005	0.0514	0.0008	0.0595	6E-04	0.0706	0.0003	0.0127
Li	0.1492	0.0032	0.13	0.0071	0.1516	0.0098	0.191	0.0156	0.2341	0.009	0.2502	0.005	0.2762	0.0029	0.2337
Ti	0.0002	3E-07	2E-05	1E-06	1E-05	5E-06	3E-05	9E-06	8E-05	2E-06	9E-05	3E-07	0.0002	1E-05	BDL
Fe	0.0004	1E-06	3E-04	9E-06	0.0003	2E-05	0.0004	7E-06	0.0006	3E-05	0.0006	2E-05	0.0006	4E-05	0.1803
Mn	1E-05	2E-07	2E-06	0	7E-07	8E-07	2E-05	5E-07	0.0095	3E-05	0.1113	4E-04	0.2088	0.0005	0.1929
Ni	2E-05	3E-07	4E-05	3E-07	5E-05	4E-07	6E-05	4E-06	0.0007	5E-06	0.0028	4E-05	0.0044	2E-05	0.0067
Cu	1E-05	1E-06	BDL	0	BDL	0	BDL	0	BDL	0	2E-05	0	0.0001	6E-06	0.0033
Pb	1E-05	0	BDL	0	BDL	0	BDL	0	1E-05	0	2E-06	0	BDL	0	BDL
As	BDL	0	BDL	0	BDL	0	2E-05	2E-06	6E-05	2E-06	0.0014	3E-05	0.0004	1E-05	BDL
Se	BDL	0	3E-04	4E-06	0.0003	1E-05	0.0006	3E-05	0.0006	2E-05	0.0006	2E-05	0.0006	2E-05	0.0004
B	0.0011	7E-05	0.396	0.0059	0.9801	0.0255	1.2664	0.0026	1.4255	0.0209	1.6545	0.052	1.7493	0.0118	1.5978
Cd	BDL	0	BDL	0	BDL	0	BDL	0	BDL	0	9E-06	1E-05	3E-05	2E-06	BDL
Zn	0.0004	8E-06	1E-04	6E-06	5E-05	1E-07	9E-05	1E-06	0.0001	3E-06	1E-04	1E-05	0.0015	7E-06	0.0046
Co	2E-05	3E-07	5E-05	1E-06	7E-05	2E-06	8E-05	4E-06	0.0001	3E-06	0.0005	2E-05	0.0009	7E-06	0.0011
V	4E-05	6E-08	4E-04	4E-07	0.002	1E-06	0.0226	6E-05	0.0235	0.0002	0.0297	2E-04	0.0242	0.0002	0.0107
Al	0.009	0.0001	0.079	0.0009	0.0803	0.0011	0.0028	0.0003	0.0036	6E-05	0.0005	1E-04	0.0029	9E-05	0.2145
Si	0.0211	0.0001	0.097	0.0008	0.0946	0.0017	0.2899	0.007	0.3058	0.0052	0.8893	0.002	3.199	0.0297	3.948
Sr	0.5525	0.0092	0.636	0.0073	0.7332	0.0052	0.8321	0.0033	0.8824	0.0066	0.982	0.002	1.1059	0.0117	1.1745
Cr	0.0012	2E-06	0.021	3E-05	0.0236	0.0001	0.0216	0.0002	0.0191	0.0001	0.0159	1E-04	0.0109	1E-05	0.0026
Mo	0.0004	3E-06	0.002	2E-05	0.0019	8E-06	0.0015	1E-05	0.0016	6E-06	0.0015	5E-05	0.001	9E-06	0.0006
SO_4	0.0375		0.97		2.0434		4.5276		3.3188		3.4993		3.4432		3.4832